FUNCTIONAL STEM-CELL BASED TISSUE ENGINEERED VASCULAR GRAFTS FOR HIGH-RISK DONOR POPULATIONS

by

Jeffrey T. Krawiec

Bachelor of Science, Pennsylvania State University, 2010

Submitted to the Graduate Faculty of

The Swanson School of Engineering in partial fulfillment

of the requirements for the degree of

Doctor of Philosophy

University of Pittsburgh

2015

UNIVERSITY OF PITTSBURGH

SWANSON SCHOOL OF ENGINEERING

This dissertation was presented

by

Jeffrey T. Krawiec

It was defended on

November 23rd, 2015

and approved by

J. Peter Rubin, MD, Professor, Departments of Plastic Surgery and Bioengineering

Sanjeev G. Shroff, Ph.D., Professor, Department of Bioengineering

William R. Wagner, Ph.D., Professor, Departments of Surgery and Bioengineering

Yadong Wang, Ph.D., Professor, Department of Bioengineering

Justin S. Weinbaum, Ph.D., Research Assistant Professor, Department of Bioengineering

Dissertation Director: David A. Vorp, Ph.D., Professor, Departments of Bioengineering, Cardiothoracic Surgery, and Surgery

FUNCTIONAL STEM-CELL BASED TISSUE ENGINEERED VASCULAR GRAFTS FOR HIGH-RISK DONOR POPULATION

Jeffrey T. Krawiec, PhD

University of Pittsburgh, 2015

Despite the significant progress made in the field of tissue engineered vascular grafts (TEVG), there still exist a number of barriers that inhibit the clinical translation of many TEVG designs. This is illustrated by the high number of pre-clinical evaluations, but limited number of clinically tested grafts. The goal of this dissertation was to identify the most paramount of these barriers and address them in the adipose-derived mesenchymal stem cell (AD-MSC)-based TEVG previously developed within the laboratory of Dr. David Vorp. First, as many pre-clinical investigations that fail to assess cells derived from clinical populations who would routinely require a TEVG therapy, AD-MSCs from two prominent clinical populations – diabetics and elderly were evaluated. Utilizing both in vitro and in vivo approaches to identify altered functions with regards to TEVG maturation and patency, it was shown that diabetic patients in particular produce TEVGs that readily occlude via thrombosis. Additionally, decreased fibrinolytic activity was shown to be one altered pathway contributing to the pro-thrombotic phenotype. Second, as many approaches are practically limited by extensive fabrication times, a freshly-derived adipose-derived cell population – the stromal vascular fraction (SVF) – was utilized to fabricate TEVGs. This was compared to donor-matched culture expanded AD-MSCs to demonstrate the use of a new cell source free from the necessity of culture expansion. The results of this study showed similar in vitro and in vivo functionality of both cell populations in the context of TEVG applications. Finally, a cell-free alternative TEVG design was proposed

with a proof of concept study that is alleviated from either barrier. A novel technology – termed as “artificial stem cells” – was developed that combines the stem cell secreted products with a microsphere-based delivery system to replace the in vivo cellular activity of AD-MSCs. Together, the work of this dissertation advanced the field of stem cell-based TEVGs by investigating the use of cells clinically realistic populations and proposing novel cell sources (SVF and artificial) to practical barriers to propel TEVGs towards clinical translation.

TABLE OF CONTENTS

LIST OF TABLES

LIST OF FIGURES

1.0 INTRODUCTION

The goal of this dissertation is to develop functional tissue engineered vascular grafts (TEVGs) that overcome key clinical and practical barriers essential for enabling the translation of this technology. To do so, tissue engineering utilizes the combination of cells, materials, and/or bioactive factors to repair or replace tissues of interest – in this case the blood vessels. In order to develop an effective TEVG that addresses current barriers, one must first have an understanding of the vascular anatomy the TEVG is trying to recreate, comprehend the limitations of current approaches, and what define what barriers remain to be conquered in the field of TEVGs that hinder their translation. This introductory chapter will review the current state of the scientific field within these areas providing an overview of scientific knowledge contributing to this body of work. In this way, the reader is presented with a clear perspective in understanding the limitations of the previous scientific endeavors leading this work and the significant impact and novelty that it achieves.

The TEVG being investigated within this study is an autologous mesenchymal stem cell-based design that is intended to be used for small diameter revascularization procedures. In this way cells are isolated from a patient, fabricated into a cell-scaffold construct, and implanted within that same patient for small diameter applications such as the coronary artery, peripheral arteries, or for use as an arteriovenous fistula during hemodialysis. While in a broad sense this TEVG could utilized in larger settings (e.g. in the case of pediatric vein reconstruction

procedures), the current scope of this work is to apply this those patients who possess cardiovascular disease and are thus prone to small diameter vascular complications. The work of this dissertation is specifically meant to guide the TEVG being developed within the laboratory of Dr. David Vorp towards clinical translation by defining and addressing current rate-limiting barriers.

The introductory chapter of this dissertation will first provide a broad overview of the arterial anatomy to define the main constitutive components of a TEVG (Section 1.1). Next, an overview of cardiovascular disease, its prominent patient populations, and the etiology of those populations will be described to identify the intended target for our TEVG (Section 1.2). Following this, an overview of various TEVG design components of a will be given (Section 1.3). Then, as the scope of this dissertation is to begin directing our TEVG towards clinical translation, an in depth discussion and criticism of TEVG approaches that have successfully engaged in clinical trials will be provided (Section 1.4). Finally, the current clinical barriers will be distilled and discussed (Section 1.5) to guide the specific aims of this dissertation.

1.1 ARTERIAL ANATOMY: WHAT ARE THE MAIN CONSTITUENTS OF A TEVG?

1.1.1 The Cardiovascular System and General Arterial Anatomy

The cardiovascular system is responsible for the circulation of fluids, cells, nutrients, bio-active factors, and heat throughout the body [1]. It consists of two main circulatory loops –pulmonary and systemic – which are driven by the pumping effects of the heart [1]. The pulmonary loop directs blood to the lungs where it receives oxygenation prior to being returned to the heart where it will enter the arteriovenous loop to be delivered to the rest of the body [1]. While the pulmonary loop has similar features to the arteriovenous system, the latter is ultimately more complex [1]. The arteriovenous system begins as a major artery (the aorta) which undergoes multiple branchings (largest to smallest: aorta, artery, arterioles) where it decreases in both diameter (aorta: 30 mm aorta, arteriole: 10 μm) and thickness, but increases in number and total system cross sectional area (aorta: 7 cm^2, arteriole: 150 cm^2) [1]. The smallest of arteries then connect to a network of capillaries (the smallest vessels) which are thin walled and responsible for exchange between the blood and body, such as delivery of oxygen [1]. These vessels then converge into the venous tree (smallest to largest: venuoles, veins, vena cava) where they group to one single vessel to return blood to the heart where it can be oxygenated [1].

Besides the classification of vessels based on their anatomical location and size, they can also be characterized based on their function and composition. For example, the aorta is a conducting vessel where its main function is to deliver blood received from the heart [1]. To overcome the volatile and high pressure environment experienced during ejection of blood from the heart, the aorta possesses a structure with a high number of fibers allowing it to recoil the

deformations it undergoes in comparison to other vessels [1]. This ability to recoil – otherwise known as elasticity – is imparted to the vessel by elastin (i.e. elastic fibers) which will be discusses in Section 1.1.5 (“Elastin”). Smaller arteries – mainly arterioles – can be classified into another vessel type called resistance vessels [1]. These are mainly responsible for contracting and relaxing to regulate blood pressure within the circulation and as such are highly muscular [1]. The smallest vessels – capillaries – are classified as exchange vessels which, create a system of transport between the blood and tissues [1]. Finally the vessels within the vein system are classified as capacitance vessels and are highly compliant and thin walled [2] so they can receive the high volume of blood from the capillaries which is transported it back to the heart [1].

Despite the variety of the different vessel types within the circulatory system, their wall anatomy consists of a three layered structure (with the exception of capillaries) consisting of the intima, media, and adventitia with each layer having its own unique composition [1, 3]. The intima – the innermost layer – is composed mainly of endothelial cells and the vascular basement membrane while the media – the middle layer – consists of smooth muscle cells, elastic fibers, and collagen. Finally the adventitia – the outermost layer – consists of fibroblasts and connective tissue [1]. This however, this is a simplification as there additionally exist a variety of other minor vascular structures, cell types, and proteins associated with the cellular and micro-architectural environment of the vessel wall. These include the glycocaylx coating on the luminal surface of endothelial cells [4], matricellular proteins [3], vascular progenitor cells [5, 6], nerves present within the adventitia [1], and depending on the size of the vessel a self-sustaining capillary network known as the vaso vasorum [1]. However due to their contribution as the main functional components of the vessel wall – and thus a TEVG – only the primary components – EC, SMC, collagen and elastin – will be discussed below. Information on vascular extracellular

components such as fibulins, fibronectin, basement membrane associated proteins, proteoglycans, and matricellular proteins can be found reviewed by Kelleher et al. [3] Additionally, information on the cell subpopulations within the vascular wall such as progenitor cells can be found reviewed by Pacilli et al. [5] and Torsney et al. [6] and with their debated contribution to vascular pathology found discussed in work by Song Li [7-10].

1.1.2 Endothelial Cells

Endothelial cells are one of two primary cell types within the vessel wall and are located as a monolayer lining along the lumen of the vessel. These cells arise during embryonic development from mesodermal lineage-derived angioblast cells [11, 12] and are of critical importance for the regulation of many aspects of physiology. This importance is illustrated by the considerably large quantity of endothelial cells present in the adult body with their surface area covering approximately 1000 m^2 [13]. Broadly, endothelial cells regulate 5 main functions: transport (e.g. nutrients to tissues), vascular tone (vasoconstriction and dilation), host defense (leukocyte rolling and extravasation; inflammation), hemostasis (coagulation and fibrinolysis), and angiogenesis [14-16]. In each of these cases, endothelial cells possess a high number of inducible genes allowing a duality to either promote or decrease each of these functions [15]. As an example endothelial cells can regulate vessel size through constriction via production of endothelin-1 or dilation via NO [11]. As another example, ECs can express a variety of anti-coagulant (NO, surface heparin sulfate) and fibrinolytic (uPA, tPA) factors but also express pro-coagulant (TF, ET-1) and anti-fibrinolytic (uPAR, PAI-1) factors depending on their activation state [11].

Endothelial cells display a high degree of structural, functional, and molecular heterogeneity based on their location in the vascular bed or organ [12, 15]. Structurally for

instance, artery endothelial cells are long and aligned with blood flow in straight vessel segments whereas in branch segments and veins they are not [2, 15, 17]. Structural heterogeneity also occurs with regards to the intended organ function where endothelial cells are located, such as the fenestrated pattern which occurs in filtration based organs (e.g. kidney, liver) allowing for increased transport instead of the continuous configuration seen in high blood flow situations [12, 15]. In addition, capillary endothelial cells – where the majority of transport occurs – are more permeable than that seen in greater vessels [15, 17]. Functionally, different areas of the vascular beds can have a different balance of anti- and pro-coagulant factors [17], venules mediate the majority of inflammatory responses [2, 17], and arterioles mediate the majority of vascular tone regulation [2, 17]. Finally, endothelial cells can have unique location-dependent molecular markers such as ephrinB2 which is expressed in arteries as opposed to EphB4 in veins [2, 18]. However, endothelial cells also display a high degree of plasticity when subjected to different environmental stimuli allowing them to alter their phenotype [2, 15]. Two examples are the increased expression of eNOS adopted by vein endothelial cells when placed under arterial flow conditions in the case of a coronary bypass graft [2], and the high degree of heterogeneity seen in tumors [15].

While endothelial cells offer a variety of functions, for the purposes of TEVGs the most important characteristic is their anti-thrombogenic effect. From a design standpoint, anti-thrombotic effects preserve the main purpose of a vascular graft: to act as a patent conduit to allow for blood flow. The other characteristics of endothelial cells such as vessel tone regulation to alter blood pressure, trafficking of immune cells, angiogenic sprouting, and nutrient transport while important in their own merits, are secondary to the main performance of a vascular graft. Acquiring autologous endothelial cells for use in TEVGs have their drawbacks as these must be

acquired through sacrifice of a vessel segment which could likely be utilized clinically as a vascular graft itself. In more recent years acquisition of endothelial cells has shifted towards differentiation of stem cells such as adipose-derived mesenchymal stem cells [19-28] as these can be isolated more desirably through liposuction.

1.1.3 Smooth Muscle Cells

Smooth muscle cells are the primary cell type located in the medial layer of the vascular wall [1]. Under normal physiologic conditions (particularly in resistance vessels) these cells are responsible for contractile functions which alter vessel diameter to regulate blood pressure or maintain rigidity of the wall via isometric contractions [1, 29, 30]. In these situations SMCs remain quiescent and proliferate at a slow rate [29]. However unlike other muscle cells (cardiac, skeletal), smooth muscle cells also have a strong degree of plasticity to them and change their phenotype to proliferate, migrate, and synthesize extracellular components in response to injury [1, 29]. The phenotypic sensitivity seen with these cells provides a usefulness to injury repair but can be a detriment as they are also affected by pathologic signals [29, 30]. Indeed, SMC plasticity has been implicated in multiple vascular diseases such as intimal hyperplasia [8, 10, 31], aortic aneurysm [32-35], calcification [36-38], hypertension [29], and atherosclerosis [1, 31, 39, 40].

The plasticity of smooth muscle cells can be characterized based on the presence of contractile proteins and the morphological features of the cell [41, 42]. As a SMC becomes more differentiated to a contractile phenotype it adopts markers such as smooth muscle alpha actin (early), calponin (intermediate), and myosin heavy chain (late) while displaying a spindle-like morphology [31, 41, 42]. As it transitions to become a synthetic SMC, these markers will be lost

for proliferative, migratory, and protein synthesis markers such as PDGF, MMPs, and collagens [41]. A variety of signals exist which can promote SMCs to assume a contractile or synthetic phenotype such as biochemical factors [30, 41, 42] (TGF-beta, AngII: contractile, PDGF, bFGF: synthetic), extracellular matrix [41, 42] (fibrillar collagen I: contractile, monomeric collagen I: synthetic), mechanical stress [41, 42] (environmental dependent), substrate stiffness [43] (stiffer: synthetic), endothelial cell signals [30, 31, 42, 44, 45] (environmental dependent), and inflammation [42] (increased inflammation: synthetic). However, many contractile proteins which are utilized to label SMCs and identify their phenotype are non-unique and expressed in other cell types present in the vascular wall such as fibroblasts [29] and progenitor cells [7]. This has ultimately made the study of SMCs difficult, especially with regards to lineage tracing [8, 9, 29].

As with endothelial cells, acquiring SMCs for autologous vascular tissue engineering requires sacrifice of a vascular segment which can be non-ideal as this could likely have been utilized as a suitable graft itself and requires the patient to undergo an extra-surgery to isolate. Additionally, obtaining a suitable quantity of SMCs requires in vitro expansion but SMCs possess a limited proliferation capacity [46]. This, coupled with their propensity for phenotypic switch makes it difficult to acquire native-like quiescent, contractile SMCs. However, having a TEVG populated with SMCs is critical to the success of a vascular graft. In particular SMC content indicates a higher degree of vascular maturity [47] and mechanical properties such as tensile strength and stiffness are correlated with SMC content [48, 49]. Without these properties, TEVGs can be prone to failure by intimal hyperplasia or aneurysmal rupture [50]. As with endothelial cells AD-MSCs have also been utilized in recent times to generate them [19, 27, 51-57].

1.1.4 Collagen

Collagen is an abundant and ubiquitously expressed class of proteins within the body and is one of two primary extracellular components of the vascular wall [3]. Primarily collagen functions to provide mechanical tensile strength to the wall [3, 58] however this must be within an appropriate range. If too little collagen is present the wall will have insufficient strength to overcome hemodynamic forces at which point the wall can rupture or dilated. If the wall has too much collagen it will stiffen causing adverse cellular effects such as encouraging a pro-fibrotic phenotype [59], increasing systemic resistance, and increasing the risk of cardiovascular disease [60]. The arrangement in collagen is layer-dependent with medial collagen being aligned circumferentially to resist hemodynamic pressure and adventitial collagen being aligned longitudinally to resist changes in length [1]. While being mainly a structural component, collagen can also provide cell signaling events via adhesion of cellular integrins (e.g. $\alpha 1\beta 1$) and is thought to contribute to SMC quiescence under normal physiologic conditions [3, 46].

Despite the abundance of collagen in the body, it can exist in many different forms and is encoded by large array of genes with 17 types of collagen having been identified (each denoted by a roman numeral suffix, e.g. collagen IV) [3]. Each of these collagen types form the basic collagen fiber structure consisting of a woven triple helix but can be altered in assembly and prevalence [3]. The most important collagen types for the vasculature are collagens I, III, and IV [3]. Within the arterial wall, types I and III are the most abundant residing in the medial and adventitial layers [1, 3] consisting of an elongated fiber-like structure with type III assisting the regulation of the diameter of type I collagen [3]. Collagen type IV is present in the basement membrane adjacent to endothelial cells and consists of a network-like structure rather than an elongated fiber like the other types [1, 3].

Unlike the other vascular components (EC, SMC, and elastin) collagen can be easily acquired for use in vascular tissue engineering as it can be both produced in vitro by cells [61, 62] and produced in vivo [63-66].

1.1.5 Elastin

The other main extracellular structural protein within the vascular wall is elastin which mainly occurs in the form of elastic fibers/lamellae. While elastin can provide cellular signals such as maintaining SMC cell senescence [67], its primary role is to impart the biomechanical property of elasticity to the vascular wall [3, 58, 68]. This provides a direct contrast to collagen as its tensile strength is insignificant comparatively but its elasticity is essential for arteries to recoil and recover the deformation they experience under the cyclic loading throughout the cardiac cycle [58, 68, 69]. Additionally, the amount of elastic fibers present in a vessel are linearly proportional to the pressure they experience [3].

Structurally elastic fibers consist predominantly of an elastin core which is surrounded by relatively small proteins known as micro-fibrils [68]. Unlike collagen which is coded by many genes, elastin is only coded by one [3] but is associated with a plethora of different molecular components with regards to elastic fiber composition and assembly [68, 70]. In particular, the main players in the process of elastic fiber formation are elastin binding protein, fibrillins (particularly 1, 3 and 5), MAGPs (1 and 2; 2 is more specialized), fibulins (1,2, and 5), and lysyl oxidase [67, 68, 70, 71]. Formation of elastin first occurs through translation, splicing, and shuttling of the soluble precursor to elastin – tropoelastin – to the cell surface for secretion via elastin binding protein [67, 68, 70, 71]. The secreted tropoelastin then self-aggregates via coacervation where it is chaperoned via fibulin to be deposited onto a microfibril scaffolding.

This scaffolding consisting mainly of fibrillins with MAGPs acting to assist in both the binding of tropoelastin to fibrillin and maintaining structural integrity of the microfibrils [3, 67, 68, 70-72]. The combination of coacervated elastin deposited on a micro-fibril scaffold leads to a "beads on a string" architecture [68]. As a final step, lysl oxidase links the tropoelastin globules via crosslinking lysine residues [67, 70, 71] generating elastin. An interesting side effect of the cross-linking process is the generation of fluorophore structures which impart elastin with auto-fluorescent properties [73].

Loss or fragmentation of elastic fibers and genetic abnormalities in elastin-associated genes have been shown to result in debilitating diseases (reviewed [3, 67, 68, 71]) and adverse cellular effects. Two examples are aneurysmal dilation (i.e. progressive dilation of the artery) [69] and Marfan syndrome [67, 68, 71]. Additionally, during the process of elastin fragmentation soluble elastin products can result and act as cell signaling molecules inducing negative effects such as SMC hyper-proliferation [67], inflammation [74], and calcification [36]. However, unlike collagen which can easy be replaced by de novo synthesis throughout adulthood, elastin production can be exceedingly difficult. This is for two reasons: 1) the genes coding for elastin and elastin-related proteins are downregulated post-natally [3, 75], and 2) the highly orchestrated process of elastic fiber formation is difficult to recreate in vitro [76]. The down regulation of elastin-related genes is a conserved process occurring across a variety of species [3, 75].

This difficultly in adulthood elastin formation has posed a great challenge for vascular tissue engineers in the development of elastic fiber-rich TEVGs. This has led to several studies investigating the fabrication of elastin-based scaffolds (reviewed [67, 77]). However, processing elastin is a difficult process due to its insolubility, limiting these constructs in terms of size, shape, and supply [67]. Elastin can be hydrolyzed to enhance its solubility but comes at an

expense of mechanical properties and propensity to induce inflammation [67]. However, the use of synthetic peptides and fabrication techniques such as electrospinning is helping to advance this work [67]. The generation of elastin through cellular mechanisms has also been investigated as a way to generate functional elastic fibers. This includes alterations to gene expression [78] and regulation [79-81] of elastin-related proteins, stimulation of cells through TGF-beta [82-84], and administration of tropoelastin to vascular SMCs [76]. Another route to recreate the biomechanical effects of elastin has been to use synthetic elastomeric materials (see Section: "1.3.2 Scaffold Considerations"). However, as these are intended to break down eventually in vivo, development of elastin will ultimately be necessary to compensate.

1.2 TYPES OF CARDIOVASCULAR DISEASE: WHERE IS A TEVG APPLIED?

Cardiovascular disease can take many forms but often necessitates the need for a vascular replacement or bypass due to the occlusive nature of these diseases. While an in depth discussion of all forms of cardiovascular disease is beyond the scope of this dissertation, a brief overview of the main forms and their associations will be presented below. Further discussions relevant to this body of work such as their occurrence with advanced age and diabetes will be discussed in the following sections (see Sections: "1.2.2 Elderly Etiology and Vascular Related Effects", "1.2.3 Diabetes Etiology and Vascular Related Effects"). It is important to note that while a brief summary is provided below, it is not a definitive explanation of their pathology as many factors can play a role on a cellular (e.g. SMC phenotype switch – see Section: "1.1.3 Smooth Muscle Cells"), mechanical [85], genetic [86, 87], or inflammatory level [88, 89]. The most prominent

vascular diseases will be introduced including intimal hyperplasia, atherosclerosis, aneurysms, hypertension, calcification, and thrombosis.

Intimal hyperplasia is characterized by a narrowing of the lumen of a vessel caused by thickening of the intimal layer and is induced by the inward migration, proliferation, and matrix synthesis of SMCs [90]. The main mechanism by which this occurs is due to the phenotypic switch in SMCs [8, 10, 31] seen during cases of vessel injury (e.g. during surgical intervention), inflammation, or increases in wall shear stress (e.g. vein graft) [90].

Atherosclerosis results in the development of a fatty plaque within the arterial wall causing its narrowing and is a result of endothelial cell dysfunction, SMC phenotypic switch, inflammation, and penetration of lipids into the vascular wall [13, 39, 40]. This disease is heavily associated with diabetes (see Section: “1.2.3 Diabetes Etiology and Vascular Related Effects”) and is often associated with other co-morbidities such as calcification [37, 40]. Atherosclerosis occurs more frequently in certain areas of the vascular bed such as branch points and vessels with tortuous geometries [2]. Plaques may also rupture – triggering thrombosis – and a higher vulnerability is seen in ones that have high inflammation and a larger lipid core size [13].

Aneurysms are characterized by progressive dilation of the arterial wall and triggered by an initial insult to elastin [69, 91]. Subsequent changes will occur due to this dilation such as synthetic SMC phenotype switch [32-35], stiffening of the wall [91], and loss of strength [69, 91-93]. Aneurysm can be different in shape such as the saccular aneurysms occurring in the cerebral arteries [69] or the fusiform aneurysms occurring in the abdominal aorta [91]. Additionally, in the case of abdominal aortic aneurysms they can be accompanied by an intraluminal thrombus which induces hypoxia, reduces strength, and causes loss of SMC [92, 93]. Aneurysms are

commonly associated with age (elderly), gender (male), and smoking [91, 94] and occur more frequently in the abdominal aorta, thoracic, and cerebral arteries.

Hypertension is persistent elevation of blood pressure in the arteries and is associated with progressive stiffening of the blood vessel wall. This is commonly seen in aged patient populations with related associations (see Section: “1.2.2 Elderly Etiology and Vascular Related Effects”) including loss in EC function, synthetic phenotype SMC, and loss in vessel elasticity [95].

Calcification is the presence of calcified mineral deposits within the arterial wall and predominantly occurs in the medial layer. This is associated with a variety of dietary (e.g. high glucose), inflammatory, and metabolic conditions ultimately resulting in expression of osteogenic signals that cause phenotypic modulation of SMCs into osteoblast-like cells [36-38].

Thrombosis is the end result of an insult to the fluid dynamics within blood flow [96] or perturbations to the biochemical factors within the coagulation cascade [97, 98] and/or fibrinolysis [99] cascade causing development of an blood clot (thrombus). Many factors can influence thrombosis but two examples relevant to this dissertation are the increase in fibrinolytic inhibitors in diabetes (see Section: “3.4 Discussion”) or improper methods of achieving cellular coverage of TEVG materials (e.g. cell seeding, see Section: “1.3.4 Cell Seeding Techniques”) which both increase the propensity for thrombosis.

The following section will detail two patient cohorts which are at a high risk for these cardiovascular diseases [100], outlining their etiology and adverse effects to the native vasculature.

1.2.1 Cardiovascular Risk Patient Cohorts

In the development of an ideal TEVG, it is imperative that the appropriate patient populations are considered as these will be the most likely recipients of this technology. While there are many demographics that have been shown to act as predictors to cardiovascular disease such as gender, BMI, smoking, and family history, the two most prominent factors are the presence of diabetes and advanced age [101-103]. This is a major concern in the United States as both of these cohorts have reached exceedingly high numbers within recent years. Diabetes occurs in approximately 10% of population (~30 million people) [104] and the currently sizable elderly population within the U.S. (35 million) is expected to double by 2030 [105]. Diabetes is particularly troubling as cardiovascular related mortality rates have been reported in upwards of 70% in diabetics [28]. It is also important to note that while aging and diabetes have their own independent mechanisms, the occurrence and subsequent pathological effects of both can happen concurrently [106].

1.2.2 Elderly Etiology and Vascular Related Effects

The pathologic consequences of aging are not completely understood but are believed to be due to shortening of telomeres during cellular replication (i.e. mitosis) leading to cellular senescence [106-108]. During the DNA replication stage of mitosis two new strands of DNA are formed by DNA polymerase. However, due to the unidirectional activity of DNA polymerase, each strand has to be synthesized by different mechanisms. To synthesize the strand that is opposite to the direction of DNA polymerase, RNA primers must be laid down. However, as these are later removed rather than overwritten, each replication will result in the end of being shortened in in

the repetitious sequence-rich end regions known as telomeres [106, 107]. In these regions enzymes known as telomerases exist which repair the missing ends, but in most cell types these are inactive [106]. Over the multitude of replications a cell will undergo within a lifetime, shortening will happen to a critical point and pathologic effects will occur such as chromosomal end-to-end fusions, replicative senescence, and apoptosis [106, 107].

Aging related changes in the vascular extracellular matrix typically manifest as an arterial stiffening contributing to the pathology of hypertension [105, 109]. The end result is an increase in both collagen and elastin cross linking [105, 109] leading to a stiffened vascular wall. Additional changes to the extracellular components include increased collagen content and elastin fragmentation [105, 109]. While it is unclear the exact mechanism that causes these changes, associations have been made with age related decreases in endothelial NO production, synthetic phenotype SMC switch resulting in hypertrophy and collagen production, age related loss in elasticity, genetics, and a high salt diet [95]. Additionally, senescent SMCs are present in hypertensive patients and secrete factors which result in hypertrophy of non-senescent SMCs [110]. This hypertensive stiffening results in increases in blood pressure [111] and subsequent cardiac afterload [95, 109, 112] which can be predictive of cardiovascular mortality [109, 111].

Aging can also create dysfunctional effects in both the endothelial cells and SMCs within the vascular wall contributing to vascular pathologies. For endothelial cells, aging results in endothelial dysfunction via reduced eNOS and presence of increased ROS [106, 107, 113], both of which are associated with telomere loss [106]. eNOS function is one of the most important for endothelial cells and helps resist a variety of pathologic effects due to its vasodilative (protects hypertension) and anti-platelet properties (prevents platelet aggregation and thus thrombosis), as well as its ability to reduce SMC proliferation (implicated in multiple vascular pathologies) and

reduces reactive oxygen species [113]. Endothelial cell proliferation is also stunted [106] with increasing age and a higher degree of permeability is seen [114]. For SMCs, telomere shortening is associated with loss of proliferative ability [106] converting the cell to a senescent phenotype but these cells also release secreted factors which promote hypertrophy of surrounding SMCs [110] contributing to the pathology of hypertension [95]. Aged SMCs and increased oxidative stress can also present with increased alpha-SMA (potentially leading to higher tension), increased collagen and MMP expression, as well as an apoptotic phenotype [115]. Finally, senescent EC and SMC with shortened telomeres are typically located at the sites vascular disease such as atherosclerotic lesions [106].

1.2.3 Diabetes Etiology and Vascular Related Effects

Diabetes has a ubiquitous pathologic effect on the vascular system which can present as complications such as retinopathy, stroke, peripheral artery disease, and coronary artery disease [116]. Diabetes most commonly occurs in the type II form where it is characterized by an increased blood glucose concentration coupled with insulin resistance [116, 117]. Unlike type I which is triggered by an auto-immune response, type II can ultimately be preventable with tight glycemic control [118]. The induced insulin resistance present within diabetes reduces the effectiveness of insulin to trigger glucose uptake from the blood into the liver, muscle, or fat where it can be stored as glycogen. This results in the hallmark of diabetes: hyperglycemia, which develops pathological consequences due to the inability of endothelial cells to regulate glucose uptake thus rapidly importing it [119]. This is due to the endothelial cell expression of Glut1 (as opposed to Glut4 in other tissues which can be regulated) transporters which are not signaled by or change their regulation based on insulin concentrations [120-122]. Under normal

conditions where glucose would be utilized for either storage (conversion to glycogen), energy (glycolysis), or building of amino acids (pentose phosphate pathway), the now overabundance of glucose is shunted to the polyol pathway [119, 123] which leads to the development of ROS and AGE. Respectively, ROS leads to an increase in oxidation within the wall promoting an inflammatory environment and AGEs result due to glycation reactions which alter the functions of reacted proteins. For example, AGEs can lead to faster stiffening of the arterial wall [30]. In addition to these changes, the endothelium becomes more permeable [123].

Following the changes induced by hyperglycemia, dyslipidemia (elevated plasma triglycerides and cholesterol) which occurs in 97% of diabetic patients [116], leads to an abundance of LDL that penetrate the vascular wall leading to atherosclerosis initiation [13]. This LDL can also undergo glycation which further prolongs its half-life leading to more prolonged effects [116]. Furthermore, the abundance of ROS within the vessel wall causes oxidation of LDL particles which recruit blood leukocytes, instigating an inflammatory response [13, 116, 124]. Ultimately these events work in tandem to develop the fatty streak and SMC proliferation seen in atherosclerotic plaques [13].

While this illustrates a few primary mechanisms by which diabetes exerts its pathologic effects, several other mechanisms such as altered cell signaling of PKC, generation of other AGE products, and other metabolic changes (glucose conversion in hexosamine) can also occur [119, 123, 125, 126]. However, it is apparent that glucose-induced ROS is central to these mechanisms [123] which is in part due to an increase in incomplete glycolysis – resulting in mitochondrial electron transport chain intermediate products – due to the overabundance of intracellular glucose [123].

Besides the aforementioned changes in the diabetic vasculature as a whole, diabetes also induces phenotypic changes to the cells within the vessel wall. It causes the endothelial cells to become more permeable and decreases endothelial produced NO [118, 123]. Without NO, SMCs lose their quiescence where they proliferate causing vascular complications [123, 126] (see Section: "1.2 Types of Cardiovascular Disease") and the endothelium-dependent vaso-dilative properties of the wall are lost [118]. Additionally, the increased blood insulin concentration that occurs during diabetic insulin resistance increases endothelial adhesion molecules which exacerbate the recruitment of inflammatory cells ultimately accelerating atherosclerotic progression [118]. Other changes include decreased thrombo-resistance [122] and calcific changes to SMCs [36].

1.2.4 Current Clinical Treatment Options

Cardiovascular disease is the leading cause of death and results in over 600,000 [127] revascularization procedures being performed annually in the United States. This, coupled with 7.3 million deaths due to coronary heart disease [128, 129] and 17% of the national expenditures being attributed to cardiovascular diseases [130] highlights the critical need for functional vascular replacements. Additionally, hemodialysis which utilizes vascular grafts for access occurs in 340,000 patients each year in the U.S. [131]. However, the gold standard vascular replacements used in the clinic such as non-degradable synthetic material grafts or autografts (i.e. a vessel from a patient utilized on themself) have drawbacks making them non-ideal treatment options.

Non-degradable synthetic grafts such as ePTFE (expanded Polytetrafluoroethylene) or Dacron® (Polyethylene terephthalate) are the most common non-native materials used for

vascular conduits and see wide success in large diameter applications despite their aberrant lack of endothelium [129, 132]. However, as the diameter of these grafts decrease to less than 6 mm (defined as a “small diameter” application), the lack of endothelium results in thrombotic failure (39% patency for lower limb bypasses) [129, 132, 133]. Mechanistically this occurs by the deposition of blood proteins such as fibrin onto the hydrophobic graft surface initiating thrombosis [132]. Additionally, platelet activation – which amplifies thrombosis – also occurs more readily on hydrophobic surfaces [132]. In large diameter grafts this concern effect is minimized due to the high flow rates which achieve removal of these proteins. However, in smaller sized grafts have an increased as the surface-to-flow ratio, thrombotic complications are critical. Additionally, blood becomes more coagulant under low-flow conditions [96] or if flow is perturbed leading to a pro-thrombogenic phenotype of endothelial cells [134]. This commonly occurs in the case of a compliant-mismatched vein graft wherein a ballooning effect happens resulting in improper flow [135]. Thrombotic failure of grafts typically occurs at acute time points (< 30 days) [129].

Autografts – such as the saphenous vein, internal mammary artery, and radial artery [129, 136] – are preferred vascular replacements due to their similarity to native vessels. However, these grafts are accompanied by their own set of drawbacks. The IMA is the current gold standard, particularly in the case of coronary artery bypass grafting wherein it achieves a 5-year patency of about 90% [136-138]. The IMA also is less prone to atherosclerosis than the saphenous vein as it has higher NO production, less fenestrated endothelium, higher tPA activity, more heparin sulfate, and similar mechanical properties to native arteries [139]. However, this vessel is limited in availability to only two vessel segments [137] which may exclude its use during additional operations or in the case if it was previously used. Additionally harvesting of

this vessel requires strong surgical proficiency, results in increased surgical time, and possess risks of sternal infection [136, 137]. Patency rates of artery grafts can also decline with age [140] however in the cases of coronary procedures, artery autografts are preferred to vein grafts as they show an improved performance [138].

The greater saphenous vein is another gold standard vascular conduit but healthy vein segments for this are quite limited with only 45% of patients having suitable vein grafts [28, 141]. However, while the saphenous vein is preferred to other vein segments [141], its patency is remarkably low as shown by a 60% patency rate over 5 years when used for lower extremity bypass grafting [141] and 45% when used for coronary procedures [138, 142]. Selection choice of an appropriate vein segment is also a concern. A vein segment utilized for a coronary grafts requires a segment of approximately 10 cm [143] and a larger diameter is preferred due to the correlation between loss in patency and decreased diameter [141]. The primary cause of patency reduction is due to their high compliance compared to arteries they replace [50, 62]. This mismatched compliance will induce a significant dilation in the vein triggering the vein SMCs to adopt a proliferative and migratory state inducing intimal hyperplasia (or stenosis) resulting in a narrowing of the graft and eventual occlusion of the graft [143]. Intimal hyperplasia could also be induced by harvest-related endothelial trauma [144]. However, failures resulting from this develop at an extended time course [129] take upwards of 12 years [145].

Both these clinical vascular conduits have highlighted two main mechanisms by which vascular grafts fail: thrombosis due to lack of endothelium or thrombo-resistant mechanisms (as seen in synthetic grafts) and intimal hyperplasia due to improper mechanical properties (as seen in autografts). Methods such as endothelialization have been developed to enhance the patency of ePTFE grafts but this still only achieves patency indistinguishable to vein grafts and their

patency is reduced as size decreases (71% for 7mm vs 55% for 6 mm at 10 years) [146]. Additionally, many factors in the coagulation system have been targeted to reduce the coagulation of synthetic graft materials [132]. While these show an improved efficacy, human data and long term performance still remain to be seen. Notably, in the case of anti-platelet therapy in the context of vascular access for dialysis, no effect on improving patency is observed [147]. Additionally, use of drug therapeutics could lead to bleeding complications or systemic effects [132].

In the case of vein grafts, methods have been developed to enhance their mechanical properties by coating them with an electrospun sheath [148]. The development of this technology has shown promising results and is currently underway by Neograft Inc. [149]

Despite the attempts to resolve the failure mechanisms seen in these two clinical conduits, there are still irreparable characteristics that make them non-ideal. In the case of synthetic grafts, these cannot grow in patients preventing their use in pediatric applications and are prone to calcification [150]. Additionally, graft infection is infrequent (up to 5%) [151] but is admittedly higher than seen in autografts [132] and presents with devastating mortality rates (75%) or limb amputations (70%) [151]. In the case of autografts, the availability of appropriate vessel segments is limited compared to the need.

1.3 TISSUE ENGINEERING APPROACHES

In the near three decades since the pioneering work of Weinberg and Bell in 1986 [152] in the development of a living vessel composed of a collagen tube seeded with vascular cells, vascular tissue engineering has expanded to include a plethora of different methodologies. At its core,

tissue engineering utilizes the combination of cells within a scaffolding material intended to functionally replicate the tissue type being studied. More recently, the field of tissue engineering has expanded to the use of a variety of materials, cells, biologic factors, and culture methods. While the review of all the contributing individual studies to this body of work is beyond the scope of this dissertation, the following section will summarize the broad categories of approaches. Additionally, as this dissertation is specifically focused on considerations related to clinical translation of the TEVG within the Vascular Bioengineering Laboratory, an in depth discussion of the TEVGs which have underwent clinical trials will be discussed separately (see Section: “1.4 Current Clinical TEVG Approaches).

1.3.1 General Considerations

As stated above, a TEVG consists of the combination of cells, scaffolding materials, biologic factors, and culture methods. However, these components must be combined in such a way that present a feasible design in terms of both functionality and practicality. Ideally, a TEVG will possess attractive characteristics in the following three broad criteria: biocompatibility, mechanical properties, and manufacture [129].

Biocompatibility when broadly defined is the ability of a material to elicit an appropriate application-specific response when applied to a biological system. For the field of vascular engineering this consists of the following characteristics: non-toxic (including scaffold and scaffold breakdown products), has no susceptibility to infection, is non-immunogenic, and is anti-thrombogenic [129]. While the criteria of non-toxicity and susceptibility to infection are self-evident, the latter two require more explanation. Non-immunogenicity refers to the ability of the graft to not elicit an immune/inflammatory response that can cause rejection of the graft (i.e.

in the same manner that can occur during organ transplantation). This is typically an antigen mediated phenomenon by T and B cells and does not imply that inflammation should be entirely absent in vivo. On the contrary, mild inflammation has been shown to be a key component in TEVG success (see Section: “1.5.3 In Vivo TEVG Mechanisms”). Anti-thrombogenicity refers to the ability of the TEVG to resist formation of a luminal blood clot (i.e. thrombus) leading to graft occlusion. This can be done in a variety of methods from tailored materials [153], bioactive factor incorporation [154-156], use of heparin [156], and most commonly endothelialization [19, 157].

A TEVG must also have suitable mechanical properties including elasticity, burst pressure, and compliance similar to that of native vessels. Elasticity allows the vessel to recoil to recover its deformation following loading with pulsatile blood pressure. Under normal physiology this is accomplished via the extracellular matrix component elastin (see Section: “1.1.5 Elastin”) but for tissue engineering this can also be achieved through use of elastomeric materials. Without proper elasticity vessels can become prone to progressive dilation as seen with aneurysm pathology (see Section: “1.2 Types of Cardiovascular Disease”). A TEVG must also have enough strength to withstand the loading induced by blood pressure or else it will be at risk for rupture. Most commonly, strength is reported as measure of vessel burst pressure with that of the saphenous vein (~1680 mmHg) [158, 159] being the gold standard. Finally, the TEVG must have a similar compliance to the tissue it is replacing. As discussed in the case of a vein graft used as an arterial bypass (see Section: “1.2.4 Current Clinical Treatment Options”), too much compliance can induce intimal hyperplasia but as in the case of a calcified graft, too little can cause adverse cellular effects such as a pro-fibrotic phenotype (see Section: “1.1.4 Collagen”) . Adding to the difficulty of matching the mechanical properties of a native vessel is

that these conditions must be preserved throughout the time course in vivo when substantial remodeling and architectural changes are occurring (see Section: “1.5.3 In Vivo TEVG Mechanisms”). Indeed, mechanical properties have been shown to change throughout the duration of an implanted TEVG [49, 63, 64, 160].

Two more essential properties of a TEVG are the ability to resist tearing of the anastomotic sutures and kinking. The ability to resist the tearing of sutures is measured by the suture retention force and should be adequate enough such that the graft can be easily secured by a surgeon and not tear after placement. The necessity for kink resistant grafts is application specific – such as the case of a coronary artery bypass which presents a non-linear geometry – but a critical aspect as a kink will result in immediate impediment of blood flow through the graft. Despite this, susceptibility to kinking is not a reported parameter in TEVG literature and can often be missed as initial animal studies utilize linear interposition grafts such as at the abdominal aorta or carotid artery locations [47, 66, 161-163].

Finally, the practicality in regards to manufacture of the TEVG must be considered. In particular, a fabrication process that is both rapid and at low cost is ideal as there are many barriers to translation with regards to extended or costly fabrication methods (see Section: “1.5.2 Fabrication Time”). Additionally, a graft should be capable of being made to a variety of sizes, able to be sterilized, and easily stored.

1.3.2 Scaffold Considerations

Choosing an appropriate scaffolding material to utilize for a TEVG is a critical consideration as it both establishes the 3D architectural support for the cells and the initial mechanical properties of the TEVG. Throughout the development of TEVGs many different scaffolding materials have

been utilized – each with their own advantages – including non-degradable synthetic materials, degradable synthetic materials, natural polymers, decellularized vessels, and fully biological materials.

Some the earliest TEVG studies (prior to 1996) utilized synthetic materials that were non-degradable [158] such as Dacron. However, the inability to degrade carries a variety of negative aspects. First, tissue ingrowth into a non-degradable graft will ultimately only be able to stiffen the graft potentially resulting in a loss in compliance [158]. Additionally, the use of non-degradable materials has shown to induce calcification [150] in newly formed tissue around the synthetic graft exacerbating this issue. Finally, non-degradable materials do not offer the same remodeling potential as degradable or purely biological tissue and as such cannot change their size in vivo preventing their potential use for pediatric applications. As such, most of the focus of TEVG development has subsequently shifted to use of biodegradable synthetic or biological materials.

Biodegradable synthetic materials offer several advantages for the development of TEVGs as they can be cheaply fabricated, have tunable properties, can be elastomeric, and offer the ability to resorb to allow for newly formed native-like tissue to develop (i.e. neotissue) throughout the TEVG. Tuning this latter aspect is particularly important as a graft which degrades too quickly – such as that seen with PGA – will result in loss of mechanical properties which have not yet been adequately established by the neotissue [158]. The most common material to be utilized are polyesters due to their ability to break down via hydrolysis and their common use in the clinic with the most popular being PGA, PLA, PCL and their various co-polymers [158, 164]. Various properties of these materials can be found discussed by Tara et al [164]. Other example materials include degradable polyurethanes [161] and PGS [162]. One

attractive aspect of biodegradable synthetic materials is that they can be fabricated in multiple ways generating porous or fibrous structures [162, 165, 166]. However, most of these materials often require seeding with vascular or stem cells as a means to prevent thrombosis (see Section: "1.5.3 In Vivo TEVG Mechanisms"). Criticisms have been made against synthetic grafts due to their biological inertness [158], and the lack of cellular signals which natural materials possess [158], and low amount of functional groups to bind axillary molecules such as growth factors [167].

Natural materials and polymers can also be utilized together to create scaffolds [168]. While collagen can be easily isolated [159], the isolation of elastin is difficult due to its insolubility and typically results in a loss of mechanical properties (see Section: "1.1.5 Elastin"). Other natural materials have been utilized such as silk [167], hyaluronan [169], and fibrin [159]. In particular, fibrin presents an attractive alternative as its components (fibrinogen, thrombin) can be easily isolated from a patient's own blood and its properties can be heavily customized [170]. However, in order to have enough strength it must undergo a lengthy culture with cells in a bioreactor [171]. The drawbacks of natural materials are plentiful as they commonly lack adequate strength [159], have high cost, and possess a high degree of variability [158]. Due to these deficits, obtaining biologically-derived materials is more commonly done through decellularization of vascular tissue.

Decellularization is the process of removing cellular material from tissue through the use of detergents and enzymes leaving only the extracellular matrix components [164, 172]. Commonly, this is accomplished with detergents such as SDS (ionic) or triton-X (non-ionic) and enzymes such as nucleases, dispases, and trypsin [159]. Physical forces such as freeze drying can be used in addition [159]. While this ultimately results in a scaffold with a similar matrix

composition to that of a native vessel, there are several challenges to this approach. Specifically, scaffolds can be prone to shrinkage due to loss of proteoglycans in the decellularization process [173], have reduced mechanical properties [173], and can exhibit degeneration of the scaffolding material in vivo [174]. Additionally, if this scaffold is obtained from a human, the sacrifice of a potentially suitable vessel already prepared for clinical use is required. Conversely, if the vessel segment is obtained from animal tissue there are worries of disease transmission (example: HIV in non-human primates [175]). Ultimately this limits the size, shape, and supply of obtained these types of scaffolds. Additionally, decellularized scaffolds possess exposed collagen – which possesses a high degree of thrombogenicity [158, 176] – and therefore cell seeding must be utilized to resist thrombosis. However, cell seeding of these scaffolds is be challenging due to their low porosity and presence of elastic lamellae in within the vascular matrix [177]. Recent studies have been investigating other methods to produce scaffolds similar to a decellularized scaffold by stimulating the production of vascular ECM with SMCs cultured in a bioreactor [61, 62] circumventing the need for isolation from a patient.

The final method to produce a TEVG scaffold is through the use of completely biologically generated materials. Multiple methods have been utilized to develop these materials with two main examples being growing cells to obtain a cell sheet which is subsequently rolled to obtain a tubular construct or utilizing the foreign body response to generate a fibrous tissue around a subcutaneously implanted material. Cell sheet engineering was pioneered by by L'Heureux in 1998 [178] and has progressed to the point of clinical trials (see Section: "1.4.2 Approach 2 – Cell Sheet Technology"). Many other groups have adopted this technology making improvements to the mechanical properties, sheet adhesiveness [179, 180], switching to an more proliferative cell type such as MSCs instead of the traditionally used SMCs or fibroblasts [181],

and growing cells on thermo-sensitive polymers to allow for lifting of cell sheets without mechanical tearing [159]. However, despite these advances there are two main drawbacks of this approach: the enormous amount of fabrication time and the difficultly switching synthetic cells back to a contractile phenotype (see Section: “1.1.3 Smooth Muscle Cells”). The second example which utilizes subcutaneously implanted tubular materials that are subsequently encapsulated with fibrous tissue due to the foreign body response [182] generate tissue that is both autologous and has substantial strength. However, the resulting graft still requires performing an additional surgery on the patient to obtain and requires an extended fabrication time.

1.3.3 Cellular Considerations

As a means to provide functionalization to scaffolding materials to overcome hurdles such as anti-thrombogenicity and poor remodeling, cells are often utilized. At minimum, cells must be viable, non-immunogenic, and able to perform specialized functions [159]. However, from a practical and translation standpoint it is ideal for cells to also be highly proliferative and easily harvested [159]. Additionally, autologous cells are preferred due to the risks of disease transfer and immune-rejection associated with xenogenic or allogenic cells, respectively [159].

Vascular cells such as SMCs and ECs are common cell choices for vascular engineering as these intrinsically possess specialized functions available within the vasculature. However, isolation of autologous cells requires sacrifice of a vascular segement which must be isolated from the patient via surgery and often times are acquired at low quantities [159]. In addition, vascular cells have a limited proliferation capacity and can often undergo phenotypic changes in culture [158]. Genetic alterations to these cells such as induction of telomerase have been utilized but genetic manipulation raises risks and regulatory barriers [159]. Due to this, MSCs

have been proposed as one mechanism to acquire vascular cell phenotypes (see Sections: “1.1.2 Endothelial Cells”, “1.1.3 Smooth Muscle Cells”).

Much of the focus of vascular engineering has shifted to the use of adult stem cells which can be isolated autologously from a patient, present more attractive isolation sites, and have an high proliferation potential. Mesenchymal stem cells are one adult stem cell type which can be isolated from bone marrow, muscle, and adipose tissue [19]. These cells are multipotent and secrete a variety of angiogenic, mitotic, and anti-thrombogenic factors [183-189] making them ideal for tissue engineering. Their use has followed two main functions where they have either been coaxed to differentiate into vascular cell phenotypes prior to implantation, or utilized directly in their undifferentiated state as a source of potent bioactive factors to enable in situ development of vascular cells [19, 190] (see Section: “1.5.3 In Vivo TEVG Mechanisms”). This latter approach is preferred as it substantially reduces the time to implantation. The other adult stem cell type frequently utilized is the hematopoietic-derived endothelial precursor cell (EPC) [19]. This cell type can be isolated from the peripheral blood [19], adipose tissue [191], or bone marrow [19] of a patient and displays similar properties to endothelial cells but with an increased proliferation rate [19]. Most commonly these cells are seeded to provide thrombotic resistance in the same manner as endothelial cells. A more in depth review of these cell types can be seen in a separate publication (Krawiec and Vorp [19]).

Other cell types which have the potential to be utilized in vascular engineering are embryonic stem cells and the related iPS cells [192] (somatic cells coaxed via viral vectors back to a pluripotent state). Due to ethical concerns, embryonic cells are not routinely utilized but both cell types present substantial challenges due to lengthy and difficult differentiation protocols which limit their translatability.

1.3.4 Cell Seeding Techniques

Cell seeding is the process by which cells are incorporated within a tissue engineering scaffold. An ideal cell seeding process can incorporate cells in an efficient, rapid, reproducible, and controllable way while minimizing their injury. Additionally, cell seeding methods can be utilized to achieve either a surface or bulk (i.e. through thickness) seeding with this distinction often being a function of scaffold geometry [193]. For example, if a scaffold is intended to be seeded with a lumenal endothelial cell lining a low porosity scaffold is best suited [194], while if a scaffold is intended to have cells present throughout the thickness a highly porous [195] scaffold is preferred. Achieving proper bulk seeding with a uniform distribution of cells is challenging, but a uniform distribution is required to provide cellular activity and anti-thrombotic effects throughout the entirety of the scaffold wall. As porous scaffolds are routinely utilized in tissue engineering, utilizing bulk seeding methodologies is preferred.

However, despite the advantages which cell seeding techniques can offer, they are often an underutilized aspect of TEVG fabrication. In particular, the most commonly used approach is to simply pipette a cell solution onto a scaffold surface [193, 196]. Not only does this passive method result in poor efficiency (10-25%) and cellular penetration, but it can require additional weeks of fabrication time to allow the cells to migrate within scaffold pores [193, 196]. Due to these drawbacks several alternative seeding methodologies have been proposed utilizing active transmural forces to increase both cell seeding efficiency and penetration [193, 196]. Examples of these include the use of rotation, magnetic forces, acoustic waves, vacuum, and flow [193, 196]. However, while these may be useful in the case of seeding a flat sheet, the more complicated tubular geometry utilized in vascular engineering presents additional challenges. For example, the use of a single transmural force (e.g. vacuum) will result in an uneven

circumferential distribution due to gravitational effects [193]. To address this, our lab has investigated the combined effect of both vacuum and rotation utilizing a controllable device [197, 198]. In this way, cells are infused lumenally throughout the scaffold at which point they are subjected to rotation and vacuum. This process achieves a higher efficiency (>90%) than most other reported techniques [196] and requires no user manipulation making it ideal for translation. Additionally, we have collaborated with another group to develop a controllable vacuum-based seeding system [199] which has since had additional design features such enabling a completely closed fabrication process [200, 201]. It is important to note however that when utilizing vacuum based seeding methods, pressures must be controlled as values over 250 mmHg will have negative effects on cell viability [199].

Other techniques such as integration during scaffold fabrication have been investigated, but this can be difficult and highly dependent on fabrication or polymerization conditions. In most cases, cell survival in these processes are negatively affected [193].

1.3.5 Bioreactors and Culture Post-Seeding

Bioreactors enable post-seeding culture and maturation of three dimensional cell seeded TEVG constructs and overcome the limited nutrient diffusion in typical flask-based culture with the potential addition of mechanical stimulation [159, 202]. Bioreactors can vary in their degree of complexity from a simple spinner flask that provides convective transfer of nutrients, to the more complicated flow loop-based bioreactors where mechanical stimuli can additionally be applied (more examples have been reviewed by Blose and Krawiec et al. in Chapter 13 [202]). In vascular tissue engineering dynamic culture is utilized as a means to allow for cellular adhesion and spreading along scaffolds [197], while flow loop bioreactors place the construct in line with

pulsatile flow allowing for the application of shear and stretch to the construct [61, 62, 159, 171]. This is most often utilized as an in vitro means to encourage the development of natural proteins such as collagen [61, 62, 159, 171] or coax the differentiation of mesenchymal stem cells [203, 204] (see Sections: “1.1.2 Endothelial Cells”, “1.1.3 Smooth Muscle Cells”). However, these approaches are often accompanied with the drawback of a lengthy and costly in vitro culture time which will likely not be clinically applicable for emergency situations. Due to this loss in translatability, many approaches have shifted to utilize in vivo maturation phases instead where the body acts a pseudo-bioreactor [19, 190] enabling maturation (see Section: “1.5.3 In Vivo TEVG Mechanisms”).

1.3.6 Acellular TEVGs

While cellular incorporation within tissue engineered scaffolds has been routinely utilized as a method to reduce thrombogenicity and enhance graft remodeling (see Section: “1.5.3 In Vivo TEVG Mechanisms”), the inherent variability and fabrication concerns (see Sections: “1.5.1 Improper Cell Sourcing”, “1.5.2 Fabrication Time”) associated with these approaches has led to the development of several accellular TEVGs [65, 153-156, 162, 169, 205-223]. This is often done by functionalizing biodegradable materials with surface coatings, bioactive factor immobilization, or drug delivery vehicles, all of which have shown promising results in the development of patent and remodeled TEVGs. However, these functionalized biodegradable materials often utilize a single or limited number of factors (e.g. heparin [156, 210, 212]; hirudin [222]; phospholipids [153, 205]; antibodies [212]; growth factors such as VEGF [212, 213], bFGF [211], BDNF [155], MCP-1 [216], NGF [154], SDF-1a [156, 209, 215], and G-CSF [206-208]; TGF-beta inhibitors [221]; and adhesive proteins such as fibronectin [211, 215]), and this

approach is constrained in that a limited number of factors cannot replicate the complex, multi-factorial coordination involved in biological systems. Further, utilizing a high concentration of a single factor – which many such approaches resort to – can lead to deleterious systemic side effects [224, 225].

In some cases materials alone can be sufficient to generate patent and remodeled TEVGs. These include grafts composed of natural materials such as hylaronan [169], silk [217], SIS [218], or synthetic materials designed to be rapidly degrading [162, 226], or fabricated into woven [219, 220], nanofibrous [65], or electrospun [223] structures. However, despite the obvious advantages of being able to be utilized "off-the-shelf" which minimizes fabrication time, their degradation times or potential incorporation with bioactive factors should be carefully considered as a scaffold with a length that supersedes the migratory capacity of the remodeling process can fail [227].

1.4 CURRENT CLINICAL TEVG APPROACHES

The following section will detail the four TEVGs that have entered clinical trials. Interesting, each of these approaches utilizes entirely different methodologies. The advantages and disadvantages of each will be discussed.

1.4.1 Approach 1 – Bone Marrow Cells with Synthetic Scaffold

The first TEVG to successfully reach clinical trials [228-230] used of bone marrow cells to construct a TEVG [48]. In this method bone marrow mononuclear cells were obtained from

patient specific bone marrow aspirates to obtain 200 million cells which were seeded onto PGA/CL/LA scaffolds by manual pipetting. Following incubation in autologous blood plasma for 2 hours, the constructs were implanted. All surgeries (Fontan procedure; vena cava to pulmonary connection) performed were elective procedures and occurred between September 2001 and December 2004 in Tokyo, Japan in 25 children (average age: 5.5 years). The patients were followed on average of 6 years where all grafts showed no signs of aneurysm formation, graft failure, graft infection, or calcification. However, one graft showed partial thrombosis and 4 others showed stenosis; these complications were all treated successfully through additional interventions. This clinical study has been discussed and reviewed heavily [228, 231-234].

This study was successful for multiple reasons. First, the TEVG in this study was constructed with bone marrow cells, was cultured in autologous plasma, and post-seeding was implanted within 2 hours. This rapid and xeno-material free approach is extremely attractive in terms of clinical translation as financial burdens and culture-related risks are minimized. Additionally, this graft utilized biodegradable synthetic materials which allowed for graft remodeling and lengthening that is necessary in a growing pediatric patient. However, the major drawback of this graft was that it was tested in a low pressure environment and likely doesn't have the strength to withstand arterial conditions in its current form [66]. Additionally, while this graft showed great promise in children, considering its use in diseased populations is unclear.

Since the clinical trials of this TEVG, this group (Shinoka and Breuer) has been extremely productive. To better understand one of the main complications they experienced within their clinical trials – stenosis – they have underwent a series of studies investigating this process within their graft [221, 235, 236] which appears to be mediated by high levels of TGF-beta [221], platelets [236], and NK cells [236] and can be mitigated by cell seeding [235]. They

have also shifted to the development of a new arterial graft which presents a more challenging test bed due to the high pressure environment [65, 66, 160, 237, 238]. Despite initial studies which showed aneurysmal dilation [66], they have ultimately been successful in this endeavor. They have also performed investigatory studies into the remodeling process of TEVGs [63-66, 160, 192, 216, 221, 235, 236, 239-242] which can be coupled with long term implantations [64, 66, 160, 238, 242] and studies of explanted graft biomechanics [49, 63, 64, 160] to better understand how a TEVG mechanistically develops. These will be discussed in Section "1.5.3 In Vivo TEVG Mechanisms". Additionally, to improve upon the translatability of their TEVG they have begun development of an acellular graft [63-66, 236, 242] and developed a closed-loop seeding method to reliably incorporate cells within their scaffolds under sterile conditions [199-201, 243] without culture [243, 244]. Finally, they have performed axillary studies looking at the usage of iPS cells [192] for TEVG fabrication, guiding the development of TEVGs using computational models [64, 245], and are utilizing non-invasive in vivo imaging modalities to assess TEVG development [242, 246]. Excitingly this group is currently pursing studies which include the first clinical trial within the US to implant a TEVG in children [247].

1.4.2 Approach 2 – Cell Sheet Technology

A TEVG constructed with the cell sheet technology (see Section: "1.3.2 Scaffold Considerations") first developed by L'Heureux [178] underwent clinical testing [248-250] in Argentina and Poland between 2004 and 2007 where TEVGs were utilized as an arterial-venous fistula for hemodialysis. A total of 10 patients (ages: 29-89) were documented in this study all whom were suffering from end stage renal disease and had previously failed at least one attempt at hemodialysis. It is important to note that this model is particularly challenging for TEVGs as it

utilizes patients who already possess significant health problems and the repeated puncturing utilized during hemodialysis can result in disruption of hemostasis and graft remodeling. However, it also has several advantages in that it allows for easy monitoring of the TEVG and failures are tolerated well since they are not life or limb threatening.

TEVGs were fabricated by culturing fibroblasts taken from patient skin biopsies supplemented with ascorbate until cell sheets were formed at which point they were wrapped around a mandrel and allowed to mature until the sheets fused together. Following maturation, the inner layers of the graft were devitalized via air drying and seeded with patient endothelial cells isolated from saphenous veins. The average time of fabrication was 7.5 months. Upon implantation no antiplatelet therapies were used unless the patient already had a catheter in place.

Throughout this study, one patient withdrew and 5 adverse events occurred among the 9 other patients. These included 2 cases of aneurysm, 1 dilation, 1 thrombosis, and 1 death unrelated to the TEVG. No infections were present. The TEVGs displayed a 78% (7 out of 9) primary patency – meaning no interventions were used to restore patency – at 1 month and a 60% (5 out of 8) primary patency at 6 months. The authors commented that the dilation-based complications the TEVGs experienced were not due to the strength of the vessels since their burst pressures were sufficiently high, but most likely due to delamination between the layers of the TEBV or weakening due to repeated puncturing. Despite these complications, this study shows great efficacy for this TEVG due to the extraordinary patient cohort and challenging model that was used. Additionally, unlike the graft designed by Shinoka (see Section: “1.4.1 Approach 1 – Bone Marrow Cells with Synthetic Scaffold”), this was the first clinical TEVG to have enough strength to be placed in the high pressure arterial environment.

While this TEVG offers many advantages having underwent such a challenging clinical study in terms of both the test bed and being part of a multi-center study, it has a large downfall of taking many months to manufacture. This is a very large concern for translation since the longer the time it takes to grow the less likely it could be used in emergency situations and possesses high costs. In particular, it is still economically challenging to produce a TEVG in this manner due to the high production cost and low patient reimbursement potential [250, 251]. Another criticism is that multiple interventions to the patient (skin biopsy, saphenous vein isolation) had to be performed in order to obtain cells.

The creators of this graft (now called Lifeline^{TM}) are now established as a company – Cytograft – and have begun another clinical trial for lower limb bypasses. However, their documented progress in scientific literature has been limited since the first clinical trial [252, 253]. Published studies have shown their investigations into the mechanical properties of their TEVG showing that it had similar strength and suture retention force as the IMA but less compliance [252]. However, at 6 months post-implantation compliance levels had increased [252]. Additionally, three allogenic-derived TEVGs were implanted within patients that were constructed in the same manner as above but completely devitalized and not seeded with endothelial cells prior to implantation [253]. Grafts were not afflicted with immune reactions and withstood up to an 11 month time course implantation without degradation but continually reduced flow and encountered cases of thrombosis due to the lack of endothelium [253].

1.4.3 Approach 3 – Decellularized Vein

Another type of TEVG that has reached clinical trials took place in Gothenburg, Sweden (published 2012) which was utilized to alleviate portal vein obstruction (thrombosis) in a 10 year

old girl [254]. The graft was fabricated from a decellularized 9cm segment of a deceased allogenic donors iliac vein (age 30) and then populated with SMCs and ECs generated from the patient's own bone marrow cells. The total fabrication time took a total of 12 days. However, unlike other dual seeding approaches [47, 163, 206, 255-258] which incorporate SMCs prior to ECs to achieve medial and intimal presence of the two cell types, respectively, this study did the opposite. The complete TEVG was utilized as a bypass between the superior mesenteric vein and the intrahepatic left portal vein and was chosen as a therapy due to the patient's lack of suitable vein segments and to avoid life-long immuno-suppression in the case of a liver transplant.

Upon implantation the TEVG immediately provided functional blood flow and was stable to 9 months but decreased its flow at one year due to narrowing and mechanical obstruction. At this point the clinicians intervened to remove the section of the graft which was narrowed and proceeded to attach a segment of newly fabricated, identical TEVG to compensate for the length loss which resolved the obstruction. The patient was not maintained on immuno-suppressive drugs but was maintained on anticoagulants (aspirin) for 6 months.

This TEVG, like the prior (see Section: "1.4.2 Approach 2 – Cell Sheet Technology"), shows that materials (but not cells) derived from allogenic sources can indeed be utilized. Through the use of a decellularized vessel they were able to more rapidly generate a suitable vascular matrix as opposed to having to utilize extensive culture methods. Additionally, utilizing natural materials which can be remodeled in vivo will allow for the implanted vessel to grow with the adolescent patient. Despite these advantages there are still a few drawbacks. First, using a multiple step culture method still possesses a risk of contamination for the TEVG and as SMCs were generated from bone marrow cells which required cellular differentiation, potential adverse transformations could occur. Also, the authors noted that the vascular matrix was dissimilar to

native vessels following the decellularization procedure and postulated that it may not be suitable for the more mechanical robust arterial environment.

1.4.4 Approach 4 – Bioreactor Produced TEVG

The final and most recent (2014) TEVG clinical study has not yet published scientific literature and evidence of their progress is only limited one brief conference abstract [259]. This graft originates from Niklason [61, 62] – and the subsequently established Humacyte company – which utilize SMCs grown in a degradable PGA scaffold within a pulsatile bioreactor to generate a vascular matrix with no residual scaffolding material. This matrix is then decellularized and re-cellularized with endothelial cells prior to implantation. The advantage of this approach is that once the matrix is fabricated and subsequently decellularized, it can be stored until ready for use with a patient. Additionally due to the lack of immunogenicity seen with allogenic matrix materials in other clinical studies (see Sections: “1.4.2 Approach 2 – Cell Sheet Technology”, “1.4.3 Approach 3 – Decellularized Vein”), these matrices can be fabricated ahead of time through non-patient specific (i.e. allogenic) cells. Indeed, this group has created grafts of both animal and human cadaver cells [61, 62]. Grafts fabricated in this manner have shown strength, compliance, and suture retention forces similar to that of native vessels [62].

The clinical study, which is currently underway [259], utilizes this TEVG for hemodialysis vascular access in patients with end-stage renal disease and is the first to test this application within the United States. Pre-clinical studies for this graft in large animal and nonhuman primate models have been documented with results showing suitable mechanical properties for arterial conditions, promising remodeling to a vascular-like tissue, and no adverse events [62, 259]. However the early term clinical results have not yet been published.

While this approach has several advantages particularly in terms of developing TEVGs scaffolds from non-patient specific (i.e. non-autolgous) approaches and that they maintain their mechanical properties even after 12 months of storage [62], there are some concerns due to practicality. The fabrication of this TEVG utilizes both a pulsatile bioreactor and long term culture (10 weeks) which induce significant cost. As cells for developing this primarily collagen-based scaffold utilize cells isolated from cadavers [62], a more practical and less costly method is to utilize a decellularized cadaver vessel. This will also provide the added benefit of containing more prominent elastin.

1.5 CURRENT BARRIERS TO CLINICAL TRANSLATION

Despite the extensive amount of pre-clinical testing seen in the field of cell-based TEVGs with both small [63-66, 160, 161, 181, 192, 216, 221, 235-241, 243, 255, 260-266] and large [47-49, 61, 62, 163, 178, 206, 242, 244, 256-258, 263, 267-279] animal models, few TEVG approaches have progressed to clinical trials (see Section: “1.4 Current Clinical TEVGs”). Indeed, there are a number of inhibitory barriers encountered during the clinical translation of TEVGs with regards to usage of cells, establishing feasible and consistent modes of manufacture, difficult regulatory pathways, and financial concerns. While many studies have begun to address these barriers through the in vivo use of human cells [62, 178, 216, 237, 240, 255, 260-264, 266], and/or the development of large animal sized scaffolds [47-49, 61, 62, 163, 178, 206, 244, 256-258, 263, 267-279], many barriers still remain unaddressed. This is abundantly clear when criticizing the drawbacks of the four TEVG approaches which have reached clinical trials. In particular, Approach 1 and Approach 3 tested their grafts in children who are physiologically healthy and

displays minimal relevance to the adverse conditions see in cardiovascular disease patients. Additionally, many of the studies have concerns related to fabrication such as cost (Approach 2, Approach 4), time (Approach 2), potential for cellular transformation (Approach 3), and practicality (Approach 4). The final concern comes from both a regulatory and development stand point in understanding the mechanisms and processes by which a TEVG remodels in vivo. The following section will detail these three prominent barriers still currently present in the field of TEVGs.

1.5.1 Improper Cell Sourcing

When developing a cell-based therapy it is critically important to evaluate the functionality of the intended patient's cells as this will directly impact the efficacy of the treatment. However, despite the many advances in the field of TEVGs, studies have yet to assess TEVG functionality when comprised of cells from realistic clinical populations. Instead, many preclinical evaluations of cell based TEVGs utilize cells from healthy humans or animals [47-49, 61, 62, 161, 163, 178, 181, 206, 216, 235, 237, 239, 240, 244, 255-258, 260-264, 267-277, 280]. While these studies have shown that incorporating cells within scaffolds promotes patency and regenerative effects, these are not directly representative of patients at high risk for cardiovascular disease. Diabetic and elderly individuals are two such demographics (see Section: "1.2.1 Cardiovascular Risk Patient Cohorts") and cells isolated from these cohorts have specific deficits which brings into question their therapeutic utility. As cells are fundamental to the success of many TEVG approaches, evaluating the suitability of each cell source is an essential step towards clinical translation.

1.5.2 Fabrication Time

Another major hurdle in the development of TEVGs – and one that is seen in tissue engineering as a whole – is fabrication time. While fabrication of the TEVG components such as a scaffold can take an extended period of time, many of these can be produced in large quantity and stored minimizing the actual burden of this process. Cells on the other hand are living and must be maintained with careful observation; depending on the cell type, these can grow at a prohibitively slow pace. Ultimately, the cells (and the combined cell-scaffold construct) are the most common rate limiting step in TEVG fabrication.

Having a TEVG approach that utilizes an extended culture period can encounter many detriments with regards to clinical application. Creating excess waiting time for the patient may make the TEVG inapplicable for acute situations. In particular, the risk of mortality while waiting for coronary artery bypass graft procedures increases by 11% each month [281] and most patients (>70% [282]) are operated on in less than 6 months. Additionally, extended fabrication can incur significant costs [250] and raises concerns about potential cellular transformation. These, coupled with the number of hurdles already present for cell-based tissue engineered products [283] such as the need for extensive pre-clinical testing, funding shortages, complicated regulatory pathways, and poor commercial reimbursement [250] only amplify the difficulty in translating a TEVG. However, having a method to rapidly fabricate a TEVG at a low cost would make a large step towards alleviating many of these concerns. To illustrate this, one of the few TEVGs that has made it to clinical trials – that of Shinoka and Breuer (see Section: “1.4.1 Approach 1 – Bone Marrow Cells with Synthetic Scaffold”) – utilizes a non-cultured bone marrow derived source and uses methods to quickly fabricate their graft. Despite this, it is still a common occurrence for cell-based TEVGs approaches to utilize extensive in vitro culture

periods – with many on the order of a week or longer – after primary cells have been successfully expanded [47, 163, 178, 179, 181, 206, 237, 256-258, 262, 268, 270, 272-278, 280]. Therefore, in order to successfully translate TEVGs to the clinic, it is important to utilize an available and easily obtainable cell source.

1.5.3 In Vivo TEVG Mechanisms

Stem cell-based TEVG approaches allow for two maturation mechanisms by which they can develop into native-like vascular replacements [19, 51, 129, 190]. In one case the stem cells are utilized as a source for vascular cells – such as SMCs [19, 27, 51-55] and EC [19-28] – which are then used in combination with scaffolding materials and often times bioreactors [202] (see Section: “1.3.5 Bioreactors and Cultures Post-Seeding”) to generate a vascular-like construct. This is mainly induced by stimulation with growth factors known to induce specific routes of differentiation and/or by physiologically relevant mechanical stimulation. In this case the stem cells can spend weeks to months under in vitro culture before a construct is available for use. From a practical standpoint this extended culture can act as a barrier to clinical translation due to the high costs [250], potential risks for cellular transformation, and waiting time for a patient (see Section: “1.5.2 Fabrication Time”).

The second maturation mechanism [19, 51, 129] is where stem cells are implanted directly after incorporation into TEVG scaffolds and the body is utilized as a “bioreactor” for maturation. This process allows for quicker generation of useable TEVG constructs but the exact mechanisms behind this process are still being determined. While it was originally proposed that these cells differentiate in vivo [48], recent studies have disproved this hypothesis by showing that stem cell retention within TEVGs only lasts on the order of 1 week [192, 216, 239, 246, 261,

262]. This instead designates them as initial mediators of the TEVG remodeling process. Adding to this, studies have shown that remodeling happens through adjacent migration of vascular cells [239] and that stem cells both secrete factors that induce SMC migration [51] and provide initial anti-thrombogenicity [261, 284](see Aim 1-2). This is further corroborated by studies showing acellular TEVGs (see Section: “1.3.6 Acellular TEVGs”) are also repopulated with SMCs and ECs [153-156, 162, 169, 212, 217-221] including scaffolds with low porosity [153, 169, 217, 220] or scaffolds with bound growth factors specifically designed to recruit host cells [154-156, 216]. Additionally, TEVGs that have undergone this first type of maturation step (i.e. already developed vascular layer) experience host-based remodeling as implanted TEVGs with already intact SMC layers [276] or EC only [47, 62] are shown to be populated with host SMCs. Similar dynamic remodeling processes occur whether the implanted graft is fully synthetic [153, 162, 205, 219, 220] fully biological [62, 169, 217, 218] or a hybrid of the two [156, 216, 235, 239, 261, 262, 276].

Cell seeded scaffolds have also been suggested to be superior to non-seeded counterparts. In particular, the usage of cells [47, 161, 216, 260] or their bioactive products [154-156, 216] are able to generate grafts with a higher degree of cell density [47, 154, 155, 161, 216, 260] and EC/SMC maturity [47, 156, 161, 260] than non-seeded ones. Additionally these grafts are more resistant to failure mechanisms such as thrombosis [161, 260, 261] and stenosis (aka intimal hyperplasia) [235, 242, 261]. Cell seeding also produced TEVGs with significant longitudinal growth in a growing animal model [242], display better controlled MMP activity [242] and inflammation [216, 235], and contain higher GAG content indicating a more mature graft [242] compared to their unseeded counterparts. It has also been reported that TEVGs seeded with MSCs were able to generate more elastin in vivo compared to those without seeded cells [261].

Finally, as humans achieve much slower transanastomotic migration than animals due to their inability to adequately heal their vessels or spontaneously endothelialize [285-287], cell seeding may be a potential avenue to encourage this process thus achieving a functional TEVG. Additionally, utilization of a highly porous scaffold may also aid higher porosities have been shown to lead to a higher degree of cell ingrowth [288].

The mechanisms that ultimately lead to a functional TEVG (i.e. one that is fully populated with vascular cells and matrix) is just beginning to be understood with inflammation being considered as one of the key components [65, 66, 216, 235, 236, 239, 246, 262]. In particular, studies have shown that monocyte/macrophage infiltration is one of the first events and occurs on the order of 3 days [216, 235, 239, 262] immediately following an initial deposition of fibrin and platelets [235], but preceding any vascular tissue development. Adding to this, grafts composed purely of monocytes [240] or an inflammatory cytokine (MCP-1) [216] can produce remodeled TEVGs. However, the amount of inflammation a TEVG experiences is critical to its success. Too much inflammation in the form of macrophage infiltration has been shown to induce stenosis within TEVGs while none at all completely negates the remodeling process [235]. This study [235] also revealed that acellular grafts are more prone to a high degree of inflammation which can be attenuated by cell seeding [235]. Additionally, utilizing an animal with a functional immune system is essential to assess TEVG remodeling. In particular, it was shown that when an acellular scaffold is implanted into a mouse with dysfunctional NK cells and platelets (*bg* mutation) the TEVG will achieve an appropriate level of inflammation and remodel successfully, but in a mouse with wild type immunity will fail due to high levels of inflammation [236].

The time course of events at which vascular tissue develops within a TEVG is also beginning to be understood. Multiple studies have noted that initial population with endothelial cells begins on the order of 2-4 weeks and further matures in a time dependent manner [62, 156, 216, 235, 239, 261, 262]. SMC development also occurs with the same timing [62, 156, 162, 216, 235, 239, 261, 262]. Extracellular matrix development begins with an initial burst of collagen types I and III over the first 4 weeks achieving a quantity much higher than that or native arteries, but tapers over time to achieve native levels [63-66]. This activity is mirrored by the presence of MMPs within TEVGs [63, 66, 241]. Ultimately this newly formed tissue coupled with the presence of an intact scaffold that has yet to achieve significant breakdown at early time points, leads to an initially stiffer than native TEVG [49, 63, 64]. Collagen type IV, which is present in the basement membrane behind the endothelium, develops at a later time point than the other collagen types [241]. Finally, there is an initial burst of fibrillin at 1 week [63, 241] which abruptly drops off laying the initial scaffolding structure for elastic fiber assembly (see Section: “1.1.5 Elastin”) which will then occur and continue to increase over time [63, 65, 160, 241].

Despite the advances in understanding the TEVG remodeling process, these studies only lay the initial ground work and further investigation is required. The remodeling process can be dependent on features of the TEVG such as porosity [288] and length [62], but also change within different animal models [62]. Additionally, long-term studies should eventually be carried out at a time point where the implanted scaffolding material has been completely degraded and the remodeling has been stabilized. However, one study has shown the remodeling process of TEVGs to conclude by 24 weeks and remain stable for up to 2 years [64] but admittedly, this is parameter will be unique to each TEVG.

1.6 TEVG STUDIES IN THE VORP LAB

The TEVG developed in the Vascular Bioengineering Laboratory – which is the subject of this dissertation – was initiated during the PhD work of Lorenzo Soletti, who established the methodology and began initial preclinical testing [193]. This body of this work can viewed in depth in the following thesis and journal publications [153, 161, 165, 193, 195, 198, 205, 260, 265]. The original concept for the graft was created by combining a cellular source – rat muscle derived stem cells [197] – with a porous scaffolding material created from thermally induced phase separation of a biodegradable polyurethane based material – poly(ester urethane)urea (PEUU) [165]. This scaffolding material offered pores which were large enough for cellular incorporation (50 μm [260] vs ~20 μm for a trypsinized cell (see Section: "5.1.1 Seeding of Artificial MSCs – Determining Appropriate Diameter) and these cells were successfully incorporated via a rapid (< 5 min), efficient (> 90%), and repeatable rotational vacuum-based bulk seeding process [195, 198]. Post-seeding the construct is incubated for 2 days in a spinner flask to allow for cellular adhesion and spreading where no changes to cell phenotype or viability were seen [193, 197]. Initial testing with this TEVG showed aneurysmal dilation [161] at which point an external electrospun sheath was applied and resulted in mechanical properties similar to that of native vessels [165] and circumvented the dilations initially seen [161]. This TEVG was shown to result in good patency within a rat model and exhibited remodeling that generated the presence of vascular-like components [161]. Other studies have involved the use of different cell types such as human pericytes [260], human AD-MSCs (unpublished), or rat SMCs [265]; the

development of an acellular vessel [153, 205]; methods to scale fabrication from small to large animal models [193]; and a year-long implantation (unpublished).

This approach possess several advantages such as the minimal time between fabrication and implantation, the controllable seeding process, ability to remodel in vivo due to the biodegradation properties of the scaffold, and appropriate mechanical properties to be utilized in arterial conditions. However, there are still many areas to improve this TEVG, particularly with regards to the barriers to clinical translation outlined in Section "1.5 Current Barriers to Clinical Translation". This includes use of a clinically relevant cell source, fabrication time and the need for cell culture, and understanding the mechanism. These concerns inspired the aims to this proposal detailed below.

1.7 HYPOTHESES AND SPECIFIC AIMS

The work of this dissertation will utilize the autologous AD-MSC-based TEVG previously developed by the Vascular Bioengineering Lab and – based on the critical analysis of literature – will direct it toward clinical translation by addressing key rate-limiting barriers. In particular, these include the testing of the current clinically relevant cell sources and removing the need for cell culture thus reducing fabrication time. This study includes the three following Specific Aims and Hypotheses:

Specific Aim 1: *Characterize AD-MSCs from two high-risk patient cohorts – diabetic and elderly humans – as functional or dysfunctional by evaluating their ability to serve as the cellular component of TEVGs.* Studies in the field of TEVGs utilize stem cells for two essential functions: inducing their differentiation into vascular cell phenotypes and/or utilizing their

paracrine (i.e. secreted factor-based) effects to inducing host repopulation via migration of adjacent SMCs. We hypothesize that AD-MSCs are capable of performing both of these essential functions and these are less efficacious in high-risk donors, and this will attribute a poorer performance as TEVGs in vivo.

Specific Aim 2: *Develop a more clinically-feasible TEVG by utilizing freshly isolated SVF cells and evaluating them in both in vitro and in vivo studies.* For cellular approaches, it is more desirable to use cells directly from harvest (i.e., fresh AD-MSCs) as this removes the need for an in vitro expansion period, thereby alleviating costs and potential cellular transformation issues, reducing regulatory barriers. We hypothesize that fresh AD-MSCs will function as well as cultured AD-MSCs in a TEVG and will test this using in vitro and in vivo approaches from Specific Aim 1.

Specific Aim 3: *Develop a more clinically-feasible TEVG by utilizing secreted factors from AD-MSCs alone; i.e., without seeded cells.* If AD-MSCs from any high-risk cohorts are unable to develop functional TEVGs (as evaluated in Specific Aim 1) it would be imprudent to simply exclude these patient populations from the promise of an engineered graft. Further, the regulatory pathway is challenging for any implantable device containing cells. In this aim, an alternative TEVG will be designed by saturating it with factors secreted by healthy AD-MSCs. We hypothesize that this acellular TEVG will function as well in a rat model as a TEVG seeded with AD-MSCs. This aim will consist of a pilot study to illustrate the feasibility of this design.

This research project was designed to address two primary barriers related to the clinical translation of TEVGs utilizing an adipose-derived stem cell source. First, AD-MSCs from two clinically relevant patient cohorts whose respective demographic pathologies are known to effect cell function were evaluated for use as an autologous TEVG through both in vitro and in vivo

methods (Chapter 2). Then resulting complications that were observed specifically in one patient cohort – diabetics – were mechanistically investigated (Chapter 3). Secondly, a non-culture adipose derived cell population –raw SVF cells – was utilized for development of a TEVG (Chapter 4) and tested for their ability to perform essential functions contributing to a TEVG in vitro as well as their in vivo performance. Finally, in an attempt to alleviate the complications seen in the high cardiovascular risk patient cohorts from Specific Aim 1, secreted factors – which are a primary contributor to TEVG success – were utilized to create a microsphere-based drug delivery system (Chapter 5). These AD-MSC secreted factor encapsulated microspheres were termed as “artificial AD-MSCs” due to their resemblance in geometry and ability to be utilized with similar methodology to AD-MSCs themselves. A pilot study was performed demonstrating the feasibility of this technology. Finally, a summary of results and thoughts on future directions will be provided (Chapter 6).

2.0 SPECIFIC AIM 1, PART 1:

EVALUATION OF HIGH-CARDIOVASCULAR RISK DONOR AD-MSCS FOR USE AS TEVGS

2.1 INTRODUCTION

Tissue engineering of small-diameter blood vessels is a promising alternative to currently-used vascular grafts having shown both reduced intimal hyperplasia and thrombosis compared to standard grafts [19, 61, 161, 163, 206, 235, 260, 267]. However, when developing an autologous cell-based therapy – such as the stem cell-based TEVG within this dissertation – it is critically important to evaluate the functionality of the intended patient's cells as this will directly impact the efficacy of the treatment. The cell type utilized in this dissertation will be adipose-derived mesenchymal stem cells (AD-MSCs) due to their attractive isolation via liposuction and the prowess of MSCs as a cell type compared to traditional vascular cells (see Section "1.3.3 Cellular Considerations"). However, AD-MSCs of patients at high cardiovascular risk, such as diabetics and the elderly (see Section: "1.2.1 Cardiovascular Risk Patient Cohorts"), have not yet been evaluated in the context of TEVG applications leaving it unclear if cells from these patient populations are suitable for producing autologous functional TEVGs and thus eligible for the promising treatments tissue engineering offers (see Section: "1.5.1 Improper Cell Sourcing"). Additionally, many cells utilized in pre-clinical studies are isolated from commercial sources

which do not represent realistic clinical populations. Metrics for evaluating the effectiveness of a cell for a TEVG have also not been clearly defined. The purpose of this aim is to define metrics for evaluation of different donor cells within the context of TEVGs and to evaluate those cells using both in vitro and in vivo methodologies. In this aim we hypothesize that diabetic and elderly AD-MSCs will function poorly in terms of the aforementioned metrics and this will provide a poor performance in vivo.

2.1.1 AD-MSCs and the Effect of Donor Populations

It has been clearly established that the use of adult stem cells –particularly MSCs –represents a critical step in increasing the translatability of autologous tissue engineered technologies (see Section: “1.3.3 Cellular Considerations”). As previously stated, these cells can offer a variety of advantages over primary cells that include an easier isolation process, the ability to self-renew, the potential to differentiate into multiple cell types, and the ability to secrete a wide spectrum of bioactive factors with varying functional effects [183, 187-189, 289-291]. Indeed, in tissue engineering as a whole, MSCs have seen use in multiple applications [19, 292-296] including for TEVGs [19].

While MSCs can be isolated from a variety of tissues, the most attractive source is from adipose tissue due to its ease and abundant isolation via liposuction. In general, all MSCs – independent of their isolated location – display similar characteristics in terms of morphology and immuno-phenotypic marker profiles, but display slight variation in their propensity to differentiate into various mesodermal lineages [297]. This similarity and occurrence in multiple organs is thought to be due to MSCs being located in a perivascular location within blood vessels throughout the body [298, 299]. For AD-MSCs in particular, in addition to the classic

mesodermal markers that are used to classify MSCs (e.g. CD44, CD73, CD90, CD105 [300]), AD-MSCs also transiently express markers such as CD34 which decrease over extended culture [301, 302] and distinguishes them from bone marrow MSCs [303]. This is likely a function of the various subpopulations present within the AD-MSC population upon initial plating [191] and will be discussed separately in Aim 2 when comparing the use of freshly isolated SVF cells to the subsequent culture expanded AD-MSCs. When considering which fat depot to isolate AD-MSCs from, studies have shown similar functionality in terms of proliferation, lipid accumulation upon adipogenic differentiation, and efficiency of osteogenic differentiation in female populations but some differential effects can be seen in terms of their susceptibility to apoptosis or osteogenic differentiation in male populations [304-306].

Historically (approximately 3 decades ago), AD-MSCs were termed as “preadipocytes” and mainly studied in the context of obesity and adipogenesis [307-310]. However, upon their definition as a multipotent stem cell (i.e. MSC) in 2001 [311], their research has expanded to fields including multiple regenerative medicine applications [312-322] and cancer [184, 323, 324]. Additionally, while it was initially suggested decades ago that these cells consist of multiple populations [325, 326], it was only until recently that their surface marker profile, genome, and composition has been sufficiently characterized [191, 327-330].

When considering the two prominent cardiovascular disease patient cohorts which this dissertation will utilize (i.e. diabetics, elderly; see Section: “1.2.1 Cardiovascular Risk Patient Cohorts”), AD-MSCs have been shown to be adversely affected. AD-MSCs isolated in the presence of diabetes were shown to possess increased ROS [331], increased susceptibility to apoptosis [331, 332], decreased differentiation potential (osteo [331, 333], adipo [333], endothelial [28]), decreased production of secreted factors (angiogenic [332, 334], fibrinolytic

[335]; also see Aim 1-1 for promigratory effects and Aim 1-2 for fibrinolytic effects), and decreased functional performance (angio [333], wound healing [333, 334], vascular stability [332]). AD-MSCs isolated from elderly donors have also been shown to possess similar dysfunctional characteristics such as a decreased differentiation potential (osteo [336], adipo [304], myogenic [337]), altered secreted profile [338], and decreased functional performance (angiogenesis [339], myogenic regeneration [337]). However, no differences in isolation efficiency or proliferation have been seen with either diabetic [28] or aged AD-MSCs [20, 304, 336]. Despite this work, the function of AD-MSCs from these two cohorts has yet to be evaluated in the context of vascular tissue engineering. As such, the next section will aim to define a set of criteria to evaluate the function of these cells within this context. Understanding these effects is paramount for autologous cell which is preferred as the use of allogenic cells which would require immuno-suppression diminishes the viability and survival of AD-MSCs [340].

2.1.2 Definitions of Essential Cellular Functions and Performance Criteria for Vascular Engineering

To define the essential functions which an AD-MSC must perform in order to be a successful cell source in the context of vascular tissue engineering one must consider the manner in which it is utilized and the mechanistic nature of the processes involved in vivo for TEVG generation (see Section: “1.5.3 In Vivo TEVG Mechanisms”). As outlined in Section “1.5.3 In Vivo TEVG Mechanisms”, there are two main methodologies in which stem cells are utilized to achieve a matured, vascular-like TEVG. The first is through the differentiation of stem cells into vascular phenotypes prior to implantation in vivo and the second is through the use of the cells in their

undifferentiated state which act to secrete bioactive factors that recruit host vascular-like cells. Considering both of these options reveals two critical performance criteria of stem cells: 1) the ability to differentiate into vascular cells (e.g. SMCs), and 2) the ability to secrete SMC pro-migratory factors. Beyond these functions on a cellular level, however, the cells must also be able to be successfully incorporated within a tissue engineered scaffold leading to a third performance criteria: 3) the ability to successfully seed and attach to tissue engineered scaffolds. For this dissertation, this is particularly a concern for elderly cells as age has been shown to be associated with cell size [341] which could hinder the seeding process. Finally, one must consider the end goal of a TEVG which is to generate patent, vascular-like grafts which establishes the final criteria: 4) in vivo performance. For this Specific Aim both diabetic and elderly AD-MSCs will be evaluated within these 4 contexts to consider their suitability for a clinical TEVG. If these criteria cannot be met by a specific cohort's cells, an acellular TEVG for these patients will be developed and discussed in Aim 3.

2.2 METHODS

2.2.1 Isolation and Culture of Cells and Collection of Conditioned Media

AD-MSCs were isolated from human patients using previously described methods [51, 191, 304]. All AD-MSCs were isolated (or had been previously isolated and banked) under the surgical service of Dr. Peter Rubin during elective procedures. All tissue was obtained through use of an approved Institutional Review Board (IRB) exemption status protocol allowing the following information to be gathered to protect patient confidentiality: gender, age in years,

presence of diabetic condition, and body-mass index (BMI). Isolated adipose tissue was then minced and digested in a collagenase solution (1 mg/mL, type II) for 30 minutes to remove cells from their surrounding matrix. The solution was then filtered through gauze to remove debris and centrifuged to remove the buoyant adipocytes. The pellet was then resuspended in an NH4Cl erythrocyte lysis buffer (154 mM) to remove red blood cells, and finally centrifuged again to obtain a cell pellet. That cell pellet was plated and cultured to obtain AD-MSCs. In this study cells were used between passage numbers 2 to 6.

For the purposes of this study AD-MSCs of various patient demographics were selected and classified into the following groups: "healthy" (< 45 years of age, non-diabetic), "diabetic" (< 45 years of age, diabetic (type 2)), and "elderly" (> 60 years of age, non-diabetic). Both the diabetic and elderly groups were considered as high cardiovascular risk, clinically relevant cohorts whereas the healthy group was utilized as a control. The age thresholds were established based on SCORE (Systematic COronary Risk Evaluation [102]) charts provided by the European Society of Cardiology and represented a point where aging demonstrated a high (in the case of elderly) or low (in the case of healthy) cardiovascular risk. To isolate the specific effects of each individual factor (i.e. diabetes or elderly compared to healthy), the ages were kept similar in a younger bracket for diabetic patients, and only non-diabetics were considered for the elderly group. Additionally, all cells were isolated from female patients to isolate gender effects between these comparisons, however to allow for a gender based comparison for the in vitro studies, a healthy male group was also established. A list of donors, their demographics, and the experiments which they were used for are listed in **Table 1**.

All AD-MSCs were cultured in 75-cm^2 tissue culture flasks (Corning) and grown under defined culture media [1:1 Dulbecco's modified Eagle's medium (DMEM; Gibco #11965) to

DMEM/F12 (Gibco #113300) with 10% fetal bovine serum (Atlanta Biologics #S11550), antibiotics (1% Pen/Strep, 0.5% Fungizone, 0.1% Gentamycin), and 10 µL of 10 mM dexamethasone] mixed with 25% Preadipocyte Growth Medium (#C-27410, #C-39425; PromoCell). Culture media was changed every 2-3 days and when AD-MSCs were expanded to near confluence, they were passage expanded utilizing 0.25% trypsin-EDTA (#25200-056; Gibco) or utilized for subsequent experimentation.

To obtain conditioned media, culture media was replenished in near confluent flasks of AD-MSCs (~80%) and cultured for an additional two days upon which it was collected. The conditioned media was then centrifuged (#Sorvall Legend RT, 1200 rpm, 5 min) to remove any cellular material or debris. It was stored at –80ºC until use.

Additionally, human aortic SMCs were purchased from ATCC (#PCS-100-012) and grown in a similar manner to AD-MSCs but in their own culture media (Cell Applications, #311-500, #311-GS).

Table 1. List of AD-MSC donors utilized in Aim 1-1. “X” marks use in particular experiment whereas multiple “X” identify multiple in vivo implantations of the same line.

AD-MSCs Utilized for Aim 1-1 Experiments									
Vorp Lab ID Number	Grouping	Gender	Age	Diabetic	BMI	Differentiation	Migration	Cell Seeding	In Vivo
1	Healthy	Female	38	No	33	X	X	X	
2	Healthy	Female	35	No	28.6	X	X	X	XX
5	Healthy	Female	33	No	29.9	X	X	X	X
8	Healthy	Female	32	No	21.4	X	X	X	X
20	Healthy	Female	36	No	30	X			
21	Healthy	Female	45	No	25.5	X			
22	Healthy	Female	32	No	21.4	X			
SVF5 p4	Healthy	Female	26	No	32.8				X
SVF7 p4	Healthy	Female	40	No	25.5				XX
SVF8 p4	Healthy	Female	38	No	35.2				X
3	Diabetic	Female	39	Yes	23.7	X	X	X	
13	Diabetic	Female	43	Yes	22.2	X	X	X	XX
14	Diabetic	Female	45	Yes	30.6	X	X	X	XXX
15	Diabetic	Female	39	Yes	27.4	X	X		XX
6	Elderly	Female	68	No	28.8	X	X		XXX
16	Elderly	Female	65	No	27.8	X	X	X	XX
18	Elderly	Female	65	No	25.8	X			
19	Elderly	Female	64	No	29.8	X	X	X	XX
25	Elderly	Female	61	No	28.3	X	X	X	
4	Male (healthy)	Male	36	No	23	X	X		
9	Male (healthy)	Male	24	No	26.4	X			
10	Male (healthy)	Male	42	No	34.7	X	X		
11	Male (healthy)	Male	22	No	24.3	X	X		
12	Male (healthy)	Male	31	No	37.5	X	X		

2.2.2 Differentiation of AD-MSCs into SMCs

To induce differentiation of AD-MSCs into SMCs, AD-MSCs were plated at on PLL coated coverslips (Neuvitro, GG-22-pll) at a density of 10,000 cells per coverslip. They then subsequently cultured in a differentiation media based on MEMα (Life Technologies, #12561-056) containing angiotensin II (AngII, 1 μM, Sigma #A9525) and 10% serum for 4 days [342]. After 4 days, AD-MSCs were fixed using 4% paraformaldehyde for 30 minutes and were evaluated using a standard immuno-fluorescent chemistry protocol to detect the SMC contractile markers calponin (1:250, Abcam #ab46794), myosin heavy chain (1:250, Abcam #ab77967), and smoothelin (1:250, #ab8969). F-actin (1:250, Sigma #P5282) was additionally used to assess the presence of an SMC spindle-like morphology. Calponin was chosen as a marker as it is expressed in aortic SMCs across their phenotype diversity [41, 42, 343]. Myosin heavy chain and smoothelin were chosen in addition as they are both indicative of fully mature, contractile SMCs [41, 42, 343]. In this study SMA could not be utilized as it is inherently expressed in AD-MSCs during flask culture. All images were acquired with an epi-fluorescent microscope with NIS Elements software (version 4, Nikon Instruments Inc., Melville, New York) and results were quantified using built-in tools. Expression of SMC contractile markers was quantified as the percentage of expressing cells and cell morphology via F-actin stain was quantified as shape factor (4*pi*area/perimeter2, ~0 = ellipsoid, ~1 = circular). Primary human aortic smooth muscle cells (ATCC, #PCS-100-102) were used as controls. AD-MSCs were utilized to compare across the basis of diabetes, age, gender, and BMI.

2.2.3 Ability of AD-MSCs to Promote SMC Migration

SMCs were plated within 24 well plates (TPP) at 10,000 cells/cm^2 (~20,000 cells per well) one day prior to experimentation to achieve confluent monolayers. Initial pilot studies were performed to determine this as the optimal cell density as SMCs plated at too high of a density will produce extracellular matrix and induce contractile effects that will inhibit their migratory effects (see Appendix A). To perform the migration assay (**Figure 1**), each well of SMCs had their media removed and were scratched with a single stroke of a 200µL pipette tip (scratch wound length: 682µm ± 105µm (avg ± SD, n=48). SMCs were then washed with 1X Hanks' Balanced Salt Solution to remove any cellular debris. SMCs were then incubated for 30 minutes with SMC media containing 1µL/mL of Cell Tracker Red (Invitrogen, #C34552) for 30 minutes for fluorescent visualization. The media was then replaced with AD-MSC conditioned media from healthy, diabetic, elderly, or healthy male donor groups and allowed to migrate over 24 hours. Non-conditioned AD-MSC media was used as a control.

For all experiments comparing between donor groups, conditioned media was diluted with stock culture media to 100,000 conditioning cells/mL. However, additional experiments were performed utilizing heathy AD-MSC-derived conditioned media for dose dependent studies. Here, media was diluted from 500,000 conditioning cells/mL (termed dose 1:0) to various dilutions of 1:2, 1:4, 1:9, and 1:19. Finally, healthy conditioned media was also heat-inactivated where it was raised to a temperature of 56ºC for 30 minutes.

To acquire images throughout the time course of migration the plates were placed in a closed, thermo-controlled (37^{0}C) stage top incubator (Tokai Hit Co., Shizuoka-ken, Japan) atop the motorized stage of an inverted Nikon TiE fluorescent microscope (Nikon Inc., Melville, NY) equipped with a 10X, 0.5NA plan apochromat lens (Nikon Inc., Melville, NY). This allowed

cells to be maintained under typical cell culture conditions (20% O_2, 5% CO_2, 37^{0}C). NIS Elements software (version 4.0) was utilized to automatically image cell migration every 2 hours. The resulting images were analyzed by measuring the area of the wound normalized to the area at the initial time point for each well. Migration rate was calculated by averaging the difference in normalized area between the first 4 time points (equivalent to 8 hours) and was normalized to non-conditioned controls.

Additionally, to detect one bioactive factor was indeed produced by AD-MSCs, an enzyme-linked immunosorbent assay (ELISA) kit (R&D Systems, #DVE00) was utilized to probe for vascular endothelial growth factor (VEGF) within the conditioned media of AD-MSCs. All protocols were followed according to manufacturer instructions. However, in this study only healthy donors (i.e. <45 years of age, non-diabetic) were utilized and a higher number was utilized to get a greater sense of the population variability (n=12; inclusive of donors 1, 2, 5, 8, 20, 21, 4, 10, 11 in **Table 1** plus the following: [#7, Healthy, Female, 26, No, 21.3], [#23, Healthy, Female, 25, No, 29], [#24, Healthy, Female, 34, No, 27]). The donors utilized spanned a wide range of BMI (avg±std: 27.3±4.3, range: 21.3 to 34.7).

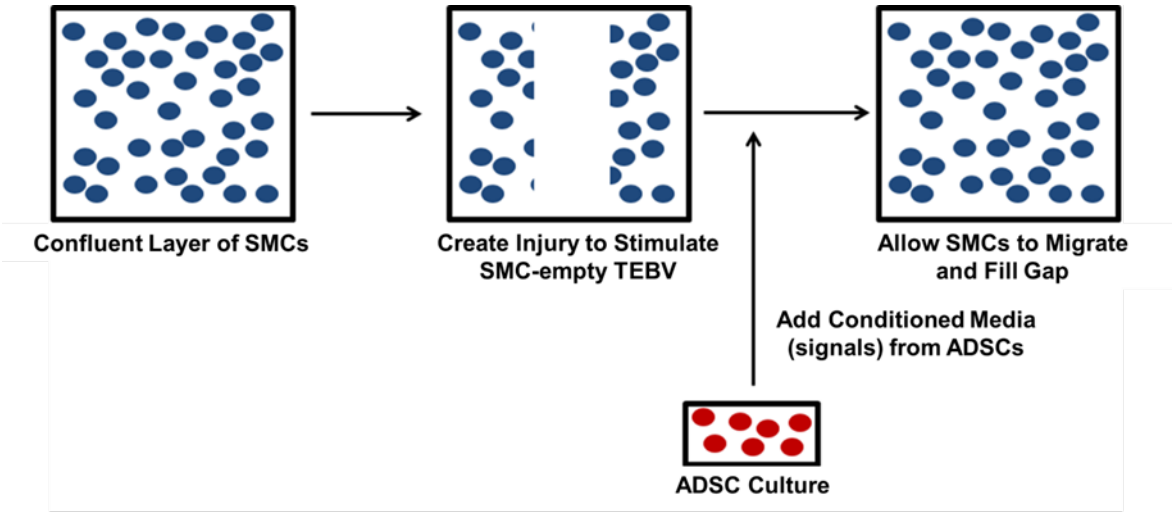

Figure 1. Experimental schematic of SMC scratch wound Migration Assay. SMCs are induced to migrate via a scratch wound assay while being stimulated with AD-MSC conditioned media over the course of 24 hours. Example images of this assay can be seen in Appendix A.

2.2.4 PEUU Scaffold Fabrication

Bilayered, tubular, biodegradable, elastomeric scaffolds (1.3 mm ID, 10 mm length) were created from poly(ester urethane)urea (PEUU) as previously described [165, 344, 345]. PEUU was synthesized utilizing polycaprolactone diol, 1,4-diisocyanatobutane, and putrescine [344] then fabricated in two different layers [165, 345]. This is a design which has been previously utilized by David Vorp's laboratory [161, 165, 260, 265]. Thermally induced phase separation (TIPS) was utilized to fabricate the inner layer of the scaffold which creates a highly porous network allowing for cellular integration [260]. This scaffold was then placed on a rotating mandrel where it was finished by electrospinning PEUU to create a fibrous outer layer to provide mechanical stability (~400 µm TIPS thickness, ~70 µm ES thickness [260]).

2.2.5 Cell Seeding into TEVG Scaffolds

AD-MSCs were seeded into PEUU scaffolds using the previously developed and validated Rotational Vacuum Seeding Device within David Vorp's laboratory [197, 198]. Briefly, PEUU scaffolds were mounted within the device chamber where they were infused lumenally with a cell suspension containing 3 million AD-MSCs (suspension concentration: 1 million cells/mL, total volume: 3 mL, infusion rate: 2 mL per minute). During this time, the chamber was closed and a vacuum force of -127 mmHg was applied. Following seeding, constructs were statically rested for 4 hours in media to allow for cellular adhesion and were then moved to 500 mL spinner flasks (Kontes #Cytostir 882911-0250) where they were cultured for 48 hours (stir rate: 15 rpm). At this point the constructs were considered prepared for in vivo implantation.

2.2.6 Measurement of Uniform Cell Seeding

As part of our TEVG design cells are incorporated into scaffold pores in a uniform manner (i.e. similar density and distribution across the radial (thickness), circumferential, and longitudinal directions). As a means to ensure that cell seeding was not altered across AD-MSC donor groups causing confounding effects during in vivo studies, the cell seeding of each donor type was validated (healthy (n=4), diabetic (n=3), elderly (n=3)). This is particularly a concern for elderly cells as age has been associated with an increase in cell size [341] which can directly affect cell seeding. Post-seeding and following spinner flask incubation, the constructs were fixed in 4% paraformaldehyde for 30 minutes, cut into three longitudinal pieces, and frozen for histologic analysis using standard protocols (30% sucrose for 30 min them embedded in OCT compound (#Fisher). To analyze cell seeding, sections were stained with DAPI to identify cell nuclei and F-

actin (Phalloidin, 1:250; Sigma #P5282) to show cellular spreading along scaffolding material. Images were acquired at 10x using an epifluorescent microscope with NIS Elements software (version 4, Nikon Instruments Inc., Melville, New York).

Due to the cumbersome and time consuming nature of manually counting cells, an automated cell counting tool was developed utilizing scripts within ImageJ (1.47, Rasband, Bethesda, Maryland) (see Appendix B for script). This tool was designed such that it could detect the presence of cells within a stained fluorescent image and output cell density. Acquired 10x images from each seeded construct were first stitched together utilizing ImageJ toolboxes (MosaicJ Plugin) to acquire complete cross sectional views and were counted with the aforementioned script. Then to compare across the circumferential and radial directions, each cross section image was virtually segmented (non-automated) into circumferential or radial pieces. Cell densities per area were compared across all directions (i.e., radial, circumferential, and longitudinal).

2.2.7 In Vivo TEVG Implantation

Seeded scaffolds (n=8 healthy, n=7 diabetic, and n=7 elderly; some donors had multiple grafts implanted as indicated by the "XX" in **Table 1**) were implanted as abdominal aortic interposition grafts in Lewis rats for 8 weeks as previously described [153, 161, 260, 265]. For the purposes of this study all rats were kept similar between all groups (i.e. in a healthy status: non-diabetic, non-elderly). All AD-MSCs in this study had a BMI range that was consistent ($p=0.62$) between the groups: 29.4±4.8 (healthy), 26.7±4.2 (diabetic), 28.7±0.8 (elderly). Implantations were performed as follows. Briefly, rats were anesthetized (4% Isofluorane and 50 mg/kg ketamine for induction; 1% Isofluorane for maintenance), placed in a supine position, and administered an

injection of cefazolin (100 mg/kg, intramuscular) as a prophylactic. A midline incision was then made and the infrarenal abdominal aorta was exposed via manual dissection. Microclamps were then applied and the aorta was transected. An AD-MSC seeded construct was then sutured as an end-to-end anastomosis with interrupted 10-0 prolene sutures. After the graft was secured, the microclamps were released to restore blood flow. The patency of the graft was verified by direct observation of distal pulse pressure prior to closing the animal where the muscle and skin layers of the rat were sutured in a continuous style with 3-0 polyglactin resorbable sutures.

Following surgery all animals were maintained on both antibiotics (Baytril, 10 mg/kg, oral, twice per day) and analgesics (buprenorphine, 0.5 mg/kg, subcutaneous, twice per day) for 3 days, in addition to antiplatelet therapy for the first 4 weeks (dipyridamole – 250 mg/kg for the first 7 days, 100 mg/kg for the following 3 weeks, oral; aspirin – 200 mg/kg for the first 7 days, 100 mg/kg for the following 3 weeks, oral). All implantations were carried out to the 8 week study endpoint unless obvious distress was observed due to thrombotic complications, at which point animals were euthanized.

Upon euthanasia, an angiography was performed to assess the patency of the TEVG prior to explant wherein a catheter was placed in the descending thoracic aorta and infused with an x-ray contrast agent (Renograf). TEVGs were then explanted TEVGs and were fixed in 4% paraformaldehyde for 30 minutes, bathed in 30% sucrose for 30 minutes, and then frozen for histologic analysis.

Three native aortas were explanted from non-operated rats to be utilized as a positive control.

It is important to note that one of the TEVGs in our study from the elderly group was patent but aneurysmally dilated upon explant and appeared to be due to abnormal fragmentation

of the electrospun scaffold layer. As this was an anomaly that has not been observed in any of our previous studies [161, 260, 265] this sample was excluded from analysis of composition. Histologic results from this sample can be seen in Appendix C.

For discussion on the use of human cells within the inbred Lewis rat model, see Section 2.7.5 (“T cell and B cell Activity Within Implanted TEVGs”).

2.2.8 Histologic Evaluation and Immuno-fluorescence

Frozen TEVGs were sectioned via a cryo-microtome at an 8 μm thickness mounted on gelatin coated slides (for recipe see Appendix D) to improve their adhesion throughout the staining process. Sections were then stained with hematoxylin & eosin (H&E) or immuno-fluorescent chemistry both using standard techniques. Antibodies were used to detect the presence of ECs (von Willebrand Factor (vWF) – 1:250; US Biological #V2700-07), SMCs (smooth muscle alpha-actin (SMA) – 1:1000; Sigma #A5228 and calponin – 1:250; Abcam #ab46794), and elastin (1:100; EPC #RA75) with fluorescent secondary antibodies (Rockland #611-1202 (1:1000); Invitrogen #A10521 (1:1000), Sigma #C2821 (1:300)). When performing elastin staining an etching procedure was utilized prior to staining to expose elastin from potentially surrounding microfibrils which can block immuno-based staining. Briefly, sections were incubated in solution of Guanidine and DTT (6M Guanidine-HCl in 20 mM Tris pH 8.0, with 0.8g dithiothreitol (DTT) per 10 ml) for 15 minutes to dissociate disulfide bonds and then in a solution of iodoacetamide (0.19g iodoacetamide per 10 ml in 20 mM Tris pH 8.0) for 15 minutes to prevent reformation. All images were acquired at 20x using an epifluorescent microscope with NIS Elements software. Analysis was restricted to the newly developed luminal tissue within

TEVGs (see Section: “2.3.4 In Vivo Gross Observations and Patency of Healthy, Diabetic, and Elderly TEVGs”).

2.2.9 Morphometric and Quantitative Analyses

To perform morphometric analyses, the following metrics were acquired manually using tools in NIS Elements software: cell density, neotissue thickness, nuclear shape factor, percentage of cells positively expressing SMA or calponin, percentage of luminal perimeter occupied by vWF positive cells, and percentage of thickness occupied by elastin. Neotissue thickness was defined as the thickness of the newly developed vascular-like tissue which is present on the luminal side of the explanted TEVG. Nuclear shape factor (defined as [4π x area/perimeter^2]) measured the circularity of cell nuclei giving an indication of cellular alignment. For each image parameter, measurements were made using 4 replicate images from each explanted TEVG.

2.2.10 Multiphoton Analysis of Collagen Architecture

To analyze the presence of collagen within explanted TEVGs we utilized multiphoton microscopy as previously described by our group [346, 347]. Briefly, an Olympus multi-photon microscope (Model FV10, ASW software, Olympus America Inc., USA) was used via second-harmonic generation (excitation wavelength: 780nm, emission wavelength: 400 nm) acquired at 25x magnification. To quantitatively assess the collagen architecture within acquired images, we employed a custom image-analysis MATLAB script specifically designed to output the following parameters: fiber intersection density, segment length, fiber tortuosity, mean fiber orientation with 90 degrees set as the circumferential direction, and the mean fiber diameter.

These methods have been previously described in detail by our group [346, 347]. In brief, the script identifies fibers and intersection points between fibers within a multi-photon image. Fiber intersection density is defined as the number of intersection points per area, segment length is defined as the average length of fibers between intersection points, and tortuosity is the segment length divided by the direct line length between intersections. In addition, the orientation of each fiber segment is calculated with respect to the circumferential direction (i.e. 90 degrees) and the average diameter of each fiber segment is calculated.

2.2.11 Statistics

All statistical analysis was done utilizing Minitab software (version 16) to perform either a t-test, ANOVA, or linear regression. Statistical significance was accepted at $p<0.05$. All data were verified for parametric tests by confirming normality and homogeneity of variance (not shown). Appropriate post-hoc tests when using ANOVA analyses were performed (Fisher's LSD, Tukey).

When performing comparisons across donor groups (i.e. healthy, diabetic, elderly) and between donors of different genders (i.e. female, male) during the in vitro SMC differentiation and SMC migration studies, t-tests were performed to elucidate differences between each pair. While this experimental design could be classified as a two-way ANOVA, this was not performed as all group combinations were not present required to run the test (e.g. male diabetic) and these comparisons were not the end goal of this study (i.e. altering a single factor while controlling for all others; e.g. comparing the female healthy and male elderly would introduce multiple biasing effects and is thus irrelevant to this study).

2.3 RESULTS

2.3.1 Differentiation of AD-MSCs from Diabetic and Elderly Donors into SMCs

To assess whether AD-MSCs from diabetic donors had a reduced ability to differentiate into SMCs compared to healthy donors, they were stimulated with angiotensin II for 4 days. Diabetic AD-MSCs revealed a less efficacious differentiation compared to healthy AD-MSC controls indicated by a significantly lower expression of the SMC marker calponin (**Figure 2**). Additionally, diabetic AD-MSCs failed to adopt the typical SMC spindle-like morphology (**Figure 3**) observed in healthy AD-MSCs as shown qualitatively by F-actin staining and quantified by a lack of a significant reduction in shape factor. No positive staining was seen with myosin heavy chain or smoothelin in either healthy or diabetic donor differentiated AD-MSCs (data not shown). Unstimulated AD-MSCs from both groups did not express calponin, myosin heavy chain, or smoothelin (data not shown) and display a flat morphology (see **Figure 3**). SMCs were used to confirm the functionality of the antibodies for these three markers (data not shown) and the SMC spindle-like morphology.

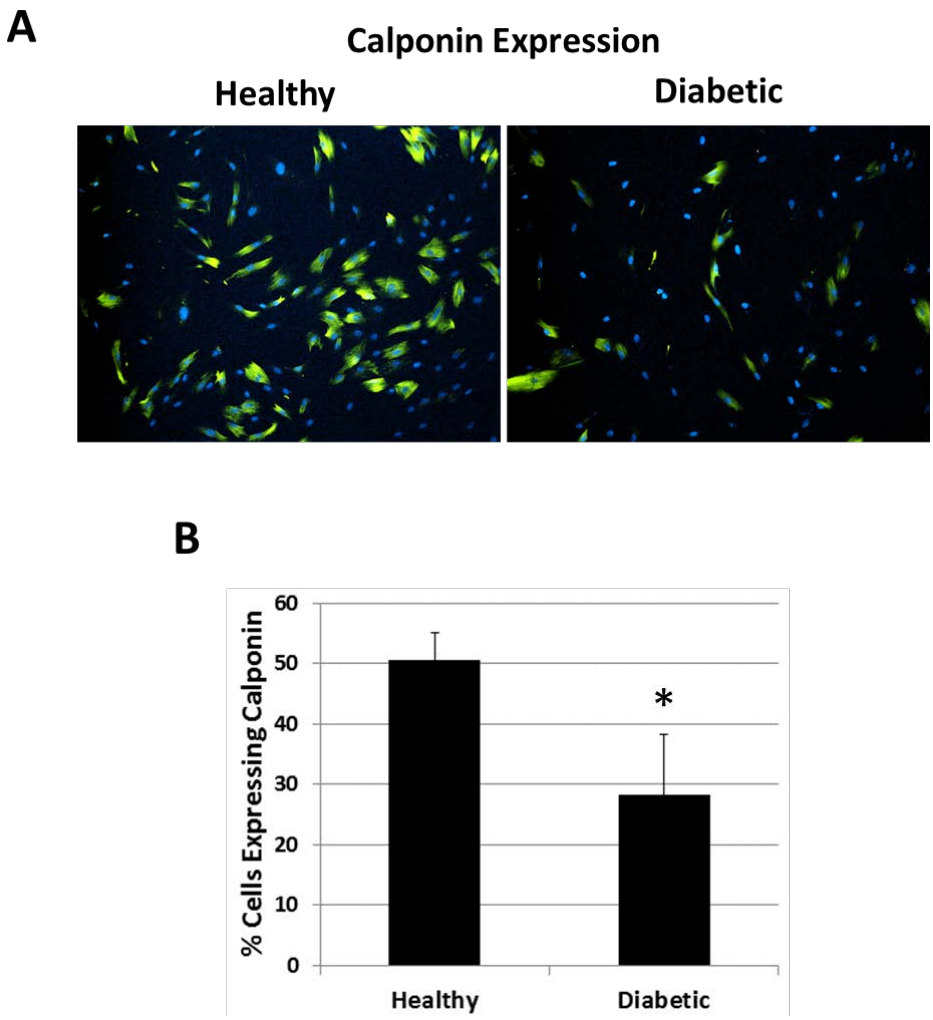

Figure 2. AD-MSC differentiation into SMC is decreased for diabetic patients based on calponin expression. Diabetic AD-MSCs displayed a less efficacious SMC differentiation compared to healthy AD-MSCs in terms of the expression of calponin ((A) – immuno-fluorescence for calponin (green) with counterstained nuclei (blue)). This was quantified by percentage of calponin expressing cells (B). Data is presented as mean ± SEM with *= significant difference at $p<0.05$. For calponin expression n=7 was used for the healthy group and n=4 for the diabetic group.

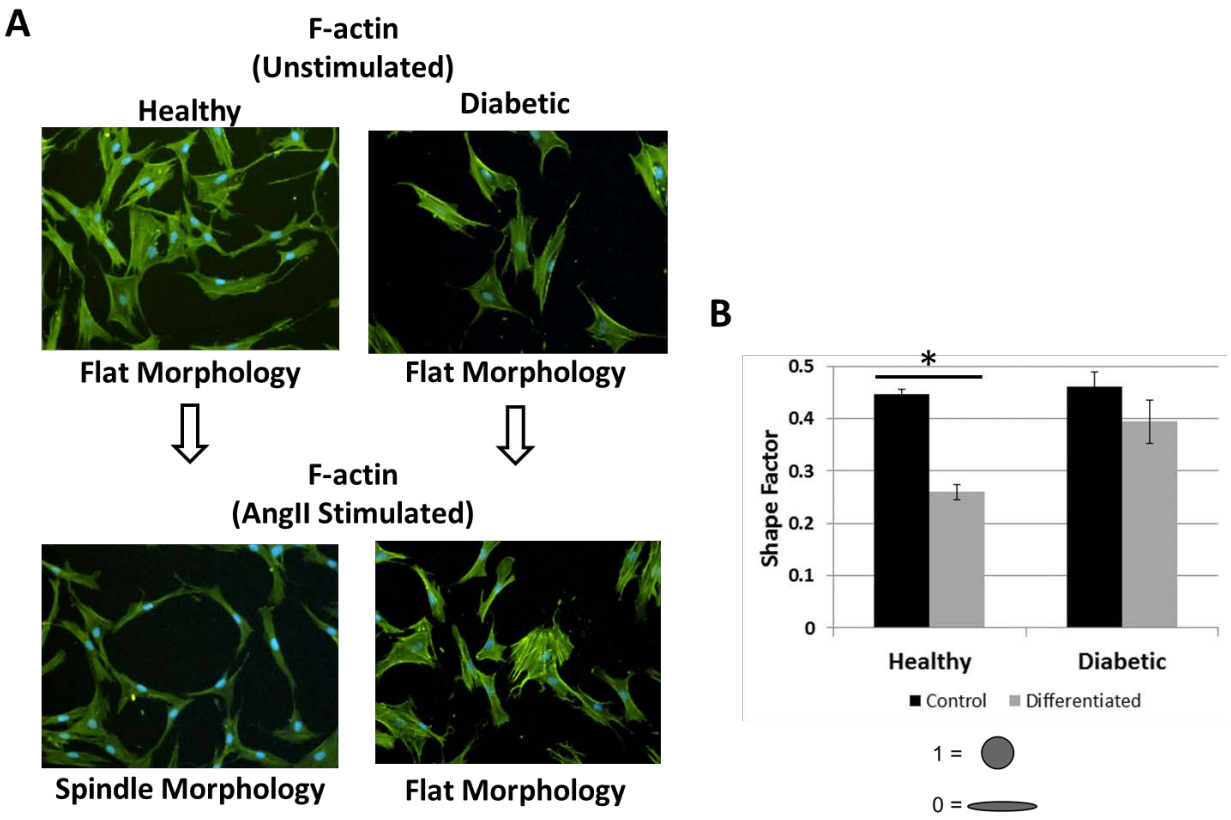

Figure 3. AD-MSC differentiation into SMC is decreased for diabetic patients based on cell morphology. Upon differentiation AD-MSCs did not acquire an SMC spindle morphology ((A) – immuno-fluorescence for F-actin (green) with counterstained nuclei (blue)). This was quantified by measuring the shape factor of the cells ($4\pi \times$area/perimeter2, ~0 = ellipsoid, 1 = circular) (B). Data is presented as mean ± SEM with *= significant difference at $p<0.05$. n=4 was used per group for shape factor experiments.

Similar to the diabetic donor AD-MSCs, those from elderly donors also displayed a reduced differentiation potential towards SMCs under angiotensin II stimulation. This was shown based on the lower expression of calponin (**Figure 4**) and maintenance of a flat morphology throughout the differentiation process (**Figure 5**). Additionally, similar to healthy and diabetic donor AD-MSCs, elderly ones revealed no positive staining for myosin heavy chain or smoothelin in either stimulated or unstimilated cases (data not shown).

Gender did not affect the ability of AD-MSCs to differentiate into SMCs as both male and female donors showed equivalent results in terms of expression of calponin post-differentiation and were induced morphologically into a SMC-like spindle shape (**Figure 6**).

Finally, to assess the influence of BMI as a potentially confounding variable a linear regression analysis was performed across all donors (**Figure 6**). No significant BMI-dependence was seen across calponin expression ($R2 = 0.001$, $p=0.96$).

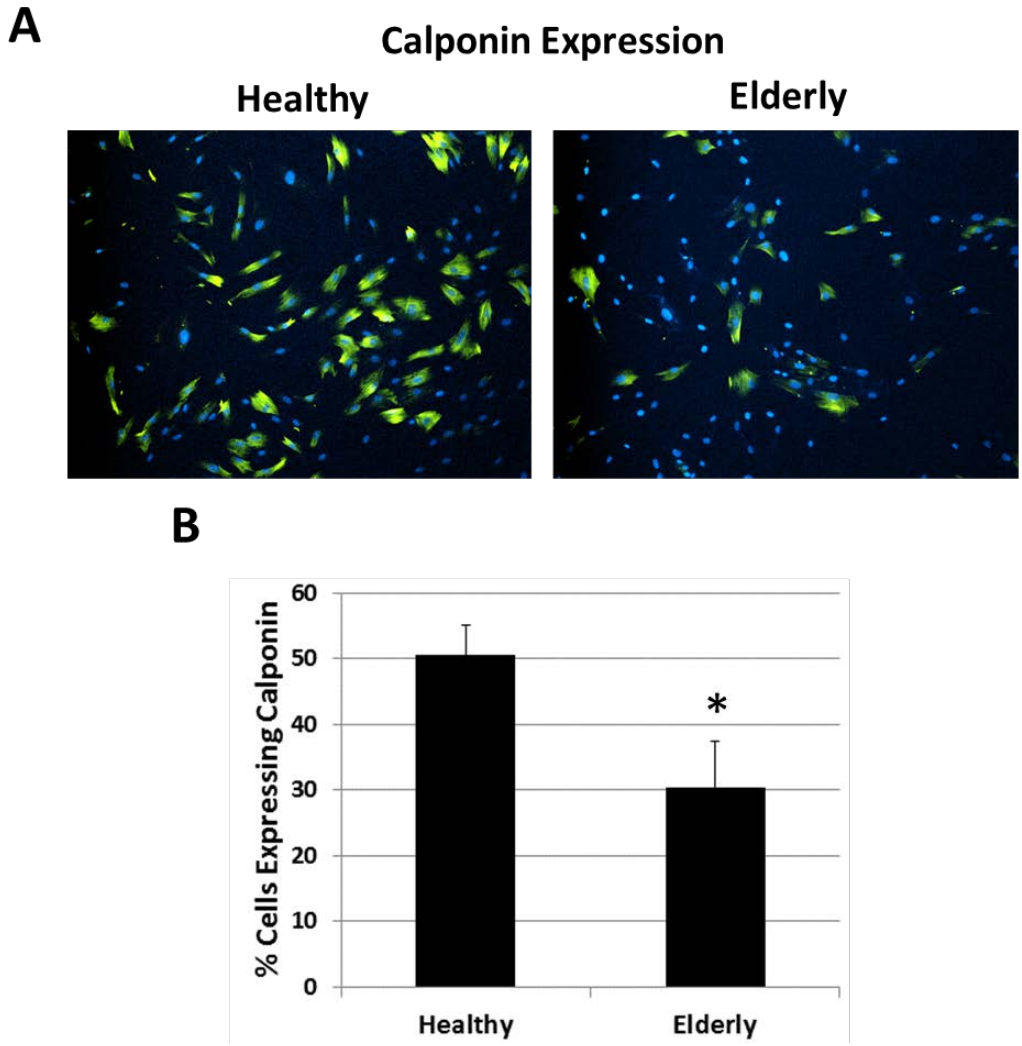

Figure 4. AD-MSC differentiation into SMC is decreased for elderly patients based on calponin expression. Elderly AD-MSCs displayed a reduced ability to differentiate into SMCs under AngII stimulation for 4 days. AngII stimulated AD-MSCs showed a significantly lower expression of calponin ((A) – immuno-fluorescence for calponin (green) with counterstained nuclei (blue)). This was quantified by number of calponin expressing cells (B). Data is presented as mean ± SEM with *= significant difference at $p<0.05$. For calponin expression n=7 was used for the healthy group and n=5 for the elderly group.

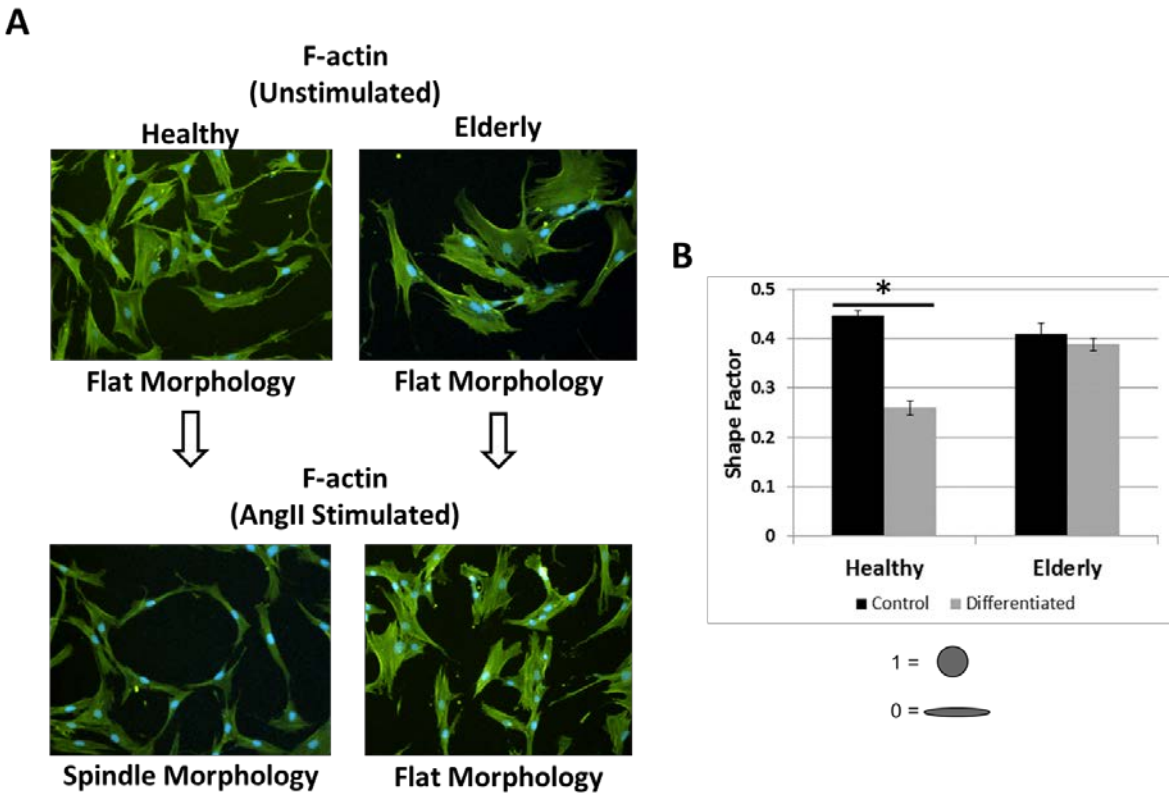

Figure 5. AD-MSC differentiation into SMC is decreased for elderly patients based on cell morphology. Differentiated AD-MSCs did not acquire an SMC spindle morphology ((A) – immuno-fluorescence for F-actin (green) with counterstained nuclei (blue)). This was quantified by measuring the cells shape factor ($4\pi \times$area/perimeter2, ~0 = ellipsoid, 1 = circular) (B). Data is presented as mean ± SEM with *= significant difference at $p<0.05$. n=4 was used per group for shape factor experiments.

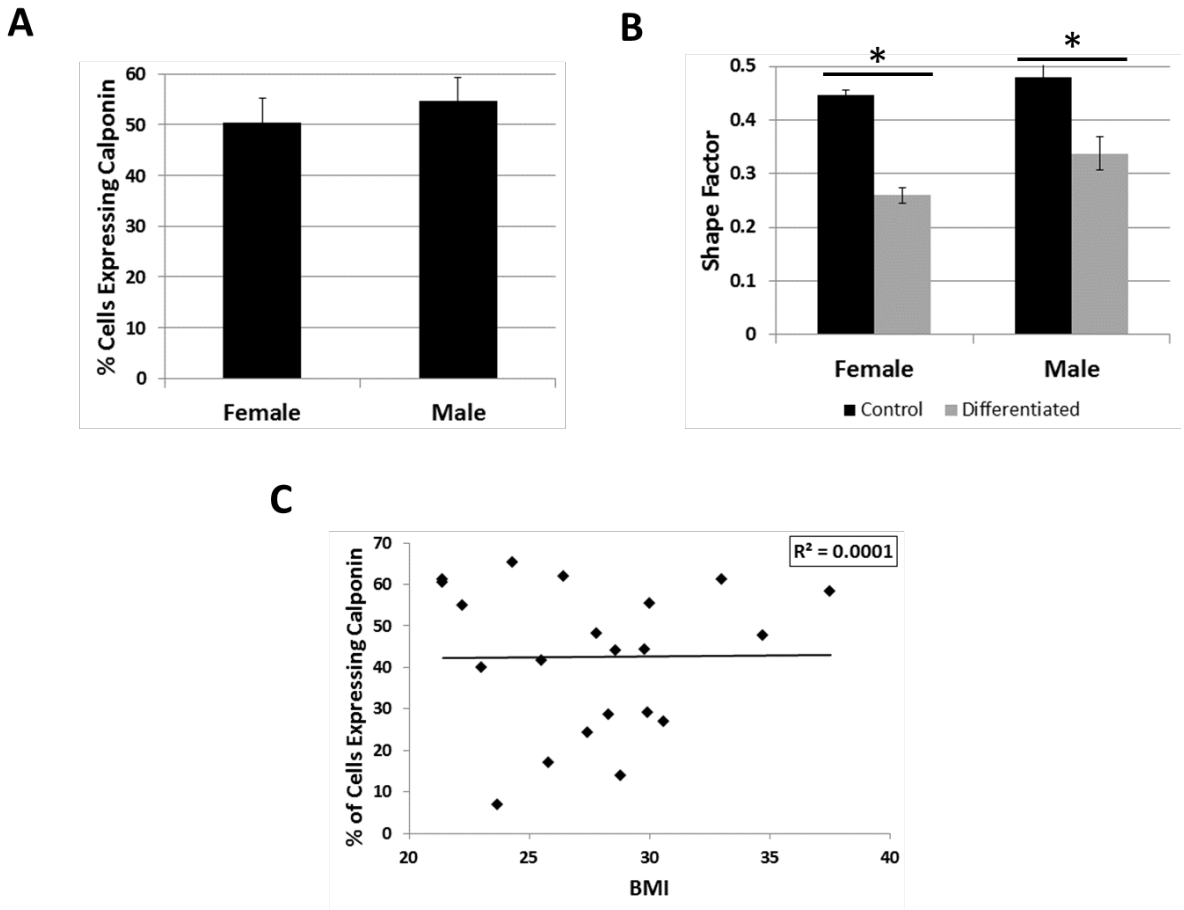

Figure 6. Gender and BMI do not affect AD-MSC differentiation into SMCs. Comparing gender of AD-MSCs from both healthy male and female donors produced equivalent results when AD-MSCs were stimulated to differentiate into SMCs with AngII based on calponin expression (A) and change in cell morphology (B). Performing a regression analysis utilizing BMI from all donors produced no correlation for the percentage of cells expressing calponin (C). Data for bar graphs is represented as mean ± SEM with *= signficant difference at $p<0.05$. n=4 was used per group for shape factor experiments and for calponin expression experiments, n=7 was used for the female group and n=5 for the male group.

2.3.2 Ability of AD-MSCs to Produce SMC Pro-Migratory Factors in Healthy, Diabetic, and Elderly Donors

To investigate the ability of AD-MSCs to exert a secreted factor-based pro-migratory effect on SMCs and assess how this critical function for TEVGs is altered in high-cardiovascular risk donor demographics, conditioned media was collected from AD-MSCs of healthy, elderly, and diabetic patients and utilized in a scratch wound SMC migration assay. Upon stimulation with AD-MSC conditioned media from healthy donors, SMCs showed a more rapid wound closure rate when compared with non-conditioned control media (**Figure 7**). This data was expressed as migration rate per hour (over the first 8 hours prior to inevitable slowing due to plate filling). Additionally, the pro-migratory effect was removed upon heat inactivation indicating the heat-liability of the secreted factors (**Figure 7**). The AD-MSC conditioned media also showed a dose dependent response as dilution to varying levels of conditioning cells/mL produced a less rapid migration rate with a 20-fold dilution producing a similar effect to non-conditioned media (**Figure 7**). Finally, a representative growth factor that is responsible for SMC migration [348] – VEGF – was probed for in media conditioned by healthy AD-MSCs and was shown to be present at 4091±1903 pg/10^6. Additionally, the correlation of production of VEGF with BMI showed no significant trend (data not shown, R^2=0.01, p=0.74).

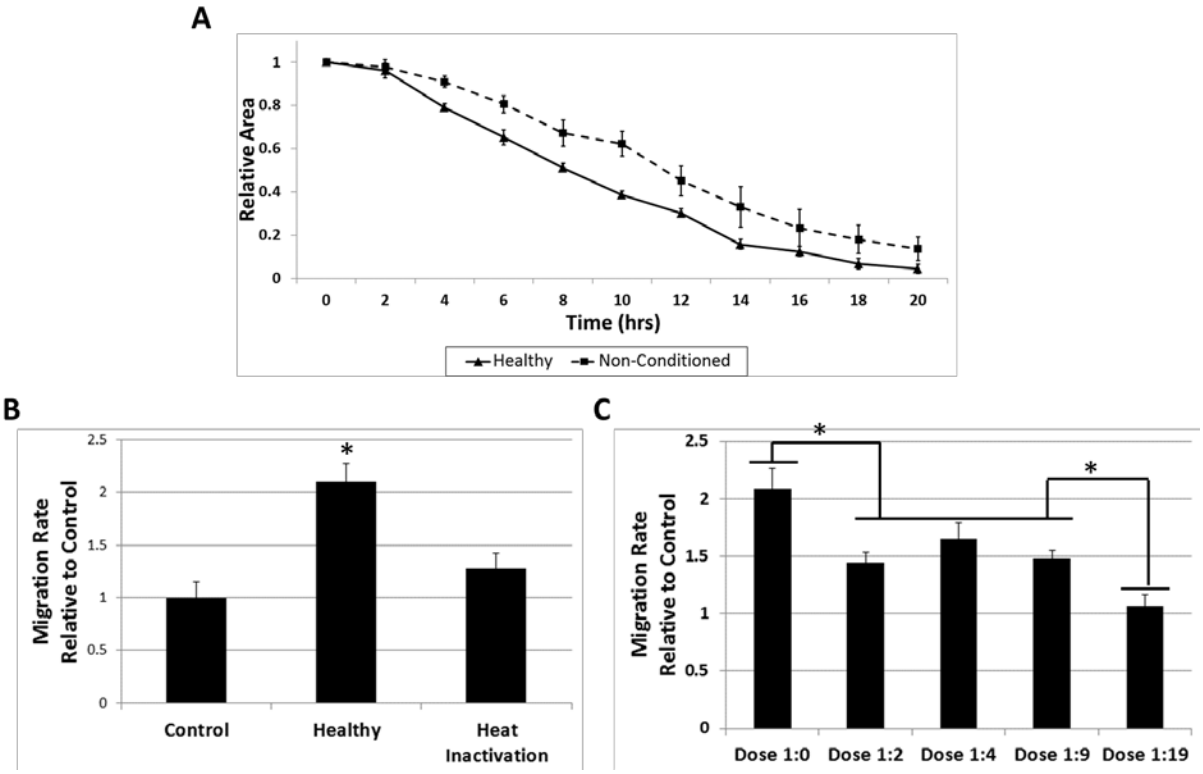

Figure 7. AD-MSC secreted factors can promote SMC migration. SMCs are induced to migrate via a scratch wound assay while being stimulated with AD-MSC conditioned media over the course of 24 hours. AD-MSCs promote the migration of SMCs compared to non-conditioned controls (A). This data was quantified by measuring the normalized wound area over time. This data converted to migration rate per hour relative to controls, expressing a significant difference between AD-MSC conditioned media and non-conditioned controls (B). Additionally, heat inactivating conditioned media caused a significant loss in functionality indicating SMC pro-migratory effects happen at least in part on a protein level. Diluting AD-MSC conditioned media to varying levels of conditioning cells/mL produced a dose dependent effect (dose 1:0 = 500,000 conditioning cells/mL) (C). Data is presented as mean ± SEM with *= significant difference at $p<0.05$. n=4 was used per group in all experiments.

To then determine differences related to donor demographics, we analyzed the potency of AD-MSC conditioned media from two high cardiovascular risk populations: diabetics and the elderly. Similarly to healthy AD-MSC conditioned media, SMCs stimulated with conditioned media from diabetic patients also induced a more rapid wound closure compared to non-conditioned media (**Figure 8**). However, AD-MSC secreted factors from elderly donors were unable to induce pro-migratory effects (**Figure 9**). It is also noteworthy that all AD-MSCs in this study were cultured in high glucose growth media (~17 mM which is equivalent to 306 mg/dl which is above the diabetic threshold) indicating that the diabetic hyperglycemic environment does not limit the ability of AD-MSCs to produce SMC pro-migratory factors.

As all the donors utilized for the previous experiments were female to reduce confounding effects, it was important to assess whether gender played a role in AD-MSC secretion of SMC pro-migratory factors. Comparing the migration rate induced by healthy female and healthy male cells revealed the effect not to be gender specific (**Figure 10**) as there was no difference between the groups.

Finally, to assess a potential confounding variable of BMI a linear regression analysis was performed including all donors utilized in this study (**Figure 10**). No significant trend was seen (migration rate: $R^2 = 0.05$, $p=0.4$)

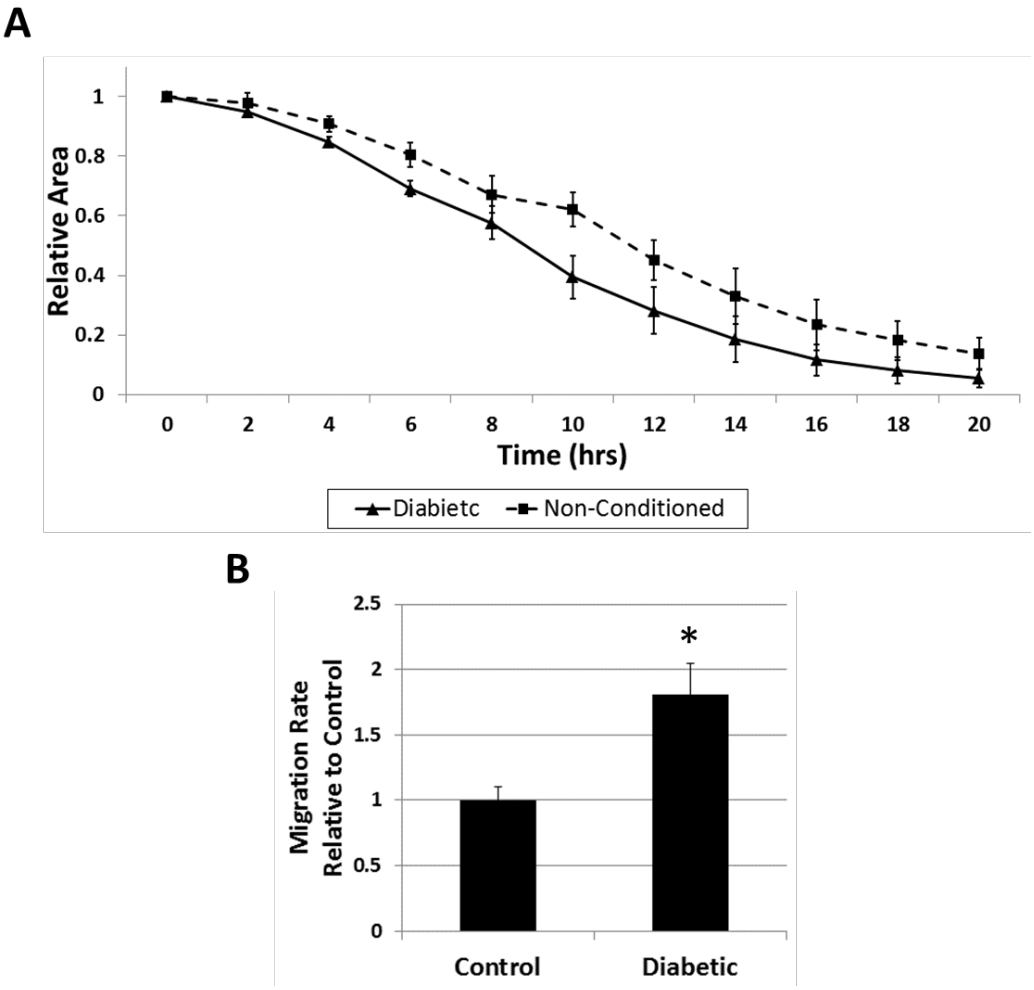

Figure 8. AD-MSCs from diabetic patients produce SMC pro-migratory secreted factors. Investigating diabetic patient AD-MSCs for the ability of their secreted factors to promote SMC migration, showed an increased migration compared to non-conditioned media ((A) – wound closure over time; (B) – wound closure rate per hour). This increased migration rate was similar to that seen with healthy AD-MSCs. Data is presented as mean ± SEM with *= significant difference at $p<0.05$. n=4 was used per group in all experiments.

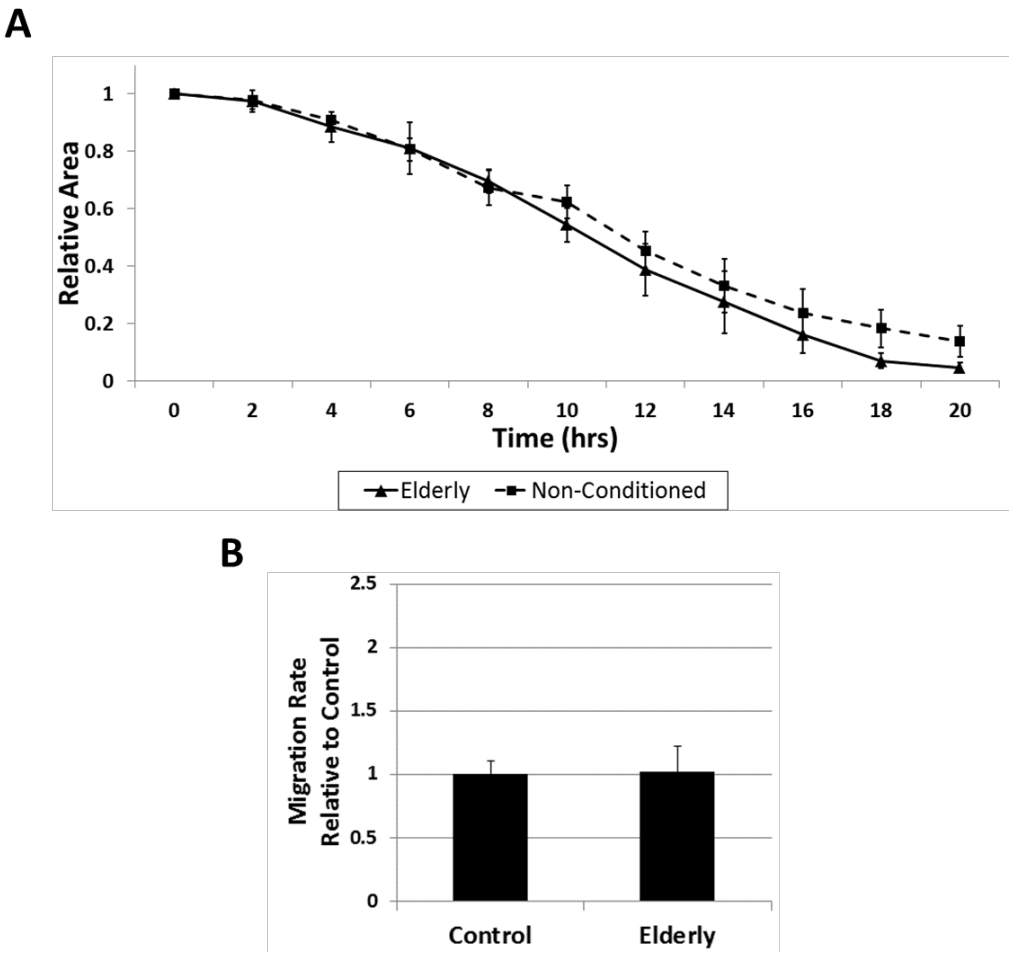

Figure 9. AD-MSCs from elderly patients do not produce SMC pro-migratory secreted factors. When comparing between healthy and elderly patient AD-MSCs, those from elderly patients displayed an inability of their secreted factors to produce SMC pro-migratory effects ((A) – wound closure over time; (B) – wound closure rate per hour). Data is presented as mean ± SEM with *= significant difference at $p<0.05$. n=4 was used per group in all experiments.

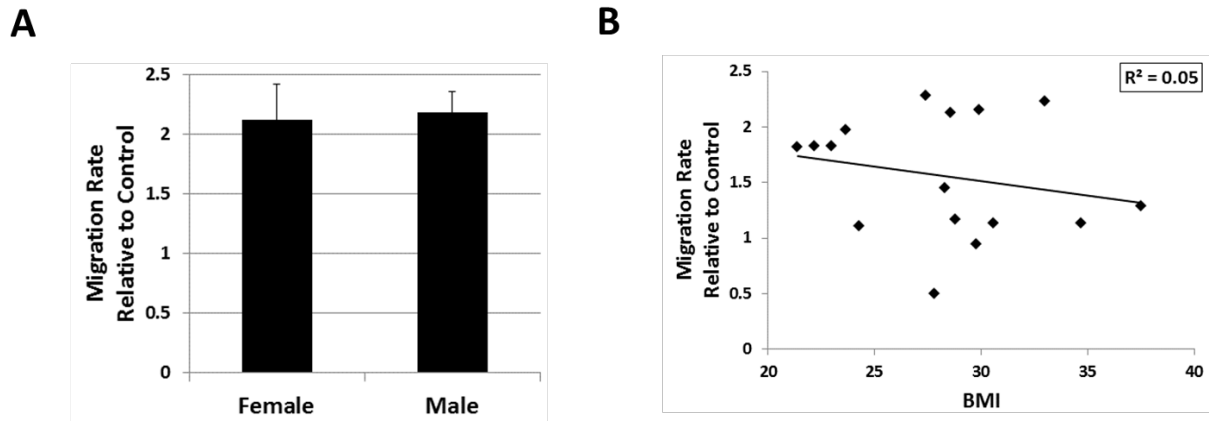

Figure 10. Gender and BMI do not affect AD-MSC secreted SMC pro-migratory factors. Comparing across the gender of AD-MSCs from both healthy male and female donors produced equivalent SMC pro-migratory responses (A). Performing a regression analysis utilizing BMI from all donors produced no correlation for migration rate (B). Data for bar graphs is represented as mean ± SEM with *= signficant difference at $p<0.05$. n=4 was used per group for migration.

2.3.3 Uniform Cell Seeding Analysis for Healthy, Diabetic, and Elderly AD-MSCs

To ensure consistent TEVG fabrication across all groups, the cell seeding process was investigated and compared for uniformity. As first step to overcome the potential error associated with manually counting as well as to increase throughput of experiments requiring quantification of cells, a cell-counting tool was developed utilizing scripts in ImageJ. First, this tool imports a multi-channel (i.e. colored) image and then extracts the desired channel which was utilized for the detection of cells. In most cases this is the blue channel due to the common use of DAPI staining for cell nuclei. Next, the tool applies a Gaussian blur to the image and subtracts this from the original to eliminate background noise and develops more sharply defined particles. An Otsu threshold [349] is then applied to form a binary image utilized in subsequent counting steps. This method converts a gray scale image to one consisting only of two binary pixel colors (black and white) by defining the optimal pixel gradient between immediate separations. The particles

are then eroded and subsequently dilated. In this situation, particles which are of normal size will remain the same but particles that are sufficiently small and likely imaging artifacts (as opposed to cells) will be eliminated. Finally a watershed transformation is applied prior to counting which separates touching circular objects. A visual representation of these steps can be seen in **Figure 11**. The script with now isolated cells can output various parameters within ImageJ toolboxes such as number of cells, area, perimeter, etc. To validate the accuracy of this tool compared to manual counting, three images were manually counted by three lab members and subsequently analyzed using the automated analysis tool which showed a striking similarity (**Figure 12**).

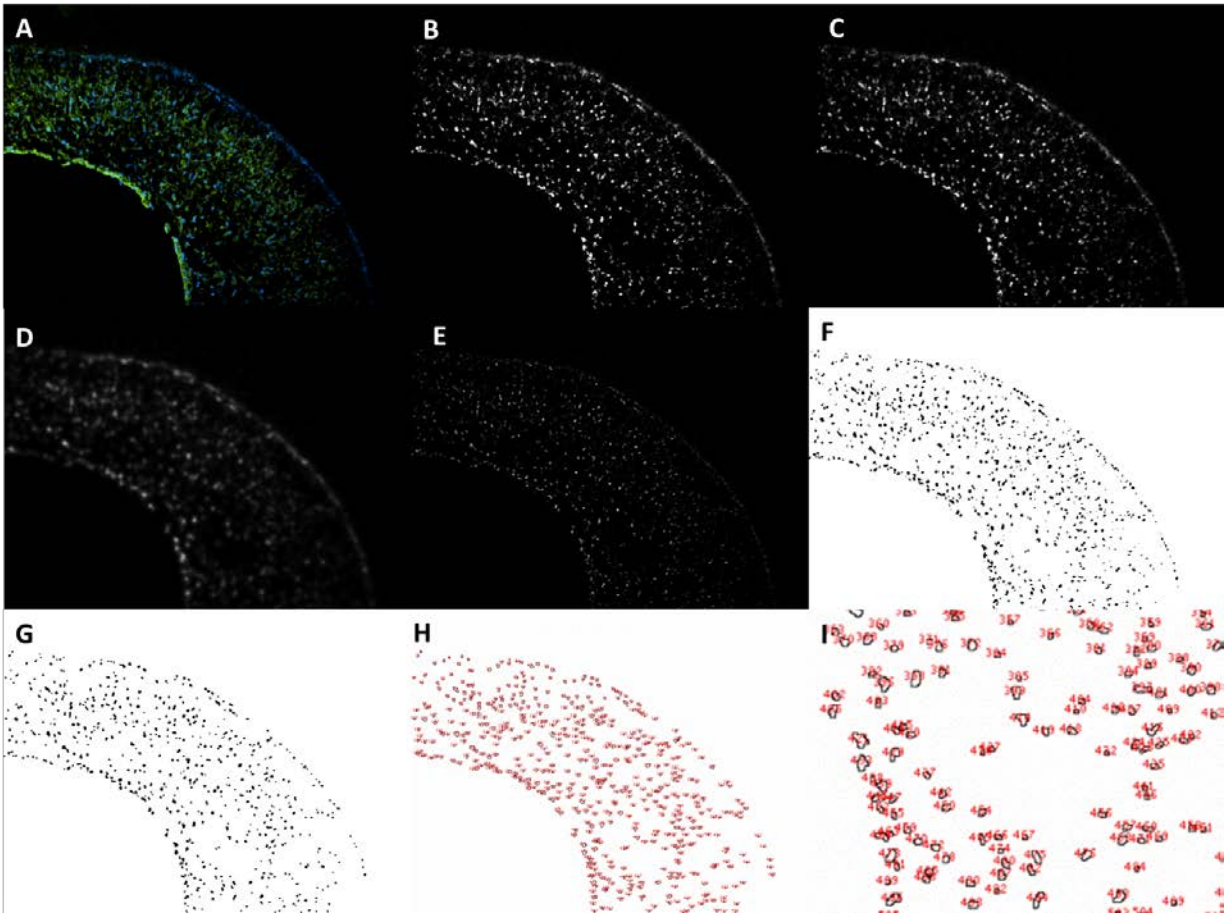

Figure 11. ImageJ cell counting tool procedure. (A) An original multicolored image (or single color) is imported into ImageJ for analysis. (B) The specified individual channel representing the cell nuclei is selected and converted to grayscale. A Gaussian Blur of Radius 1 pixel (C) and 4 pixels (D) is applied to the image and subtracted from one another to reduce background noise and develop more punctate cell nuclei (E). (F) Otsu's Threshold is performed to transform the image to a binary format where all cell nuclei are converted to black and the background is converted to white. (G) Both "Open" and "Watershed" commands are performed to remove small pixel artifacts and separate overlapping cell nuclei, respectively. (H) Finally, each cell nuclei is identified and counted. Blowup image shown in (I).

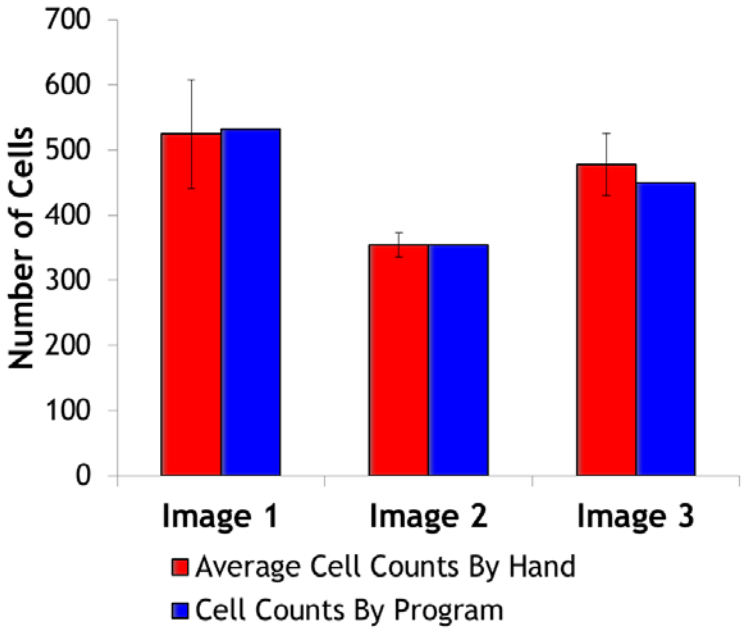

Figure 12. The automated ImageJ cell counting tool produces equivalent results to manual counting. Three lab members performed manual cell counting for three cell seeded TEVG scaffold images. Equivalent results were observed when comparing to the program output.

As a next step, to ensure that cell seeding was consistent between different AD-MSC donor cohorts, scaffolds were seeded with AD-MSCs from each donor (healthy, diabetic, elderly; n=3 per group) and subsequently analyzed with the aforementioned code. In all cases AD-MSCs were successfully seeded within scaffolds at high efficiency (>95% of the infused cells became entrapped within scaffolds) and achieved qualitative uniformity (**Figure 13**). Additionally, F-actin staining revealed that the cells were appreciably spread on the scaffold. Quantitative analysis comparing the number of cells per area across segmented longitudinal, circumferential, and radial directions confirmed this uniformity (**Figure 14**). As an example, when cross-section images were segmented into three radial pieces, approximately one-third (~33%) of the total cells were present in each segment. In all cases statistical analysis revealed a non-significant p-value was shown via one-way ANOVA (radial: 0.94, 0.75, 0.77; circumferential: 0.96, 0.48,

0.65; longitudinal: 0.76, 0.05, 0.26; for healthy, diabetic, and elderly, respectively) confirming uniformity.

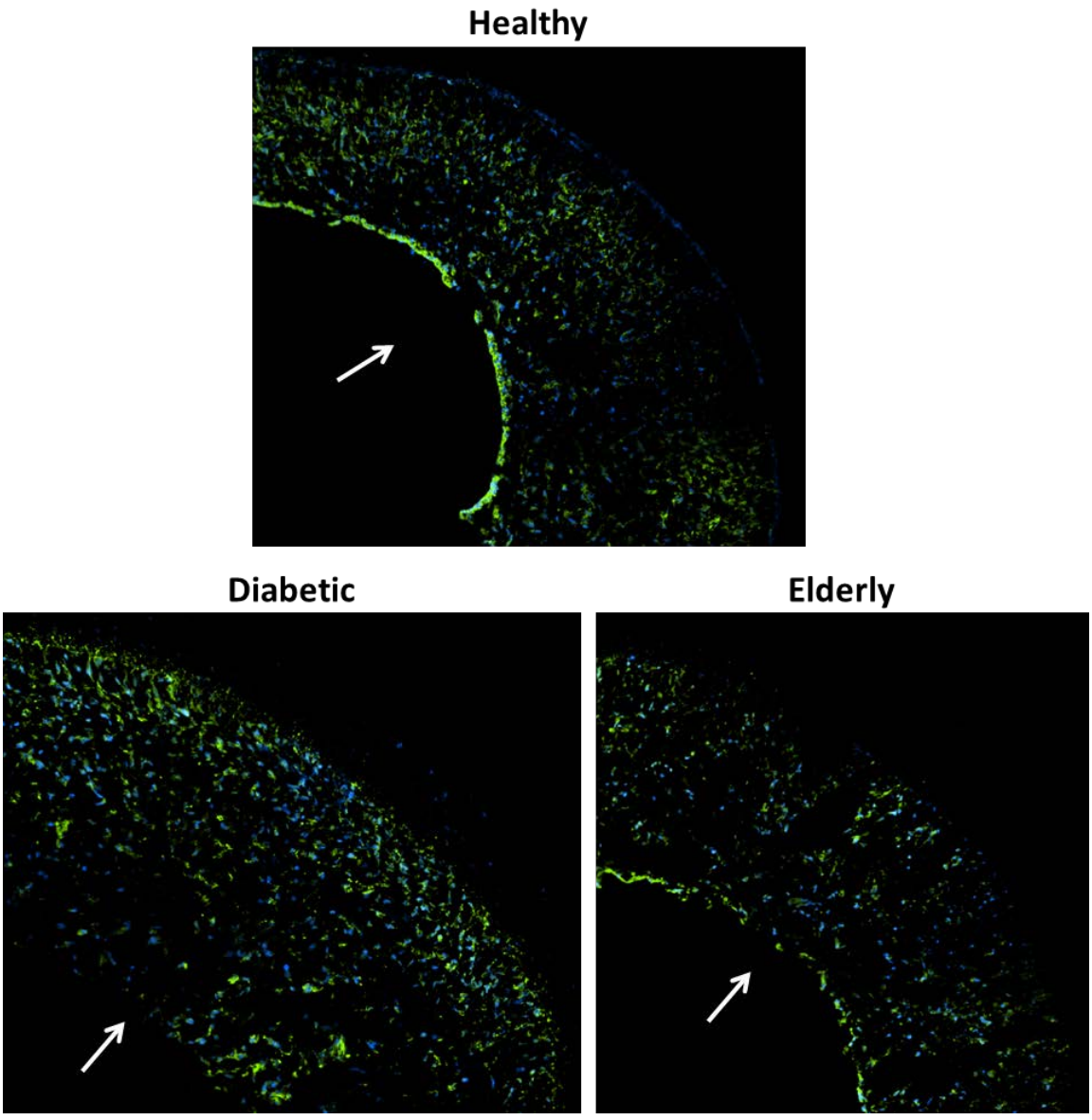

Figure 13. AD-MSCs from healthy, diabetic, and elderly donors qualitatively seed successfully within scaffolds. AD-MSCs from healthy, diabetic, and elderly donors were seeded into scaffolds (n=3) and stained for cell nuclei (blue: DAPI) and F-actin (green: Phalloidin). All scaffolds showed a uniform distribution of cells and consistent spreading along the scaffold. White arrow indicates the lumen.

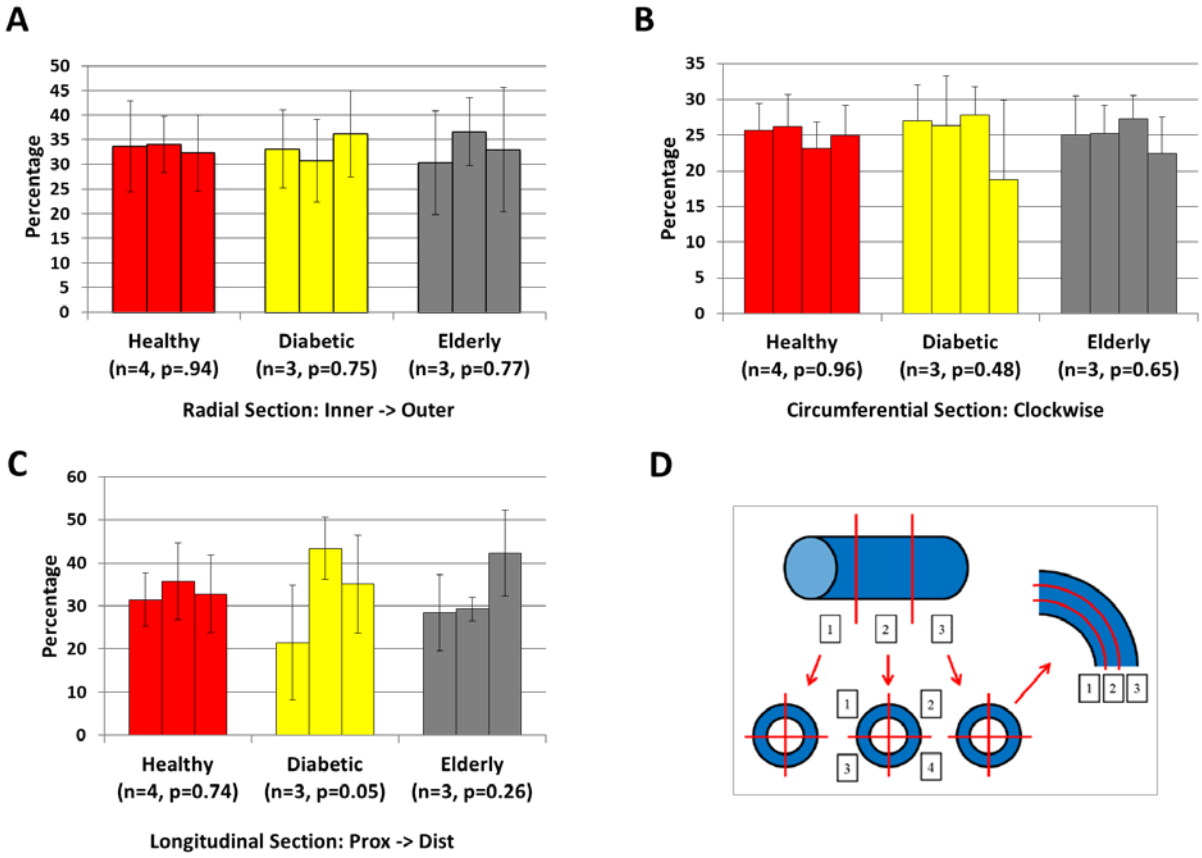

Figure 14. AD-MSCs from all donor groups seed quantitatively uniformly in TEVG scaffolds. TEVG Scaffolds seeded with AD-MSCs from healthy, diabetic, and elderly groups were confirmed as quantitatively uniform by measuring the cell numbers (presented as mean percentage of total ± SD) across radial (A), circumferential (B), and longitudinal (C) segments. The results show that each donor group achieves similar cell numbers regardless of segment or direction (No significant difference was observed with $p>0.05$.). These values are also comparable to a perfectly even distribution (e.g. three radial segments results in 33% for each). When comparing the radial segments adjustments were made based on area as the increasingly larger concentric circle segments would inherently possess more a higher number of cells. A schematic of the segmentation strategy can be seen in (D).

However, one drawback in performing the approach above is that obtaining appropriately paired circumferential segments (i.e. the same scaffold spot for each longitudinal ring analyzed) to compare is difficult due to manufacture artifacts in scaffold and rotation that occurs through processing. This is not experienced while segmenting across the radial and longitudinal directions as the pairs are obvious. As a means to further refine the circumferential analysis, we increased the number of segments to 9 to improve the detection of circumferential uniformity. An illustration of the superiority of this approach can be seen in **Figure 15**. As shown by the example, if significant clumping occurs it is possible to achieve a numerical indication of either uniformity or non-uniformity depending on where the segmentation occurs. However, by increasing the number of segments this error is minimized. Segmenting all AD-MSC seeded TEVGs in this manner utilizing 9 segments still resulted in a uniform circumferential distribution of the cells (**Figure 16**). Additionally, the average variability experienced across these segments was similar between all groups (**Figure 17**) and experienced a normal distribution (**Figure 18**) indicating that any variation experienced in cell seeding was due to random chance and not due to anomalies (which would be experienced if clumping occurred). Admittedly this approach still is not perfect and further refinement could be made in the future by measuring average inter-particle distances.

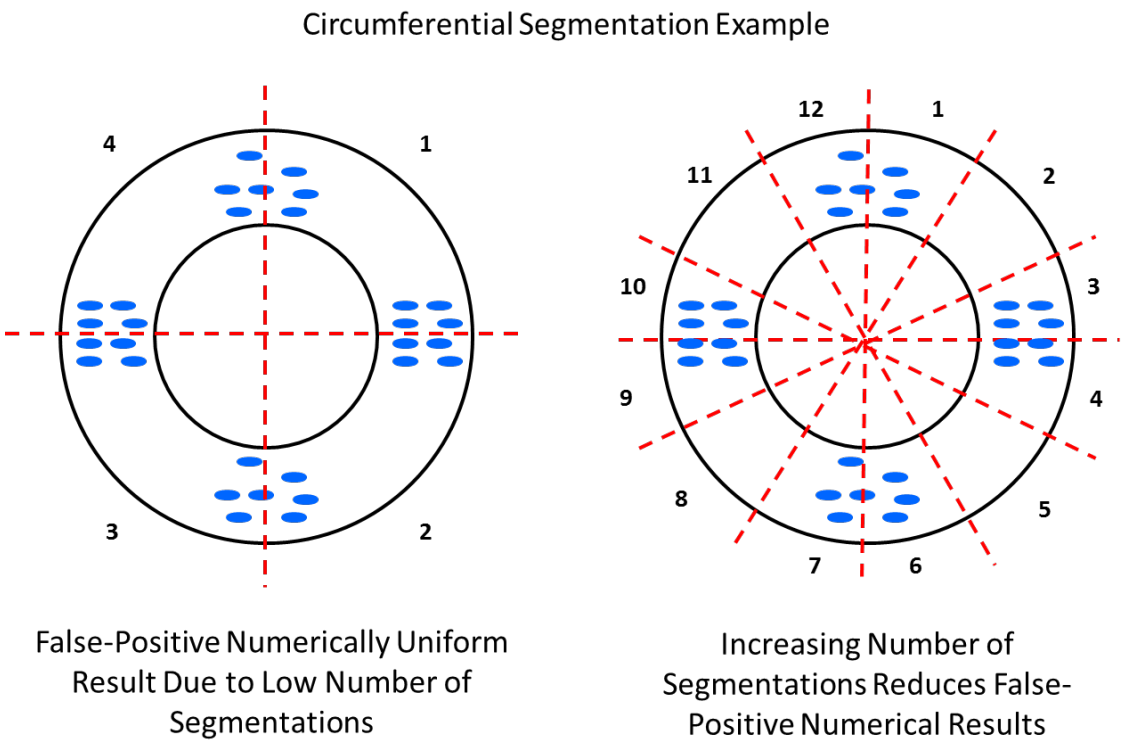

Figure 15. Illustration of a false-positive example of cell seeding analysis and the superiority of an increased number of circumferential segments. An example case is given where if only four segments are utilized (left) the automated cell counting method will determine the cell density per region as similar comparing circumferentially despite the qualitatively obvious non-uniform distribution. However, increasing the number of circumferential segments (right) reduces the chance of this happening.

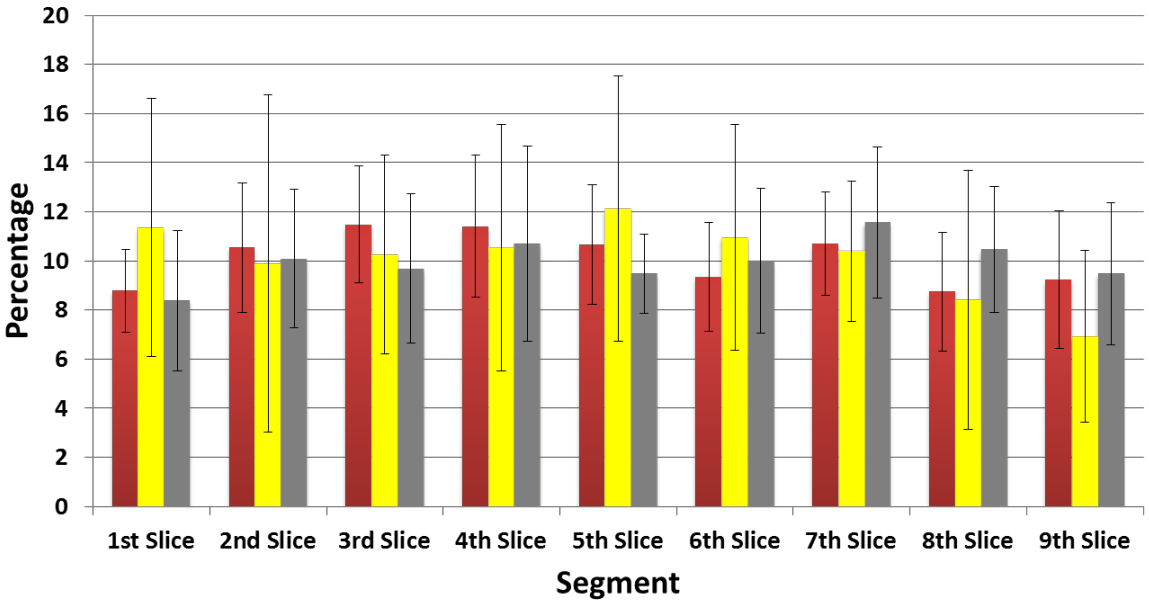

Figure 16. Circumferential analysis of cell seeded TEVG scaffolds with an increased number of circumferential segments. The circumferential analysis seen in Figure 14 was advanced by using a higher number of circumferential segments (9 slices instead of 4 slices). The resulting data further confirm the circumferential uniformity AD-MSC seeded scaffolds composed of cells from all donors (healthy (red), diabetic (yellow), elderly (gray)).

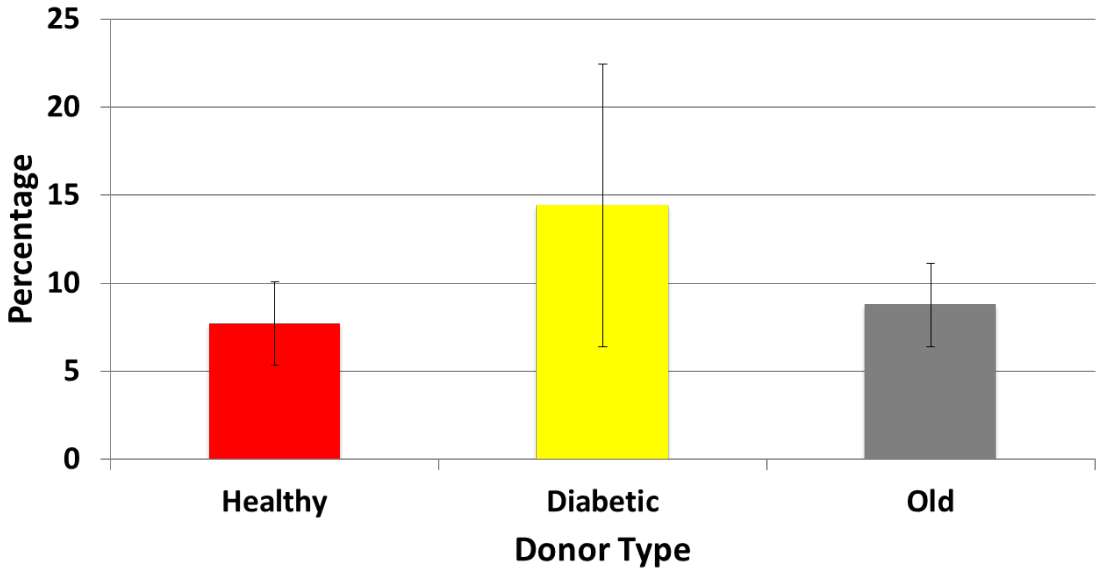

Figure 17. AD-MSC seeded scaffolds have similar variability in the circumferential direction. The average variability between the 9 circumferential slices in Figure 16 was compared between healthy, diabetic and elderly groups and displayed similarity ($p=0.22$). This indicated that there are no anomalies in the seeding distribution (i.e. a uniform seeding was achieved) which would have resulted in unusual increases in variability (as any variability induced strictly by random chance is would be similar across all groups).

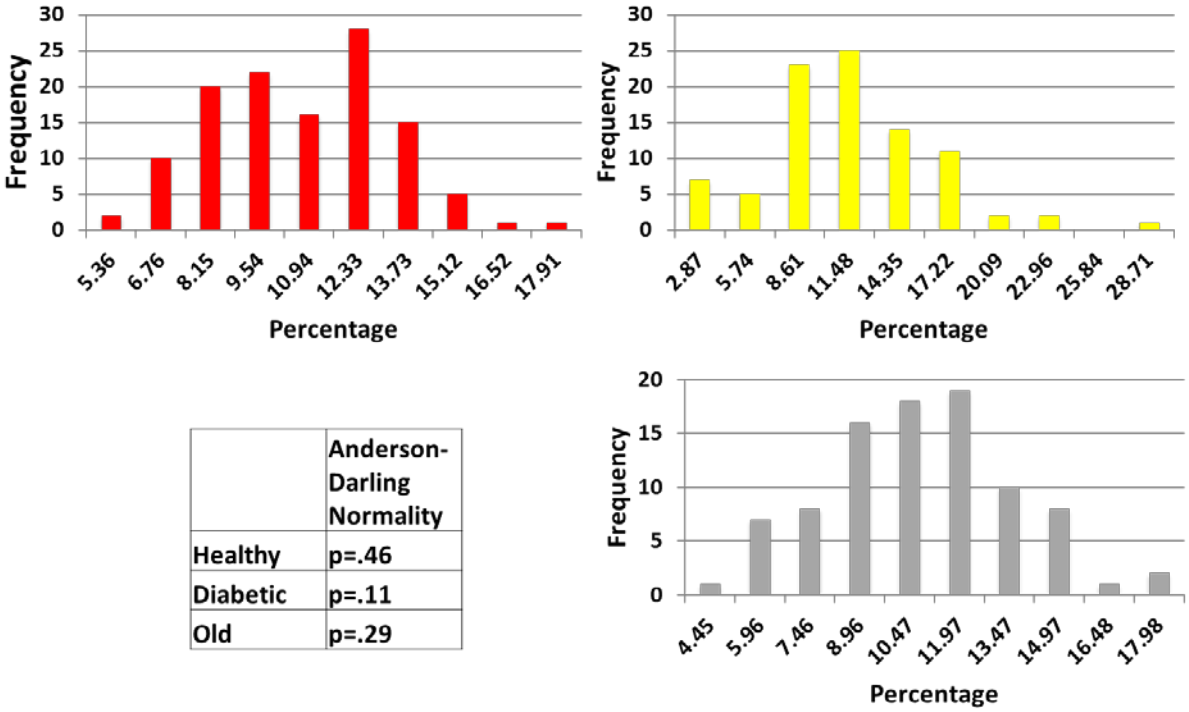

	Anderson-Darling Normality
Healthy	p=.46
Diabetic	p=.11
Old	p=.29

Figure 18. The cell density in AD-MSC seeded scaffolds across the circumferential direction display a normal distribution. The percentage of total cross sectional cell densities across each of the 9 circumferential slices (e.g. theoretical average = 100%/9 = 11%) in Figure 16 (and triplicate images) were plotted as a histogram for each healthy, diabetic or elderly group. A normal distribution resulted for each group further indicating in conjunction with Figure 17 that there are no anomalies in the seeding distribution which would have resulted in unusual increases in variability.

2.3.4 In Vivo Gross Observations and Patency of Healthy, Diabetic, and Elderly TEVGs

Upon implantation of all AD-MSC seeded grafts (**Figure 19**) regardless of donor group, obvious blood flow was observed indicated by a strong distal pulse pressure. Following 8 weeks of maturation in vivo the patency of TEVGs were assessed via angiography wherein only TEVGs which maintained patency would exhibited flow of the contrast agent past the graft to the legs (**Figure 19**). Investigating the donor-related effects revealed that whereas healthy and elderly AD-MSCs were able to produce patent vessels (100% and 71% of the time, respectively), diabetic AD-MSC-based had a marked reduction in this ability (28%) (**Figure 19**). Nearly all animals with non-patent grafts showed debilitating occlusion related symptoms at acute time points (< 1 week) at which point they were euthanized and TEVGs were explanted. Due to the acute timings of these occlusions and due to literature evidence suggesting that this is a time when stem cells are retained within TEVGs (see Section: "1.5.3 In Vivo TEVG Mechanisms") this effect was attributed to the stem cells themselves. However, one single animal with AD-MSC from diabetic donors remained free of symptoms for 8 weeks despite full occlusion of the graft which can occur due to collateral vessel growth. Gross observation of all occluded grafts revealed the presence of a lumenal clot (**Figure 20**). Observation of patent grafts revealed significant remodeling with a tissue-like appearance in the generation of TEVGs, whereas non-patent grafts – even the one that was explanted after 8 weeks – exhibited no such tissue-like appearance (**Figure 20**). In particular, a newly developed vascular-like "neotissue" developed lumenally while the PEUU scaffold TIPS layer (thermally induced phase separation, i.e. the inner layer) showed visual signs of degradation.

A

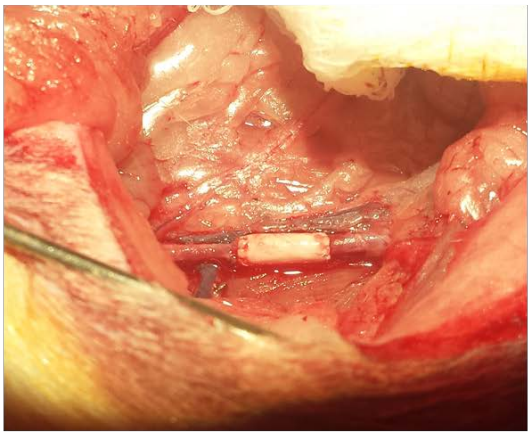

B

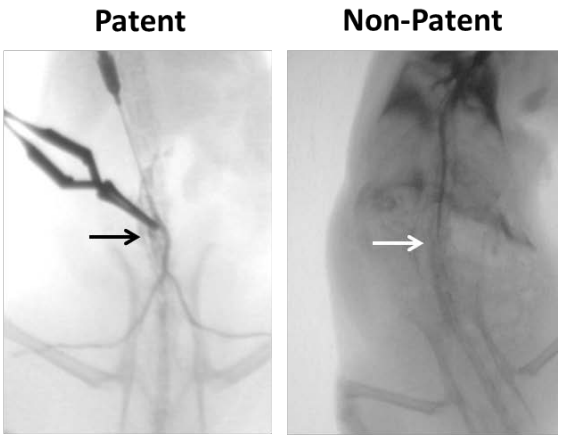

C

AD-MSC Donor Group	Patency
Healthy	100% (8/8)
Diabetic	28% (2/7)
Elderly	71% (5/7)

Figure 19. Diabetic AD-MSCs do not produce patent vessels whereas healthy and elderly do. (A) Example image of TEVG implant is shown. (B) Angiograms were performed to assess the patency of TEVGs at the 8 week endpoint with a patent vessel showing clear flow past the graft to the hindquarters (indicated by arrows). (C) Total patency rate was calculated based on the number of patent vs. total TEVGs; note that TEVGs created using cells from diabetic donors show a marked reduction in patency.

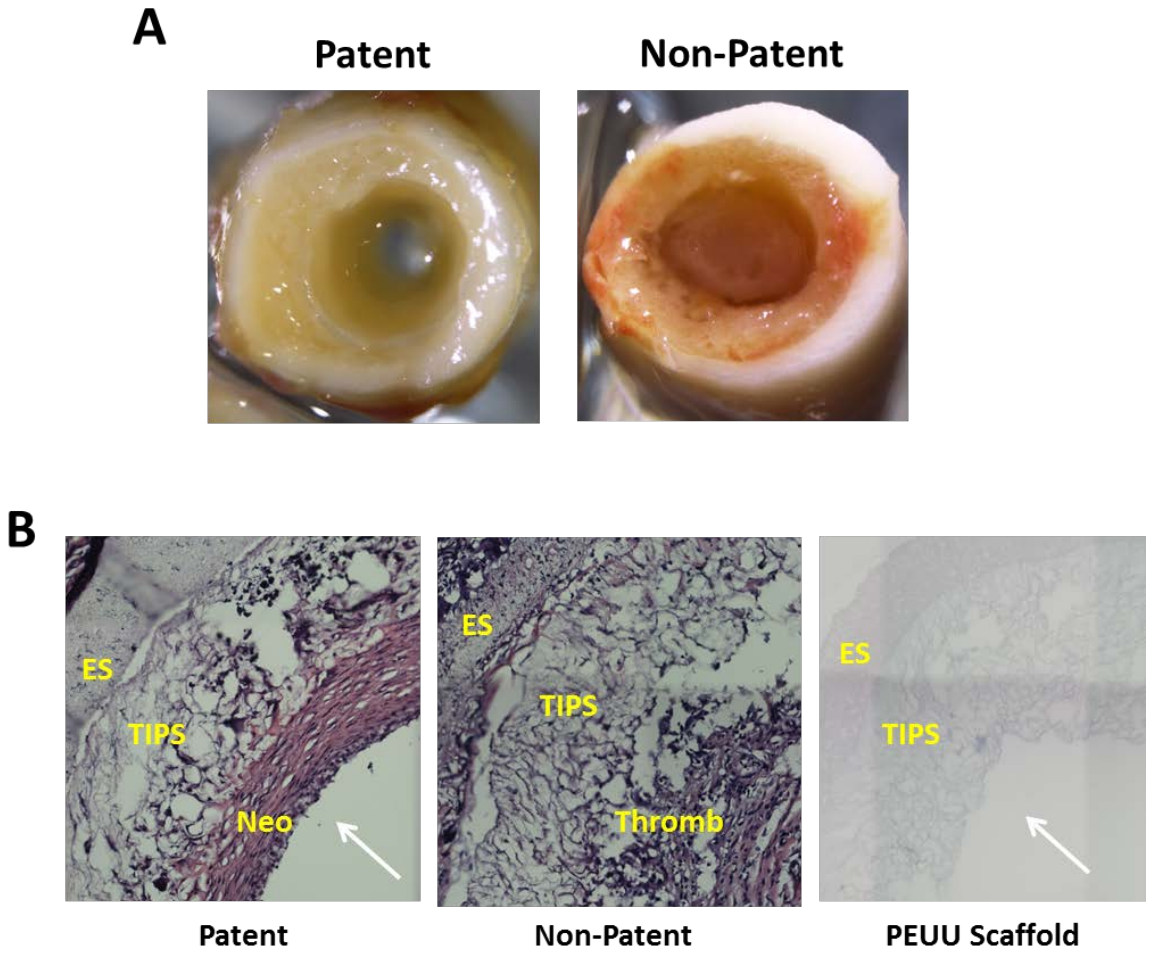

Figure 20. Occlusion of diabetic TEVGs is due to thrombosis. (A) Gross inspection of the explants revealed that the primary reason for non-patent TEVGs was occlusive thrombosis. (B) H&E stained sections of a patent 8 week TEVG, a non-patent 8 week TEVG, and a non-implanted PEUU scaffold. Significant remodeling of patent TEVGs included newly developed neotissue (Neo) lumenally and breakdown of the original PEUU scaffolding material (inner layer: TIPS, outer layer: ES). Occluded grafts displayed presence of a thrombus and no remodeling. Arrows indicate lumen.

2.3.5 Morphometric Measurements of Explanted TEVGs

Three morphometric measurements were performed on all patent TEVGs explanted at 8 weeks (n=8 healthy, n=2 diabetic, n=4 elderly): cell density, neotissue thickness, and nuclear shape factor (an indication of circumferential alignment). All of these parameters were equivalent across donor groups (**Table 2**; one-way ANOVAs for cell density ($p = 0.7$), neotissue thickness ($p = 0.22$) and nuclear shape factor ($p = 0.68$)). Comparing to native artery controls however, neotissue thickness and shape factor were similar but TEVGs had a higher cell density (**Table 2**).

Table 2. All quantified morphometric, histological, and micro-architectural parameters of patent TEVGs. No statistical significance was seen comparing between healthy, elderly, and diabetic parameters.

	Healthy	Elderly	Diabetic	Native Artery
Cell Density	5.1 ± 1.6	5.3 ± 0.6	4.3 ± 0.8	2.4 ± 0.1
Neotissue Thickness	102.3 ± 28.7	115.2 ± 23.0	141.1 ± 23.6	87.4 ± 7.6
Shape Factor	0.81 ± 0.04	0.79 ± 0.04	0.81 ± 0.05	0.78 ± 0.04
% Cells SMA-Postitve	99.8 ± 0.4	96.7 ± 4.1	100 ± 0.0	100 ± 0.0
% Cells Calponin-Postitve	77.6 ± 14.8	74.1 ± 8.4	81.7 ± 8.4	100 ± 0.0
% Lumen vWF-Positive	95.6 ± 5.6	96.1 ± 2.7	94.7 ± 7.4	100 ± 0.0
Fiber Intersetcion Density	13.9 ± 3.4	16.3 ± 0.16	14.0 ± 0.3	8.6 ± 1.8
Segment Length	48.7 ± 6.1	45.5 ± 1.4	50.1 ± 2.2	71.1 ± 17.5
Tortuosity	1.11 ± 0.02	1.10 ± 0.02	1.10 ± 0.01	1.13 ± 0.02
Fiber Orientation	91.9 ± 1.0	92.0 ± 0.6	92.3 ± 2.2	92.1 ± 0.7
Fiber Diameter	11.8 ± 0.4	11.9 ± 0.4	11.8 ± 1.0	13.0 ± 0.2
% Thickness Elastin	93 ± 6	92 ± 9	99 ± 1	100 ± 0

2.3.6 Cellular Composition of Explanted TEVGs

To determine which types of cells and the extent at which they were incorporated within TEVG neotissue, we performed immuno-fluorescent chemistry for the presence of vascular SMCs (SMA, calponin) and endothelial cells (vWF). All patent explanted TEVGs displayed a similar composition with the majority of the tissue thickness being comprised of SMA-positive cells with a continuous lining of vWF-positive endothelial cells along the lumen (**Figure 21**). Quantifying the percentage of cells expressing these markers revealed that SMA-positive cells were indeed distributed through the thickness of the neotissue and that vWF-positive cells were ubiquitous along the luminal surface (**Table 2**). Both of these features were equivalent to native artery controls. Further confirming the presence of SMCs, the marker calponin was also present throughout the TEVG neotissue but while similar across AD-MSC donor groups (**Table 2**; 80%, $p = 0.78$), it was lower than the 100% expression seen in native artery controls.

In this study no neovascularization in the form of vaso vasorum was observed. However this was not expected due to the lack of its presence in rodent aortas [350] and that our neotissue thickness is smaller (<150 μm) than the necessary capillary distance required by tissues (200 μm) [351].

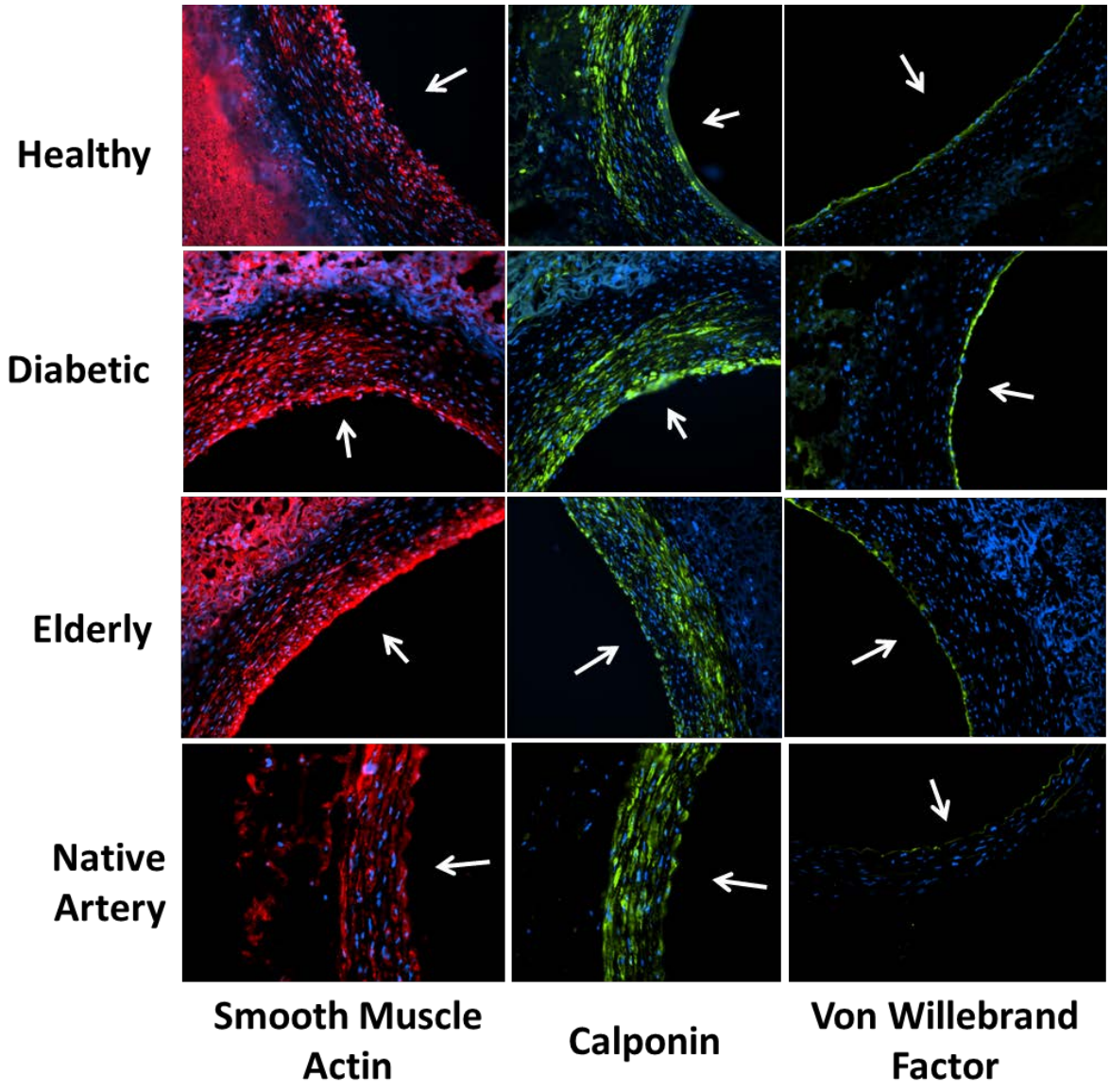

Figure 21. All patent TEVGs display similar cell phenotypes. Patent TEVGs, regardless of AD-MSC donor type, display significant remodeling with the development of neotissue composed of SMA (red; left column) and calponin (green; middle column) positive SMCs, as well as a continuous lining of vWF positive ECs (green; right column) which is qualitatively similar to native arteries (bottom row). All images were counterstained for cell nuclei (blue: DAPI). White arrow indicates the lumen. Note that the residual PEUU scaffolding material produces a significant amount of auto-fluorescence and should not be regarded as positive staining in these images.

2.3.7 Matrix Composition of Explanted TEVGs

To determine the presence of extracellular matrix within TEVG neotissue we performed two forms of microscopic analysis. Multiphoton microscopy was utilized to image collagen, which qualitatively displayed a fiber-like structure (**Figure 22**). Of note is that collagen fibers were not present entirely throughout the neotissue thickness – as they were in native arteries – and were specifically absent near the lumen (**Figure 22**). Utilizing custom scripts developed in MATLAB to analyze the micro-architecture of vascular tissue, we assessed parameters revealing information about fiber intersections, segment lengths between intersections, tortuosity, fiber orientation with respect to the circumferential direction (set at 90 degrees), and fiber diameter (i.e. thickness) (**Table 2**). For each parameter, no difference was observed between any patent TEVG which had utilized AD-MSC from healthy, diabetic, or elderly patients (one-way ANOVAs for fiber intersections: 0.48; segment lengths: 0.56; tortuosity: 0.93; fiber orientation: 0.9; fiber diameter: 0.9). Native artery controls displayed similar micro-architectural parameters with the exception of having fewer fiber intersections (**Table 2**).

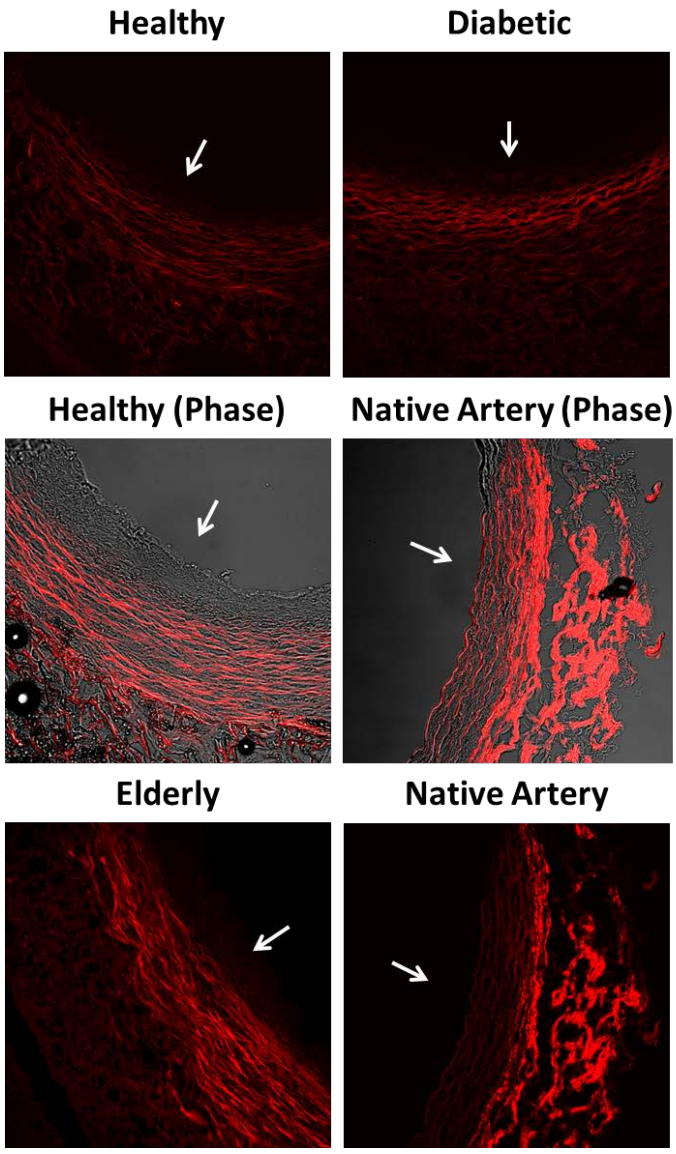

Figure 22. All patent TEVGs have a robust network of aligned collagen fibers. (A) TEVGs, regardless of AD-MSC donor type, display a development of a fibrous, circumferentially aligned collagen network (red). However, the collagen fibers present within a TEVG are not fully distributed throughout the neotissue thickness like that seen in native artery controls (see phase contrast overlay). White arrow indicates lumen.

Immuno-fluorescent chemistry was then used to detect the presence of elastin within explanted TEVGs. Elastin was qualitatively (**Figure 23**) and quantitatively (**Table 2**) present throughout the thickness of TEVG neotissue. This is the same distribution as native artery controls. However, despite the immunological presence of elastin, the pronounced elastic lamellae of native arteries and their inherent autofluorescence was not observed within TEVGs (data not shown).

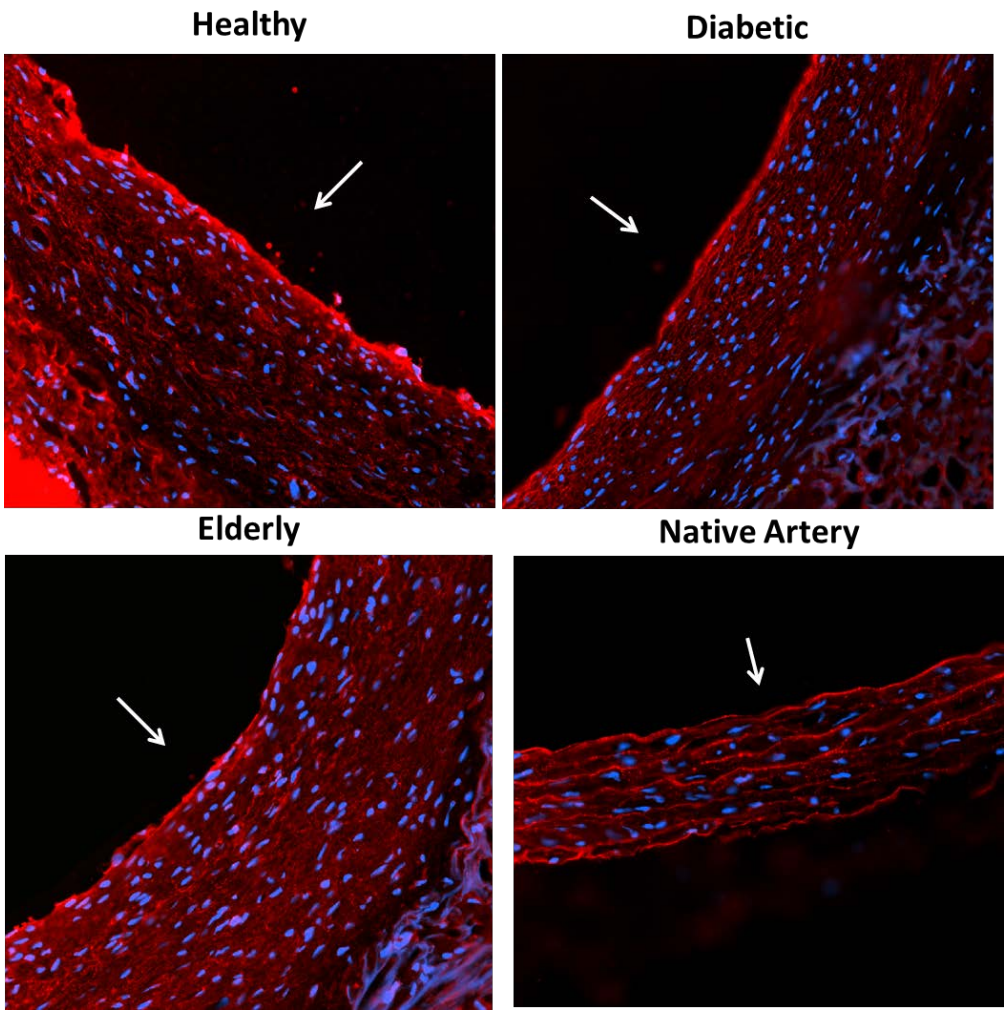

Figure 23. TEVGs display presence of elastin but no elastic lamellae. TEVGs, regardless of AD-MSC donor type, display alpha-elastin throughout the neotissue thickness (red) including a prominent layer next to the lumen. However the prominent medial elastic lamellae which are present in native arteries were absent in remodeled TEVGs. White arrow indicates. Note that the residual PEUU scaffolding material produces a significant amount of auto-fluorescence and should not be regarded as positive staining in these images.

2.4 DISCUSSION

The ability of an implanted scaffold to become populated with functional cellular constituents is a critical factor for success in tissue engineering applications. As discussed in Sections 1.1.3 (“Smooth Muscle Cells”) and 1.5.3 (“In Vivo TEVG Mechanisms”), a TEVG with higher SMC content indicates a greater degree of contractility and correlates with desirable mechanical properties. As many tissue engineering approaches employ biodegradable scaffolds, if insufficient vascular cells are not developed or recruited the TEVG could fail. Additionally, MSCs can guide the maturation process of a TEVG by their ability to differentiate into vascular cells and secretion of factors that can recruit them (see Section: 2.1.2 Definitions of Essential Cellular Functions and Performance Criteria for Vascular Engineering”). In this Aim it was shown that donor demographics in human AD-MSCs can affect the ability to differentiate into SMCs and the ability to produce secreted factors that are responsible for SMC migration. Age diminished both of these the abilities of AD-MSCs while diabetes only affected the ability of AD-MSCs to differentiate. Gender and BMI however did not seem to play a role in either stem cell function, which is surprising since female AD-MSCs proliferate at a higher rate than male ones [352, 353] and BMI is negatively correlated with AD-MSC differentiation capacity [354]. As we have utilized human cells in this study, particularly those from clinically realistic groups, and shown functional differences in a mechanism of action by which TEVGs remodel and the ability of AD-MSCs to form SMCs, this represents is a critical step in the clinical translation of

TEVGs. While these cells may have auxiliary functions such as providing resistance against thrombosis [261], this clearly could reduce the effectiveness of an autologous TEBV therapy.

One area of interest that was not yet investigated in the migration experiments is the effects of each AD-MSC demographic with their respective SMC demographic, such as diabetic SMCs and elderly SMCs. However, these have been previously shown to have increased [355] and deceased [356] migration, respectively, in human SMCs. This parallels the conclusions above that the combination of AD-MSC and SMC of diabetic patients is pro-migratory, where those of elderly is not.

As many TEVG approaches utilize AD-MSCs to differentiate into SMCs (see Section: "1.1.3 Smooth Muscle Cells" and "1.5.3 In Vivo TEVG Mechanisms"), those utilizing elderly and diabetic cells could be heavily affected due to the reduced differentiation potential for both groups. One point worth noting in this regard is that under 1 μM AngII stimulation for 4 days AD-MSCs do not achieve complete differentiation into SMCs as shown by positive staining of calponin (an intermediate differentiation marker) in approximately 30-50% of AD-MSCs with no staining for myosin heavy chain or smoothlin (both late differentiation markers).

We have also shown that the ability of AD-MSCs to induce SMC migration is decreased upon heat inactivation indicating that these secreted factors likely operate on a protein level. One likely explanation could be that growth factors secreted by MSCs are responsible for this pro-migratory function. Indeed we have shown that one known factor to promote SMC migration, VEGF, is present in our conditioned media. However, many growth factors produced by AD-MSCs are pro-migratory for SMC [357] but also can induce other mitogenic, proteolytic, extracellular matrix producing, inflammatory, and angiogenic effects [187]. This is concerning for studies that target elderly patients as the same growth factors that lead to the deficiency in

promoting SMC migration may also affect other applications beyond TEVGs. Additionally, with AD-MSC secreted factors showing a dose dependent response, the need to optimize the number of cells utilized in cell therapy approaches is clear.

Additionally in this Aim we have shown that scaffolds seeded with AD-MSCs from human patients can remodel into native-like TEVGs following 8 weeks of implantation. Among the three different donor populations analyzed (healthy, diabetic, elderly) – which included two cohorts at high cardiovascular risk – a low patency rate for the TEVGs was found only when using AD-MSCs from the diabetic cohort. TEVG failures were consistently due to thrombotic occlusion at an early timepoint. Throughout the study we took measures to minimize confounding effects (e.g. using the same gender, avoiding overlapping age brackets between elderly and diabetic patients) and ensured that in vivo effects were not related to fabrication (i.e. poor or non-uniform cell seeding as all TEVGs seeded similarly) of the vascular grafts. For the AD-MSC-based grafts which remained patent, remodeling resulted in a cellular composition and matrix structure closely mimicking those seen in native arteries. We note that there were some exceptions, including a lower percentage of cells expressing calponin in the TEVG, versus native artery, and both the lack of a full-thickness distribution of collagen and pronounced elastic lamellae in the TEVG. We expect that the remodeling process is incomplete at 8 weeks and further SMC maturation and extracellular matrix synthesis will occur. Indeed, several groups have shown that TEVG remodeling is a long-term process [49, 162, 276]. Providing further evidence to the continued remodeling in our TEVGs at this time point is the presence of collagen abluminally and the presence of calponin lumenally. Based on this configuration it is likely that abluminal SMCs are currently engaged in a synthetic phenotype wherein they are actively depositing collagen and those closer to the lumen are assuming a contractile phenotype.

We have demonstrated here that cells from a diabetic patient cohort fail in our TEVG application where cells from healthy patients do not. Since it is a common practice to use cells from healthy patients in pre-clinical studies [47-49, 61, 62, 161, 163, 178, 181, 206, 216, 235, 237, 239, 240, 244, 255-258, 260-264, 267-277, 280] (see Section: "1.5.1 Improper Cell Sourcing"), we would contend that testing cells from the intended patient cohort (and therefore the source of autologous cells) is critical. Additionally, while only AD-MSCs were tested in this study, other cell types routinely utilized in vascular engineering such as endothelial cells [106, 116, 358-360], endothelial precursor cells [361-367], and SMCs [106, 355, 356, 359, 360, 368] can also be affected by donor demographics. Several questions remain about the donor effects observed here, including 1) What is the mechanism for thrombotic failure seen with cells from diabetic donors?, and 2) What other high-risk donor populations could possess ineffective cells for this graft strategy? Answering these and similar questions could be the next frontier in autologous vascular engineering.

Cells from elderly patients induced successful remodeling of the scaffolds utilized for the TEVG. This was unexpected since also shown in this Aim is that AD-MSCs from elderly patients were defective at differentiating into SMC and inducing SMC migration. As such we had expected less SMCs in the explanted grafts from the elderly cohort. There are a few possible explanations why the elderly-derived cells worked in this in vivo model. One explanation relates to the concept of a "critical size defect". In many models of tissue regeneration, the size of the defect may be small enough (and the host robust enough) that regeneration is successful, while beyond some size threshold therapy is no longer effective. In the current study we employed a 1 cm long scaffold, which is significantly smaller than that required for a human-sized graft (on the order of 10 cm for a coronary artery bypass [143]). It may be that the in vitro deficiency we saw

using AD-MSC from elderly patients will become consequential upon moving to a larger sized graft. Another explanation could be the hemodynamic parameters of the rat interpositional implant model. While this model is useful for initial screening, the local flow and stress patterns will be very different (and more similar to humans) in larger and more geometrically challenging models [369, 370]. Therefore large animal models will be needed to move this technology forward.

2.5 CONCLUSION

In conclusion, the essential functions and criteria for use of AD-MSCs within a TEVG as defined in Section 2.1.2 ("Definitions of Essential Cellular Functions and Performance Criteria for Vascular Engineering") were evaluated across two clinically relevant human donor populations (diabetic, elderly) which include: 1) the ability of AD-MSCs to differentiate into SMCs, 2) the ability to of AD-MSCs to secrete SMC pro-migratory factors, 3) the ability to successfully seed within TEVG, and 4) the in vivo functional performance.

The presence of diabetes was shown to reduce the ability of SMCs to differentiate but their ability to produce pro-migratory factors was unaffected. However while these AD-MSCs were able to successfully seed within TEVGs scaffolds they displayed poor in vivo performance due to thrombotic occlusion.

AD-MSCs isolated from an elderly population also displayed a decreased ability to differentiate and in contrast to diabetic AD-MSCs, an inability to produce pro-migratory factors. However, while similar to diabetic AD-MSCs in that those from elderly patients were able to

successfully seed TEVG scaffolds, their in vivo performance was unaffected despite both analyzed cellular functions being decreased.

This Aim clearly demonstrates that patient demographics – specifically those at high cardiovascular risk – can negatively affect autologous cells and induce poor performance in TEVG applications. This is particularly shown in those patients with diabetes which fail to thrombosis. However, interestingly all patent grafts – regardless of donor group – are able to develop into robust TEVGs containing key vascular components such as SMCs, endothelial cells, collagen, and elastin. These results indicate that if methods could be utilized to alleviate these thrombotic affects, functionality could be restored to the diabetic population. Further investigation into this will be discussed in Aim 1-2.

2.6 FUTURE WORK

While this Aim makes clear progress in identifying the concerns for the use of autologous cells from realistic clinical populations, this research is still nascent and there are still multiple factors to be investigated. As this study solely isolated the effects of cells by removing biasing effects due to patient demographic cross-over and keeping all other parameters (e.g. scaffold, animal model, etc.) similar, many environmental effects which may affect TEVG performance still must be considered. As discussed above (see Section: “2.4 Discussion”) the presence of diabetes and advanced age have been shown to affect the migratory potential of SMCs. As the main TEVG remodeling mechanism relies heavily on the recruitment of host cells (see Section: “1.5.3 In Vivo TEVG Mechanisms”), understanding this effect is critically important. Adding to this, the diabetic environment has been shown to be pro-calcific which could compromise graft

performance [371] and the functions of AD-MSCs have been shown to be environmentally sensitive [372-374]. Considering both diabetic and aged animal models is an appropriate next step.

Additionally, while removing biasing via strict stratification of donor groups assisted in elucidating differences due to independent effects it did not successfully validate changes that would be observed in the highest cardiovascular risk group: elderly diabetics [100]. However, due to the independent pathologic mechanisms associated with diabetes and aging (i.e. hyperglycemia and age-related senescence, respectively) it is likely that cross-over of cellular effects unique to each group or synergistic effects could occur. Indeed, cross-over of effects have been reported between aged and diabetic conditions [335, 375, 376] and certain effects are not observed until both aging and diabetes happen co-currently [377]. Evaluating this group is a worthwhile next step.

Another concern for the use of animal models is that only a small animal model has been utilized in this study. While this animal model was suitable for this study as it acted to screen TEVGs from multiple patient groups, a larger model could offer several advantages due to their higher similarity to human hematology and vessel geometry [132, 369, 378, 379]. As an example, rodent models have quicker pro-thrombin time resulting in faster coagulation and have substantially more platelets than humans [378]. This could result in a stronger susceptibility to thrombosis. As diabetic TEVGs displayed significant thrombosis, testing in a larger animal model may assist in alleviating this effect. Adding to this, different sized vessels can lead to thrombosis via different mechanisms. For example when considering the role of tissue factor, microvascular thrombosis is dominated by circulating tissue factor whereas macrovascular thrombosis is dominated by vessel wall tissue factor [379]. Additionally, the test bed utilized in

small animal models may not be representative of the intended clinical setting due to their linear geometry. For example a coronary artery procedure will encounter complex geometries and kinking which will not be encountered in our current model [369].

One limitation is that we did not perform extensive mechanical characterization of our TEVGs upon explant which can be another critical factor to their success as discussed in Section 1.3.1 (“General Considerations”). While the mechanics of explanted TEVGs were initially rarely investigated when performing pre-clinical TEVG analysis, more studies have begun to perform these tests in recent years (see Section: “2.7.3 Explanted TEVG Mechanical Testing”). For the purposes of this dissertation a pilot study on the explanted properties of our TEVG was performed as discussed below (see Section: “2.7.3 Mechanical Testing Data”).

Another limitation of this study was that the cells present within the TEVG were not labelled or identified in explanted samples. Doing so could provide further insight into the potential mechanisms of TEVG remodeling as well as guide future experiments when designing the artificial stem cells within Aim 3. To do this, pre-implanted cells could be labelled with membrane dyes, transfected with reporters such as GFP, or identified via immuno-straining by detection of human specific markers. However, one technical challenge in identifying cells within the seeded pores is the strong auto-fluorescence in explanted TEVG scaffolds (see the smooth muscle actin column in **Figure 21** for example images displaying strong scaffold-based auto-fluorescence adjacent to the neotissue).

Finally, while it was shown how diabetes and aging affect the ability of AD-MSCs to differentiate and promote SMC migration via conditioned media, this was not shown for other vascular cells such as endothelial cells. This is due to the fact that the decline of endothelial differentiation of AD-MSCs and the ability of MSC conditioned media to be pro-migratory for

endothelial cells has been shown in other studies [28, 380]. However, differences in the pro-migratory secreted factors due to donor base remains to be investigated and could be pursued in future studies.

2.7 ADDITIONAL STUDIES AND THOSE CONTRIBUTING TO FUTURE WORK

2.7.1 Short Term Implants

In addition to the 8 week implants performed in Aim 1, shorter implants were performed at both 1 and 2 weeks (n=2 each). The implants at 1 week were utilized to confirm the lack of an immune response present when utilizing human cells within a Lewis rat model (see Section: "2.7.5 T cell and B cell Activity Within Implanted TEVGs") and to assess short term TEVG remodeling for the future tuning of the acellular TEVG proposed in Aim 3. Immuno-staining for SMA and vWF revealed the early stages of SMC recruitment to the graft but also completely lack of ECs (**Figure 24**). This is in contrast to the well-developed neotissue present at an 8 week time point.

Explants performed at 2 weeks were done as a pilot study for assessing the mechanical properties of our TEVG. The results can be seen in Section 2.7.3 ("Mechanical Testing Data").

In the future it is important to evaluate the dynamics of the remodeling process particularly for the development and tuning the release of the artificial MSC technology being developed in Aim 3. In this manner the evaluation of the TEVG composition should be performed to identify the presence of vascular components (i.e. EC, SMC, collagen, elastin) and the implanted AD-MSCs in order to understand the necessary timing of delivered factors. While

some work has been performed in the Vorp laboratory to track the presence of human cells using fluorescent in situ hybridization (FISH) showing minimal presence of human cells at 8 weeks [260], tracking can also be done through dyes, GFP labelling, or human-specific antibodies. In this study it was preliminary shown that at short timepoints (3 days from a diabetic thrombosed sample; 1 week from a patent healthy sample) human cells were present, however at later time points (8 weeks) they were absent via staining for the MSC marker CD90 (**Figure 25**). Additionally, this antibody was confirmed via positive staining in an MSC seeded scaffold and negative seeding in a rat artery (data not shown). This staining also suggests that the poor patency observed in diabetic TEVGs is due to their diminished anti-thrombogenicity due to their persistence in TEVGs at times when clotting occurs.

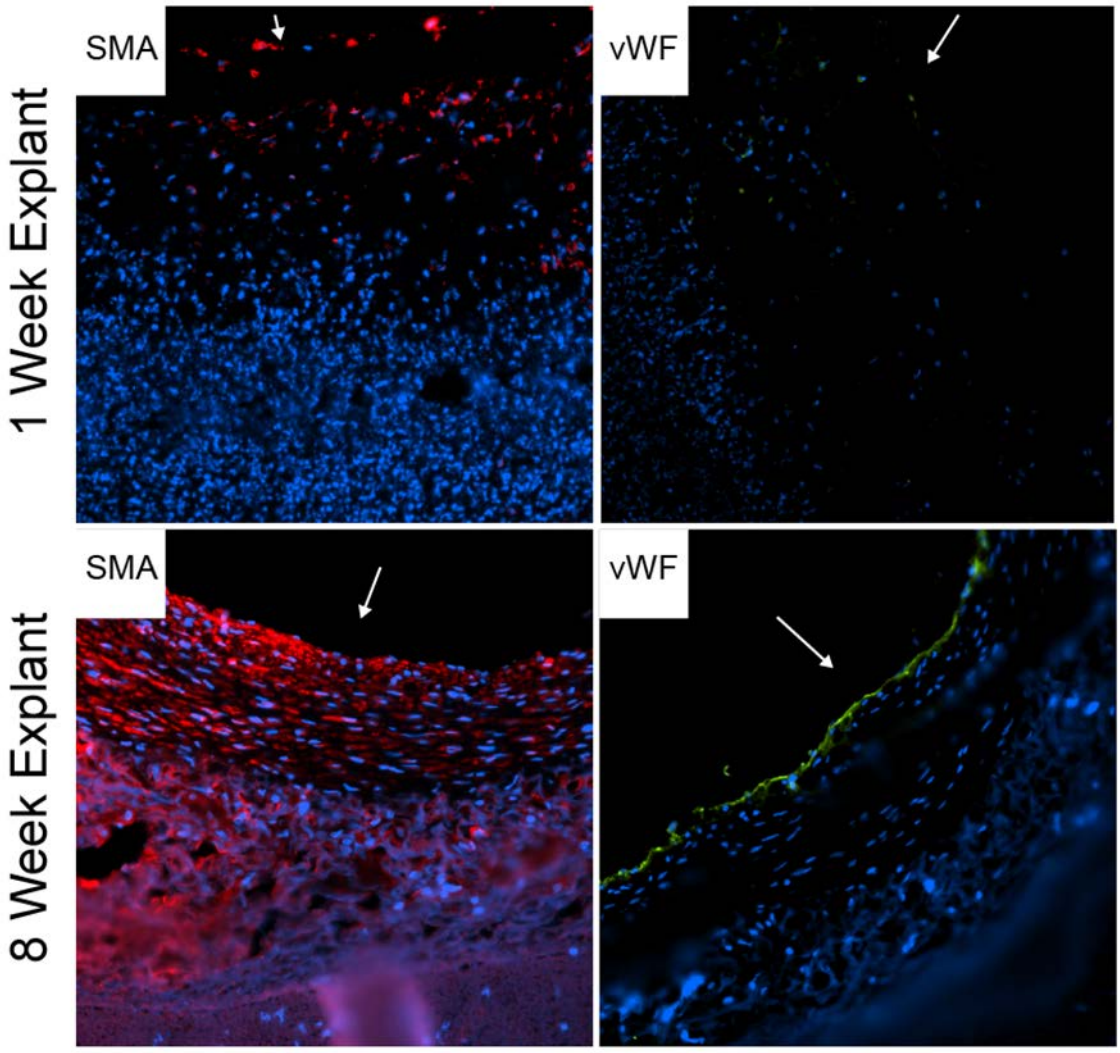

Figure 24. Short-term implantation reveal incomplete recellularization with vascular components. PEUU scaffolds seeded with AD-MSC were implanted for 1 or 8 weeks (see Aim 1-1). After explantation, the vessels were analyzed for using immuno-fluorescent staining for the SMC marker smooth muscle alpha-actin (SMA) or the EC marker von Willebrand Factor (VWF). Recellularization is incomplete with 1 week of implantation, but complete by 8 weeks. (n=2, lumenal surface is indicated by white arrows).

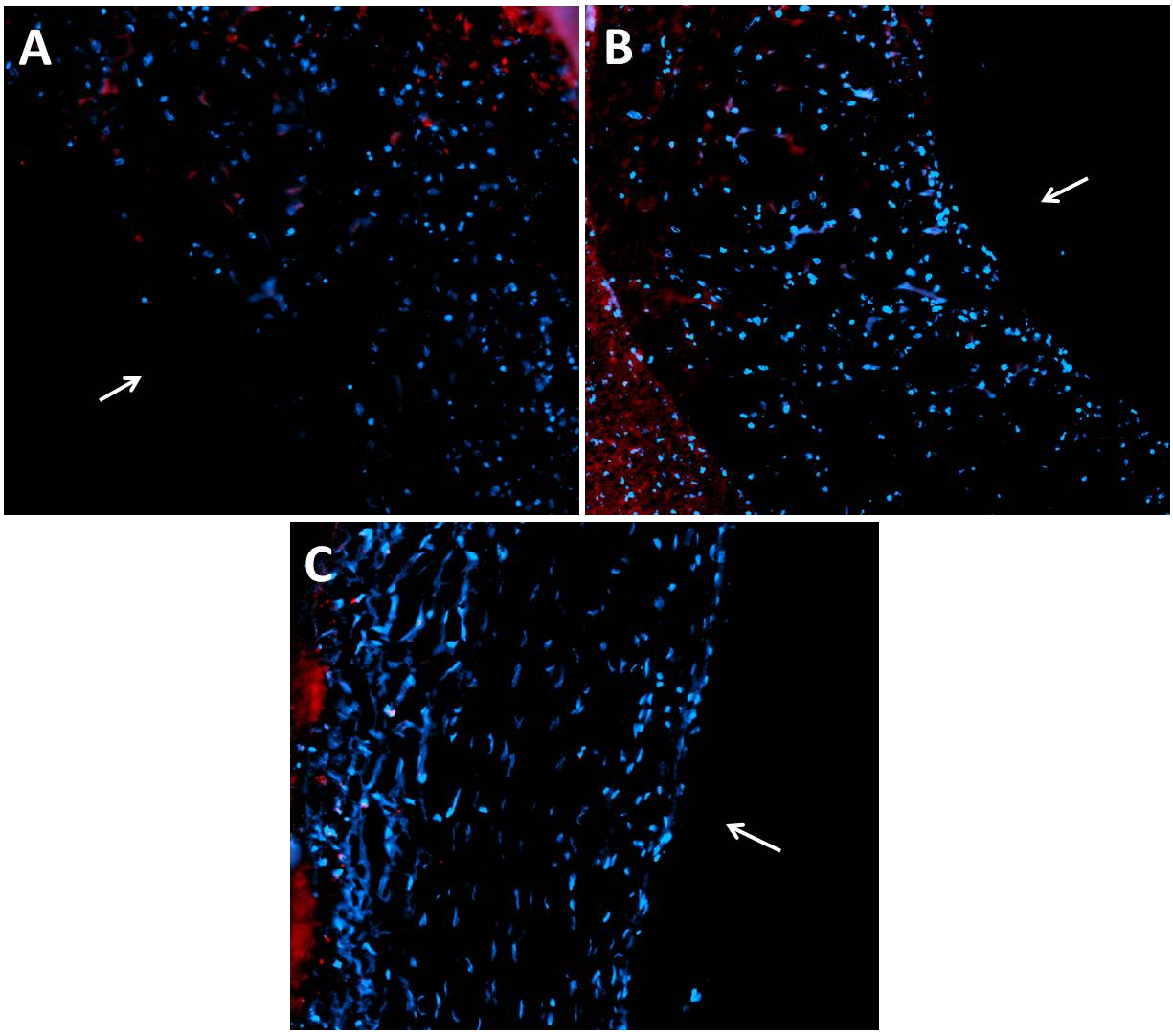

Figure 25. Immuno-staining for human CD90 reveals presence of implanted cells during short term implantations. Explanted TEVGs were stained with human specific CD90 (red; counterstained with DAPI (blue)) to identify the presence of implanted AD-MSCs in explants consisting of (A) a clotted TEVG seeded with diabetic AD-MSCs at 3 days, (B) a patent TEVG seeded with healthy AD-MSCs at 1 week, (C) and a patent TEVG seeded with healthy AD-MSCs at 8 weeks.

2.7.2 Further ECM Characterization via Mason's Trichrome and Verhoeff Van Gieson

In addition to the extracellular matrix data on collagen and elastin generated from immuno-fluorescent microscopy, a subset of TEVG explants were stained with Verhoeff-Van Gieson (VVG) and Mason's Trichrome to identify collagen and elastin, respectively. All grafts showed clear presence of elastin (black) and collagen (blue) further validating their presence within TEVGs (**Figure 26** and **Figure 27**).

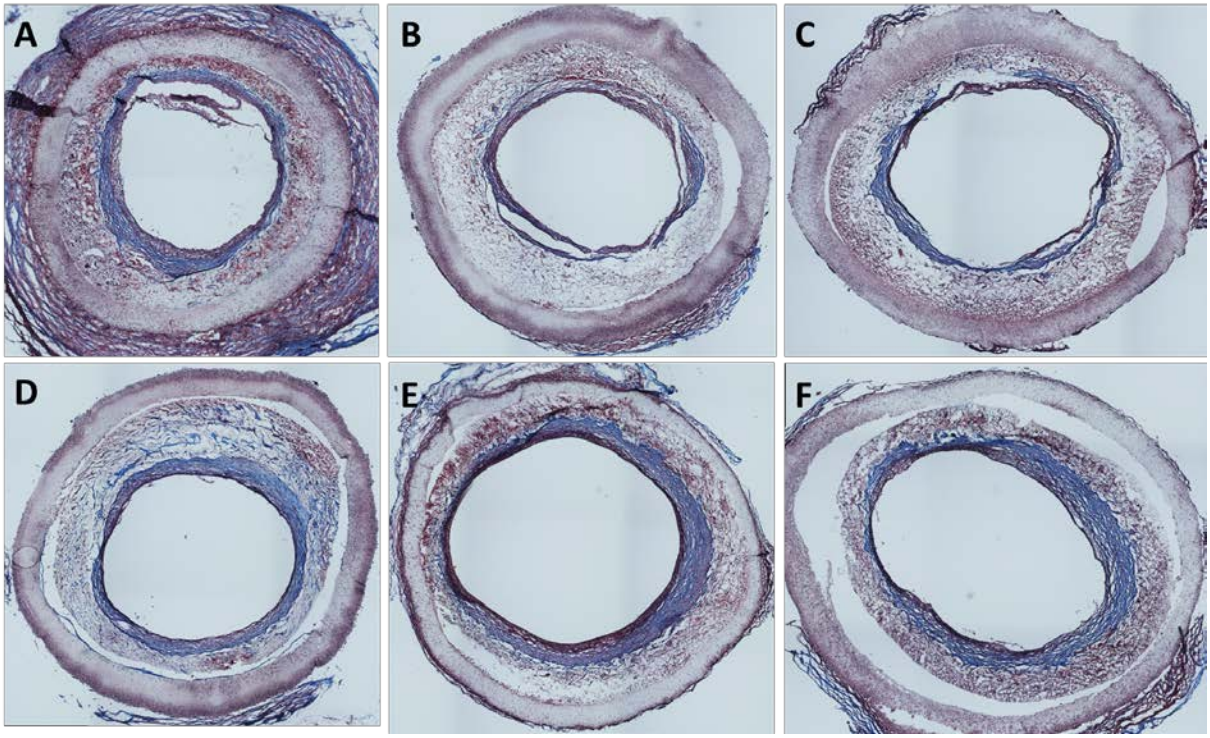

Figure 26. Characterization of 8 week TEVG explants by Mason's Trichome staining. Further characterization of the extracellular matrix was performed using Mason's Trichrome staining which indicates collagen (blue). Only healthy (A-C) and elderly (D-F) AD-MSC-based explants were used in this analysis which both displayed clear development of collagen within TEVGs.

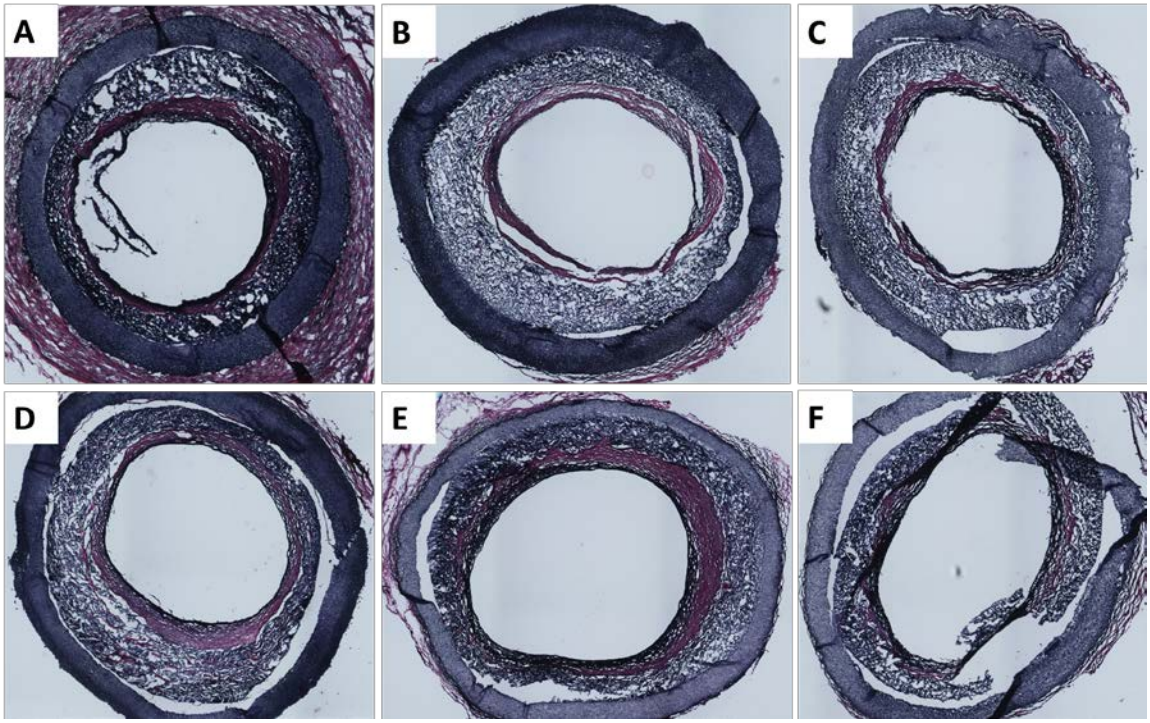

Figure 27. Characterization of 8 week TEVG explants by Verhoeff van Gieson staining. Further characterization of the extracellular matrix was performed using Verhoeff van Gieson Staining which indicates elasatin (black). Only healthy (A-C) and elderly (D-F) AD-MSC-based explants were used in this analysis which both displayed clear development of elastin within TEVGs.

2.7.3 Explanted TEVG Mechanical Testing

Understanding the mechanical properties of the TEVG throughout its in vivo development is a critical concern as they can be predictive of failure mechanisms such as intimal hyperplasia and graft rupture. However, another aspect of TEVG mechanics is that early stage mechanical properties can influence those in the long term [64]. In particular, a study performed by Khosravi et al. showed that the presence of a TEVG that possesses a higher stiffness at an early time point in vivo – than to a less stiff one, all other things being equal – will result in a stiffer graft at later time points [64]. Indeed, due to the importance of mechanical properties, studies are now beginning to emerge investigating the mechanical properties of explanted TEVGs [47, 49, 63,

64, 153, 160, 252, 273, 275]. In addition to the analysis in Aim 1, a preliminary investigation was performed to investigate the mechanics of our TEVG upon explant wherein dynamic compliance and uniaxial tensile testing were performed on a subset of the grafts. Included in this analysis is one SVF composed TEVG from Aim 2. The cell lines used for the 8 week implants from the following cell line numbers (see **Table 1**): 2, 16, SVF8, SVF 5 p4, SVF 7 p4, and SVF 8 p4.

To measure dynamic compliance, explanted TEVGs were placed within an ex vivo vascular perfusion system using previously established protocols [165] where they were subjected to pulsatile physiologic pressure waveforms (120/80 mmHg) via a Bio-Medicus pump (#520D). During this time a laser micrometer was utilized to measure the outer diameter of the TEVG with dynamic compliance was then calculated as (D120 – D80)/(D80*(P120 – P80)). Immediately following, the TEVGs were removed from the system, cut circumferentially into rings and were tested uniaxially using an Instron Tensile Tester (#5543A) following established protocols [165]. The mechanical parameters were calculated from the resulting stress(Cauchy)-strain curves: ultimate tensile stress (UTS; maximum stress experienced by the sample) and the tangent modulus in the both the physiologic region (between 120 and 80 mmHg) and the elastic region. Additionally, in both these studies sections of native rat aorta explanted proximal to the TEVG were utilized to reflect native-like properties.

Dynamic compliance testing (**Figure 28**) revealed that all TEVGs, regardless of time point or donor group, had limited compliance in comparison to native rat aorta controls. Additionally, TEVGs explanted at 8 weeks were less compliant than those at 2 weeks or our initially implanted scaffolds which have compliance similar to native vessels [165]. From this we

hypothesized that our TEVGs could be experiencing calcification which was analyzed in the following section (see Section: “2.7.4 Calcification of Implanted TEVGs”).

Tensile testing (**Figure 29**) revealed that explanted TEVGs have a tensile strength (UTS) and tangent modulus 10-fold less than that seen in native vessels. Additionally, unlike native vessels scaffolds which display a singular peak stress, explanted TEVGs displayed a biphasic response. This was noted to be due to the difference in mechanics in the inner scaffold layer (neotissue/TIPS) which fractures first compared to the outer scaffold layer (electrospun). Despite these differences, the strength of TEVGs increased with further in vivo maturation (2 weeks to 8 weeks) and all explanted TEVGs display tangent moduli in the physiologic region on the same order of magnitude as native vessels.

One noteworthy observation is that although both mechanical tests introduce circumferential stretch, a loss in compliance was shown when performing pressure-diameter testing but a higher stiffness was not shown when performing uniaxial tensile tests. There are two main reasons for these differences. First, the pressure-diameter testing is a biaxial test (circumferential and radial) and introduces longitudinal fixation whereas the uniaxial test (strictly circumferential) does not. This allows for more prominent Poisson effects (i.e. reduction of transverse dimensions during elongation of the primary direction) under the assumption of incompressibility which can drastically alter the response. Secondly, the pressure-diameter testing gives global effects of the entire explanted TEVG whereas uniaxial tests only observe local effects (i.e. you are testing multiple ring pieces of the graft as opposed to the graft as a whole). As calcification may not be uniformly distributed throughout the entirety of the graft, there are instances where these effects could be missed.

One final mechanical parameter that was only anecdotally noted was the potential for kinking of the scaffolding material when bending is experienced (**Figure 30**) which could affect TEVG tested in more geometrically complex models. However, this is only noted for blank (i.e. non-seeded scaffolds) and was not further investigated in those that were cellularized. This point remains as speculation and should be investigated in future studies.

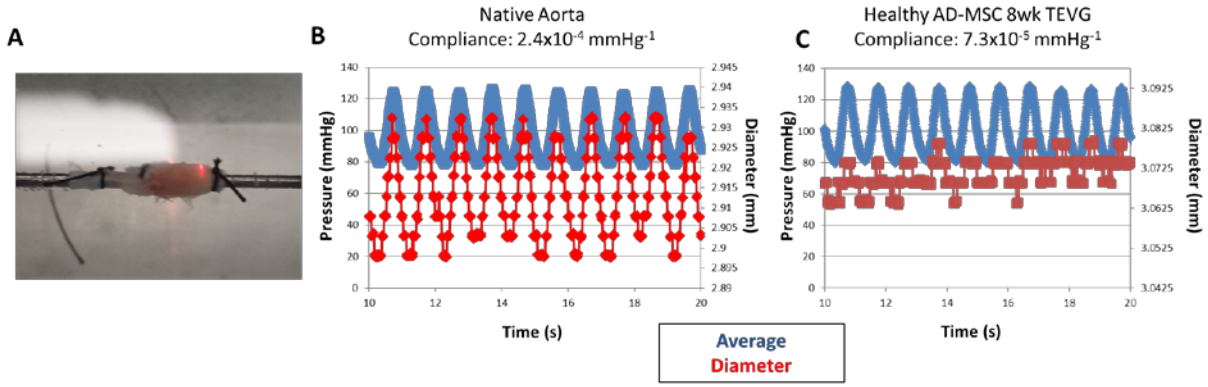

	2 Week Healthy (n=2)	8 Week Healthy (n=1)	8 Week Old (n=1)	8 Week SVF (n=1)	Native Artery (n=2)
Dynamic Compliance ($mmHg^{-1}$)	13.80 ± 3.50 E-05	5.50E-05	7.30E-05	9.79E-05	62.00 ± 53.70 E-05

Figure 28. Explanted TEVGs display limited compliance compared to native vessels. (A) Explanted TEVGs were tested in an in vitro perfusion apparatus where they were applied with a physiologic waveform (120/80 mmHg) and their diameter was monitored with a laser micrometer. While native aortas displayed a high degree of compliance (B), explanted vessels displayed little (C) (y-axis scaled to the same intervals in (B) and (C)). Calculating the compliance values (inclusive table) showed that explanted TEVGs at 8 weeks had compliance an order of magnitude or less than native vessels and this value deceased with increased in vivo maturation (2 weeks to 8 weeks).

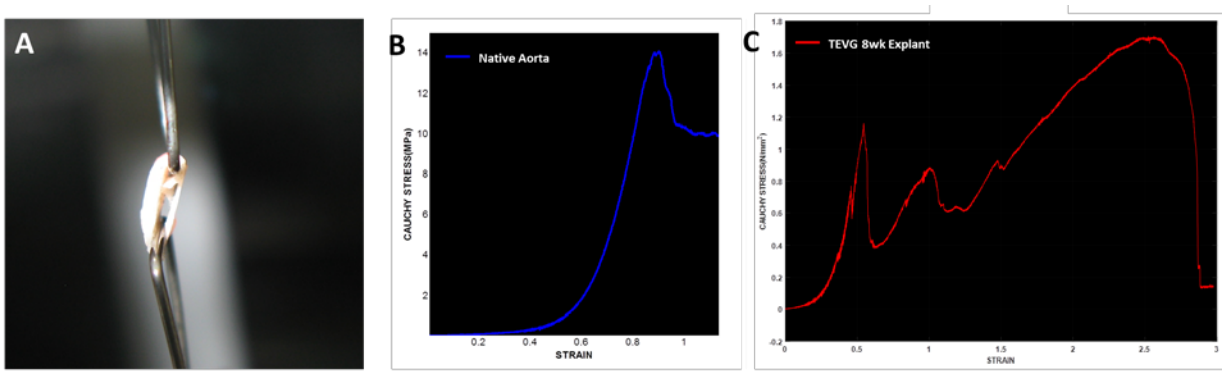

	Mechanical Properties of AD-MSC TEVG Explants				
	2 Week Healthy (n=2)	8 Week Healthy (n=4)	8 Week Old (n=1)	8 Week SVF (n=1)	Native Artery (n=3)
Ultimate Tensile Stress (Neotissue/TIPS) (MPa)	1.16 ± 0.22	1.35 ±0.34	0.60	0.89	
Ultimate Tensile Stress (full) (MPa)	1.18 ± 0.19	4.69 ± 2.31	1.01	2.34	11.81 ± 3.55
Tangent Modulus (physiologic)	0.44 ± 0.03	0.64 ±0.16	0.29	0.54	0.318 ± 0.22
Tangent Modulus (elastic)	3.44 ±2.10	4.22 ± 0.92	2.22	3.68	35.51 ± 14.72

Figure 29. Explanted TEVGs display tensile properties less than native vessels. (A) Explanted TEVGs were cut into rings and stretched uniaxially to measure tensile mechanical properties. The shown image depicts a point where the inner TEVG layer (neotissue/TIPS) has fractured and the remaining force being generated is from the outer TEVG layer (electrospun) leading to a biphasic response. Representative images of stress-strain curves from native aorta (B) and explanted TEVGs (C) as well as quantified mechanical parameters (inclusive table) are shown. The tangent modulus (unitless, i.e. MPa/MPa) within the physiologic range was defined as the slope of the stress-strain curve between 120 and 80 mmHg and the tangent modulus (unitless, i.e. MPa/MPa) in the elastic portion was defined as the slope of the linear portion of the stress-strain curve.

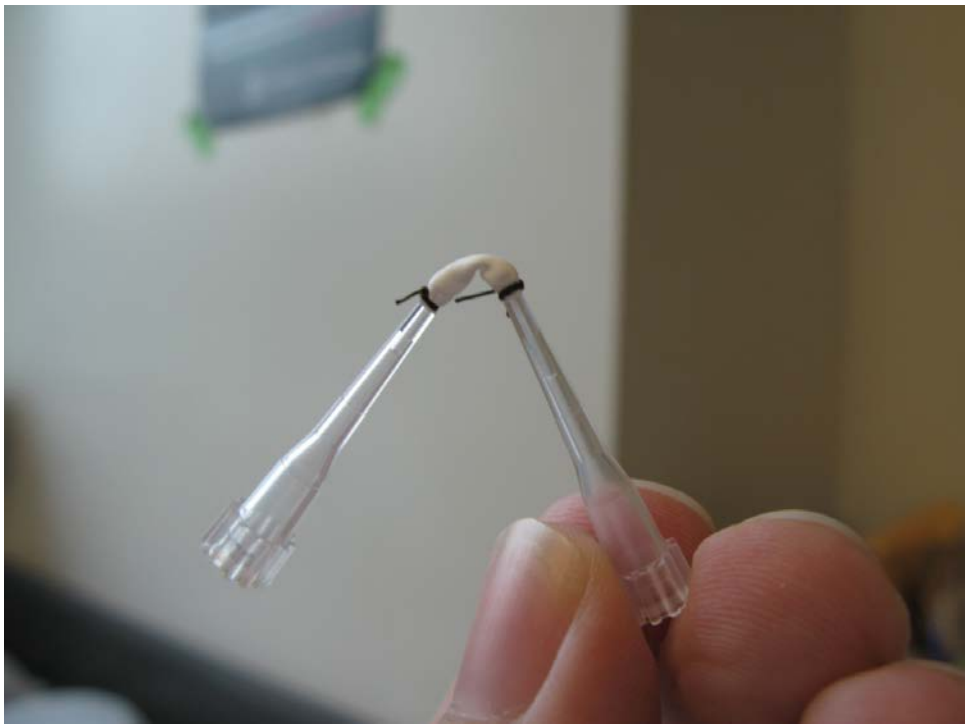

Figure 30. Bending of PEUU scaffolds results in kinking. The TEVG within this study utilizes a linear test bed (i.e. aortic interposition graft). However anecdotally it was noted that kinking can occur in bending of the TEVG scaffolds. This was not assessed further in those seeded with cells but is an important consideration in future studies which may encounter a more geometrically challenging text bed.

2.7.4 Calcification of Implanted TEVGs

As a potential explanation for the lack of compliance seen within our TEVGs – which display native-like compliance values upon implant [165] – we investigated graft calcification which has been shown to occur in vascular grafts composed of synthetic material [66, 150, 238]. Therefore we stained a small subset of our grafts for Alizarin Red (calcium: red) and Von Kossa (phosphates: black) using standard histological techniques. Stains for Alizarin Red revealed sporadic nodules throughout explanted TEVGs and occurred regardless of donor group (**Figure 31**). Additionally, as both Alizarin Red and Von Kossa staining displayed a similar staining pattern, this confirmed these nodules to indeed be composed of calcium phosphate (**Figure 32**). However this effect seems to be mediated by the host remodeling response as when thrombosis occurred in grafts (i.e. no remodeling occurs) calcification was absent (**Figure 33**). Additionally, cell seeded scaffolds revealed no positive staining for Alizarin Red prior to implantation confirming this as a post-remodeling event (**Figure 34**). To further assess whether this was not simply due to the newly incorporated adipose-derived cell type, historical explanted TEVG samples from the Vorp laboratory using human pericytes also stained positive for Alizarin Red (**Figure 35**).

Understanding and addressing the TEVG calcification is critically important for moving forward as one of the prime clinical demographics – diabetics – have been shown to possess a high propensity for calcification [371]. As our TEVGs were tested within a physiologically healthy rat model (i.e. non-diabetic) and still showed degrees of calcification, this effect could be exacerbated in diabetic patients. However, one way to alleviate this may be to alter the scaffold

pore size as TEVGs with larger pore scaffolds have been shown to be more resistant to calcification [238]. Optimization of pore size may also affect the development of extracellular matrix [381].

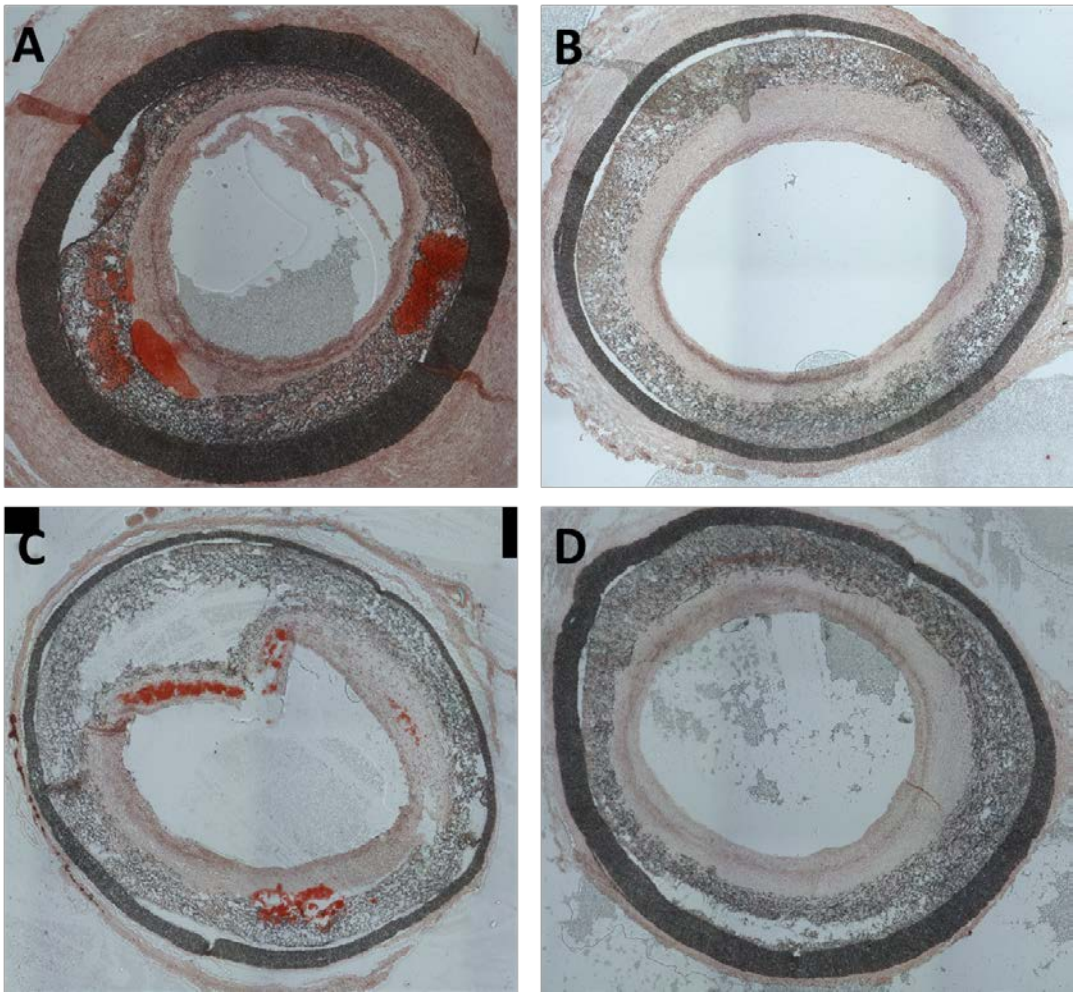

Figure 31. Calcification sporadically occurs in explanted TEVGs. Alizarin Red Staining was performed on explanted TEVG samples which sporadically displayed the presence of calcium rich nodules. This occurred in all cases, regardless of donor. Instances of calcified healthy and elderly TEVGs are shown in (A) and (C) and non-calcified ones are shown in (B) and (D).

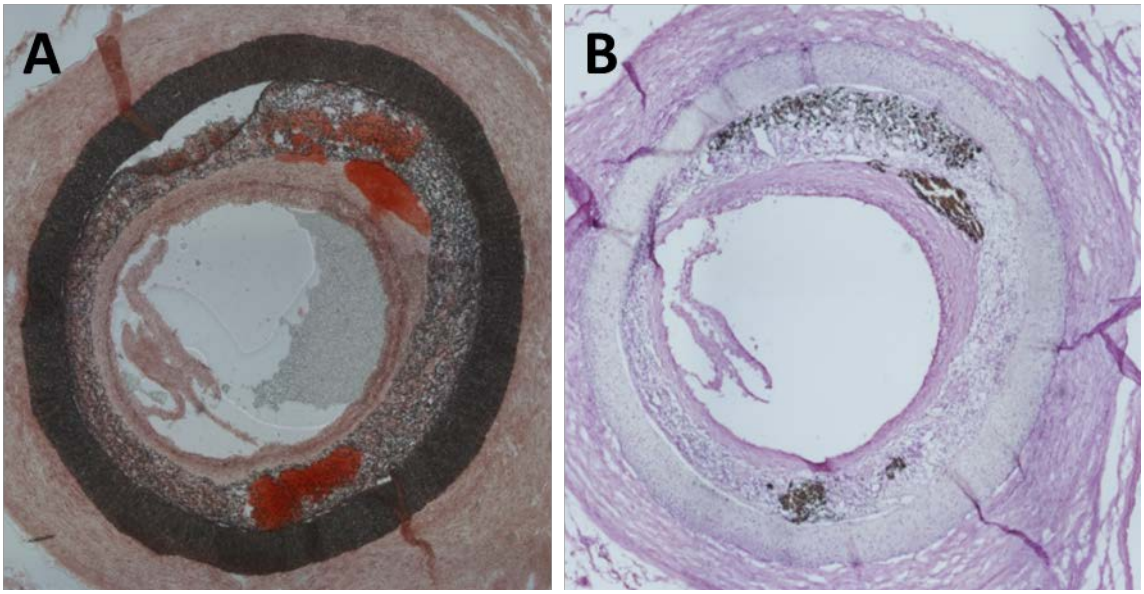

Figure 32. Alizarin Red and von Kossa staining overlap confirmed the presence of calcific nodules. In addition to staining with Alizarin Red which indicated the presence of calcium ions (red), von Kossa staining was also used which indicated phosphate ions (black). As both of these were noted to overlap in the same positions, this confirms the nodules to be calcific and thus composed of calcium phosphate.

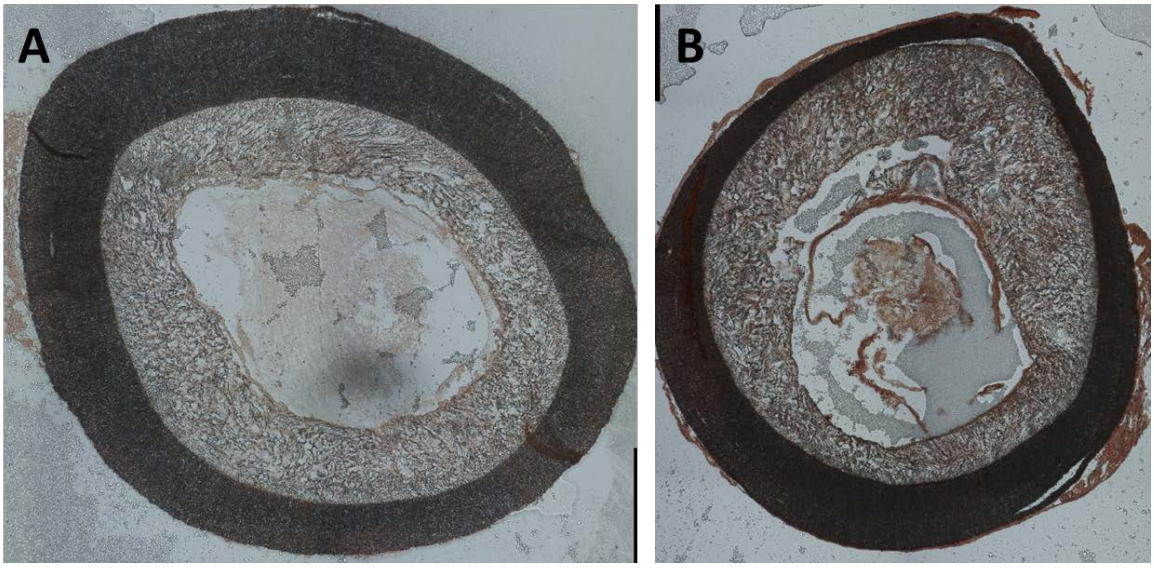

Figure 33. Calcification was not noted in instanced of thrombosis. In TEVGs which were occluded with thromosis no calcification was observed. As in occluded TEVGs in Aim 1-1 it was noted that no graft remodeling occurred and these grafts were explanted in < 1 week, this result indicates the necessity for graft remodeling prior to calcification.

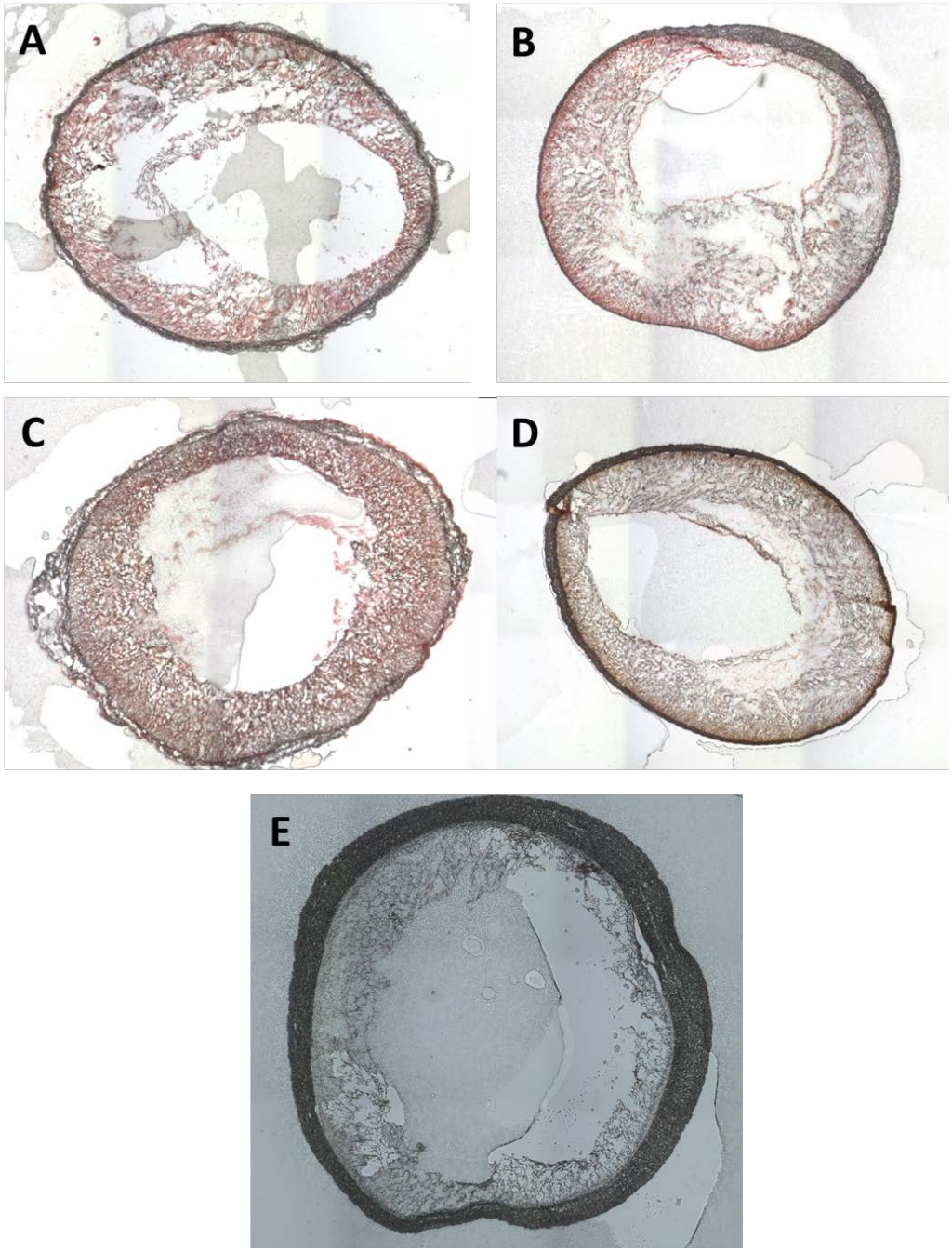

Figure 34. No calcification is observed in AD-MSC seeded scaffold prior to implantation. To confirm that no calcification was present prior to implantation AD-MSC seeded scaffolds were stained with Alizarin Red immediately after seeding (A) or when cultured in spinner flask for 2 days (B) at which point the construct would be implanted. Additionally AD-MSC seeded scaffolds cultured in spinner flasks for 5 (C) and 7 days (D) as well as non-seeded PEUU scaffolds (E) were stained. In all cases no calcification was observed suggesting it to be an in vivo process.

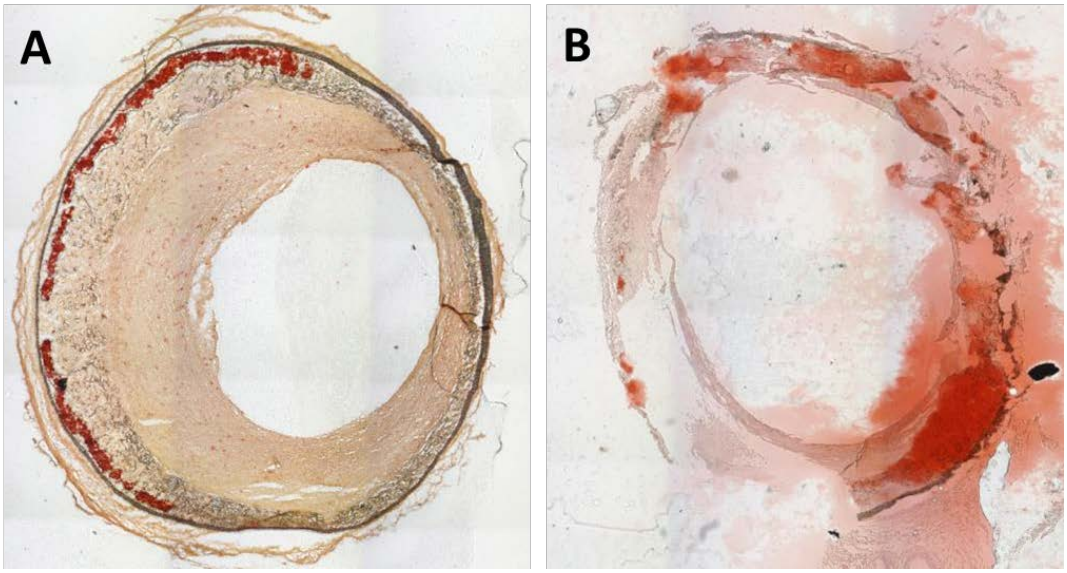

Figure 35. Historic TEVG samples from the Vorp lab using human pericytes also displayed calcification. To determine if calcification was occurring solely due to the AD-MSCs utilized within this study, historic samples from the Vorp lab (8 week implanted human pericyte graft (A) or 1 year pericyte implant graft (B)) were stained for Alizarin Red. Calcification was present in these samples.

2.7.5 T cell and B cell Activity Within Implanted TEVGs

The animal model used within this study is a Lewis rat which gains immune-tolerance due to its inbred nature. By inbreeding, these rats develop a lack of MHC gene diversity which prevents the recognition of foreign antigens [382, 383] and thus allow for the use of non-autologous cells without immune rejection. However, as this model is not fully immune-deficient (i.e. it is not athymic), it is important to confirm that the survival – and thus function – of the implanted human cells within this study were not negatively affected by a potential immune response. To confirm the lack of immunological concerns within our TEVG samples, explanted samples at 1 week were stained for CD45RA (a marker present on both T and B cells (#MCA340G, AbD Serotec) revealed no presence of lymphocytes (**Figure 36**).

Additionally, further evidence for the tolerance of human MSCs in this model has been reported by other studies showing a lack of an immune response and engraftment of human MSCs to at least 8 weeks within different applications [384, 385]. Additionally, even studies using fully immune tolerant rat models with human MSCs show survival for at least 7 days [386] which likely attests to the immuno-suppressive abilities of these cells [387, 388] further allowing for immune-tolerance. However, despite the poor survival of cells in the aforementioned study, this time point (7 days) is likely sufficient for the cells to perform the necessary functions to induce TEVG remodeling. Indeed, TEVG studies performed using fully immuno-deficient animal models have shown that implanted MSCs will be lost in approximately 1 week (see Section: “1.5.3 In Vivo TEVG Mechanisms”) regardless, due to host remodeling. As we have observed no gross inflammation in our explants, there is a lack of T/B cell activity at time points when the cells are likely around, and that sufficient remodeling is present (i.e. the cells are performing their necessary functions to generate patent and remodeled vessels) it argues that these human MSCs are well tolerated in this model.

In addition, this model may be superior to fully immuno-compromised animals when assessing TEVG remodeling as common immuno-deficient models that directly alter immune cell function such as the SCID-bg mutation can present false-positive remodeling events (see Section: “1.5.3 In Vivo TEVG Mechanisms”).

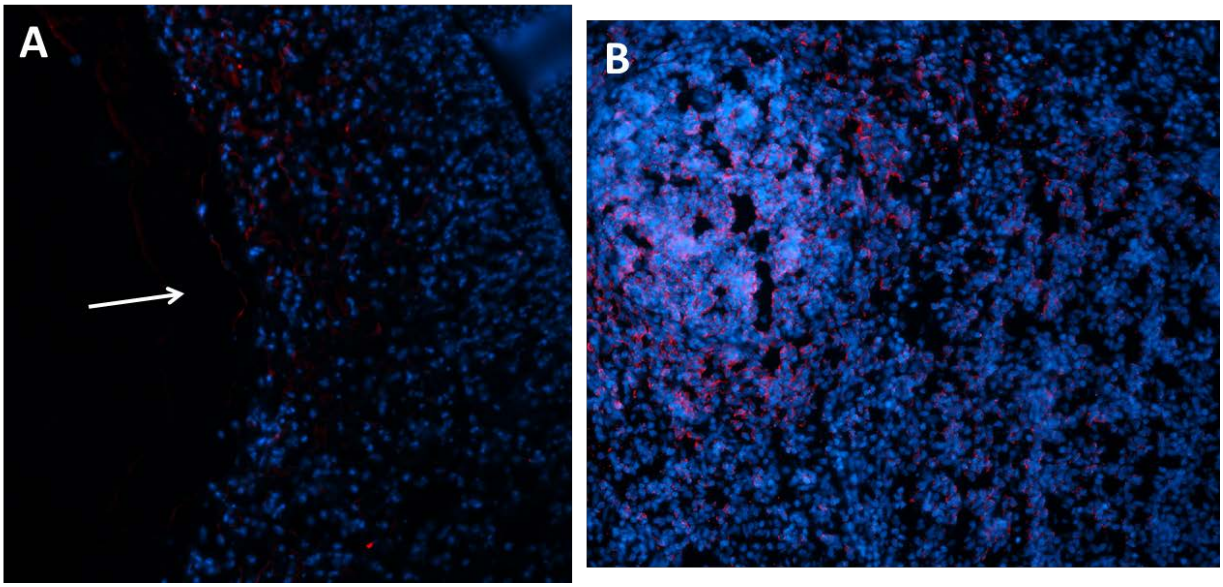

Figure 36. Lymphocyte activity is not present in TEVGs. To confirm the lack of lymphocyte activity (T-cell, B-cell) in our TEVG implants using human cells in a Lewis rat model, staining on 1 week explants was performed (A). A rat spleen (B) was utilized as a positive control to confirm antibody functionality.

3.0 SPECIFIC AIM 1, PART 2:

MECHANISM OF DIABETIC AD-MSC THROMBOSIS

After revealing that the main effect seen in Aim 1-1 was the decreased patency due to thrombosis when utilizing diabetic AD-MSCs within TEVGs, we next performed a mechanistic study to identify potential molecular players. By understanding this, modifications to the TEVG strategy could be designed to enable autologous therapy. In this study two potential processes involved in thrombosis were initially investigated: platelet adhesion and fibrinolysis. However, after initial experimentation with platelet adhesion revealed no differences between healthy or diabetic AD-MSCs, this aim mainly focused on fibrinolysis.

3.1 INTRODUCTION

Thrombosis (i.e. a blood clot) is a physiological phenomenon that occurs in the vasculature where erythrocytes and platelets will bind together and form a complex held together by fibrin at sites of injury site to prevent fatal loss of blood. While in normal physiology, thrombosis formation is a beneficial to the survival after an injury to the vascular system, in diseased conditions or during vascular interventions – in the case of a vascular graft – formation of a blood clot can lead to life- or limb-threatening consequences. Thrombosis formation occurs through a cascade of molecular pathways called termed the intrinsic [97] and extrinsic [98]

pathways. Each of these pathways involves different activators, but ultimately converge to a central pathway to generate thrombin which acts to deposit crosslinked fibrin.

In addition, regulatory pathways such as fibrinolysis act to remove thrombus material. The fibrinolysis pathway operates as a proteolytic cascade ultimately leading to activation of plasmin and digestion of the fibrin-rich thrombus. However, one potential mechanism to establish a pro-thrombogenic environment is under-activation of this pathway. Indeed, one of the initial time-course events in TEVG remodeling is the initial deposition of fibrin to the graft lumen which is removed at later time points (see Section: "1.5.3 In Vivo TEVG Mechanisms"). Activity of the fibrionlytic cascade is regulated by multiple species including two plasminogen activators (urokinase plasminogen activator (uPA) and tissue plasminogen activator (tPA)) and various inhibitors (e.g. plasminogen activator inhibitor (PAI-1), soluble uPA receptor (suPAR), alpha2-antiplasmin) (**Figure 37**).

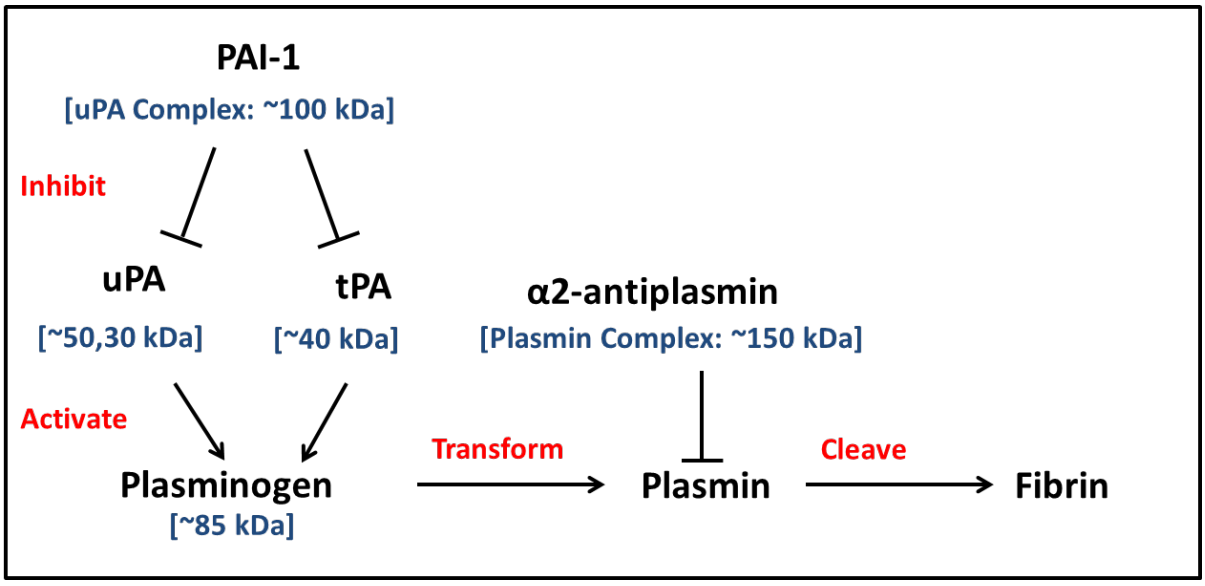

Figure 37. Fibrinolytic Molecular Pathway. The fibrinolytic pathway ultimately results in the cleavage (and thus dissolution) of fibrin. The main molecular player responsible for this action is plasmin which is regulated by multiple activators (uPA – urokinase plasminogen activator, tPA – tissue plasminogen activator), and inhibitors (PAI-1 – plasminogen activator inhibitor-1, α2-antiplasmin). The molecular weights of each of these elements is provided.

Formation of a thrombus is a heavily regulated molecular event [97, 98] but when simplified has two critical components: the adhesion of activated platelets and the deposition of the fibrin mesh. In this way when considering the pro-thrombotic effect of diabetic AD-MSCs as seen in Aim 1-2, an increase in thrombosis can be attributed to two mechanisms. First, thrombosis could occur from an increase in the degree of platelet adhesion. Second, a higher deposition of fibrin or a decrease in the degree of fibrin degradation by the cell's secreted factors could result in thrombosis. This Aim will investigate both of these phenomenon to establish a mechanistic explanation of the pro-thrombogenic phenotype of diabetic AD-MSCs.

While a pro-thrombotic phenotype can commonly be seen in diabetic individuals [389-391], a phenotypic change in this manner for cells used in vascular engineering – particularly AD-MSCs – has not been previously reported. Previous studies have shown that MSCs are capable of expressing components of the fibrinolytic pathway [184, 187, 188, 335, 392-394] and normally display an anti-thrombogenic phenotype [261] but the differential effects due to diabetic condition still remain poorly characterized [335, 392]. Investigating the mechanism behind the pro-thrombogenic phenotype of AD-MSCs from diabetic patients could provide insights on how to make these cells functional for downstream autologous vascular tissue engineering.

3.2 METHODS

3.2.1 Cell Culture

AD-MSCs and SMCs were cultured in the same manner as in Aim1-1. Additionally, conditioned media was acquired in the same way but was not diluted and the number of conditioning cells observed upon collection was the same between both groups (healthy: 0.06±0.01 x 10^6 cells/cm^2, diabetic: 0.05±0.01 x 10^6, p=0.16). The same cell lines were in Aim 1-1 were utilized but in this case BMI was noted to be similar between both groups (healthy: 28.2±4.9, diabetic: 26.0±3.8; p=0.49). For a list of donors see **Table 3**.

Table 3. List of AD-MSC donors utilized in Aim 1-2.

AD-MSCs Utilized for Aim 1-2 Experiments									
Vorp Lab ID Number	Grouping	Gender	Age	Diabetic	BMI	Platelet Adhesion	Zymography	uPA Activity	Fibrin Construct
1	Healthy	Female	38	No	33	X	X	X	X
2	Healthy	Female	35	No	28.6	X	X	X	X
5	Healthy	Female	33	No	29.9	X	X	X	X
8	Healthy	Female	32	No	21.4			X	
3	Diabetic	Female	39	Yes	23.7	X		X	
13	Diabetic	Female	43	Yes	22.2	X	X	X	X
14	Diabetic	Female	45	Yes	30.6	X	X	X	X
15	Diabetic	Female	39	Yes	27.4		X	X	X

3.2.2 Platelet Adhesion Assay

In order to test the ability of diabetic AD-MSCs (control: healthy AD-MSCs) to adhere platelets, monolayers were incubated with bovine platelet rich plasma anti-coagulated with a 7:1 vol/vol citrate dextrose for 30 minutes. This was followed by several PBS washes to remove any

unbound platelets. Bound platelets were then labeled using a standard immune-fluorescence protocol staining for CD41 (1:100, Kingfisher #CAPP2A) with counterstains for DAPI and F-actin (1:250, Sigma #P5282). Samples were imaged using NIS Elements software (version 4.0). Platelets bound to cell bodies and cell nuclei were manually counted in each image, which was then utilized to calculate the average number of platelets per cell.

3.2.3 Fibrinogen Zymography

Zymography was performed utilizing acrylamide gels with the incorporation of fibrin using previously established techniques [395]. Briefly, fibrin was mixed into the resolving phase solution prior to polymerization of a 1.5 mm thick 7.5% acrylamide gel (resolving gel formulation: 3.25 mL water, 3.37 1M Tris-HCl pH 8.8, 90 µL 10% SDS, 2.25 mL 40% acrylamide, 90 µL 10% APS, 9 µL TEMED, and 400 µg/mL fibrinogen) to achieve a final fibrinogen (Sigma #F8630) concentration of 5.33 µg/mL. The gels were loaded with conditioned media (40 µL total sample; mixed 3:1 with 4x Laemmli Sample Buffer (BioRad #161-0747)) from AD-MSCs. Following SDS-PAGE (25 mA per gel) the gels underwent several washes in water and 2.5% Triton-X prior to incubation (37°C) in a divalent cation reaction buffer (50 mM Tris-HCl pH 7.4, 1 mM $CaCl_2$, 1 mM $MgCl_2$). Digestions were performed for 7 days to allow for enzymatic degradation of the entrapped fibrin within the gel. This degradation occurs via active enzymes directly digesting fibrinogen, or reacting indirectly with contaminating plasminogen/plasmin present in the fibrinogen mixture. Following incubation, each gel was stained with Blue BANDit Protein Stain (Amresco) to visualize the degradation bands which appear as white on a blue background. The amount of degradation was quantified using gel

analysis tools within ImageJ (National Institutes of Health, Bethesda, Maryland) by integrating the mean gray scale intensity over the area of each band.

3.2.4 Western Blot for uPA

Western blot procedures were performed using standard protocols [396]. Briefly, samples (undiluted AD-MSC conditioned media or 6U uPA protein (AnaSpec, #72159)) were mixed with non-reducing sample buffer (mixing 3:1 with 4x Laemmli Sample Buffer (BioRad #161-0747)), heated for 15 minutes at 65°C, and loaded onto a 12.5% polyacrylamide gel (40 µL per lane) (formulation: 1.75 mL water, 3.37 1M Tris-HCl pH 8.8, 90 µL 10% SDS, 3.75 mL 40% acrylamide, 90 µL 10% APS, and 9 µL TEMED)). Following SDS-PAGE, the gels were electrophoretically transferred to a nitrocellulose membrane. Membranes underwent a standard immuno-staining procedure for uPA using a 5% milk blocking solution (in PBS with 0.1% Tween, 1 hr.), a rabbit anti-uPA antibody (1:500 in block, Abcam #ab24121, overnight at 4°C), and a horseradish peroxidase conjugated anti-rabbit IgG secondary (1:2000 in block, Amersham #NA934VS, 1 hr.). Blots were then developed with an in-house luminol-based ECL solution prior to imaging on a Bio Rad #ChemiDoc XRS+ imaging system.

3.2.5 uPA Fluoro-metric Activity Kit

A fluorometric microplate kit was utilized to detect the level of uPA activity within conditioned media samples (AnaSpec, #72159). All protocols were followed according to the manufacturer's instructions and all samples were repeated in triplicate.

3.2.6 Fabrication of Fibrin Constructs and Stimulation with AD-MSC Media

Fabrication of fibrin-based constructs containing entrapped SMCs was performed as previously described [395]. Briefly, fibrin gel constructs were created by immediately pipetting 200 µL of a polymerization mixture (3.7 mg/mL fibrinogen (Sigma #F4753-5G), 0.2 U/mL thrombin (Sigma #T7513-500UN), 1.25 mM CaCl2, and 50,000 cells/mL) into a 1 cm circle etched on tissue culture plastic. Gels were then incubated (37°C for 30 minutes) to allow for polymerization prior to adding conditioned media. Non-conditioned media was used as a control. Additionally, to provide for a gradation in fibrinolysis, conditioned media was supplemented with the fibrinolytic inhibitor, ε-amino caproic acid (ACA, 0.5, 1.0, or 3.0 mM). All samples were repeated in triplicate using n=3 donors per group.

To analyze the degradation of each gel, images were taken with a 16 megapixel camera at 1, 4, and 7 days. To quantify this degradation, which appeared as the gels developing a porous structure and becoming increasingly translucent, mean grayscale intensity measurements of each gel image were made in ImageJ. Specifically, gels that had a lower intensity were more translucent and thus considered as more degraded. Those gels which were incubated without ACA were found to catastrophically detach from the edges rather than showing a smooth change in translucence.

3.2.7 Compressive Mechanical Testing of Gels

To further assess fibrin degradation of fibrin-based constructs, those which were inhibited with 3 mM, 1 mM, or 0.5 mM hexanoic acid were tested utilizing mechanical compression. All gels which were administered non-inhibited conditioned media were either completely degraded or

degraded to a point that testing was not possible. Each gel was placed between two flat glass plates. The top plate was connected to a stepper motor translating at a rate of 0.005 mm/s and a 50g load cell (Transducer Techniques #GS0-50). The dimensions of each gel were measured and then loaded to 50 percent of the thickness in a non-confined state. Maximum tensile and compressive forces and energies were calculated for each sample. Samples were repeated in triplicate. Additionally, images of each gel were acquired from the sagittal plane and the contact angle of each gel was measured using tools within ImageJ.

3.2.8 Statistics

All statistics were performed in a similar manner to Section 2.2.11 (“Statistics”).

3.3 RESULTS

3.3.1 Platelet Adhesion Assay

AD-MSCs obtained from healthy and diabetic donors showed no difference in the number of bound platelets per cell (**Figure 38**) and in either case the platelet binding was lower than when human SMCs (i.e. positive control; data not shown) were used.

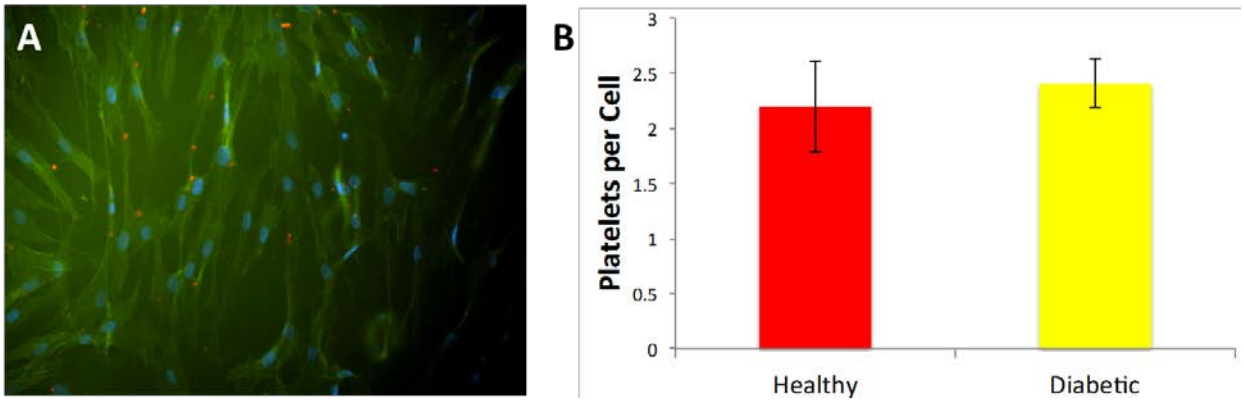

Figure 38. Healthy and diabetic AD-MSCs adhere a similar number of platelets. Monolayers of AD-MSCs from either healthy or diabetic donors were incubated with bovine platelet rich plasma to allow for platelet adhesion (example shown in (A); platelet – red; cell body (green)). The number of platelets adhered to cell bodies were counted and revealed no difference between healthy of diabetic groups (B; p=0.48, n=3)

3.3.2 Fibrinogen Zymography

To screen for fibrinolytic factors potentially secreted by AD-MSCs, fibrinogen zymography was utilized. Following 7 days of enzymatic reaction, prominent degradation bands were seen at molecular weights of 31, 40, 85, 150, and 250 kD using healthy AD-MSCs (**Figure 39**). Development of the zymograms for shorter periods (1 or 3 days) revealed less prominent bands and were thus not utilized (**Figure 40**).Visual comparisons of the degradation bands showed that media conditioned by healthy AD-MSCs produced prominent bands at 31 kD and 40 kD whereas media conditioned by AD-MSCs from diabetic donors did not. Quantifying the band areas at these molecular weights revealed a significant difference between healthy and diabetic AD-MSCs at these weights with an additional increase in the band at 150 kD (**Figure 39**) indicating a higher fibrinolytic activity in healthy AD-MSCs. Since serum alone provided a degradation band at 85 kD, we repeated the experiment using AD-MSCs cultured under serum-free conditions. In this case, bands at 40, 50, 85, 100 and 150 kD were apparent (**Figure 41**). Notably, in the serum-

free case the bands at 31 kD were lost and new bands appeared at 50 kD. Quantifying this set revealed a significant difference at 40 kD further confirming the higher fibrinolytic activity in healthy AD-MSCs. It is important to note that serum-free conditions do not represent the physiologic environment under which thrombosis occurs (i.e. within blood serum) but it confirms that AD-MSCs are capable of producing all of the bands seen within zymograms and are not confounded by the fibrinolytic factors within serum.

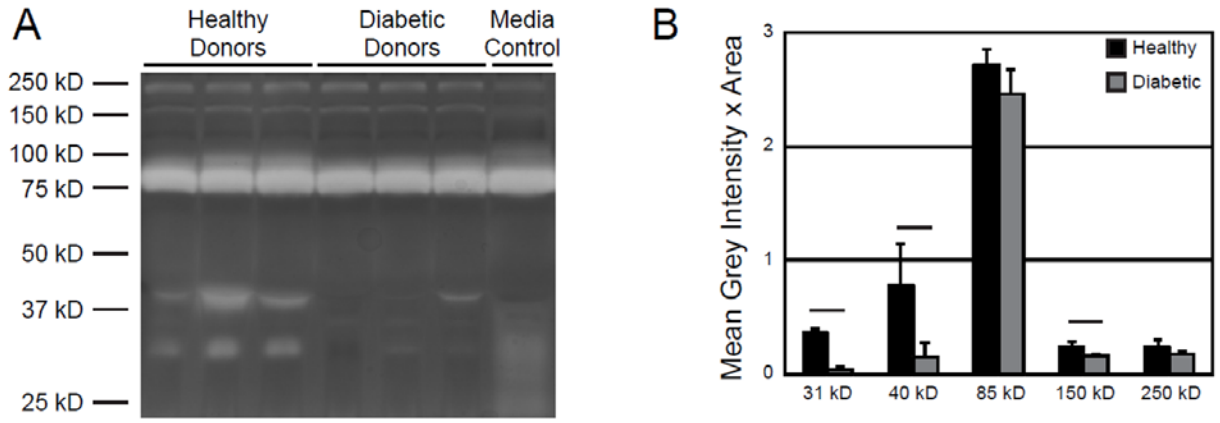

Figure 39. Diabetic AD-MSCs produce less fibrinolytic factors than healthy AD-MSCs. (A) Zymography was performed utilizing conditioned media from AD-MSCs from healthy or diabetic donors using acrylamide gels doped with fibrinogen. White bands indicate areas of fibrinogen degradation, several of which were more prominent when AD-MSC from healthy donors were used. Media control = non-conditioned serum-containing media. (B) Bands were quantified using toolboxes within ImageJ; bands at 31, 40, and 150 kD were increased in healthy samples. Data is presented as mean ± SD. Black bar = statistically significant difference with $p<0.05$.

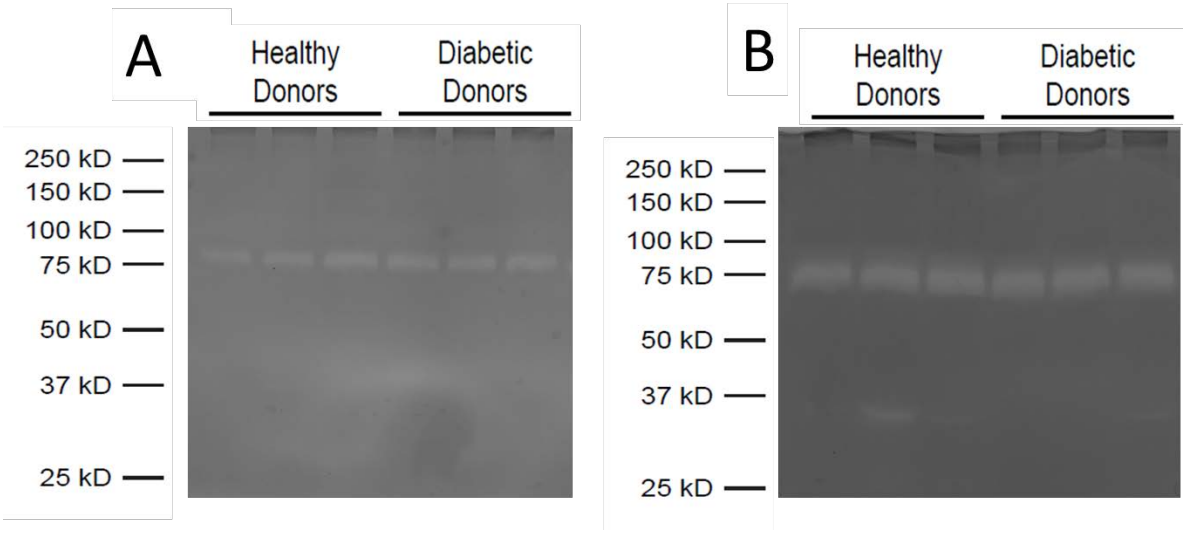

Figure 40. Zymography performed at earlier time points results in less prominent degradation bands. In addition to the 7 day zymogram performed in Figure 39, additional zymograms were performed at 1 (A) and 3 (B) days. Less prominent bands are seen at both days with bands occurring at lower molecular weights (31 kD) beginning to appear at 3 days.

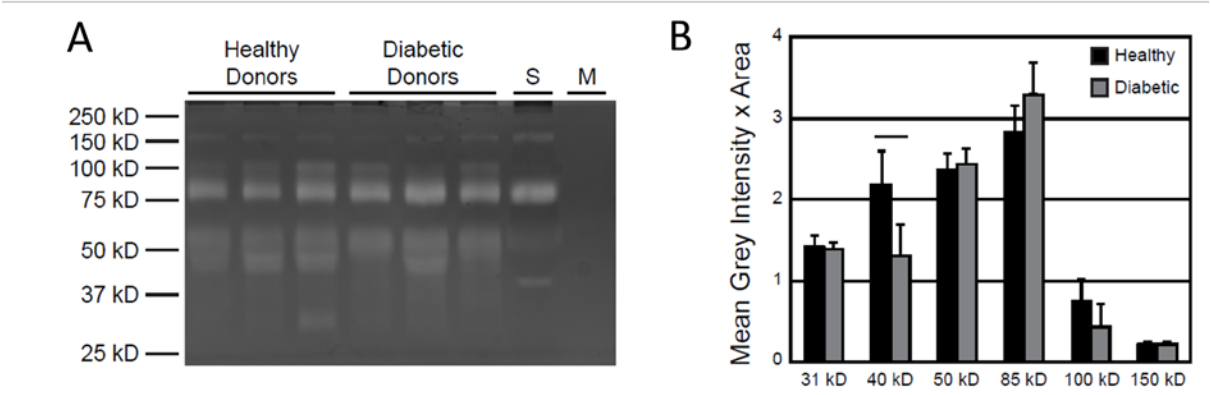

Figure 41. Fibrinogen zymoraphy performed under serum-free conditions confirm AD-MSC produced fibrinolytic factors. (A) Zymography performed using conditioned media isolated under serum-free demonstrated that all bands are capable of being produced by AD-MSCs and not masked by fibrinolytic serum factors. S = non-conditioned media containing serum. M = non-conditioned media without serum. (B) Additionally, quantification of bands in (A) demonstrated elevation of the 40 kD band in media conditioned by AD-MSC from healthy donors.

3.3.3 Western Blot for uPA and uPA Activity Kit

Prior literature [397-403] suggested that uPA would be present at three of the band weights observed in our zymography results: 31, 50, 100 kD (see **Figure 37**). Performing a Western blot using purified human uPA protein confirmed the location of uPA bands at these molecular weights and suggested the identity for the 31 kD zymographic band (**Figure 42**). However, we were unable to detect uPA in conditioned media using Western blot procedures with the same antibody and this was likely due to the levels of protein present in the media being below the detection limit. Instead, to specifically detect uPA we utilized a high sensitivity fluorometric uPA activity assay kit. Conditioned media from both cell types displayed uPA specific protease activity and that the activity of cells from diabetic patients was approximately 67% of that seen with cells from healthy patients (**Figure 42**).

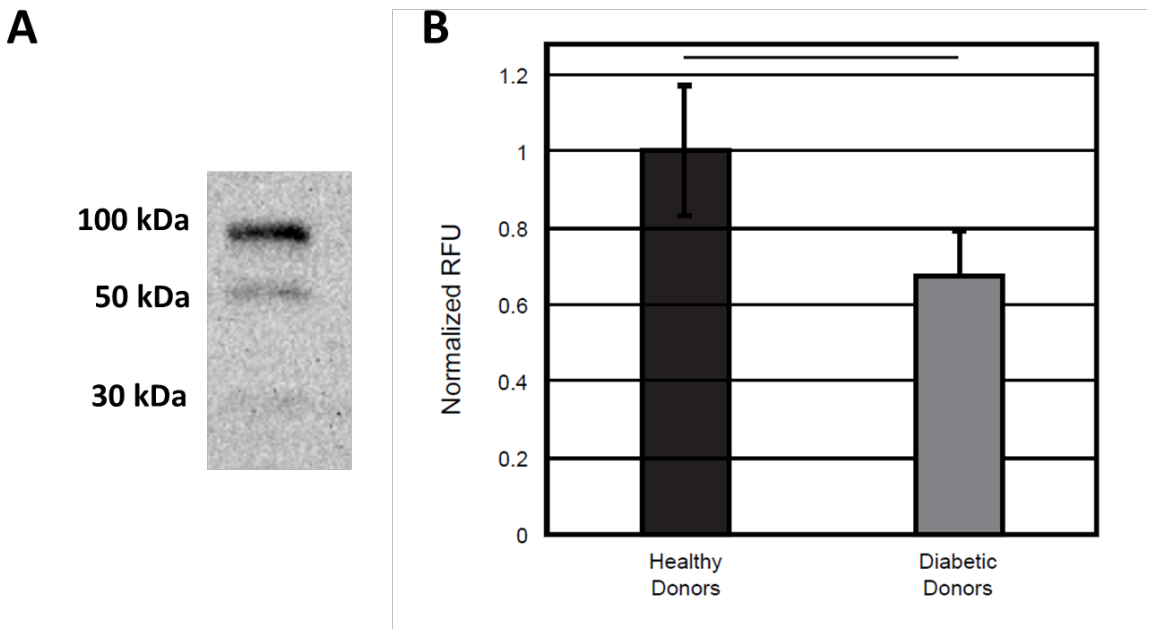

Figure 42. Urokinase plasminogen activator (uPA) is in part responsible for the differences in fibrinolytic ability between AD-MSCs from healthy and diabetic donors. (A) A Western blot was performed utilizing dilutions of human uPA protein standard. Positive signal appeared at molecular weights of 31, 50, and 100 kD matching zymographic bands seen in **Figure 39** and **Figure 41**. (B) A uPA fluorometric microplate activity kit was performed on conditioned media samples. A significant reduction in uPA activity was observed when cells sourced from diabetic donors were used. Data is presented as mean ± SD. Black bar = statistically significant difference with $p<0.05$.

3.3.4 Fibrin Based Construct Degradation

As a final means to show that healthy AD-MSCs produced more potent fibrinolytic factors than those isolated from diabetic patients, we created fibrin-based constructs containing SMCs and exposed them to AD-MSC conditioned media. Due to the fibrinolytic nature of SMCs themselves, this assay was designed to address how AD-MSC in a vascular graft might influence the fibrinolytic potential of host SMCs and thus the local anti-thrombogenic environment. In gels cultured in the absence of ACA (Aminocaproic acid, i.e. hexanoic acid) and under stimulation with media conditioned by AD-MSCs, catastrophic detachment and compaction of constructs resulted due to a high degree of degradation (**Figure 43**). This effect was observed to be reduced by using media conditioned by cells from diabetic patients. It is also important to note that AD-MSC based gels did not detach or substantially degrade (data not shown).

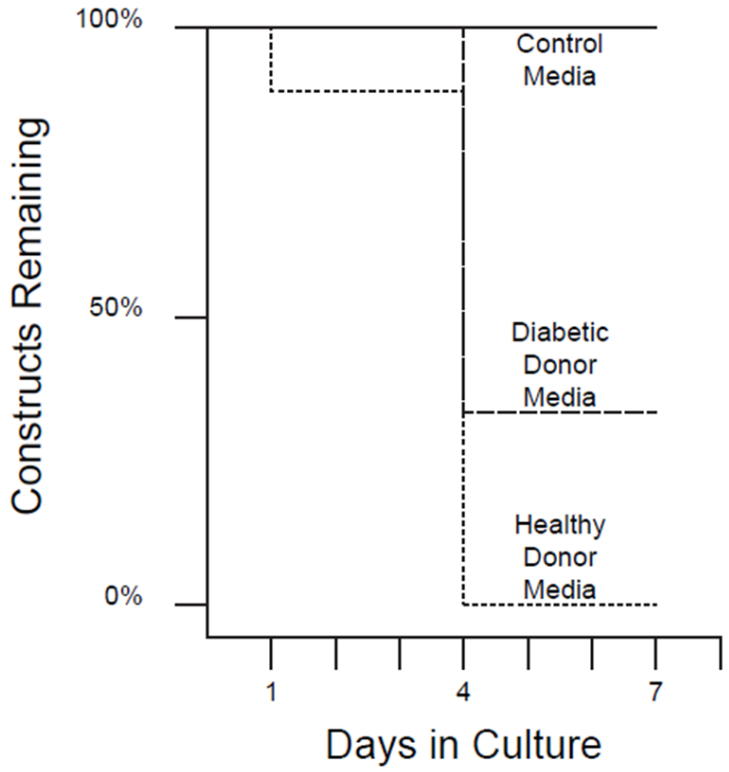

Figure 43. Secreted factors from AD-MSCs promote fibrin construct degradation. Fibrin-based constructs were fabricated and cultured with control (non-conditioned) media or media conditioned by AD-MSC from one of three healthy or diabetic donors. Each group was run in triplicate. The percentage of each set of nine constructs remaining at 1, 4, or 7 days is plotted by analogy to a "survival curve" to illustrate the loss of constructs when conditioned media what used.

As the degradation of these uninhibited gels occurred so rapidly, we treated a separate set of constructs with varying concentrations of the fibrinolytic inhibitor ACA to allow visual resolution of the degradation rate differences between the healthy and diabetic AD-MSCs. Inhibiting degradation with 3 mM ACA was sufficiently potent to prevent any degradation over 7 days regardless of group (**Figure 44**). On the other hand, inhibiting with 0.5 mM ACA was not sufficient enough to differentiate the effects between the healthy and diabetic groups. However, the intermediate inhibitor concentration of 1 mM was able to discriminate between the groups where it revealed a significant drop in grey intensity of gels treated with healthy AD-MSC conditioned media, particularly at the 4 and 7 day time points (**Figure 45** shows day 1 and 4 time points). This indicates that AD-MSCs from healthy donors have a strong enough fibrinolytic activity to overcome inhibition by 1 mM of ACA while cells from diabetic donors do not.

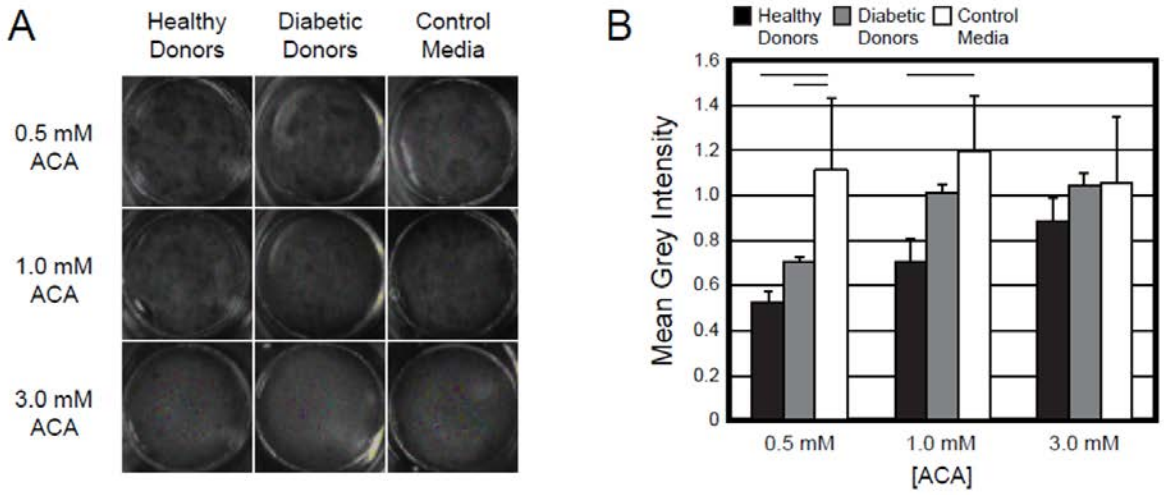

Figure 44. Media conditioned by AD-MSC from healthy donors promotes higher degradation of fibrin-based constructs than media conditioned by AD-MSC from diabetic donors. (A) To achieve a higher resolution on the degradation of fibrin constructs stimulated with AD-MSC conditioned media, we inhibited gels with either 0.5, 1, or 3 mM ε-amino caproic acid (ACA). Images are shown from an overhead view of fibrin disks at a 7 day time point. (B) Quantifying the mean grayscale intensity of each gel normalized to the background reveals that AD-MSCs from healthy patients promoted more fibrinolysis, when inhibited at an intermediate 1 mM ACA concentration. Images and measurements were also taken at days 1 and 4 and are shown in Figure 45. Data is presented as mean ± SD. Black bar = statistically significant difference with $p<0.05$.

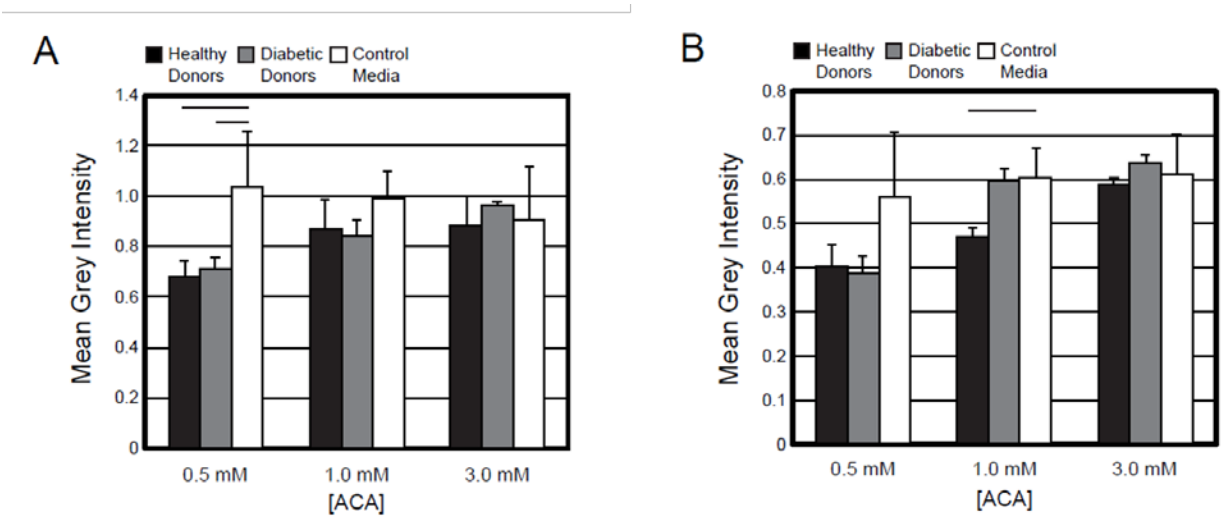

Figure 45. Earlier time points of fibrin construct degradation by analogy to **Figure 44**. Using the same method described in **Figure 44**, quantification of construct degradation was performed at day 1 (A) or day 4 (B). Data is presented as mean ± SD. Black bar = statistically significant difference with $p<0.05$.

3.3.5 Mechanical Compression Testing of Fibrin-based Constructs

To further show these fibrin gels stimulated with healthy AD-MSC conditioned media were indeed more degraded their diabetic counterparts, we performed compressive mechanical testing of the gel constructs obtained following the 7 day degradation. As stated above, only gels which were exposed to a fibrinolytic inhibitor were able to be tested as those from non-inhibited samples were near-completely degraded. Each gel revealed two distinct loading phases under compression (**Figure 46**). The first phase occurred when the gel initially made contact with the compressive plate breaking the surface tension of the gel. In this phase, substantial compressive loading had not yet occurred allowing the force to dominated by a tensive (i.e. negative) force imparted by the surface tension of each gel onto the plate. The second phase occurred as the gel underwent further compressive loading where it displayed a clear increase in load. Quantification of the mechanical parameters (compressive energy and maximum stress) during the second phase revealed no discernable differences between any groups or inhibitor concentration (**Figure 47**). However, quantifying the maximum negative stress and energy seen in the first phase of loading (**Figure 48**) reveals similar trends to **Figure 44**. Specifically, through the use of a mid-range inhibitor concentration (1 mM) a difference between the two groups can be observed where as too high (3 mM) or too low (0.5 mM) it is indiscriminant. In particular, gels stimulated with healthy AD-MSC conditioned media display an increased tensive force and energy which likely occurs as the more degraded gels become more hydrophilic (occupied by a higher water:fibrin ratio). This increased hydrophilicity was confirmed by decreased contact angle observed in gels stimulated with healthy conditioned media (**Figure 49**).

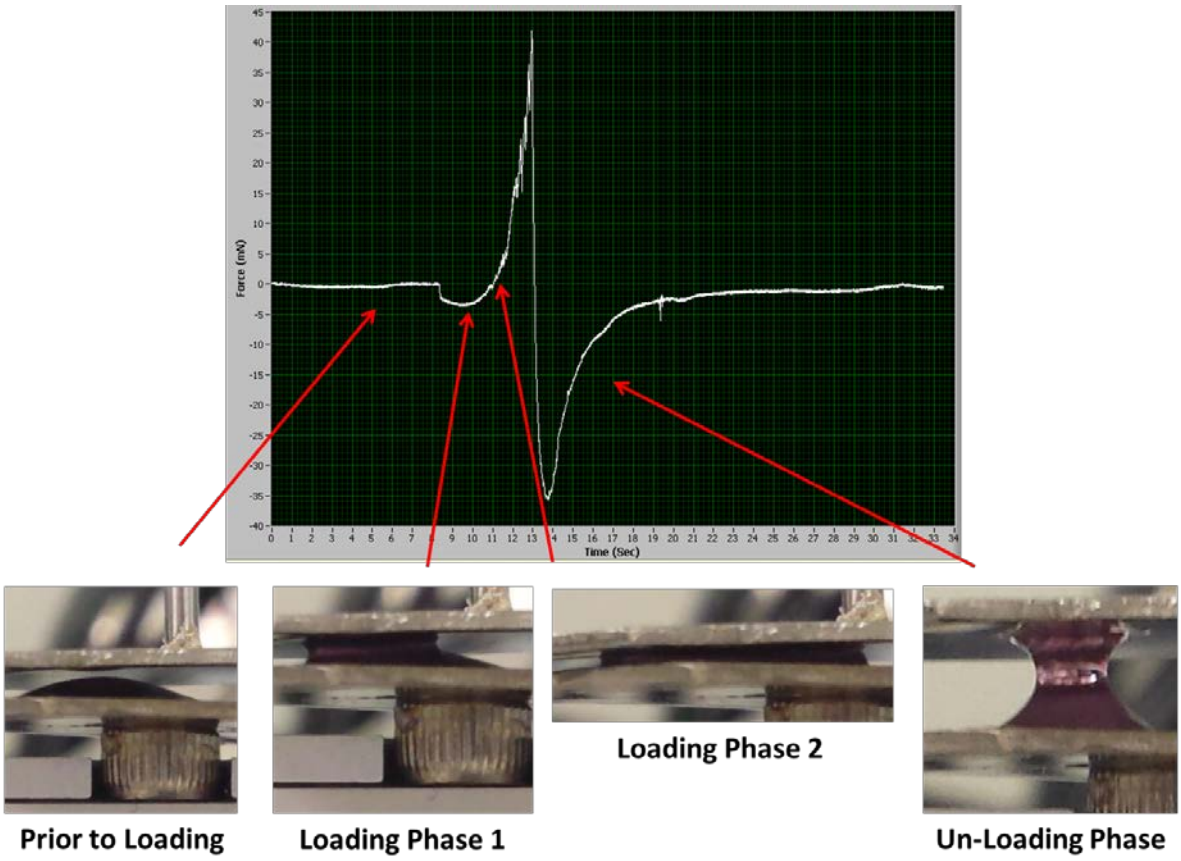

Figure 46. Mechanical compression testing of fibrin constructs has distinct loading phases. Compressive loading of fibrin gel constructs initially reveals a negative (tensive) force as the compression plate initially makes contact with the surface tension of the gel. Further loading produces a linear increase. Upon unloading of the gel a tensive force is seen as the gel retracts from the top plate.

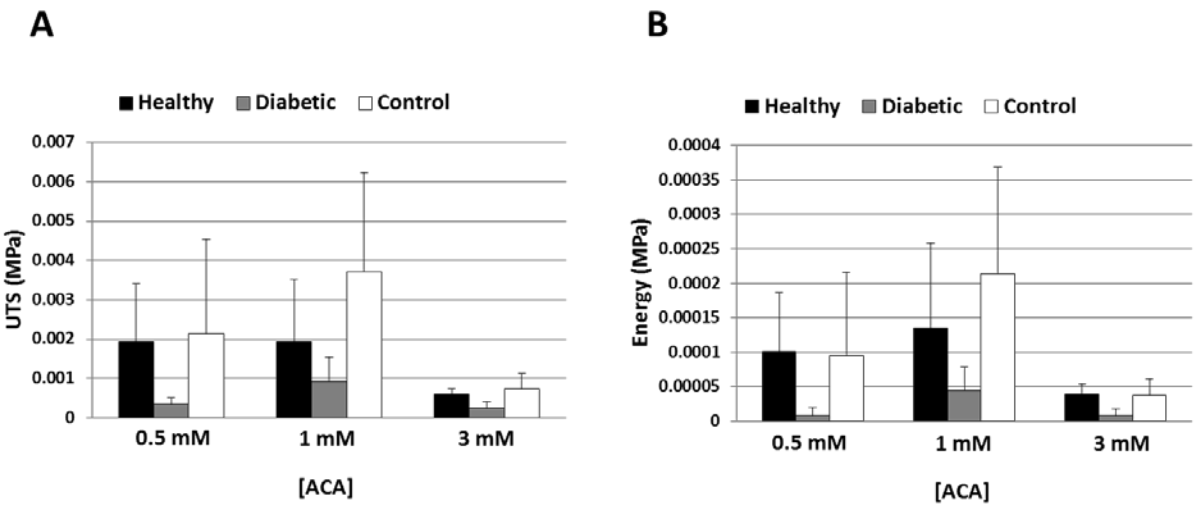

Figure 47. Compressive tensile strength and energy reveal no differences between any fibrin gel construct. The compression testing illustrated in **Figure 46** was performed on the fibrin gels after 7 days of degradation in **Figure 44**. Both the compressive strength and energy were calculated from stress-strain curves and displayed no difference for any gel, regardless of group or concentration of inhibitor.

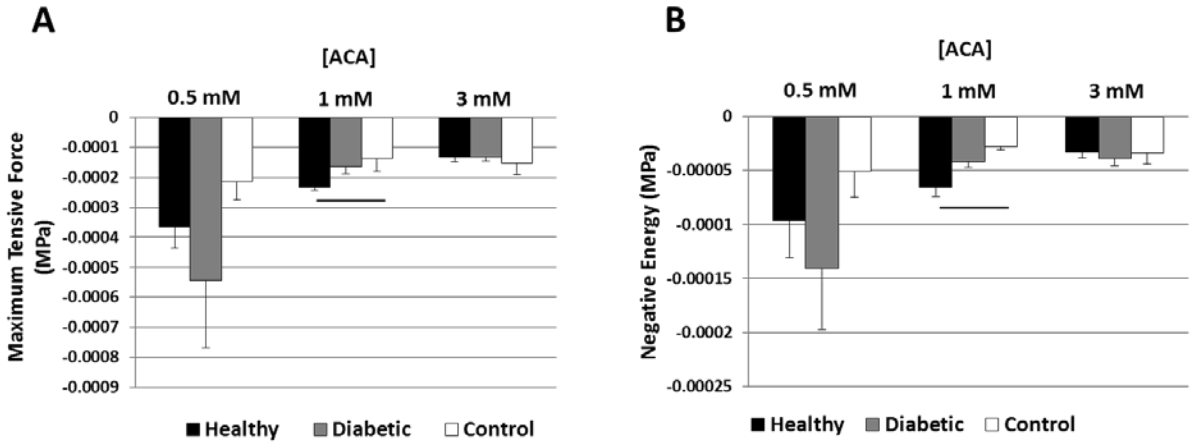

Figure 48. Initial tensive forces from fibrin construct surface tension reveal differences between healthy and diabetic constructs. Analysis of the tensive properties experienced by the surface tension after the initial contact of the compression plate with the fibrin gel surface (as illustrated in **Figure 46**), similar trends to **Figure 44** can be seen for both the maximum tensive force (A) and energy (B). Namely, both a high (3 mM) and low (0.5 mM) inhibitor concentration reveal indiscriminant differences between groups, but an intermediate level of inhibitor (1 mM) a difference can be observed. Black bar = significant difference at $p<0.05$.

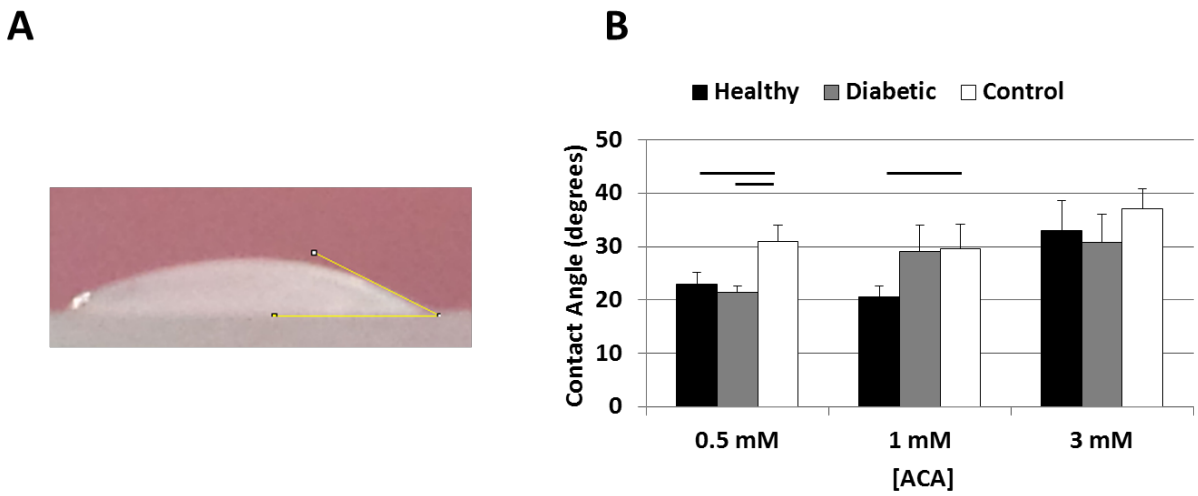

Figure 49. More degraded fibrin gels experience a reduced contact angle. The results seen in **Figure 48** can be explained by the hydrophilicity of the gel. As the gel becomes more degraded it will release a higher amount of energetically free water which increase the hydrophilicity of the gel and contribute to stronger surface tension forces. Indeed, the contact angle of the gels (A) were shown to decrease (B) as gels became more degraded and these trends mirror that seen in both **Figure 44** and **Figure 48**. Black bar = significant difference at $p<0.05$.

3.4 DISCUSSION

In this study we sought a mechanistic explanation for the thrombotic failure seen when using AD-MSCs derived from diabetic donors as shown in Aim 1-1. Here utilizing age and sex matched human donors, it is shown that presence of diabetes reduces the fibrinolytic ability of AD-MSC secreted factors compared to non-diabetic (i.e. healthy) counterparts, which can explain in part their pro-thrombotic phenotype. This broad fibrinolytic phenotype was demonstrated in vitro using fibrinogen zymography and fibrin-based constructs. At the molecular level, we used an enzyme kinetics assay to show that cells from diabetic donors have decreased uPA activity, which is a potential mechanistic explanation for the thrombotic failure. Investigating static platelet adhesion revealed no differences between the two groups.

Our zymography performed with serum revealed fibrinolytic activity within conditioned media at 31, 40, 85, 100, 150, and 250 kD. Qualitatively and quantitatively, the bands at 31 and 40 kD were more abundant in media conditioned by AD-MSC from healthy patients. Based on literature reports (see **Figure 37**), the 31 kD band is consistent with low molecular weight uPA (molecular weight: 33 kD [398, 400, 401, 404]). We observed that the low molecular weight uPA form was highly prevalent in conditioned media isolated under serum conditions but was barely present under serum free conditions. This is likely a result of plasminogen in serum, which is activated by uPA then cleaves uPA from its high to low molecular weight form [397]. Additionally, bands were noticed at 50 and 100 kD which likely correspond to high molecular weight uPA (molecular weight: 54 kD [397-402]), and high molecular weight uPA in complex with its inhibitor PAI-1 (molecular weight: 54 kD + 43 kD (PAI-1) = 97 kD [397, 399, 402, 403]). While it is counterintuitive that activity would be seen for the inhibitory complex, reactivation can occur under zymography conditions [403]. The activity of this complex also indicates the presence of the active double-chain form of high molecular weight uPA (as opposed to the inactive single-chain form [397, 399]), which PAI-1 selectively binds to it [402, 404] and this form is indistinguishable at the 50 kD band due to activation of the single-chain form via zymography conditions.

The lower amount of active uPA in AD-MSCs from diabetic donors can potentially be explained by upregulation of uPA receptors (such as uPAR [405-408], and suPAR [409-415]) in diabetic conditions. Increased uPAR causes more localization of uPA to the cell membrane [397, 399, 401], whereas a higher amount of suPAR scavenges uPA from the surrounding solution [397, 401, 409]. As uPA bound to its receptor is not readily released [401], and suPAR scavenged uPA is inhibited, these two mechanisms effectively reduce uPA activity in the bulk

solution and decrease overall fibrinolysis. Additionally, low molecular weight uPA does not bind to these receptors [401, 404, 416], and therefore has prolonged activity.

A significant increase was additionally seen at the 150 kD band under serum conditions. Literature reports suggest that the 85 and 150 kD bands are likely plasminogen/plasmin and a plasmin-α2 antiplasmin complex, respectively [395, 397]. Plasminogen activation is also suggested in our fibrin construct degradation experiments, as ACA slows degradation which occurs in a plasmin-dependent manner [417-420]. Finally, as there is a higher degree of uPA activity produced by AD-MSCs from healthy patients, an increase in downstream active plasmin is expected.

One limitation of this study is that we have not conclusively identified the 40 kD band, which differs in abundance between the two groups of cells. Literature reports suggest that this band could be tPA [421-424]. Typically, tPA (molecular weight: 70 kD) is enzymatically active upon cleavage from its single to double chain form. The two component chains are 33 and 39 kD, with the latter responsible for catalytic activity. We were unable to confirm the 40 kD band as the catalytically active chain of tPA by Western blot, and similar to uPA (which was undetectable via Western Blotting) this could be due to tPA's low concentration in conditioned media. ELISA, immuno-precipitation, or tPA activity assays offer alternative approaches in the future.

The results of this study are further corroborated by systemic reports of diabetic patients displaying a greater pro-thrombogenic phenotype with reduced fibrinolysis [425-429]. Studies have reported that diabetics have lower levels of fibrinolytic stimulators (tissue plasminogen activator [425]) and higher levels of fibrinolytic inhibitors (PAI-1 [405, 425-428, 430], uPAR [405-408], suPAR [409-415]), which contributes to an overall reduction in fibrinolysis.

Additionally, the high glucose environment seen in diabetes reduces plasmin activity via glycosylation [429], and reduced uPA activity can be seen in wound healing [431] and trophoblast invasion [432] applications. Other fibrinolytic factors altered specifically in AD-MSCs from diabetic donors include thrombospondin [392], tissue plasminogen activator [335], and PAI-1 [335]. To the best of our knowledge, our work is the first report to highlight a reduction in uPA activity by AD-MSCs from diabetic donors, and the first to implicate a donor-linked stem cell deficiency as a method of TEVG failure.

3.5 CONCLUSION

In conclusion, we present that fibrinolytic ability of AD-MSCs is decreased when the cells are sourced from diabetic donors, which offers an explanation for the high rate of thrombotic failure seen when these cells are used as the basis for tissue engineered vascular grafts. Additionally, we have identified loss of uPA activity as one potential mechanism for the thrombotic failure seen when AD-MSCs from diabetic patients are used in grafts. While other fibrinolytic mediators may also contribute to thrombotic failure in this application, we can now consider pursuing modulation of uPA activity in the short term as a method for enabling autologous TEVG therapy for the diabetic patient.

3.6 FUTURE DIRECTIONS

While we have shown that one molecular explanation for the decreased functional performance (i.e. ability to develop patent TEVGs) in diabetic cells is decreased uPA activity, this still does not provide the complete framework for a mechanism as to how the diabetic condition directly causes these cellular changes. Adding to this, compositional differences between healthy and diabetic AD-MSCs have also not been considered. However, one likely candidate for how diabetic cells acquire a pro-thrombotic phenotype is by the pathologic hallmark of diabetes – hyperglycemia – which results in a high intracellular glucose concentration leading to high levels of ROS (see Section: "1.2.3 Diabetes Etiology and Vascular Related Effects"). Indeed, this has been shown to be a contributing factor promoting damage of AD-MSCs causing losses in angiogenic function [433]. Another explanation could be from changes in the cellular composition of diabetic AD-MSCs compared to healthy ones which are more fibroblastic and present less stem cell markers such as CD105 and CD133 [434]. This effect is mirrored by fibrotic changes to adipose tissue which is seen during obesity [435] which can occur concurrently to diabetes.

Future directions for this portion of Aim 1 can encompass two components: performing more mechanistic studies and utilizing the mechanistic data to increase the pro-thrombotic activity of diabetic AD-MSCs thus restoring their use for autologous therapy. The platelet adhesion assay performed in this study revealed no differences between the healthy or diabetic group but this was far from conclusive. In particular this was performed under static conditions which are not physiologically representative and flow induces a higher degree of platelet activation [96] which would allow for more sensitivity when distinguishing between the groups. Future experiments utilizing a physiologic flow system and an AD-MSC seeded scaffold (as for

measuring dynamic compliance; see Section 2.7.3 Explanted TEVG Mechanical Testing) could be employed. Additionally, no studies were performed to show that a pro-thrombotic phenotype would be acquired via knockdown of uPA activity (e.g. genetic alteration, molecular inhibitors) in healthy cells to definitively complete the mechanistic investigation. Finally, other pathways contributing to thrombosis could be investigated in future studies. For example, Tissue Factor is one of the key regulators of the coagulation cascade leading to thrombosis initiation [436] and could be checked for upregulation in diabetic AD-MSCs. Additionally, as pro-inflammatory cytokines such as TNF-α, INF-γ, and IL-8 can cause upregulations in Tissue Factor production [436] and induce neutrophil extracellular DNA traps (NETs) which contribute to thrombosis [437]. These could also be investigated to play a major role. The activity of membrane bound inhibitory compounds such as thrombomodulin [436] and heparin [261] could further be investigated for alterations in the diabetic phenotype.

Pursing strategies to restore the changes in anti-thrombotic properties of diabetic cells could take a few avenues. First, AD-MSCs have been shown to be highly plastic and can undergo restorative changes under different environmental conditions (e.g. culture conditions). For example, diabetic cells removed from the diabetic environment can revert their metabolic properties under normal culture conditions [372], differences in adipogenic differentiation observed fat depots of different genders is not reflected in AD-MSCs when cultured [373], and weight loss can restore losses in AD-MSC adipogenic differentiation potential [374]. However, as the AD-MSCs used in this study are already passage expanded to at least four times, this may suggest the change to be irreversible via culture expansion alone. However, the opposite approach – using diabetic cells which have not undergone culture expansion (see SVF in Aim 2) – could hold promise. Indeed, culture expansion has a number of negative side effects which

affect both the function and composition of the AD-MSC population. First, extensive cell expansion reduces the differentiation potential of AD-MSCs and these changes can occur to a significant degree after as early as four successive passages (assuming that approximately 2 doublings per passage occur) [308]. These changes that occur via culture expansion have been attributed to a loss in stemness of these populations [308-310]. Further validating this point is that successive culture expansion reduces the presence of endothelial cells (CD31+) and progenitor cells (CD34+) within the AD-MSC culture (see Section: "4.7.1 Marker Profile of SVF Seeded TEVG Scaffolds"). As these cells can display anti-thrombogenic properties, preserving these within the population could potentially assist in restoring diabetic cell function. Additionally, the presence of CD34+ cells have been shown to enhance functional performance of the AD-MSC population [438, 439]. However one road block here is that endothelial cells from diabetic patients have decreased functions (see Section: "2.4 Discussion"). Thus the artificial stem cell concept defined in Aim 3 or supplement with additional anti-thrombotic factors may be ideal. While another consideration would be to perform alterations to the biomaterial utilized in this study (PEUU) which was performed previously to reduce its thrombogenicity [153, 205, 440, 441], it is unlikely that this would aid significantly in the case of cellularized TEVGs due to the insulating effect achieved by the cells spreading along the polymer surface protecting it from blood contact. Another solution could be to use genetic alteration to stimulate the production of uPA. Indeed increased production of certain proteins have been shown to alleviate dysfunctional effects [442], however this is not advisable due to the regulatory hurdles and risk present for genetic alteration. Finally, the administration of additional anti-coagulants could be utilized to alleviate the pro-thrombotic diabetic phenotype. The currently used dipyridamole and aspirin during in vivo studies both work to block mechanisms of

platelet adhesion however as this was at least preliminary this was shown that this effect was not as significant as other thrombotic pathways (i.e. fibrinolysis), drugs that target additional coagulation pathways could be used. For example, administration of uPA could be used to target the fibrinolysis pathway, heparin to enhance the activity of anti-thrombin, and warfarin could be used to inhibit the synthesis of multiple vitamin-K dependent factors.

3.7 ADDITIONAL STUDIES LEADING TO FUTURE WORK

3.7.1 Identification of tPA in AD-MSC Conditioned Media

While it was established throughout this Aim that the significant difference at the 31 kD zymographic band was due to uPA, the 40 kD band which showed a significant effect still remained to be quantified but was conjectured to be tPA. Similar to uPA, Western blot was performed but was unable to detect the presence of tPA likely due to low concentrations. This was attempted with both reducing (Abcam, #157469) and non-reducing (Abcam, #ab82249) antibodies.

4.0 SPECIFIC AIM 2: USE OF CULTURE FREE SVF CELLS FOR TEVGS

4.1 INTRODUCTION

As highlighted in Section 1.3 (“Tissue Engineering Approaches), vascular tissue engineers have developed a plethora of vascular grafts which have shown promising results and represent excellent progress on the way towards a clinical solution. However, despite the significant degree of pre-clinical testing that cell-based TEVGs have undergone (see Section: “Improper Cell Sourcing”), multiple barriers still exist which inhibit clinical translation of this technology. This is illustrated by the few TEVG approaches to reach clinical trials (see Section: “1.4 Current Clinical TEVG Approaches”). As outlined in Section 1.5 (“Current Barriers to Clinical Translation”), these barriers include the incorporation and testing of human cells, feasible and consistent modes of manufacture to appropriate sizes, and fabrication time. However, while advances have been made addressing the both the use of human cells (including Aim 1 which tests clinically relevant human cells) and scaffold production methods, minimizing fabrication time is still a major concern.

While human adipose-derived mesenchymal stem cells (AD-MSCs) are a very attractive cell source as they are abundant, easily obtained, and can be rapidly expanded in vitro, they still require culture expansion to isolate [443]. However, adipose tissue itself is uniquely advantageous to the field of vascular tissue engineering as its raw population (the stromal

vascular fraction (SVF)) is progenitor rich, containing AD-MSCs, pericytes, endothelial progenitor cells, and endothelial cells [191, 444] which have all been successfully used in vascular tissue engineering [19]. Additionally, adipose tissue also offers a large quantity of cells and typical liposuction volumes can provide suitable quantities for construction of a "human-sized" graft without additional in vitro expansion [445-448]. Together this illustrates that SVF cells represent an ideal cell population for TEVGs as these can be utilized without the need for a culture step thereby minimizing fabrication time. This would relieve many regulatory and financial concerns with regards to clinical translation. Ultimately this strategy is analogous to use of bone marrow mono-nuclear cells which can also be utilized without culture and has led to the development of a clinically applied TEVG [244](see Section: "1.4.1 Approach 1 – Bone Marrow Cells with Synthetic Scaffold").

However, while use of the SVF could provide a substantial reduction in time to fabricate an implantable TEVG construct it must also be coupled with a reliable seeding methodology to incorporate cells within scaffolds. The rotational vacuum seeding device developed by our laboratory which provides rapid (< 5 min), efficient (> 90%), and uniform cell seeding of tissue engineered scaffolds [193, 197, 198, 449, 450] is ideal for this application. By combining our current RVSD technology with SVF cells, it is possible to quickly fabricate an adipose tissue-based TEVG without the need for cell expansion.

In this Aim, we investigated the use of SVF cells (i.e. freshly derived adipose cells) for use in vascular tissue engineering through both in vitro and in vivo studies. Similar to Aim 1 the defined essential functions of a cell for vascular engineering were utilized (see Section: "2.1.2 Definitions of Essential Cellular Functions and Performance Criteria for Vascular Engineering"). These included the ability of SVF cells to differentiate into SMCs, the ability to secrete SMC

pro-migratory factors, the ability to seed within TEVG scaffolds, and the ability to achieve effective in vivo performance. Additionally, a head-to-head comparison with culture expanded AD-MSCs generated from the same SVF populations was performed.

4.2 METHODS

The methodology performed in this Aim is nearly identical to that which was performed in Aim 1-1 but instead with the use of a non-cultured cell type. For simplicity, many of the following sections below will refer back to those previous methods while discussing any potential differences.

4.2.1 Isolation and Culture of SVF cells

SVF cells were obtained from human patients in the same manner as AD-MSCs (see Section: "2.2.1 Isolation and Culture of Cells and Collection of Conditioned Media") but were utilized directly for seeding within a TEVG (see Section: "2.2.5 Cell Seeding into TEVG Scaffolds") as opposed to culture expansion. The list of donors can be seen in **Table 4**. However, a fraction of the obtained SVF (approximately 1 million cells) was obtained and passaged four times to establish a paired cultured AD-MSC control. These were grown in the same manner as the AD-MSCs in Aim 1 (see Section: "2.2.1 Isolation and Culture of Cells and Collection of Conditioned Media").

Table 4. List of donors utilized in Aim 2.

SVF/AD-MSCs Utilized in Aim 2 Experiments									
Vorp Lab ID Number	Grouping	Gender	Age	Diabetic	BMI	Cell Seeding	Differentiation	Migration	In Vivo
SVF 1 (same #1 from Table 1)	Healthy	Female	38	No	33	X			
SVF 2	Healthy	Female	33	No	28	X			
SVF 3	Healthy	Female	43	No	26	X			
SVF 4	Healthy	Male	44	No	23		X	X	X
SVF 5	Healthy	Female	26	No	33		X	X	X
SVF 7	Healthy	Female	40	No	26				XX
SVF 8	Healthy	Female	38	No	35		X	X	XX
SVF 4 p4 (from SVF 4)	" "	" "	" "	" "	" "		X	X	X
SVF 5 p4 (from SVF 5)	" "	" "	" "	" "	" "		X	X	X
SVF 7 p4 (from SVF 7)	" "	" "	" "	" "	" "				XX
SVF 8 p4 (from SVF 8)	" "	" "	" "	" "	" "		X	X	X

4.2.2 Differentiation of SVF cells into SMCs

This assay was performed in the same manner as Aim 1 (see Section: “2.2.2 Differentiation of AD-MSCs into SMCs”) with SVF cells being plated directly onto glass coverslips instead of PLL coated ones. Three donors were utilized (see **Table 4**) with paired cultured AD-MSCs acting as controls.

4.2.3 Ability of SVF Cells to Promote SMC Migration

SVF cells were also probed for their ability to secrete soluble products to induce the migration of SMCs. This occurred in the same manner as Aim 1 (see Section: “2.2.3 Ability of AD-MSCs to Promote SMC Migration”) and with culture paired AD-MSC conditioned media as a control. To obtain SVF conditioned media, non-cultured SVF cells were plated at high density (near confluence) and allowed to attach overnight. The media was subsequently changed and collected two days following.

4.2.4 Scaffold Fabrication, Cell Seeding, and In Vivo Implantation

All procedures regarding the fabrication of scaffolds, seeding of cells, and implantation in vivo were done in the same manner as Aim 1 (see Sections: “2.2.4 PEUU Scaffold Fabrication”, “2.2.5 Cell Seeding into TEVG Scaffolds”, “2.2.6 Measurement of Uniform Cell Seeding”, “2.2.7 In Vivo TEVG Implantation”). SVF cells (n=6, see donors **Table 4**) and donor paired cultured AD-MSCs (n=5) were utilized. Some donors were used to fabricate multiple grafts as denoted by the number of “X” in the table.

4.2.5 Assessment of Cellular, Extracellular, and Morphometric Parameters of Explanted TEVGs

The analysis of explanted TEVGs was done using the same methods as Aim 1 (see Sections: “2.2.8 Histologic Evaluation and Immuno-fluorescence”, “2.2.9 Morphometric and Quantitative Analyses”, “2.2.10 Multiphoton Analysis of Collagen Architecture”). This allowed for the detection of morphometric parameters, as well as the cellular and extracellular components.

4.2.6 Statistics

All statistics were performed in a similar manner to Section 2.2.11 (“Statistics”).

4.3 RESULTS

4.3.1 Ability of SVF Cells to Perform Essential Functions: SMC Differentiation and Secretion of SMC Pro-Migratory Factors

To initially investigate the relevance of SVF cells for TEVG applications, the ability of SVF cells to differentiate into SMCs and induce SMC migration was analyzed (see Section: "2.1.2 Definitions of Essential Cellular Functions and Performance Criteria for Vascular Engineering"). Compared to donor matched AD-MSCs – acting as a positive control as demonstrated in Aim 1 – SVF cells underwent differentiation into SMC like-cells and secreted factors to promote SMC migration on equal levels. SMC differentiation was shown by induced expression of the SMC marker calponin (**Figure 50**) and a morphologic change to a more spindle-like cell shape (**Figure 51**). It is important to note as described in Aim 1, this assay does not induce complete differentiation but is still able to produce discernable effects from different cell types.

The ability of SVF cells to promote migration of SMCs was evident by the significant increase in migration rate observed in SMCs when stimulated with conditioned media of SVF cells (**Figure 52**). The was similar to that seen with donor matched AD-MSCs. Taken together these results verify that SVF cells indeed have functions that can be utilized in the context of vascular tissue engineering.

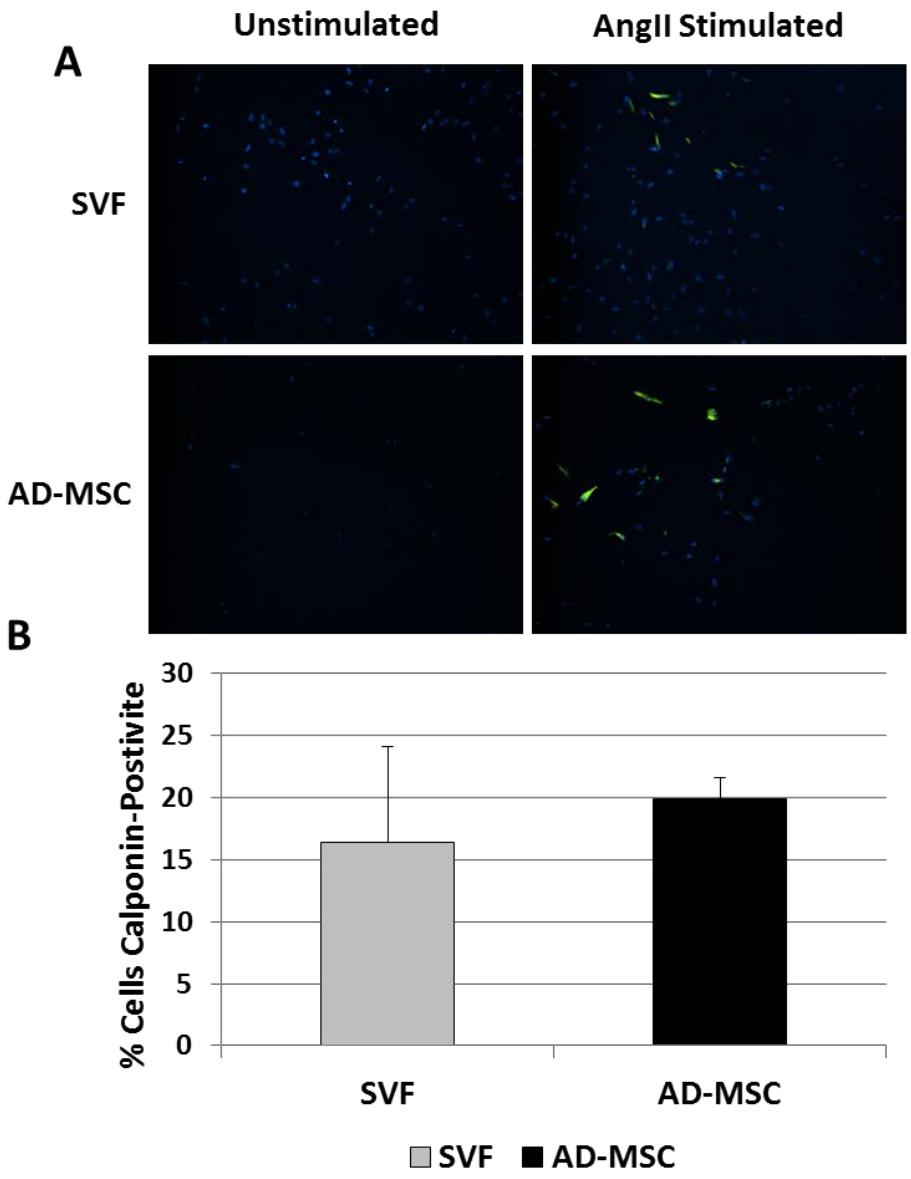

Figure 50. Human SVF cells performed an essential function of vascular tissue engineering: SMC Differentiation. (A) SVF cells and donor-paired cultured AD-MSCs were differentiated towards SMCs via Angiotensin II stimulation. SVF cells show an acquisition of the marker calponin similar to that of AD-MSCs. Images shown are representative of donor paired SVF and AD-MSCs. Data is presented as mean ± SD with a statistically significant difference defined at with $p<0.05$. n=3 donors were used per group.

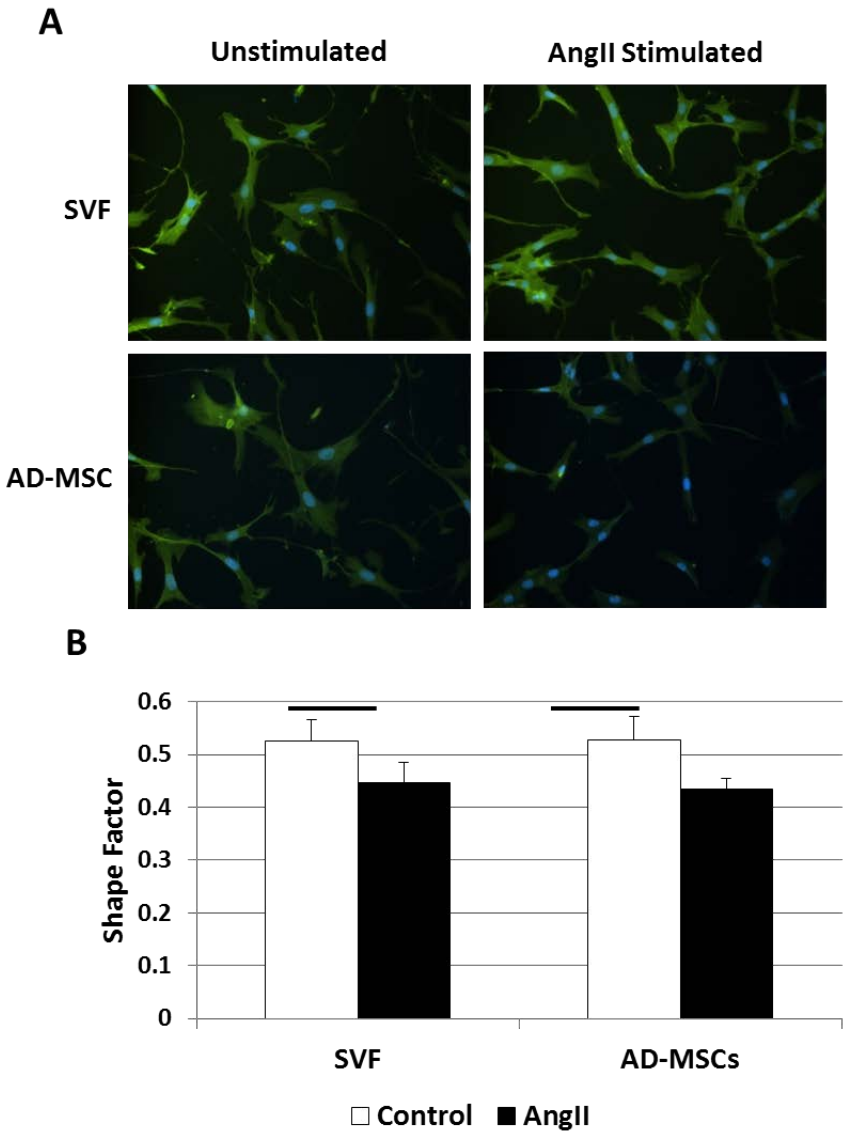

Figure 51. Stimulation with AngII induced a morphometric change in both SVF cells AD-MSCs wherein they adopted a more spindle-like shape. (A) When stimulated with AngII both SVF cells and donor-matched AD-MSCs underwent a morphological shift to a more SMC spindle-like cell shape when stained for F-actin (green; DAPI counterstain in blue). (B) This was quantified by measuring the shape factor (4p X area/perimeter2, ~0 = ellipsoid, ~1 = circular) of the cell where both SVF cells and AD-MSCs were showed a significant decrease in shape factor. Images shown are representative of donor paired SVF and AD-MSCs. Data is presented as mean ± SD with a statistically significant difference defined at with $p<0.05$. n=3 donors were used per group.

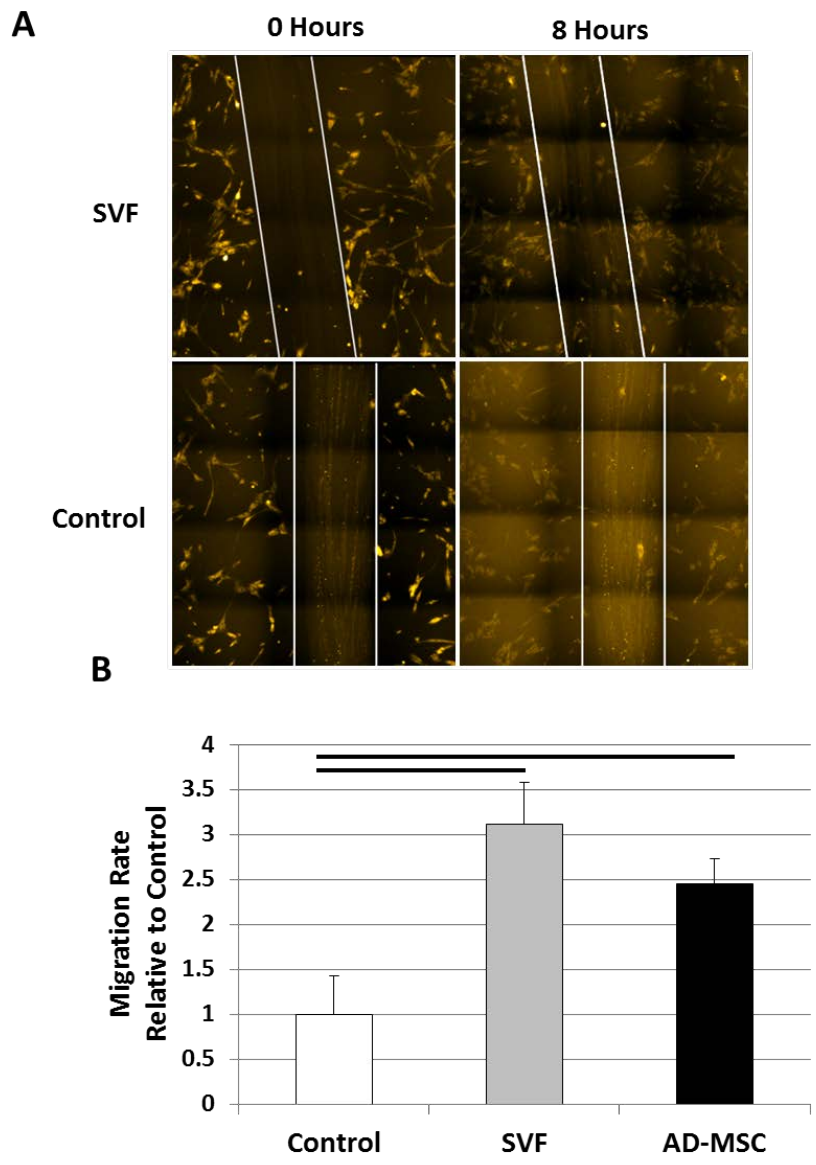

Figure 52. Human SVF cells performed essential functions to vascular tissue engineering: Promoting SMC Migration. (A) Conditioned media was acquired from SVF cells and used to stimulate SMCs in a scratch migration assay. (B) Quantitatively these cells are able to promote migration over non-conditioned controls and are on par with that seen with AD-MSCs. Images shown are representative of donor paired SVF and AD-MSCs. Data is presented as mean ± SD with a statistically significant difference defined at with $p<0.05$. n=3 donors were used per group.

4.3.2 Uniform Cell Seeding Analysis of SVF Cells

To verify that SVF cells can be seeded within tissue engineering scaffolds and as a point of quality control, the extent to which SVF were incorporated within our scaffolds using our RVSD was analyzed. Qualitatively, SVF cells were evenly seeded throughout the scaffolds in cross section and an equivalent cell densities were observed across the radial, circumferential, and longitudinal directions (**Figure 53**).

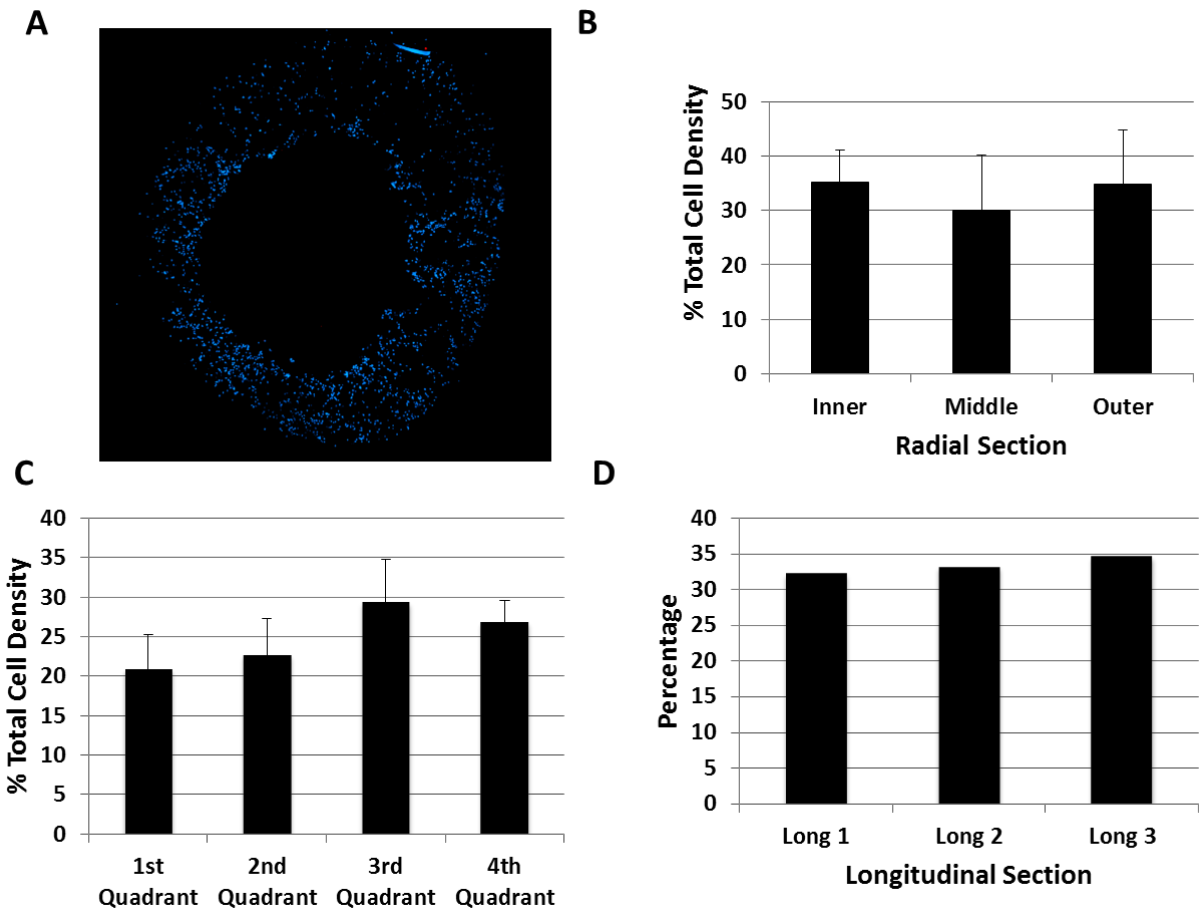

Figure 53. Human SVF cells were uniformly seeded within TEVG scaffolds. (A) SVF cells (n=3) were obtained from human patients and seeded directly into PEUU scaffolds where they seeded uniformly (blue, DAPI stain) across radial, circumferential, and longitudinal direction (not shown) of the scaffolds. (B) This uniformity was quantitatively confirmed by comparing the cell densities across virtually segmented pieces (B – Radial; C – Circumferential, D – Longitudinal). Data is presented as mean ± SD with a statistically significant difference defined at with $p<0.05$. As in **Figure 14**, adjustments were made based on area when comparing across the radial section due to increasingly larger concentric circular areas.

4.3.3 In Vivo Gross Observations and Patency

Following successful cell seeding analysis, SVF seeded scaffolds were then implanted in a Lewis rat model where after 8 weeks in vivo they remained patent, as confirmed by angiography (**Figure 54**). No dilation was observed for any implanted vessel. On gross observation, TEVGs showed an evident tissue-like appearance (**Figure 54**) and further histologic evaluation of explants (**Figure 54**) revealed clear breakdown of scaffolding material with the development of newly formed tissue lumenally (termed as neotissue). Culture paired AD-MSC-based TEVGs also displayed luminal neotissue formation (not shown) and exhibited similar patency rates (**Figure 54**). Together these results show that SVF cells are functionally equivalent to donor matched AD-MSCs for generating patent, tissue-like TEVGs.

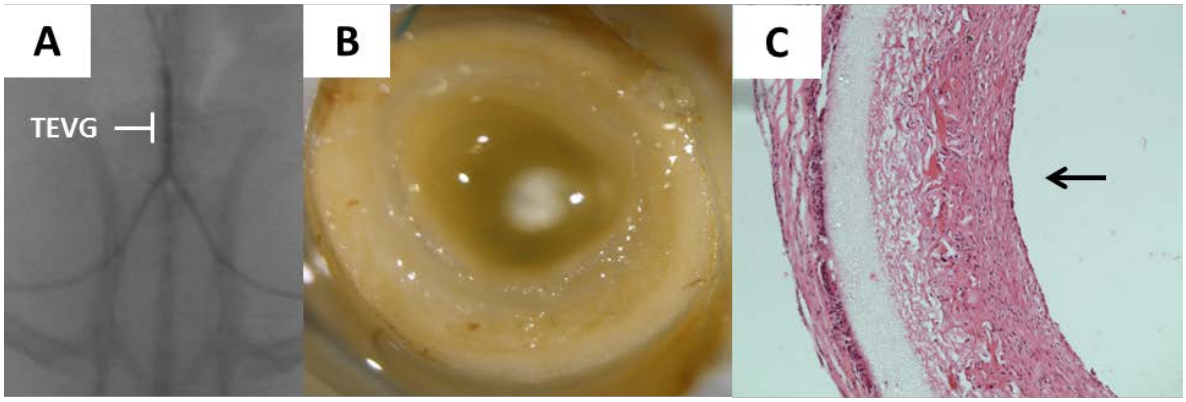

Cell Type	Patency
SVF	5/6
AD-MSC	5/5

Figure 54. Human SVF cell-based TEVGs generated patent vessels. (A) SVF seeded scaffolds were implanted in a Lewis rat model wherein they developed patent vessel at an 8 week timepoint shown by angiography. (B) Explanted SVF cell-based TEVGs displayed a clear tissue-like gross appearance. (C) Histologic H&E staining revealed SVF-based TEVGs showed signs of possessed newly developed tissue lumenally (neotissue) which showed ingrowth into scaffolding material. Both SVF cells and donor-matched AD-MSCs were equally capable of generating patent TEVGs (inclusive Table).

4.3.4 Morphometric Measurements and Vascular-Like Composition of Explanted TEVGs

To analyze the composition of the newly developed tissue within our TEVGs we probed for the primary cellular (SMC, endothelial cells), and extracellular (collagen, elastin) vascular components. Indirect immunofluorescence (**Figure 55**) revealed that the cellular components of all explanted TEVGs primarily consisted of SMCs (SMA and calponin labeling) and endothelial cells (vWF labeling). The percentage of cells expressing these markers was indistinguishable between SVF and donor-matched AD-MSC grafts (**Table 5**). Additionally, morphometric parameters to analyze cell density, cellular alignment (nuclear shape factor), and neotissue thickness were also all similar between the non-cultured SVF cells and cultured AD-MSCs (**Table 5**).

To investigate the presence of the extracellular matrix component collagen within explanted TEVGs we employed multiphoton microscopy. This imaging modality revealed prominent, circumferentially aligned collagen fibers within TEVGs produced with either SVF cells or AD-MSCs (**Figure 56**). Additionally, quantitatively assessing the fiber network revealed a similar number of intersections, segment lengths, tortuosity, diameters, and orientation between the two cell types (**Table 5**).

To investigate the presence of elastin, indirect immuno-fluorescence was utilized. This confirmed the immunological presence of elastin in both SVF and AD-MSC-based TEVGs (**Figure 56**). Additionally, quantitatively assessing its presence throughout the thickness of TEVG neotissue revealed similarity between these two cell types (**Table 5**). It is important to note however that although the presence of elastin was observed, it has not yet formed into functional elastic lamellae. Taken together, these results show that when non-cultured SVF cells

are utilized as the cell source for TEVGs they generate a vascular-like composition that is on par with that seen when utilizing cultured AD-MSCs.

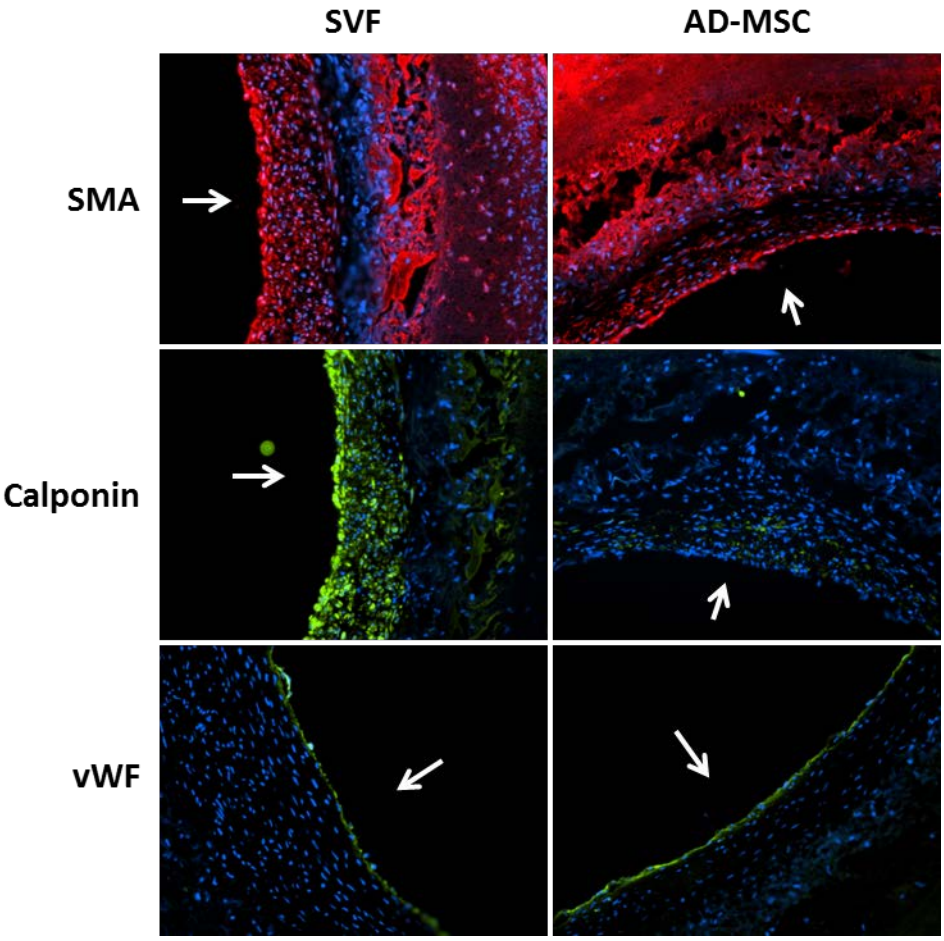

Figure 55. Human SVF cell-based TEVGs developed vascular-like tissue with primary cellular components. TEVGs, regardless of being created with SVF cells or donor-matched AD-MSCs displayed significant remodeling with the presence of vascular-like tissue. This tissue contained primary components such as SMCs (SMA (red), calponin (green)), endothelial cells (vWF (green))). White arrow indicates lumen. The presence of these components were quantitatively analyzed and all showed no significant difference (defined as $p<0.05$) between SVF cells or AD-MSCs (**Table 5**). Additionally, morphometric parameters such as cell density (# of cells per µm3 x 1000), the thickness of newly developed vascular tissue (i.e. neotissue thickness), and nuclear shape factor as a means to show alignment in the circumferential direction, all showed non-significant differences (**Table 5**).

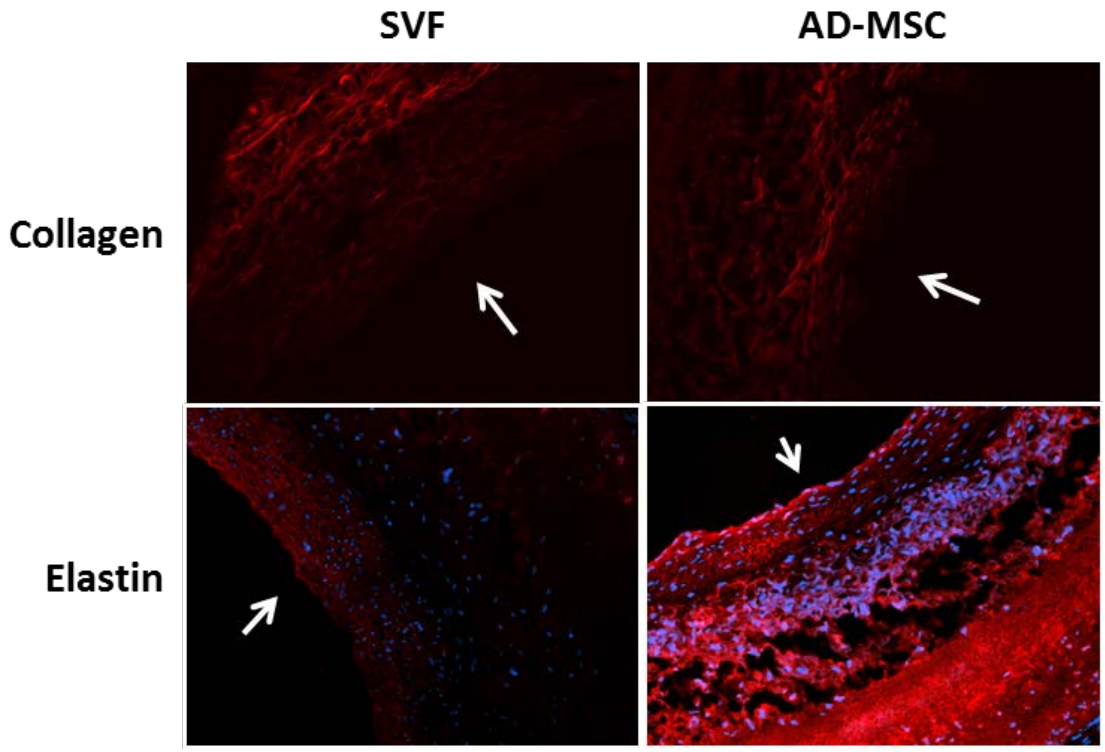

Figure 56. Human SVF cell-based TEVGs developed vascular-like tissue with primary extracellular matrix components. TEVGs, regardless of being created with SVF cells or donor-matched AD-MSCs displayed significant remodeling and contained primary extracellular matrix components such as collagen (multiphoton (red)) and elastin (alpha-elastin (red)). White arrow indicates lumen. The presence of these components were quantitatively analyzed and all showed no significant difference (defined as $p<0.05$) between SVF cells or AD-MSCs (**Table 5**). Analysis of the collagen micro-architecture for parameters such as fiber intersection density (number of intersection points per area), segment length (distance between cross-links, μm), fiber tortuosity, fiber orientation (circumferential ~90 degrees), and fiber diameter (μm) all revealed similarity between SVF and AD-MSC indicated by a non-statistically significant difference (**Table 5**).

Table 5. All quantified morphometric, histological, and micro-architectural parameters of patent SVF and paired cultured AD-MSCs. No statistical significance was seen comparing between SVF and AD-MSC parameters.

	SVF	AD-MSC
Cell Density	5.91 ± 1.66	6.12 ± 1.81
Neotissue Thickness	118.15 ± 14.85	93.57 ± 19.94
Shape Factor	0.84 ± 0.07	0.84 ± 0.03
% Cells SMA-Postitve	99.51 ± 1.09	93.37 ± 14.80
% Cells Calponin-Postitve	81.61 ± 12.54	78.41 ± 14.42
% Lumen vWF-Positive	94.37 ± 6.75	97.31 ± 3.43
Fiber Intersetcion Density	15.03 ± 2.32	12.20 ± 3.80
Segment Length	47.21 ± 7.54	52.37 ± 7.95
Tortuosity	1.11 ± 0.02	1.11 ± 0.02
Fiber Orientation	94.26 ± 2.60	94.81 ± 1.33
Fiber Diameter	11.65 ± 0.46	11.54 ± 0.38
% Thickness Elastin	80.02 ± 24.77	83.97 ± 17.89

4.4 DISCUSSION

The results of this study show that SVF cells can perform as well as AD-MSCs derived from the same population for use as a TEVG. First, these cells are capable of two stem cell-based bioactivities utilized heavily in vascular tissue engineering: undergoing differentiation into vascular SMCs and secreting pro-migratory factors. Second, it was shown that SVF cells can be incorporated within tissue engineered scaffolds and generate patent TEVGs with vascular-like tissue after implantation. The results of this study clearly indicate the functional efficacy of a non-cultured adipose-derived cell source in the context of vascular tissue engineering and that this efficacy is similar to that when using cultured AD-MSCs. Ultimately, the use of this cell source reduces rate-limiting barriers that could hinder the clinical translation of TEVGs. Indeed, the efficacy of the SVF in comparison to AD-MSCs has been shown in other applications [444, 451-454] and its use encouraged multiple clinical trials [452, 455, 456].

While non-cultured bone marrow cells have already been employed as a non-cultured cell source for vascular tissue engineering [229, 244] and can generate an equally sizable amount of cells [229, 457] as adipose tissue [445-448] (both on the order of millions per mL), the use of a non-cultured adipose-derived cell source could provide unique benefits. In addition to the attractive site which SVF cells can be harvested, performing a liposuction on a patient is associated with a reduction in cardiovascular disease risk factors [458]. This could offer resistance against recurrent vascular disease. On a cellular level, freshly isolated adipose cells (i.e. SVF) contain a higher percentage of cells that can provide anti-thrombogenic effects compared to bone marrow which could affect graft patency. These include cells such as MSCs

(30% adipose [191, 452] vs 0.001% bone marrow [216, 452]), endothelial cells (3% adipose [191] vs 0.1% bone marrow [216]), and endothelial precursor cells (14% adipose [191] vs. 2% bone marrow [216]). However, this statement remains as a conjecture as a side-by-side comparison of the two freshly isolated cell types has yet to be performed in vascular tissue engineering.

One of the major challenges currently present in stem cell-based vascular engineering is fabrication time. To reach clinical trials, tissue engineered products face a number of hurdles [283] including extensive pre-clinical testing, complicated and uncertain regulatory pathways, the necessity to improve product practicality, and funding shortages. These are amplified by the landscape of the current market where substantial reimbursement for cell-based technologies does not yet exist [250]. Additionally, regulations and recommendations set forth by the Food and Drug Administration (FDA) [459, 460] encourage the use of fresh cells as well as approaches that minimize time between isolation and use of a patient's cells for clinical trials. Indeed one of the few literature reports [228, 259, 461] in vascular engineering to make it to clinical trials utilized a non-cultured cell population (bone marrow mono-nuclear cells). The FDA also encourages controllable methods [459, 462] of manufacture which can be accomplished with cell processing devices. Utilizing our automated bulk cell seeding device in conjunction with fresh adipose-derived cells makes a significant practical step towards clinical translation. However, manual methods and xeno-genic enzymes are still required to isolate these cells [51, 191, 304, 443]. Automated technologies [451, 463] are currently being tested to alleviate these concerns and technologies [464-466] which can isolate SVF cells without enzymes are also being considered. It is foreseeable that with the combination of these

technologies, SVF cells, and our cell seeding methods, a TEVG could be fabricated at bed-side and within the same surgical procedure.

4.5 CONCLUSION

In conclusion, we have shown that a non-cultured human cell source (SVF cells) can be isolated from adipose tissue and utilized as effectively in vascular tissue engineering as AD-MSCs. These cells are capable of performing essential regenerative functions, can be seeded using a controllable device, and can generate TEVGs with a vascular-like composition. This study makes a significant step towards clinical translation of stem cell-based TEVGs.

4.6 FUTURE WORK

While this Aim acted as a proof of concept for use of a non-cultured adipose cell source for TEVG applications, there are still multiple unaddressed areas that need investigation. First, all cells used in this study were isolated from a population which would have been defined as "healthy" in Aim 1 and was chosen as such to show the efficacy of SVF cells under the best-case scenario. However this does not represent a clinically realistic population such as diabetic or elderly patients. Moreover, being a different cell population and one with a high degree of endothelial cells and EPCs [191], SVF could potentially possess a high enough anti-thrombogenicity to overcome the dearth seen in diabetic AD-MSCs in Aim 1. Second, SVF cells display a markedly different composition than AD-MSCs and understanding the cell types that

can be seeded within TEVGs is critically important for future optimization or mechanistic investigation. Third, while the use of SVF cells provides a substantial reduction in time to fabricate an implantable TEVG construct by removing the need to culture expand cells, our current protocol still includes 48 hours of dynamic culture in serum-supplemented media [161, 197, 260, 265]. This results in excess costs, the need for specialized equipment, and a potential risk for cellular contamination or transformation. Removal of this dynamic culture entirely coupled with our current RVSD technology [198] which can seed cells within minutes, would allow for an immediately usable TEVG. Adding to this the use of xeno-free enzymes [467, 468] or mechanical methods to isolate SVF cell (as discussed in Section 4.4 "Discussion") would also be preferred. Finally, while we currently utilize 3 million cells for our rat-sized construct, it may be possible to utilize a lower number to produce a functional TEVG. When scaling to a human sized construct (e.g. 4mm ID, 15 cm L) although adipose tissue can provide a suitable amount of cells (on the order of 100 million) seeding too many cells may affect the remodeling process. Indeed, one of the SMC pro-migratory factors secreted by MSCs, VEGF, actually displays a reduced effect at higher doses [348] implying that a lower number of cells could even lead to a more optimal host repopulation response so long as there is enough to provide adequate anti-thrombogenicity.

Pilot studies and further discussion of the cellular composition of an SVF seeded scaffold (see Section: "4.7.1 Marker Profile of SVF Seeded TEVG Scaffolds"), removal of a dynamic culture step (see Section: "4.7.2 Fabrication of an Implantable TEVG Without Spinner Flask Culture"), and seeding TEVG scaffolds with different cell densities (see Section: "4.7.3 TEVG Scaffolds Seeded At Varying Densities") will be discussed below.

Additionally, as one of the goals of this aim was to reduce the regulatory burden associated with TEVG translation, it is important to consider the regulatory pathway that this device could pursue. As this device would be classified as a combination product (materials and bioactive factors/cells), the FDA would the prominent agency for the market approval of this device. Additionally, as this device is implantable it would fall under the Class III which requires a strict premarket approval (PMA) process through generation of clinical safety and efficacy data. One way to expedite this process however would depend on if any of the current TEVG trials reach the market prior in which a 510k process could be pursued by showing device similarity.

4.7 ADDITIONAL STUDIES ADDING TO FUTURE WORK

4.7.1 Marker Profile of SVF Seeded TEVG Scaffolds

The composition of SVF cells is heterogeneous – unlike the more purified culture expanded AD-MSCs –and thus can result in TEVG scaffold populated with a variety of cell types. However, this composition when incorporated within scaffolds may be different than the raw SVF population. SVF cells consist of all cell types present in digested adipose tissue – which is heavily microvascularized – with the exclusion of erythrocytes and adipocytes which are removed through processing. This results in a heavily heterogeneous mixture consisting of endothelial cells, endothelial precursor cells, AD-MSCs, pericytes, leukocytes (macrophages), and lymphocytes (T-cell, B-cell) [191, 301, 302, 444, 469-471]. However, upon culture expansion this composition changes with a loss of endothelial cell markers and removal of non-

attachment dependent cells (leukocytes, lymphocytes) resulting in a purification of AD-MSCs [301, 302]. This is likely due to the high proliferative potential of AD-MSCs over the other cell types under the defined culture conditions (i.e. media recipe). Analyzing which cell types are contributing to the TEVGs is necessary not only from a quality control standpoint but also because the efficacy of cell based therapies, such as tissue engineering, are heavily impacted by the types used. From a pre-clinical standpoint this is particularly a concern; if human immune cells (lymphocytes) are entrapped within TEVG scaffolds prior to implantation within animal models it could cause adverse reactions.

A pilot study was performed to assess the cellular composition of SVF seeded scaffolds. For this, three SVF seeded TEVGs were utilized for analysis which were derived from separate donors than those detailed within Aim 2 (see **Table 4:** SVF 1, SVF 2, SVF 3). Similar fabrication methods were utilized to establish grafts prior to implantation (i.e. they underwent dynamic culture for 2 days within a spinner flask). Sections of SVF seeded scaffolds underwent immuno-fluorescent staining to detect the presence of the primary cellular components within the SVF: endothelial cells (CD31, Abcam #ab24590, 1:100), endothelial progenitor cells (CD34, BD Pharminogen #550390, 1:100), macrophages (CD68, Santa Cruz #SC-9139, 1:200), T cells (CD4, Abgent #AP1496a, 1:50), and B cells (CD20, Novus Bio #NB100-64858, 1:50). All seeded scaffolds showed presence of endothelial and progenitor markers CD31 and CD34 of the absence of the immunological markers CD68, CD4, and CD20 (**Figure 57**). As these latter markers are only present on cells which are not attachment dependent, it is likely that they were washed away during the dynamic culture despite being incorporated within scaffold pores during the seeding process.

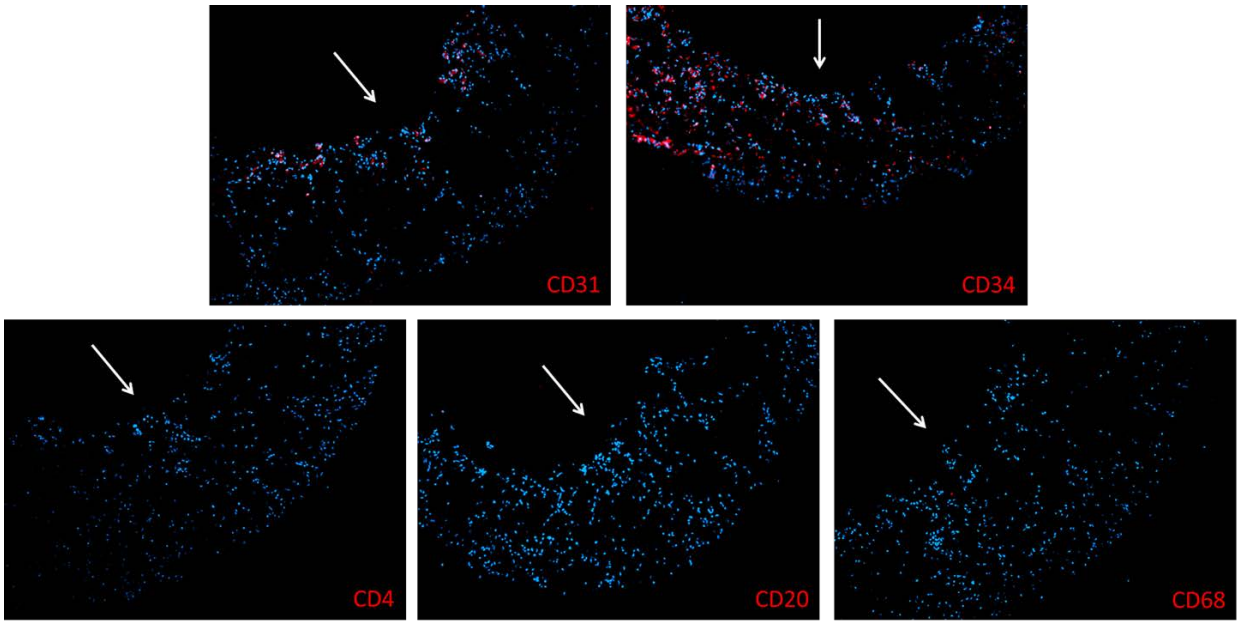

Figure 57. Phenotypic characterization of SVF seeded scaffolds. Immuno-fluorescence shows presence of endothelial cells (CD31) and endothelial precursor cells (CD34) in SVF seeded scaffolds and a lack of T-cells (CD4), B-cells (CD20), and macrophages (CD68) (n=3). White arrow indicates lumen.

Additionally, one cell line (see **Table 4**: #SVF 2) was subsequently passage expanded and a cell seeded scaffold was produced at each subsequent passage to assess the phenotypic change in SVF cells over the culture period. It was observed that both CD31 and CD34 were present during seeding of TEVG scaffolds with raw SVF cells and at early passages, but this declined during continued passage expansion (**Table 6**). This finding is consistent with studies investigating the marker profile of SVF cells throughout passage expansion in typical flask culture [299, 301, 302].

Table 6. Continued passage expansion of SVF cells results in phenotypic changes. After expanding the SVF into AD-MSCs via continual passage expansion and seeding them into TEVG scaffolds, the marker profile of seeded cells alters. In particular, CD31 expression is maintained while CD34 is lost (n=1).

Cell Type	CD31+	CD34+	CD4+	CD20+	CD68+
SVF	27%	28%	0%	0%	0%
AD-MSC P0	41%	12%	0%	0%	0%
AD-MSC P1	28%	5%	0%	0%	0%
AD-MSC P2	41%	0%	0%	0%	0%

4.7.2 Fabrication of an Implantable TEVG Without Spinner Flask Culture

As mentioned in Section 2.4 ("Discussion"), removing the currently used 48 hours dynamic culture step prior to in vivo implantation would allow an almost immediate fabrication. As many TEVG approaches utilize extended culture methods (see Section: "1.5.2 Fabrication Time") which are limited by high cost and contamination risk, this would further enhance the translatability of our TEVG. Indeed, one of the most successful TEVG approaches and one that has reached clinical trials utilizes a closed cell seeding system which prepares a graft within hours (see Section: "1.4.1 Approach 1 – Bone Marrow Cells with Synthetic Scaffold"). As an initial means to assess the potential of eliminating the need for a culture period post-seeding, a pilot study was performed where AD-MSCs were seeded in TEVGs and incubated in dynamic culture conditions (spinner flask, 15 rpm) for 0 and 2 days (n=3). Qualitatively when staining for F-actin (green) and DAPI (blue) no difference in either cell spreading or cell density, respectively, is observed (**Figure 58**). Adding to this, in a separate study, SVF seeded scaffolds following the same dynamic culture period reveal a punctate F-actin staining pattern and are not

as well spread as AD-MSCs (**Figure 59**). However, both of these cell types displayed proper in vivo functionality despite this difference in spreading. Due to these findings, achieving optimal spreading prior to implantation may be unnecessary.

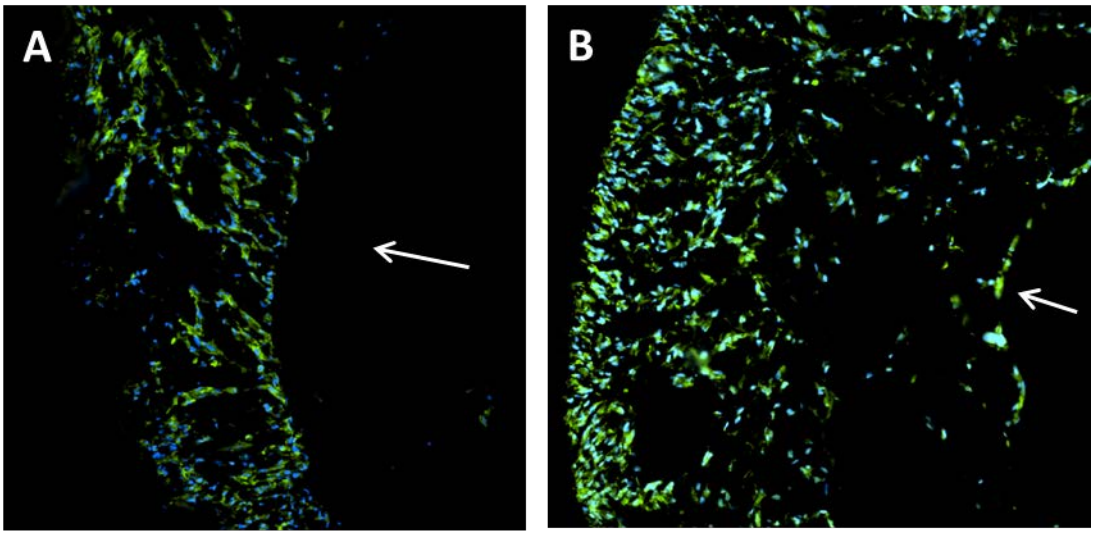

Figure 58. AD-MSC seeded scaffolds cultured in spinner flasks for 0 and 2 days reveal no qualitative differences in density or spreading. AD-MSCs were seeded in TEVG scaffolds and subjected to spinner flask culture for 0 (A) or 2 (B; current regiment) days. Staining for DAPI (blue) and F-Actin revealed no qualitative differences for cell density and spreading, respectively (n=3). White arrow indicates lumen.

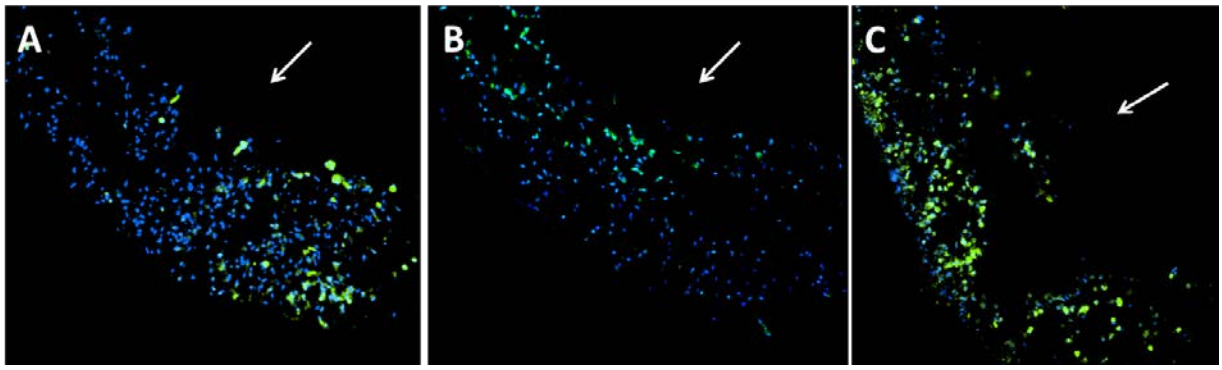

Figure 59. SVF seeded scaffolds prior to implantation reveal punctate F-Actin staining. Three SVF scaffolds (A, B, C) were stained for DAPI and F-actin prior to implantation (i.e. after a 2 day spinner flask culture). F-actin staining revealed punctate staining for SVF cells as opposed to the elongated morphology seen in cultured AD-MSCs seeded scaffolds (**Figure 58**). White arrow indicates lumen.

4.7.3 TEVG Scaffolds Seeded At Varying Densities

As stated in Section 4.4 ("Discussion"), although our current rat-sized TEVG requires 3 million cells this number has not yet been optimized and it is not clear if the number of cells will correlate with functional efficacy. Ideally, there should be enough cells to provide sufficient anti-thrombogenicity but not so much that growth factor signaling achieves supra-physiologic concentrations which could potentially reduce graft functionality. A pilot study was performed to illustrate that TEVGs could be constructed with varying cell densities while still retaining a uniform distribution is easy achievable with our methodology (**Figure 60**).

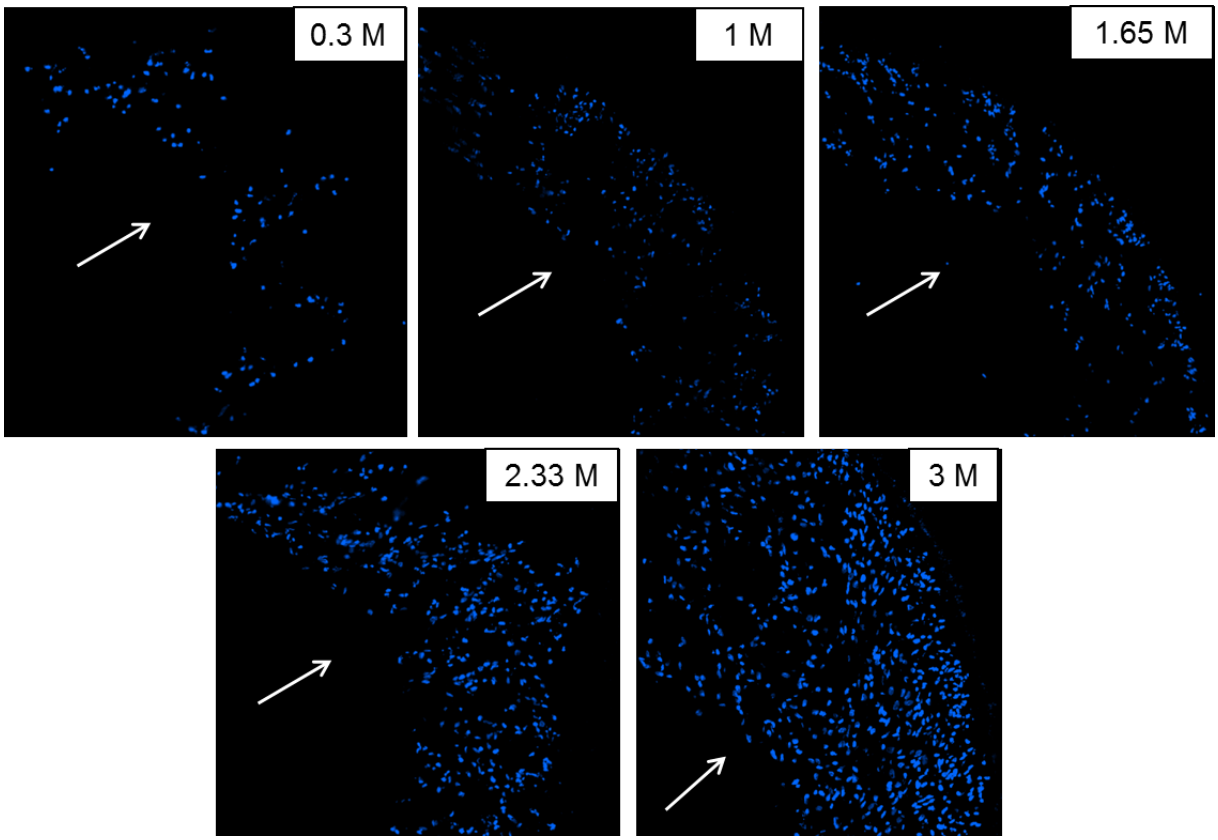

Figure 60. Seeding TEVG scaffolds with varying densities is achievable with our methodology. TEVG scaffolds were seeded with 0.3, 1, 1.65, 2.33, or 3 million AD-MSCs (n=1). A clear change in cell density is observed consistent with the number of seeded cells. Additionally, the seeding methodology preserves a uniform cell seeding, despite the change in number. White arrow indicates lumen.

5.0 SPECIFIC AIM 3: DEVELOPMENT OF AN ARTIFICIAL MSC-BASED TEVG

Autologous cell seeding of biodegradable scaffold materials is frequently utilized for TEVGs in order to offer resistance against acute thrombosis, to prevent stenosis, and to provide paracrine/secreted factors to encourage substantial remodeling of the graft in the form of host cell recruitment (see Section: “1.5.3 In Vivo TEVG Mechanisms”). However, investigatory studies into the mechanism of TEVG remodeling have shown that these seeded cells are not retained in the TEVGs long term but are needed acutely to provide these benefits until the host environment can adequately take over. This is typically performed in a paracrine (i.e. secreted factor) manner. As illustrated by this dissertation, MSCs are a potent cell type which can lead to a successful TEVG but their function is highly dependent on donor demographics (see Aim 1). Indeed, many functions that can lead to a successful TEVG are diminished in the MSC of clinically relevant populations, namely the potency of pro-migratory and anti-thrombogenic secreted factors. As such, the promise of autologous MSCs in tissue engineering approaches for vascular replacement may not be tractable for those significant patient populations. However as MSCs secrete a variety of beneficial bioactive factors which can provide pro-migratory, mitogenic, anti-thrombogenic, and immuno-regulatory effects [183-189], delivering these factors produced by a healthy MSC source could lead to a functional arterial replacement even in high-risk clinical populations. Beyond this, as a TEVG produced with secreted factors would be acellular, multiple TEVGs could be produced by one potent MSC cell line and could then be

stored for later use. This leads to an “off-the-shelf” approach overcoming many costs and risks associated with fabrication time, cellular transformation in culture, and donor-to-donor variability (see Section: “1.5 Current Barriers to Clinical Translation”).

Additionally, the approach of utilizing an artificial system is superior to utilizing a potent allogenic cell (e.g. healthy cells into a diabetic patient) line due to their practical limitations. The use of allogenic cells would require immuno-suppression therapy which could predispose the patient to life threatening diseases. As there already exist other potential therapies (e.g. the currently used saphenous vein) available without this risk, this is a significant hurdle to overcome. Additionally, generating clinical safety data to confirm the use of allogenic cells would require use of a control group which implants an allogenic graft exposing the patient to immune-rejection. As rejection of an artery could pose serious risks such as bleeding, donor site morbidity, or loss of a limb, this is not advisable.

To date, several attempts have been made to create acellular TEVGs by functionalizing biodegradable materials through surface coatings, growth factor immobilization, drug delivery, or methods to resist thrombosis (see Section: “1.3.6 Acellular TEVGs”) and have shown promising results in the development of patent and remodeled TEVGs. However, these functionalized biodegradable materials often utilize a single or limited number of factors and this approach is constrained in that a limited number of factors cannot replicate the complex, multi-factorial coordination involved in biological systems. Further, utilizing a high concentration of a single factor – which many such approaches resort to – can lead to deleterious systemic side effects [224, 225].

In this Aim an innovative TEVG approach was developed incorporating a delivery system for the broad spectrum of secreted factors derived from healthy human MSCs by

encapsulating conditioned media within degradable PLGA microspheres. These MSC conditioned media encapsulated microspheres will be termed “artificial MSCs” due to their mimicry of many facets of cell use within a TEVG. Namely these are able to replicate the paracrine activity of MSCs, be seeded within a TEVG scaffold, and display a similar geometry to that of a cell. In essence, artificial MSCs seeded within our biodegradable tubular scaffold will create a new, clinically-translatable TEVG paradigm that can be utilized in place of any MSC lacking appropriate function and be “off-the-shelf” allowing them to be produced in mass quantity while not being practically limited by fabrication time. It is also noteworthy that while in this application artificial MSCs are utilized for TEVG applications, they may hold value in other MSC cell therapies. The goal of this Aim was to demonstrate the feasibility of artificial MSCs by making initial assessments of many of the design criteria (see Section: 5.1 “Design Criteria”). Further optimization will be discussed in future work (see Section: 5.5 “Discussion and Future Directions”).

5.1 DESIGN CRITERIA

In order for artificial MSCs to be successful in releasing bioactive factors within a TEVG scaffold they must satisfy two main criteria: 1) be able to be seeded within TEVG scaffolds, and 2) release the broad spectrum of bioactive factors at appropriate potency. To satisfy both of these criteria multiple facets of each microsphere manufacture (e.g. sizing, loading, release) and seeding methodologies must be considered. The following sections will describe the subsets of these two main criteria and consider their desired characteristics.

5.1.1 Seeding of Artificial MSCs – Determining Appropriate Diameter

When considering the appropriate size of the microsphere two aspects must be considered: 1) what size will be successfully incorporated within the scaffold via the seeding process, and 2) how much cargo will be delivered. As the latter point can easy be overcome via incorporation of a higher number of microspheres or concentration of media within the microspheres, establishing the appropriate diameter based on cell seeding is considerably more important. While microspheres can have their fabrication tuned to achieve a variety of diameters (on the order of 1 [472-474], 10 [474-478], and 100 [474] μm), the sizing of microspheres for this application is ultimately limited by scaffold pore size. As our scaffold pores are approximately 50 μm in diameter, microspheres must be sized to be less than this value. Additionally, as trypsinized AD-MSCs average around 20 μm (**Figure 61**) and seed successfully, we expect microspheres around this size to be successful. To appropriately define the appropriate diameter, microspheres from sizes ranging from 1-50 μm will be seeded within TEVG scaffolds and a successful diameter will be defined as any that allows incorporation within the scaffold post-seeding.

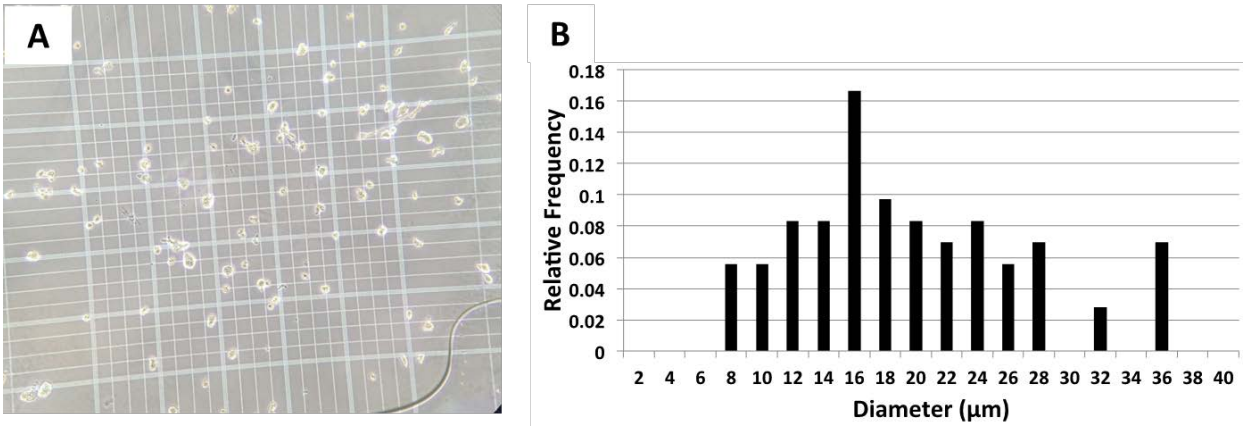

Figure 61. Size distribution of AD-MSCs The trypsinized AD-MSCs (i.e. those prior to cell seeding) placed on a hemocytometer (A) were imaged and their diameter was measured to determine their size and distribution (B).

5.1.2 Seeding of Artificial MSCs – Determining Optimal Seeding Parameters

Microspheres possess substantial differences from cells which may alter the seeding method and number of necessary microspheres. As microspheres display a high degree of structural rigidity while a cell is comparably fluid, microspheres may have difficulty navigating through scaffold pores when exposed to the transmural vacuum forces during the seeding process. However, as an initial benchmark to begin optimization of seeding parameters, microspheres were seeded to achieve a similar density and distribution (i.e. uniform in all directions) as MSCs. While admittedly, this does not determine the appropriate quantity of microspheres, this is ultimately beyond the scope of this dissertation and will require a time course in vivo investigation into the TEVG remodeling process (see Section: 5.5 “Discussion and Future Directions”). To determine methods to successfully seed microspheres to our benchmark, microspheres will be seeded with current methods and then based on the results, various parameters will be altered (solution concentration, vacuum force, etc.). It is also noteworthy that utilization of a seeding technology that can apply transmural forces such as our vacuum-based seeding is essential to the

incorporation of artificial MSCs as they cannot seeded via manual pipetting due to their lack of attachment and migratory abilities.

5.1.3 Seeding of Artificial MSCs – Retention Under Flow Conditions

Unlike cells, microspheres do not possess attachment mechanisms such as integrins to allow for adherence to scaffolding materials and can only rely on passive wedging effects within scaffold pores. However, retention of microspheres is necessary as they will encounter arterial flow conditions when placed in vivo. If the microspheres become dislodged from scaffolds it is likely that the therapeutic efficacy of the TEVG would be reduced and the microspheres could contribute to a potential embolism. To investigate if the current passive wedging effects of the microspheres are insufficient, microsphere seeded scaffolds will be placed under arterial flow conditions and monitored for their cell densities compared to static controls.

5.1.4 Bioactive Factor Release – Cell Source for Bioactive Factors

An ideal cell source to obtain MSC secreted factors to be incorporated within artificial MSCs would be one such that it can produce the necessary bioactive factors for TEVG remodeling but not be limited by donor effects which could compromise the graft such as diabetes. The current gold standard for this would be our healthy AD-MSC group from Aim 1. However, from a commercialization standpoint it is foreseeable that one potent cell line will be utilized to produce multiple artificial MSC based-TEVGs. As such, another potential cell source is a commercial MSC cell line as it offers several advantages with regards to characterization and quality control. For the purposes of this study, AD-MSCs utilized in Aim 1 were originally employed but studies

were later shifted to a commercial MSC line (RoosterBio). The distinction for which experiments were performed with each cell type will be made clear in the methods section below.

5.1.5 Bioactive Factor Release – Customizable Release

A critical design criterion for these microspheres is that they be tunable with regards to their release of cargo, which will allow the best mimicry of the action of MSCs in our TEVG. Several parameters can be controllably varied for this purpose, including polymer composition, concentration and/or composition of encapsulated factors, and microsphere porosity (pore diameter) [479]. Ideally, microspheres will release in such a way that the broad spectrum of MSC factors are released in tandem – thus mimicking the profile of a cell – and done so in correlation with regards to the number of seeded cells within a stem cell-based TEVG. However, as mentioned in above when discussing about determining the appropriate number of seeded microspheres, the exact timing of the release is unclear as we do not yet know the timing of host cell recruitment within our model system; determination of this will be reserved for future sides (see Section: 5.5 “Discussion and Future Directions”). However, as a proof of concept this study will show that the microspheres’ release can be customized to achieve a variety of release profiles with different timings.

5.1.6 Bioactive Factor Release – Processing of Media (Concentration)

In order to achieve equivalent biological activity to a batch of conditioned media, the microspheres forming artificial MSCs must encapsulate a relatively concentrated solution of secreted factors. This is because the volume of encapsulated media within microspheres is only a

fraction compared to the total volume of their surrounding solution, yet they must release a high enough concentration of factors to achieve a functionally relevant dose. Additionally, microspheres cannot continually produce factors as cells can. To determine a method which can result in the highest appropriate strategy to concentrate media, multiple concentration methods will be employed and the bioactivity of concentrated media will be verified.

5.1.7 Bioactive Factor Release – Release of Desired Factors and Maintained Bioactivity

One of the essential design characteristics of the artificial MSC technology is that it releases the broad spectrum of bioactive factors instead of solely singular or limited factors which have been employed in other TEVG approaches. We will demonstrate the release of multiple bioactive factors by measuring four representative factors: vascular endothelial growth factor (VEGF), monocyte chemotactic protein-1 (MCP-1), brain-derived neurotrophic factor (BDNF), and urokinase plasminogen activator (uPA). These are chosen since all four are known to be among the secretory products of AD-MSCs, and to be involved with aspects or mechanisms of TEVG remodeling (e.g., smooth muscle cell (SMC) migration, monocyte recruitment, angiogenesis, anti-thrombogenicity, etc.) [155, 183, 216, 357, 480-482] (also see Aim 1-2). Additionally, the factors released by artificial MSCs must remain bioactive. To confirm bioactivity, assays utilized in Aim 1 (e.g. SMC scratch migration assay) will be employed.

5.1.8 In Vivo Functionality

The ultimate success of the artificial technology is to induce similar in vivo effects to that of an MSC, namely delivering bioactive factors over the same time course seen with an MSC seeded

TEVG. This includes both delivery of the broad spectrum of bioactive factors and dosing them appropriately to the number of cells present within the TEVG (i.e. as the MSCs are removed from the graft no longer providing their secreted factor benefit, artificial MSCs are no longer releasing those same factors). In this way, artificial MSCs will induce an similar remodeling response as that seen with healthy MSCs thus alleviating concerns of donor-to-donor variability that might cause graft failure such as in the case of diabetes. While optimization of all microsphere parameters are beyond the scope of this study due to the need to perform multiple time course animal studies to successfully define the release profile needed for artificial MSCs (see Section: 5.5 “Discussion and Future Directions”), a proof of concept in vivo implantation will be performed as part of this study.

5.2 METHODS

5.2.1 Microsphere Fabrication

Microsphere fabrication will follow previously established methods to generate microspheres of different porosities and sizes utilizing double emulsion techniques to generate PLGA microspheres [483]. In this technique the size of the microsphere can be altered through changes in homogenization speed during the second emulsion formation (increase speed leads to increased size) and the size of pores can be altered by adjusting the solution osmolarity during fabrication (no adjustment leads to more pores). For determining the appropriate size of microspheres for TEVG scaffolds and when performing all seeding experiments (see Sections: “5.3.1 Seeding of Artificial MSCs – Determining Appropriate Diameter”, “5.3.2 Seeding of

Artificial MSCs – Determining Optimal Seeding Parameters", "5.3.3 Seeding of Artificial MSCs – Retention Under Flow Conditions"), microsphere populations were created to different sizes with an average diameter of 40 µm (blank), 20 µm (blank), or 10 µm (FITC-dextran encapsulated; Sigma #FD2000S). To show the ability to tailor the release of microspheres (see Section: "5.3.4 Bioactive Factor Release – Customizable Release"), conditioned media encapsulated microspheres were created to different porosities (non-porous, porous, and burst (i.e. highly porous)). As following these experiments and out of these current formulations, the size of the 10 µm and the burst porosity were found most suitable, this formulation was utilized for release studies (see Section: "5.3.6 Bioactive Factor Release – Release of Desired Factors and Maintained Bioactivity").

5.2.2 Obtaining MSC Conditioned Media

For this study conditioned media was obtained from two cell lines. The first was from utilizing healthy AD-MSCs employed in Aim 1 (**Table 1**: #1, 2, 5) and acquired in the same manner as previously described (see Section: "2.2.1 Isolation and Culture of Cells and Collection of Conditioned Media"). Briefly, near confluent flasks of AD-MSCs were given fresh media and conditioned for 2 days. AD-MSC conditioned media was utilized for the experiments controlling the release and concentrating conditioned media (see Section: "5.2.5 Concentration and Release of Microsphere Encapsulated Conditioned Media").

Due to the attractive translatability of utilizing a commercial cell line which has a high degree of characterization and quality control, all other experiments employed conditioned media derived from an MSC cell line produced by RoosterBio (#KT-002, cell line #00055). The donor

information for this cell line is as follows: 22 year old, male. Conditioned media was isolated in the same manner as with AD-MSCs and the RoosterBio MSC line was utilized between passages 0 and 3.

5.2.3 Seeding of Microspheres Within TEVG Scaffolds

Microspheres were seeded in a similar fashion to all other studies within this proposal (see Section: “2.2.5 Cell Seeding into TEVG Scaffolds”). Microspheres of size 40 µm, 20 µm, and 10 µm (FITC-dextran embedded) were utilized in this process. Prior to cell seeding microspheres were incubated in buffer (PBS) with end-over-end mixing for 1 hour to solubilize. As initial results of seeding utilizing our standard parameters were deemed inadequate, alterations to various parameters such as vacuum pressure, seeding solution volume, and seeding solution concentration were made.

5.2.4 Exposure of Microsphere Seeded TEVG Scaffolds to Physiologic Flow

Following seeding of microsphere-based TEVGs, a section of scaffold (~1/3) was removed to act as a static (i.e. no flow) control while the remainder of the scaffold was immediately placed within the pulsatile flow loop described in Section 2.7.3 (“Explanted TEVG Mechanical Testing”). Each scaffold was subjected to physiologic pressure waveforms (120 mmHg/80 mmHg) and flow (22.3 mL/min, equivalent to rodent aortic flow rate [484]) for 5 hours. Scaffolds were then removed from the system, fixed, frozen, and imaged.

5.2.5 Concentration and Release of Microsphere Encapsulated Conditioned Media

Conditioned media produced by AD-MSCs of three donors (see **Table 1**, donors #1, #2, #5) was concentrated either by filtration or lyophilization. To filter concentrate media, conditioned media samples were placed in Millipore Centrifugal Filters (3K MWCO) and centrifuged at max speed until concentrated. For lyophilization, conditioned media samples were dehydrated and reconstituted in the smallest volume of water possible to completely dissolve the sample. The degree of concentration was assessed on total protein by a bicinchoninic acid assay (Thermofisher).

To demonstrate that the release of MSC conditioned media could be tailored, microspheres were fabricated in non-porous, porous, and burst configurations (see Section: "5.2.1 Microsphere Fabrication"). Each microsphere population was incubated at 37ºC in 5 mL of PBS while being rocked end-over-end. At specified times, the microsphere populations were centrifuged (1000 rpm, 5 min), a sample was drawn, and the microspheres were re-incubated in fresh buffer. For the non-porous and porous microsphere configurations samples were drawn at 1, 3, and 7 days, and for burst release configuration samples were drawn at 1, 2, 4, and 7 days. Cumulative release was assessed based on total protein utilizing a bicinchoninic acid assay (Thermofisher). Microspheres in this experiment were encapsulated with AD-MSC conditioned media (non-concentrated) and experiments were performed in triplicate.

Next to demonstrate that relevant factors to vascular tissue engineering was present in MSC conditioned media and could be released from microspheres, ELISA kits identifying human VEGF (DVE00, R&D Systems), MCP-1 (#DCP00, R&D Systems), BDNF (#DBD00, R&D Systems), and uPA (#DUPA00, R&D Systems) were utilized following the manufacturer's instructions. Microspheres in this study were fabricated by encapsulating concentrating

conditioned media produced with RoosterBio MSCs in a burst configuration. The microspheres were released in a similar manner as above but preserved the entirety each releasate for the first three days (a time point when this fabrication of microsphere fully releases its cargo). The releases samples were then lyophilized, reconstituted, and combined such that the original volume of the pre-encapsulated sample was restored prior to performing ELISAs. Samples obtained in this study were also utilized in a bioactivity assay (see below)

5.2.6 Scratch Assay for Bioactivity of Microsphere Released MSC Conditioned Media

To confirm the bioactivity of microsphere released MSC conditioned media, a scratch assay was employed similar to that in Aim 1 (see Section: “2.2.3 Ability of AD-MSCs to Promote SMC Migration”.

5.2.7 Statistics

All statistics were performed in a similar manner to Section 2.2.11 (“Statistics”).

5.3 RESULTS

5.3.1 Seeding of Artificial MSCs – Determining Appropriate Diameter

The first design criteria for the use of PLGA microspheres with a TEVG scaffold was to appropriately assess the diameter range of microspheres which would appropriately fit within TEVG scaffolds. As a pilot study, microspheres were created with an average diameter of 20 µm

or 40μm to mimic the average size of AD-MSCs (see **Figure 61**) or to match the pore size of the scaffold (~50 μm [260]). However, it is noteworthy that each microsphere population has a wide range of diameters around this average value. The rationale for testing both of these sizes is that due to the lack of adhesive properties present on the microsphere surface, they may be physically removed under arterial flow conditions and a larger size may be necessary to "wedge" within pores to prevent this from occurring. Upon seeding of both 20 μm and 40 μm microspheres utilizing our standard methods (3 million objects seeded, vacuum pressure -127 mmHg) a majority of the microspheres did not penetrate within scaffold pores, persisting lumenally (**Figure 62**). Anecdotally, a large amount of these spheres were washed away in subsequent processing steps (fixation/freezing) as shown by a white powder eluting from the lumen of the scaffolds (**Figure 62**). Upon imaging cross sections of microsphere seeded TEVG scaffolds two phenomenon were evident: 1) microspheres of an average size around 5 μm were present within TEVG scaffolds, and 2) the microspheres themselves were difficult to visualize utilizing solely brightfield imaging. For all subsequent seeding experiments a population of microspheres with an average diameter of 5 μm utilized and were loaded with a FITC-labelled dextran for visualization. Indeed, all subsequent seeding experiments (see Sections: "5.3.2 Seeding of Artificial MSCs – Determining Optimal Seeding Parameters", "5.3.3 Seeding of Artificial MSCs – Retention Under Flow Conditions") confirmed that 5 μm or less is indeed the diameter for seeding microspheres within our PEUU scaffolds (**Figure 63**). Although this is much less that the size of cells themselves (**Figure 61**, average: 20 μm), it likely occurs due to the lack or rigidity of PLGA microspheres – as opposed to cells – which cannot deform to navigate through scaffold pores.

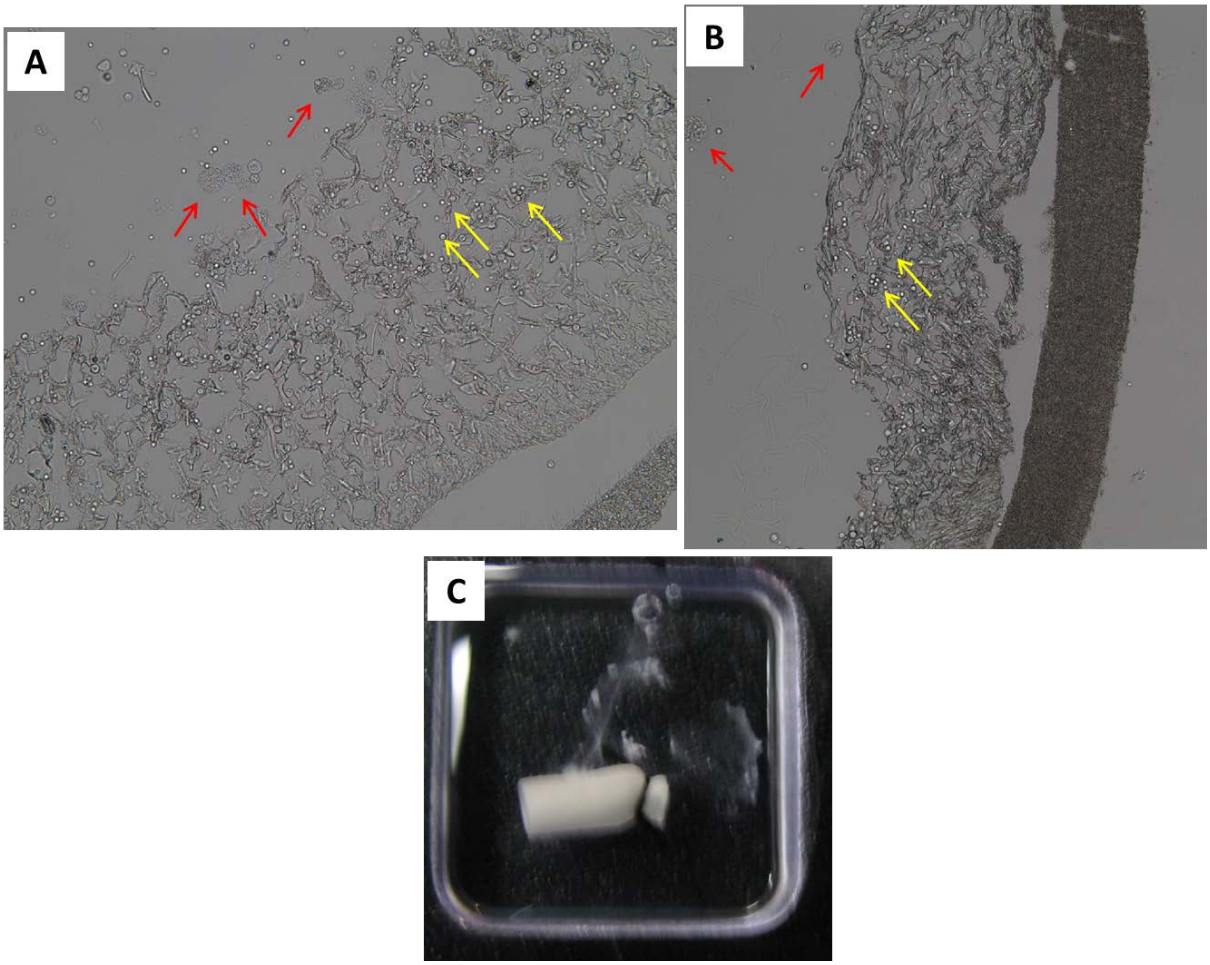

Figure 62. Only microspheres of less than 5 µm successfully seed within TEVG scaffolds. Microspheres of Average Size 20 (A) and 40 µm (B) were both seeded within TEVG scaffolds. However, only small microspheres (yellow arrows) were shown to fit within scaffold pores whereas larger sized ones are lumenally excluded (red arrows). The microspehres were quantitatively determined to be 5 µm or less. These lumenally excluded microspheres were further noted as additional histologic processing steps resulted in removal of microspheres from the scaffold lumen appearing as a white cloudiness within clear media (C).

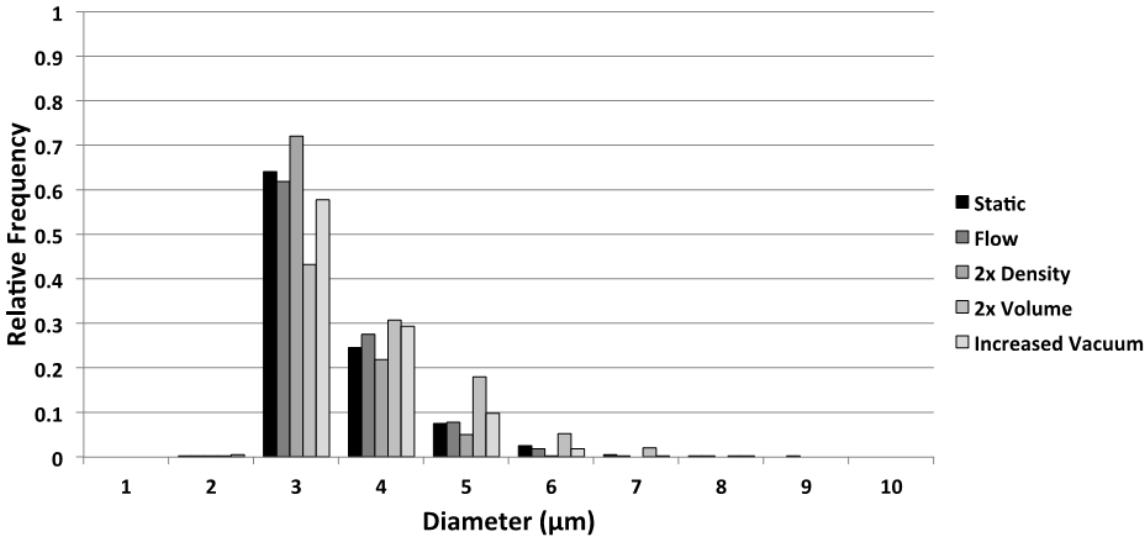

Figure 63. The diameter threshold of seeded microspheres at 5 µm or less was consistent across all experiments in this aim. The sizing of microspheres was analyzed for all seeded scaffolds within this Aim which consistently revealed a cutoff range of 5 micrometers or less.

5.3.2 Seeding of Artificial MSCs – Determining Optimal Seeding Parameters

Following determination of the appropriate microsphere size which would seed within PEUU scaffolds, we then sought to optimize the cell seeding in such a way were microspheres could be seeded to similar metrics as AD-MSCs (i.e. cell density and distribution). While admittedly future studies may prove that number of microspheres needed to induce a regenerative response may be different from that of cells, these metrics were utilized as a benchmark to evaluate potential abnormalities encountered during the seeding process when utilizing microspheres. As mentioned in the previous section, all seeding experiments utilized a microsphere population with an average diameter of 5µm with a range from 1-10 µm, and were loaded with FITC for visualization. Additionally, previous methods to count cells via the ImageJ-based automated cell counting tool (see Section: "2.3.3 Uniform Cell Seeding Analysis for Healthy, Diabetic, and Elderly AD-MSCs") developed in Aim 1-1 were utilized and indeed showed the ability to

quantify the microsphere density within seeded scaffolds (**Figure 64**). Additionally this tool allows for determination of microsphere diameter.

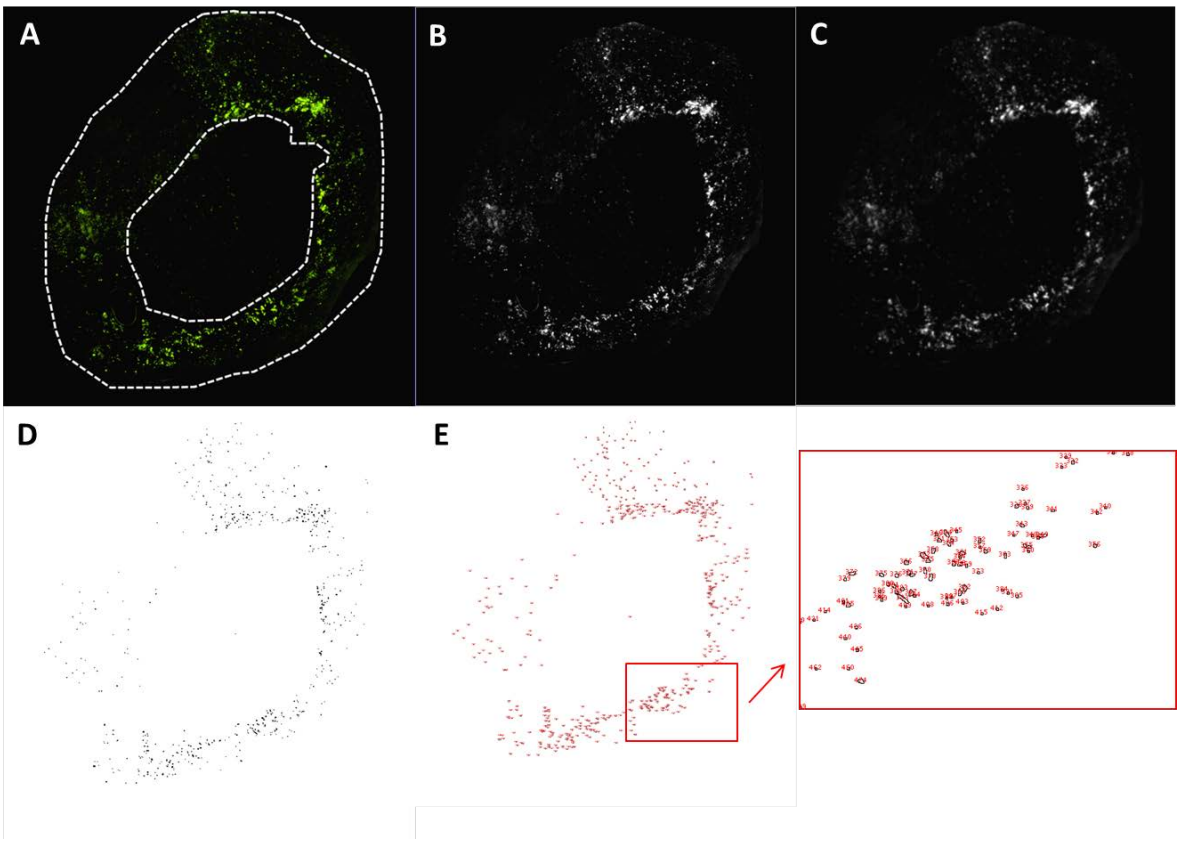

Figure 64. The ImageJ-based cell counting tool developed in Aim 1 can be utilized for analysis of microsphere seeded scaffolds. The ImageJ tool developed in Aim 1 was utilized for counting microspheres seeded within scaffolds and determining their diameter. Each step (A-E) is depicted for a microsphere seeded scaffold and is consistent with that seen in **Figure 11**.

Seeding of microspheres following standard parameters (number: 3M objects, concentration: 1 million/mL, volume: 3 mL, vacuum: -127 mmHg) was found to result in a scaffold with lower density and non-uniform distribution. Each microsphere seeded scaffold when compared to one seeded with AD-MSCs with the same number or objects (i.e. either AD-MSCs or microspheres) was shown to achieve approximately half the density (**Figure 65**). As only microspheres of diameter 5 μm or less can be seeded within our PEUU scaffolds, the observed half density is a result of only half of the microsphere diameter range occurring at less than 5 μm (range: 1-10 μm) (**Figure 66**). Additionally, when investigating the distribution of microspheres within seeded scaffolds, although the circumferential and longitudinal sections displayed uniformity, the radial distribution was skewed lumenally (**Figure 67**, see **Figure 14** for AD-MSC uniform distribution in circumferential, longitudinal, and radial directions). As stated before when considering the microsphere size, it is likely that the rigidity of the sphere results in poor navigation of scaffold pores during the seeding process.

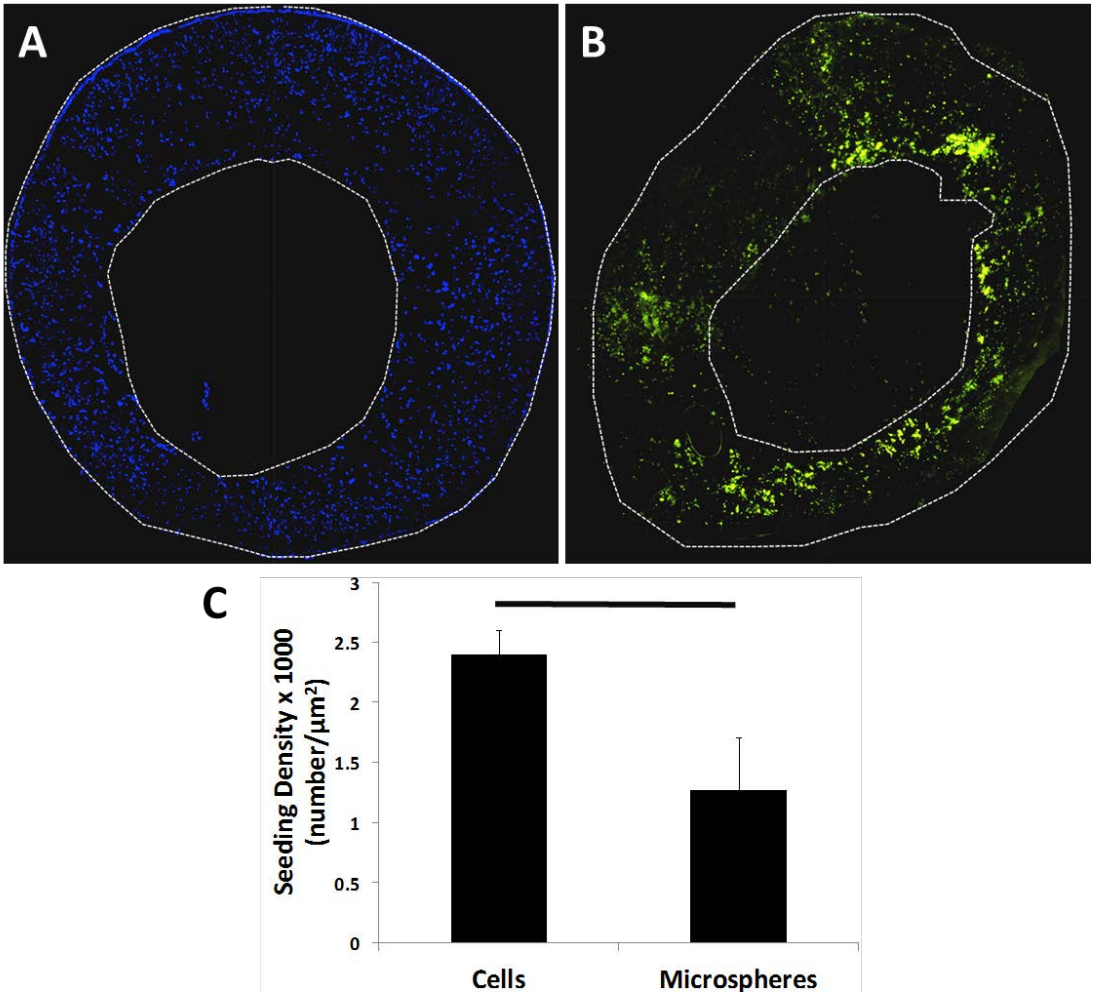

Figure 65. Microspheres seeded under current protocols for cells achieve only 50% of the seeding density. (A) Example of a cell (AD-MSCs; blue) seeded scaffold which displays a high degree of cell density and uniform distribution. (B) An example of a 10 µm FITC-embedded microsphere (green) seeded scaffold that has been seeded with an identical number to cells. Microsphere seeded scaffolds display both poor uniformity and density compared to an AD-MSC one. (C) Quantification (n=3) of the cell density using the ImageJ script in **Figure 64** revealed only approximately 50% of the density compared to cells. Black bar = significant at $p<0.05$. n = 3 each.

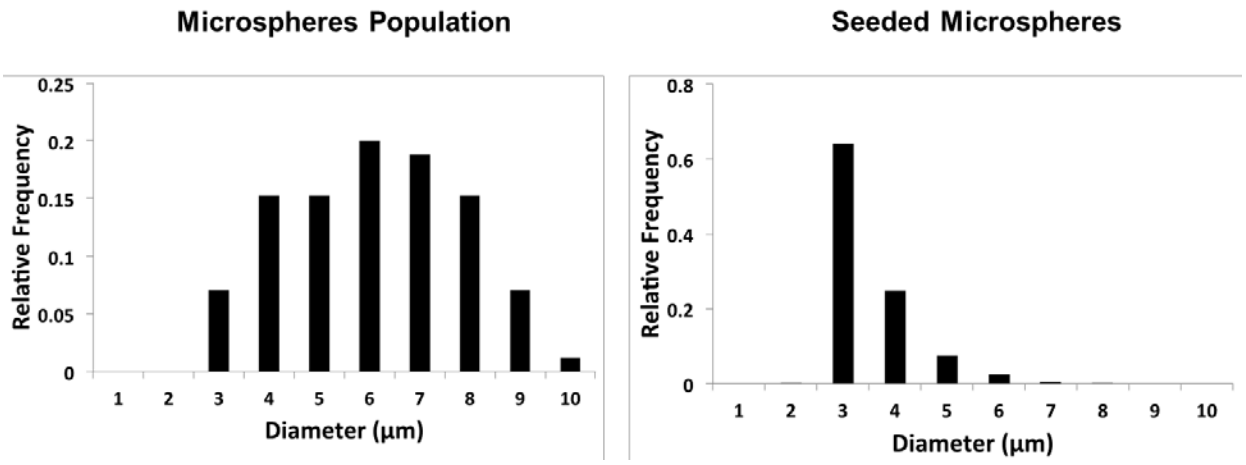

Figure 66. Only microspheres of size 5 µm or less are seeded within TEVG scaffolds. The size distribution of the 10 µm microsphere population (left) consists of normally distributed population with an average diameter of approximately 5 micrometers. However, the size of microspheres that successfully seed within scaffolds (right) only consist of diameters at 5 µm or less. As this represents approximately half of the population, this size exclusion can explain the reduced seeding density.

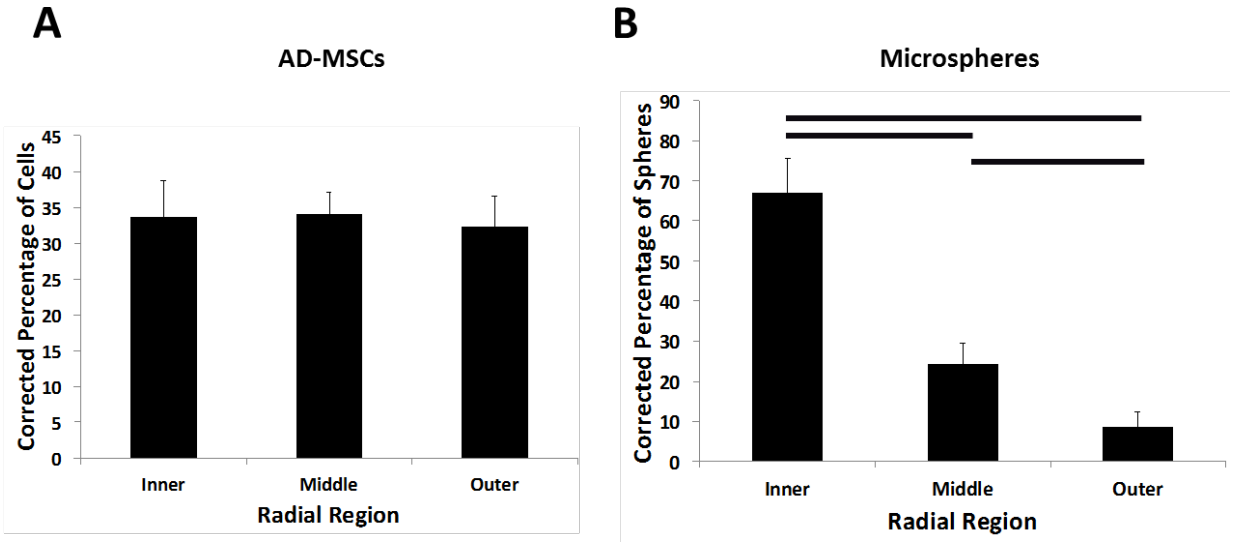

Figure 67. Microsphere seeded scaffolds have a radial distribution skewed inward. (A) Cell seeded grafts (AD-MSCs) are seeded with a uniform distribution whereas (B) microsphere seeded grafts display significant skewing towards the lumen indicating poor thickness penetration during the seeding process. Black bar = significance at $p<0.05$. n=3 each.

To compensate for the lower cell density (~50%) observed within microsphere seeded scaffolds, the total number of seeded spheres was doubled. This was done in two manners. First, this was done by doubling the concentration of the microsphere suspension utilized during the seeding process (2M/mL, 3mL volume). Secondly, a double number was achieved by increasing the total volume but keeping the concentration the same (1M/mL, 6 mL volume). Seeding microspheres in both manners produced a cell density no better than that observed prior to increasing the microsphere number and qualitatively still displayed a distribution mostly residing in the luminal region (**Figure 68**). This is likely a result of "bottle-necking" where under the current radial forces applied throughout the seeding process do not induce substantial penetration to clear luminal pores for additional microspheres.

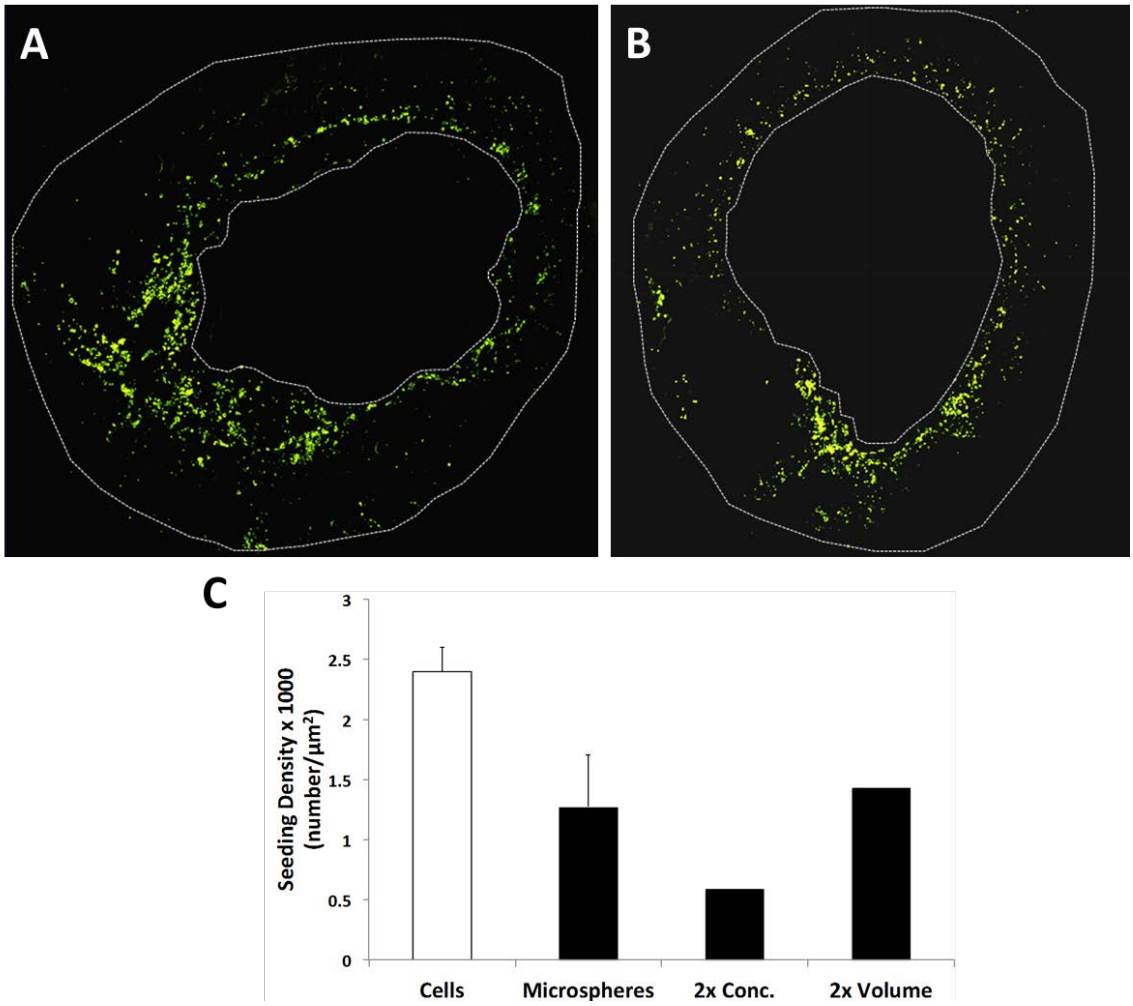

Figure 68. Compensating the 50% loss in seeding density when using microspheres with increased number is insufficient. To compensate for the 50% the loss in microsphere seeding density (**Figure 65**) the number of microspheres seeded within TEVG scaffolds was doubled by either increasing the concentration of microsphere seeding solution (A) or increasing the volume (B). Both cases (n=1 each) were unable to recover the density of microspheres to the same level as cells and a luminal skewing is still present.

To better enhance the penetration of microspheres during the seeding process to achieve both a more uniform radial distribution and to clear the aforementioned “bottleneck”, the vacuum pressure was increased to -381 mmHg (house line pressure) during the seeding process. Under a higher vacuum pressure, seeding microspheres with the increased number used in **Figure 68** was able to achieve a density similar to that observed when seeding cells (**Figure 69**). Additionally, this resulted in a uniform radial distribution (**Figure 69**). Seeding microspheres with increased vacuum but non-increased number was unable to produce this effect in terms of both distribution and density (**Figure 70**). To confirm that the increased vacuum pressure was not inducing unwanted deformation of the microspheres we confirmed the circularity (i.e. shape factor) of the microspheres post-seeding (**Figure 71**). Additionally, as the seeded microspheres throughout these experiments still displayed a diameter of 5 μm of less (**Figure 71)**, it can be argued that no deformation occurs as deformation would likely result in better penetration of larger sized spheres..

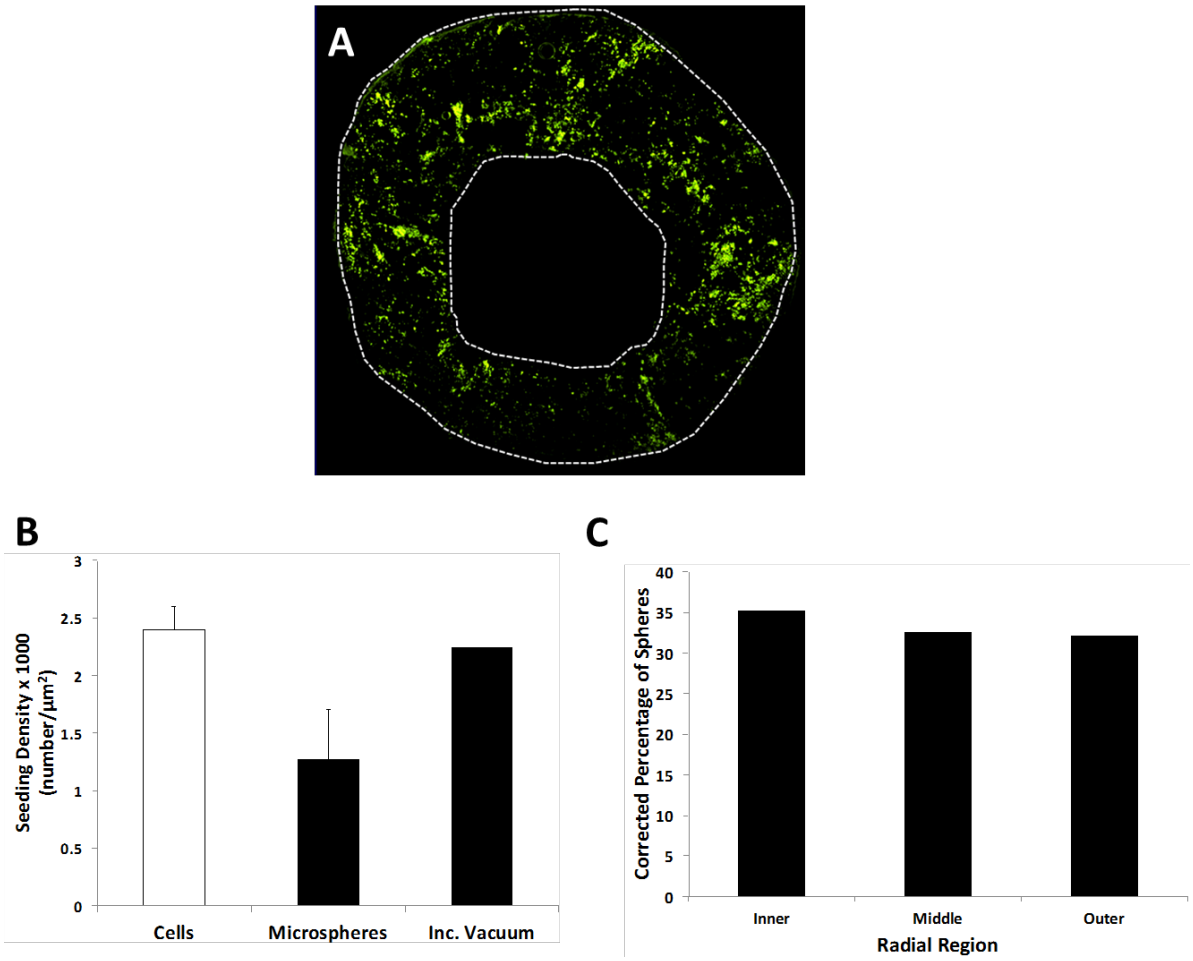

Figure 69. Microsphere seeded scaffolds with increased number and increased vacuum pressure During the Seeding Process Seed Similarly to Cells. As shown in **Figure 68**, increasing the number of microspheres alone was insufficient to increase the seeding density and a luminal aggregation is still present likely due to poor penetration of microspheres. To increase the transmural force during microsphere seeding to better distribute through the thickness, the vacuum pressure was increased 3-fold. Seeding in this manner (n=1) resulted in a microsphere seeded scaffold (A) with cell density similar to that of cells (B) with a uniform radial distribution (C).

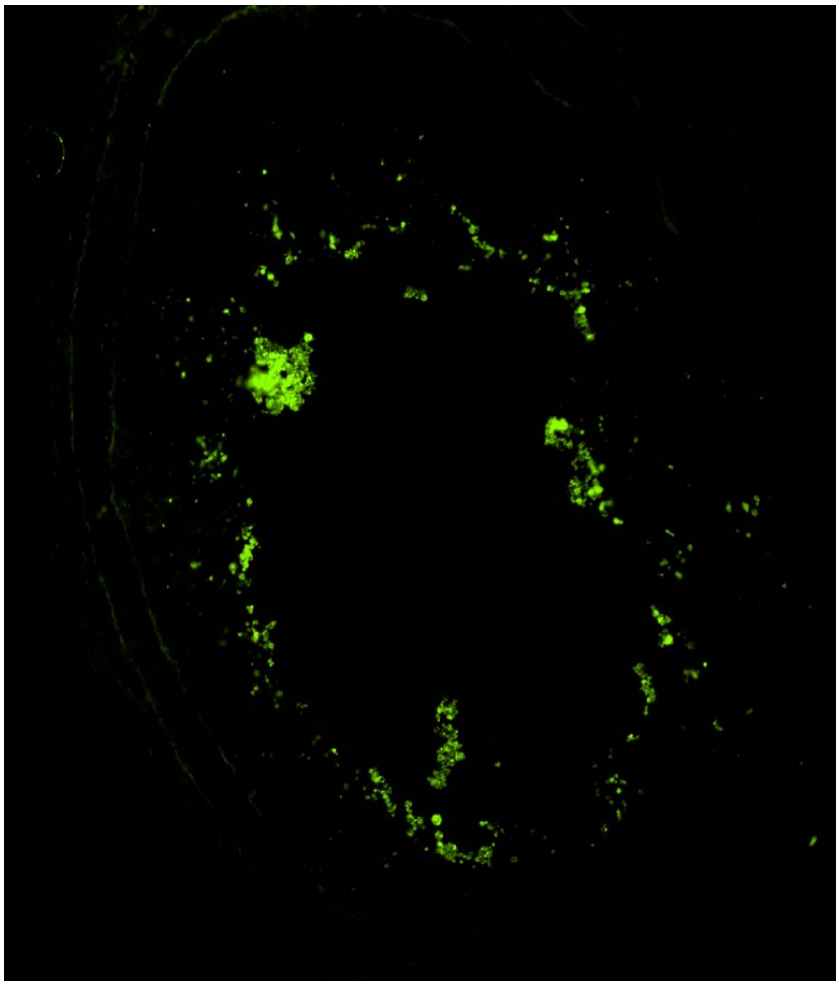

Figure 70. Increased vacuum alone without increased number was insufficient to compensate for seeding density or to obtain a uniform distribution. A TEVG scaffold (n=1) was seeded with increased but the original number of microspheres to evaluate the effect of increased vacuum pressure alone. No qualitative increase to either the seeding density or radial distribution can be observed comparing beyond that which was originally achieved in **Figure 65** utilizing the standard protocol.

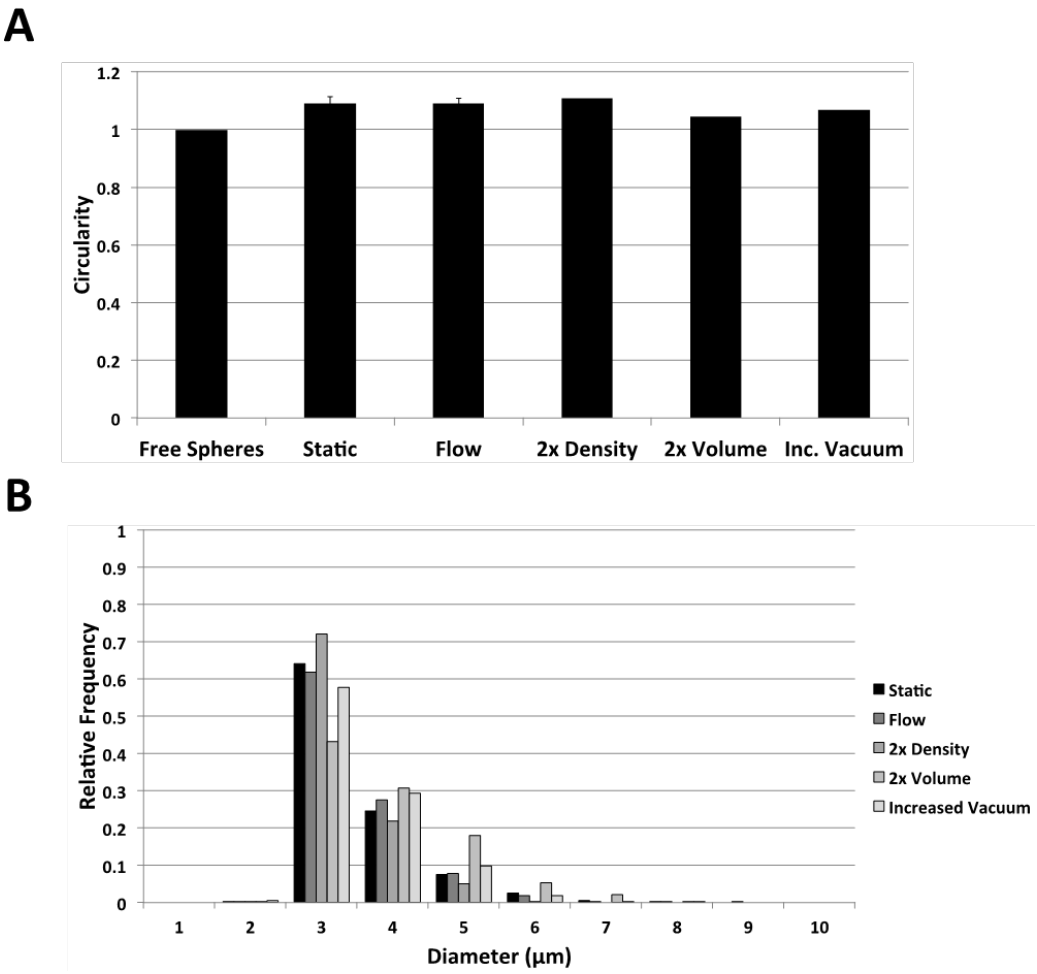

Figure 71. Seeded microspheres across all experiments remain circular and have similar sizes. To confirm that microspheres were not damaged and/or deformed when utilizing the increased vacuum pressure during the seeding process, all seeded microsphere grafts were analyzed for their (A) circularity (also known as Shape Factor; see **Figure 3**, 1 = circular, 0 = elliptical) and (B) size distribution. Similar results are seen in both cases indicating that the microspheres are not deformed during the seeding process.

5.3.3 Seeding of Artificial MSCs – Retention Under Flow Conditions

As microspheres do not have a mechanism to attach to the scaffolds in the same manner as cells do and may dislodge when subjected to flow, microsphere seeded scaffolds (3M microspheres, -127 mmHg) were subjected to arterial flow conditions for approximately 5 hours. To obtain a static control, a section of each scaffold was removed prior to flow exposure. Comparing the density of microspheres within the scaffolds exposed to flow versus static controls revealed no differences (**Figure 72**). Additionally, the sizing of microspheres within the wall remained unchanged post-flow which indicates that smaller microspheres do not become dislodged (**Figure 71**). Interestingly, the distribution of microspheres became skewed outward (i.e. deeper into the wall) (**Figure 73**) as a result of the hydrostatic pressure from arterial flow which could be protective against potential embolism of the microspheres. However, as microspheres are biodegradable, a smaller size (< 5μm) than micro-embolisms (10-50 μm) [485, 486], and a similar size to circulating blood cells [486], it is unlikely for occlusion due to embolism to be a concern. Additionally, a microsphere seeded scaffold with the optimized seeding parameters (6M microspheres, -381 mmHg) determined in the previous section was subjected to flow and still maintained a high density and uniform distribution (**Figure 74**)

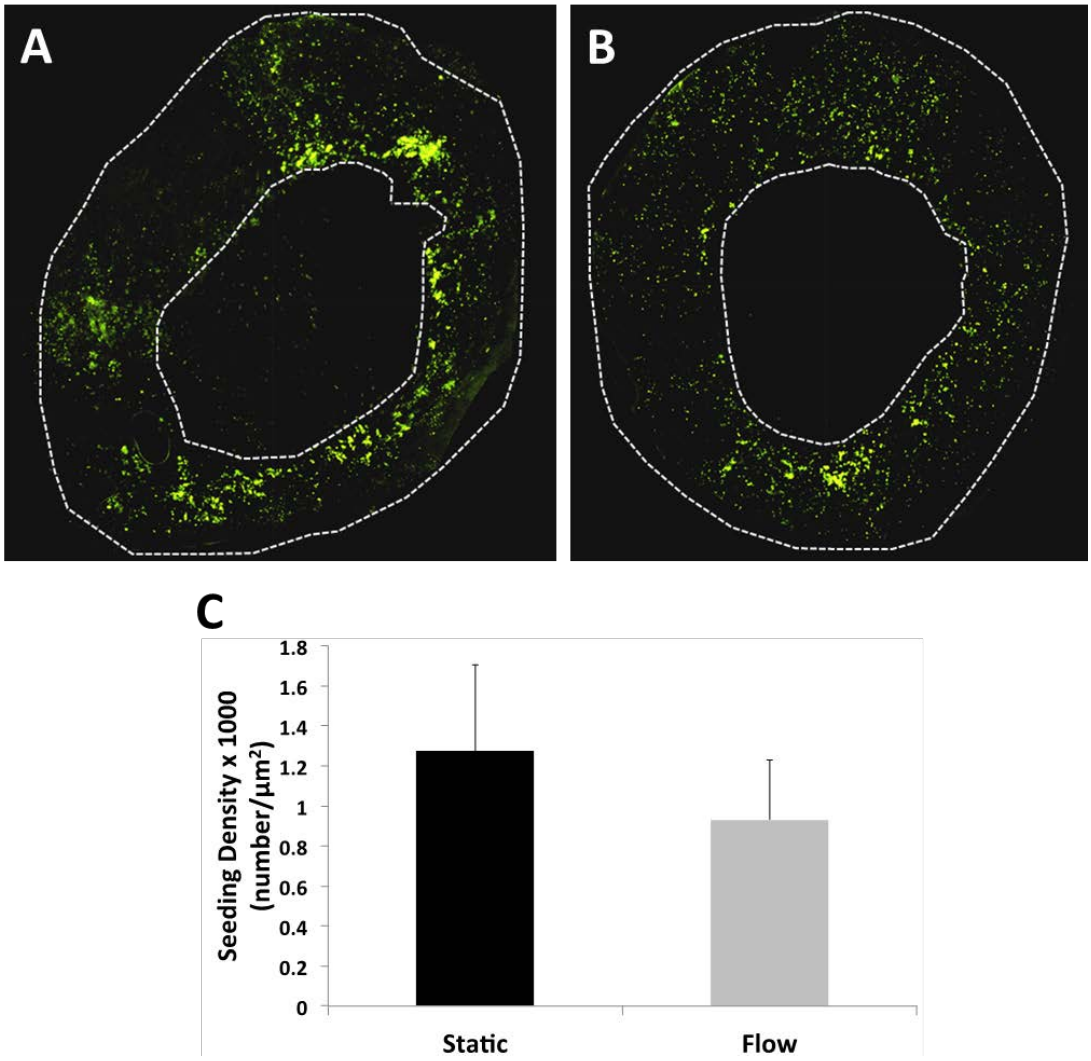

Figure 72. Microspheres placed under flow conditions showed no differences in seeding density. Microsphere seeded scaffolds (n=3) were subjected to flow conditions (120/80 mmHg physiologic waveform; 5 hours) with a static control piece removed prior. Comparing the seeding density of (A) static or (B) flow seeded scaffolds revealed (C) no differences (p=0.4)

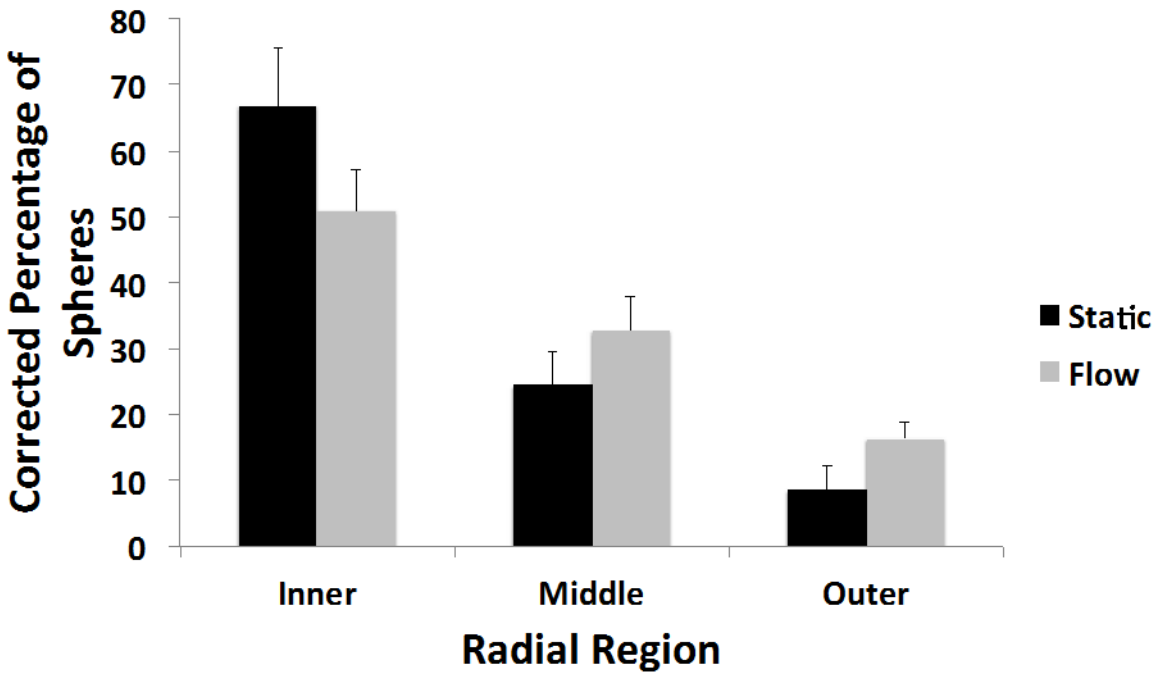

Figure 73. Analysis of the radial distribution of microsphere seeded scaffolds post-flow showed radially outward skewing. The radial distribution of the microsphere seeded scaffolds exposed to flow was analyzed and compared to static controls. As shown qualitatively if **Figure 72** and quantitatively above, a skewing outward of the microspheres is observed (n=3 each).

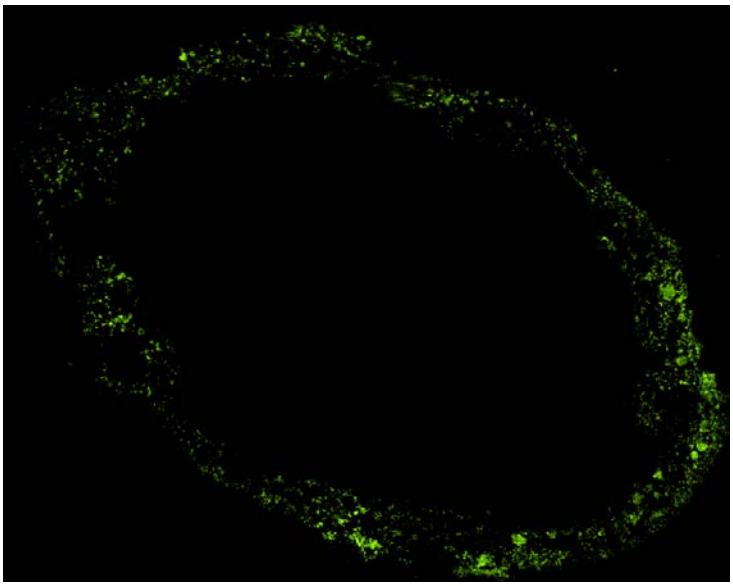

Figure 74. Microsphere seeded scaffolds with the increased vacuum/increased number seeding method shows high density and uniformity after subjection to flow. To confirm that microspheres were retained in TEVG scaffold utilizing the newly optimized seeding methodology for microspheres, one microsphere seeded scaffold under this method was subjected to physiologic flow in the same manner as **Figure 72**. Qualitatively it is observed that a high seeding density and uniformity persist.

5.3.4 Bioactive Factor Release – Customizable Release

Utilizing a standard double emulsion fabrication procedure [483], PLGA microspheres encapsulated with MSC conditioned media with non-porous and increasingly porous configurations to generate distinct release profiles (total protein, measured by the bicinchoninic acid assay). As can be seen in **Figure 75**, release is tunable by an order of magnitude as well as by as little as 2-fold by simply varying the porosity of the microspheres. It is also possible to tune the ratio of the amount delivered within the first two days compared to the amount delivered over the first week of release. The most appealing release is the highly porous release denoted by the red line in **Figure 75** which we term as the "burst" configuration. This offers the advantage of releasing of all MSC bioactive factors in concert as opposed to potentially excluding certain factors based on size resulting in drastically different functional effects in the case of a non-porous configuration. Utilizing the "burst" configuration will allow delivery of the entire combination of secreted factors, fully imparting the beneficial effects of MSCs. However, as a release in this manner will exhaust the supply of encapsulated factors at an acute time course, future studies will focus on extending the release time while still allowing delivery of the full spectrum of factors (see Section: 5.5 "Discussion and Future Directions").

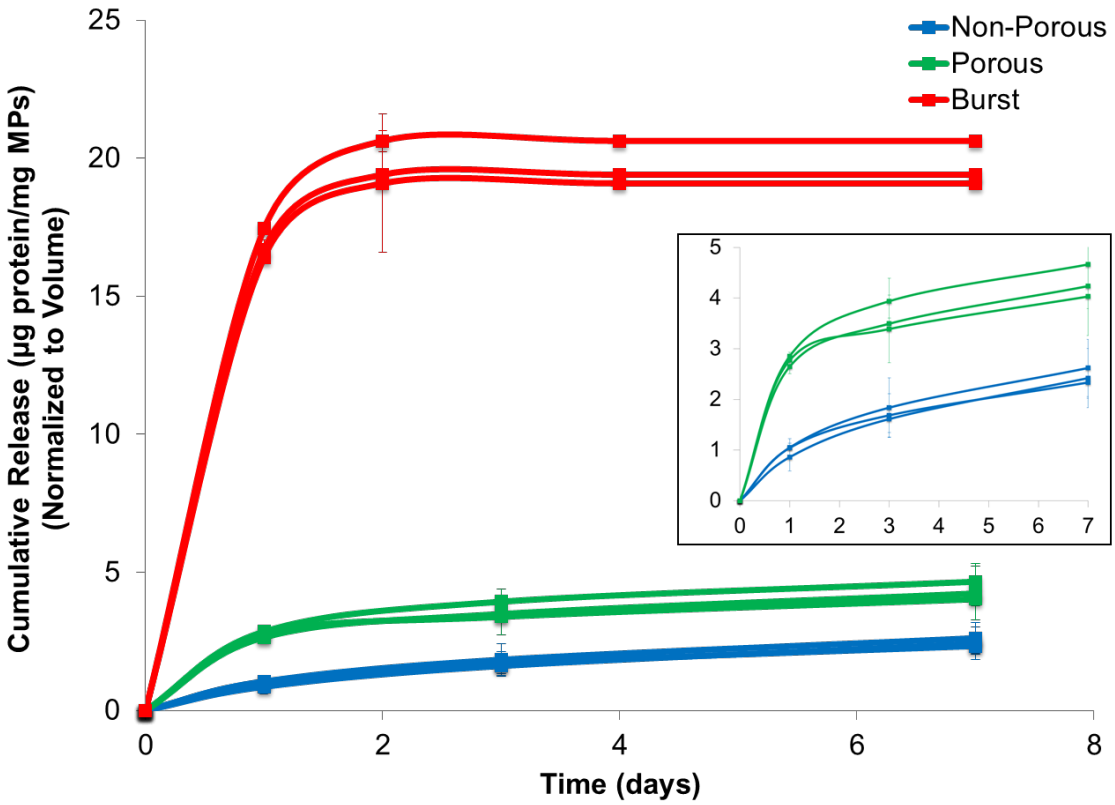

Figure 75. Cumulative release of multiple microsphere formulations. PLGA microspheres were fabricated using three different configurations (non-porous, porous, and burst). In all cases, AD-MSC conditioned media was encapsulated. Releasates were harvested daily and total protein content of each sample was measured by the bicinchoninic assay. Cumulative protein release was then plotted over the seven day period, to illustrate the three different release profiles. (data generated and utilized with permission by Dr. Morgan Fedorchak)

5.3.5 Bioactive Factor Release – Processing of Media (Concentration)

To verify that we can achieve concentration of conditioned media, we performed both centrifugal filtration and lyophilization. The highest and most consistent concentration was achieved using lyophilization and resuspension - this media was concentrated 13-fold. Concentration with filtration resulted in ~6-fold concentration but was more variable between samples (Unconcentrated: 647±4.7 µg/mL, Lyophilization: 8639±129 µg/mL, Filtration: 2859±1376 µg/mL, n=3) (**Figure 76**). From these results, all subsequent studies (i.e. release to confirm bioactivity) were performed with concentrated media via lyophilization and resuspension.

To confirm that bioactivity was retained through the lyphilization process, the lyophilized media samples were re-diluted to their original concentrations, and then utilized in a SMC migration assay. We determined from the results of this assay that the conditioned media retained its pro-migratory effect on SMCs even after lyophilization (**Figure 77**).

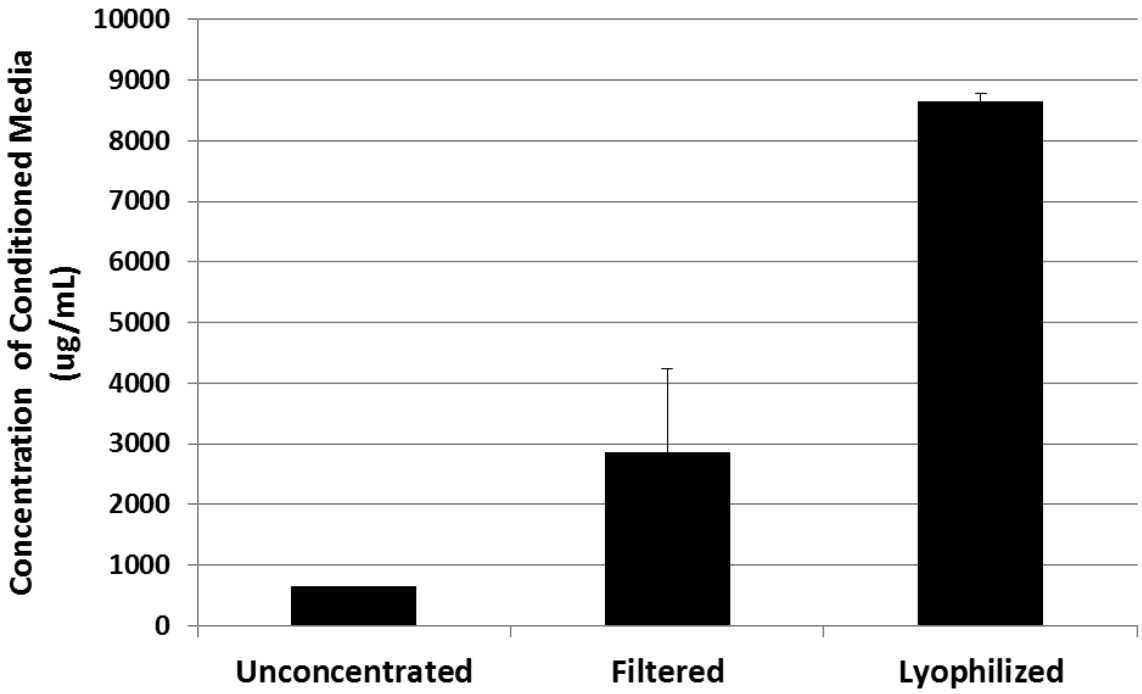

Figure 76. Conditioned media can be concentrated by filtration or lyophilization. Conditioned media from AD-MSCs (n=3, mean ± SD) were concentrated via filtration or lyophilization and reconstitution in the smallest volume possible. Lyophilization resulted in a superior concentration (approximately 10-fold) and less variability than filtration. (data generated and utilized with permission by Dr. Morgan Fedorchak)

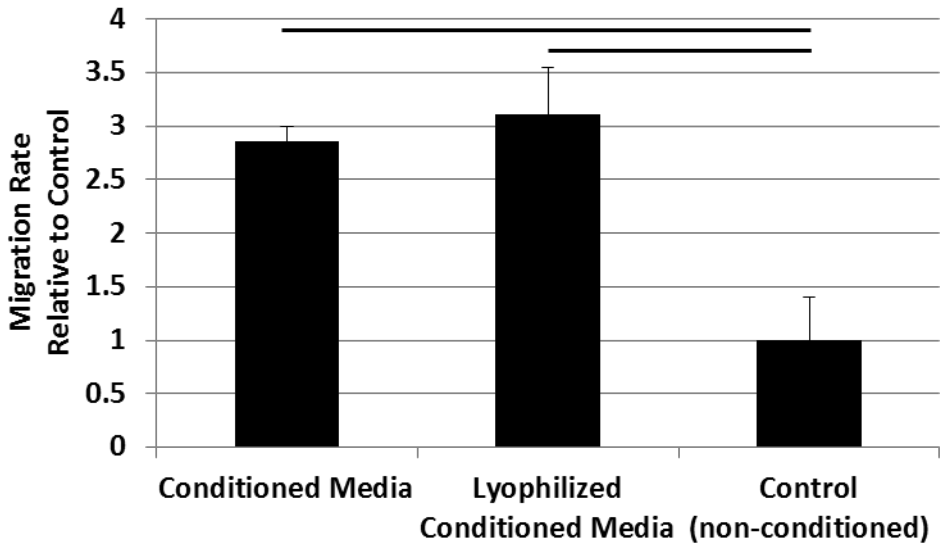

Figure 77. Lypohilized and reconstituted MSC conditioned media retains its SMC pro-migratory potential. Media conditioned by MSC (RoosterBio) was lyophilized, reconstituted to the original volume with ultrapure water, and then used in a SMC migration assay as in Figure 7. This media displayed no different in potential to promote the migration of SMCs to the positive control (unprocessed conditioned media from the same stock) and was significantly higher than control (non-conditioned) media. Black bar = significance at $p<0.05$.

5.3.6 Bioactive Factor Release – Release of Desired Factors and Maintained Bioactivity

To show that MSC secreted factors could indeed be released from microspheres (instead of total protein in conditioned media which includes serum as in Section 5.3.4 “Bioactive Factor Release – Customizable Release”) and maintain their bioactivity, we created microspheres with our current best case design: “burst” configuration microspheres encapsulated with concentrated MSC conditioned media. This allows for release of all MSC factors and provides the highest concentration delivery. Releasates from these microspheres were then analyzed via ELISA for representative factors that induce TEVG remodeling (VEGF, MCP-1, BDNF) and maintain anti-thrombogenicity (uPA). All of these factors were shown to be present in pre-encapsulated media (**Table 7**) and absent in non-conditioned media controls. However, post-released samples displayed values that were prohibitively low (**Table 7**) with only two factors (VEGF, uPA) being able to be detected. Despite the low efficacy of the release, these results still illustrate that multiple MSC secreted factors which are relevant to TEVG processes can be released from this microsphere configuration. Further studies to optimize this release will be discussed in Section: 5.5 (“Discussion and Future Directions”)

To show that microsphere encapsulated factors could be released when seeded into scaffolds, microsphere seeded scaffolds bathed in solution were compared based on total protein to an equivalent number of microsphere in solution alone. Monitoring the total protein release over the course of 7 days via a micro-BCA kit revealed similar values between both groups (**Figure 78**) indicating that released protein does not become entrapped within scaffold pores.

Additionally, these released samples were employed in an SMC migration assay to confirm bioactivity the bioactivity of released samples. The results indicate that no bioactivity was present and the released samples induced cell death. While the lack of migratory effects could indeed be due to the aforementioned low release efficiency, the occurrence of cell death may be a confounding effect due to a high salt concentration as salt containing media samples were released into PBS. Additionally, degradation of the PLGA-based microspheres could cause acidic degradation products thus causing alterations to solution pH due to the small volumes used in this assay.

Table 7. ELISA measurement of growth factors relevant to TEVG success in microsphere releases. The average generated from one cell line is provided with samples acquired from two separate culture flasks performed with measurements performed at least in triplicate. All values were subtracted from those present in non-conditioned media.

	Growth Factor Pre- vs Post-Release ($pg/10^6$ cells)	
	Pre-Release	**Post-Release**
VEGF	26751	2253
uPA	12443	24
BDNF	130	0
MCP-1	139	0

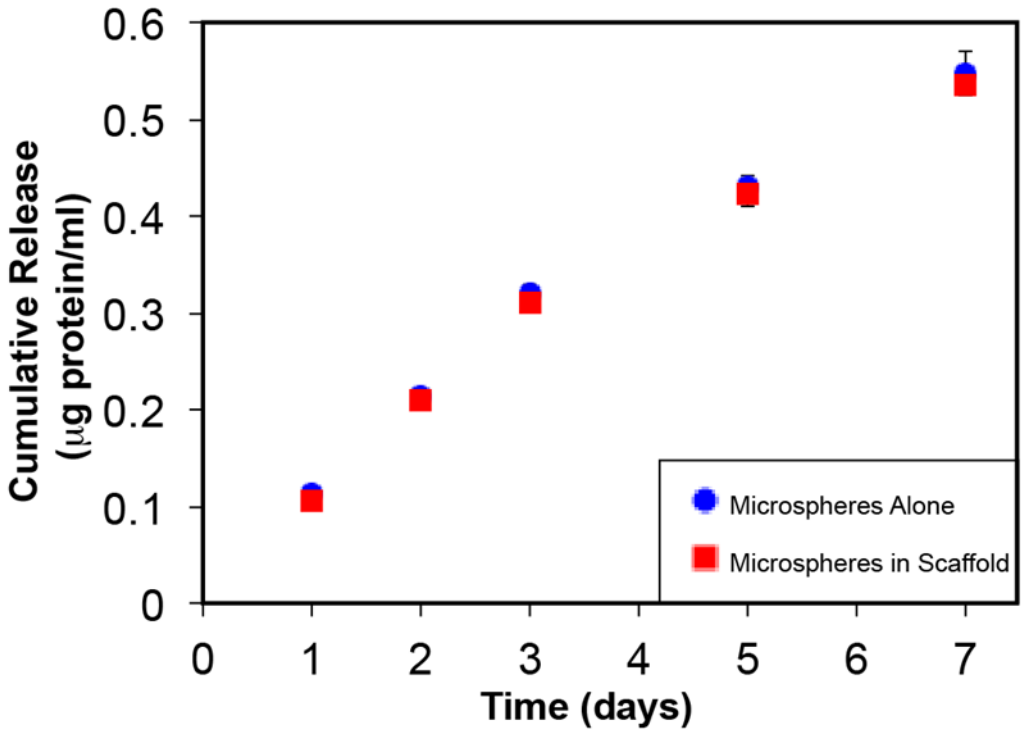

Figure 78. Microsphere release is unaffected by seeding. Microspheres were vacuum-seeded into PEUU scaffolds, assayed by BCA, and compared to release from microspheres alone in solution (mean ± SD, n=3 per group).

5.3.7 In Vivo Functionality

To demonstrate the in vivo potential of a microsphere seeded TEVG, a pilot study was performed wherein two microsphere seeded grafts were implanted for a short duration (3 days). This initial investigation was performed with FITC-encapsulated microspheres to demonstrate that microspheres will be retained within TEVG scaffolds under in vivo conditions. The microsphere grafts were successfully implanted and the patency of each was confirmed by monitoring the distal pulse pressure at the completion of surgery. Both grafts seeded with FITC-microspheres were unable to resist thrombosis (**Figure 79**). Additionally, FITC-microspheres were still present within TEVG scaffolds after exposure to physiologic flow (**Figure 79**). While it is unclear at which point the thrombosis developed during the 3 day implant as both rats were free from symptoms, in vivo flow conditions were still applied for some duration as the graft was confirmed patent upon the completion of surgery.

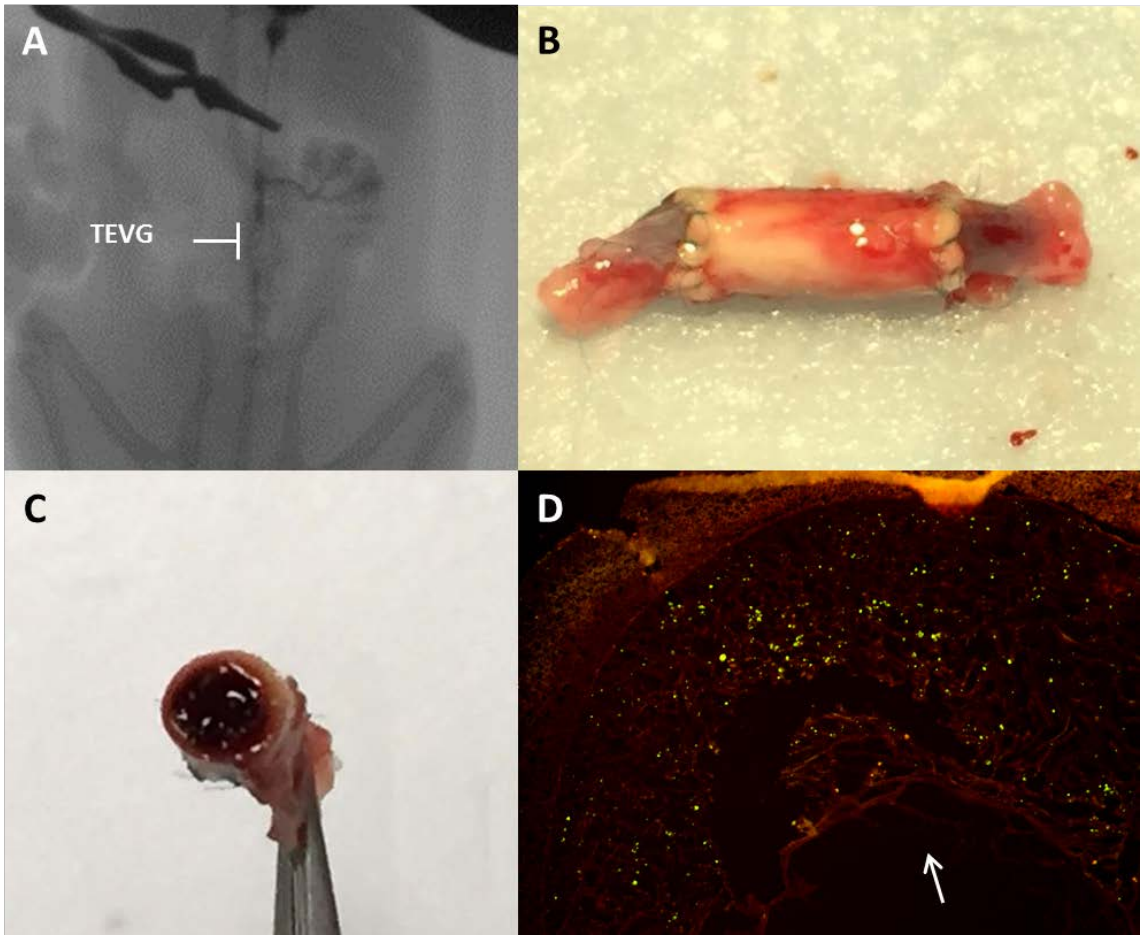

Figure 79. Implanted FITC-embedded microsphere were retained in scaffolds and induced thombosis. A pilot study was performed where two FITC-microsphere seeded scaffolds were implanted in our Lewis Rat model for 3 days. (A) Angiogram upon study completion revealed occlusion of both TEVGs. This can further be seen due to the dark color of the proximal and distal graft anastomosis (B) and the observed thrombosis when transecting the TEVG (C). (D) Microscopy revealed that FITC-microspheres were retained in TEVGs under in vivo conditions.

5.4 CONCLUSION

Through this Aim a proof of concept has been shown and the process of determining the initial design elements of the novel artificial MSC technology has begun. The diameter of microspheres that can be incorporated within our TEVG scaffold was shown to be 5 μm or less and methods to successfully seed them with the same cell density and distribution as MSCs was demonstrated. The diameter of 5 μm spheres incorporated within scaffolds was consistent regardless of using populations consisting of larger microspheres or through increasing the vacuum pressure while seeding. Additionally, seeded microspheres were not dislodged when exposed to flow conditions and showed resistance to embolism as hydrostatic pressure showed a tendency to drive them radially outward. With regards to the encapsulation and release of MSC media it was shown that conditioned media-based microspheres can be tuned to offer multiple release profiles, the media can successfully be concentrated, and that MSC factors can be released. However, in this initial trial the quantity of those factors were prohibitively low and initial bioactivity assays were unsuccessful. Despite this, the experiments performed in this Aim clearly demonstrate the feasibility of a conditioned media encapsulated microsphere-based TEVG design showing that these artificial MSCs can be successfully seeded and release relevant factors. Further refinement to this technology will be discussed in the following section.

5.5 DISCUSSION AND FUTURE DIRECTIONS

As mentioned above, while this study demonstrated the feasibility of artificial MSCs showing the ability to be successfully seeded within TEVG scaffolds, appropriate size, and possibility of release, there are still many unaddressed areas which require further investigation before the artificial MSC technology can become a reality. In particular, these include two major areas: 1) determining the desired release profile necessary for the microspheres, and 2) optimizing methods to release conditioned media at higher efficiency.

To determine the appropriate release profile it is important identify the series of in vivo time course events that lead to successful remodeling of TEVG with host cells when utilizing an MSC-based TEVG. These include four critical events: 1) the disappearance of seeded MSC, 2) the appearance of SMC, 3) the appearance of EC, and 4) the appearance of vascular ECM. While literature evidence provides evidence for some of these parameters (see Section: “1.5.3 In Vivo TEVG Mechanisms”), the resolution of these studies is insufficient for determining the release profile of artificial MSCs. Ideally, artificial MSCs will be utilized to release a similar quantity of bioactive factors to seeded MSCs and this will correlate with the disappearance of seeded MSCs. That is, as the seeded MSCs decline over time as host repopulation progresses, the release profile (and/or number of artificial MSCs) will taper off to mirror this. Ultimately a study performed in this manner will both guide the release profile as well as both the necessary number of microspheres and concentration of encapsulated conditioned media required. One criticism in this approach however is that the in vitro MSC secreted factor profile utilized to generate conditioned media for artificial MSCs may not match the profile in vivo as the secreted profile has been shown to change based on different environmental effects [480, 487-490]. However, based on the results of this dissertation and literature evidence it is clear that the MSC factors

produced in vitro (e.g. VEGF, MCP-1, BDNF, uPA) have unequivocally been shown to positively influence he TEVG remodeling process.

Another important parameter is to ensure that artificial MSCs release the broad spectrum of MSC secreted factors. While microspheres have been extensively utilized to release several compounds ranging from growth factors (VEGF [474, 491, 492], FGF [478, 493-495], PDGF [496, 497], MCP-1 [491], TGF-beta [472, 498], EGF [475], BMP-2 [499-501], BMP-7 [500], IGF-1 [498, 499, 501], NGF [502], GCNF [503]), drugs [477, 504, 505], peptides [473, 476], and siRNAs [506] these are often only delivered as single factors. Some studies have attempted simultaneous delivery of two factors through encapsulation within either the same microsphere [491, 498] or using two separate populations [499, 500]. However, achieving appropriately timed releases with microspheres has been difficult [507-509]. Indeed, mixed results have been seen when encapsulating two different factors within the same formulation of particles either showing the same release profile [499] or drastically different ones [491, 498, 501]. However, utilizing highly porous microspheres such as the “burst” release fabrication utilized in this Aim clearly shows the ability to simultaneously release multiple factors. Additionally, the collaborators (Dr. Steven Little’s laboratory) on this project have extensive experience tailoring the release profile of microspheres [510-512] and are capable of utilizing unique mathematical modeling techniques and finite element analysis to directly translate desired release profiles into several physically relevant fabrication instructions. One conceptual design to achieve a sustained release of the entire spectrum of MSC factors is to design is highly porous microspheres similar to the “burst” ones used in this Aim, but to operate different sub-populations on a time delay such that the cumulative release over time is constant..

From a technical standpoint while this Aim showed that MSC secreted factors can be released from microspheres, the release was low (< 10%) and will need additional refinement. First, the low amount of released product could be explained by poor encapsulation efficiency, a high occupancy of serum within microspheres which excludes MSC products, or potential binding to polymer fragments during release. Further investigation will be required to determine and alleviate the cause. Secondly, the bioactivity (scratch migration) assay was unsuccessful predominantly due to cell death. As the release assay was performed releasing conditioned media into PBS and with microsphere degradatory products, a high salinity (i.e. high osmotic pressure) or acidity may be contributing factors. While these issues are not relevant in the infinite sink conditions that would be experienced during implantation testing, the issue needs to be resolved when considering the small volumes used during in vitro assays. While no other bioactivity assays were attempted due to the low release efficiency, future studies could employ assays similar to the zymography performed in Aim 1-2 to detect anti-thrombotic (fibrinolytic) activity of released samples.

6.0 STUDY SUMMARY

The following sections will summarize the key findings presented within this dissertation, discuss the future directions of each Aim, and present my scientific accomplishments achieved through this work.

6.1 SUMMARY OF RESULTS

6.1.1 Specific Aim 1

Aim 1 of this dissertation investigated the use of AD-MSCs from two high cardiovascular risk patient demographics – diabetic and elderly – in the context of vascular tissue engineering. It was shown that AD-MSCs from these donors had functional deficiencies in two essential functions of TEVG maturation. First, the ability of diabetic and elderly AD-MSCs to differentiate into SMCs was shown to be less efficacious for both donor types compared to healthy controls. Second, the ability of the secreted factors from elderly AD-MSCs, but not diabetic ones, was shown to be unable to promote the migration of SMCs. However, when considering the fabrication of TEVG constructs, all donor types (healthy, diabetic, elderly) were able to successfully seed scaffolds in line with our gold standard data (i.e. at high cell density and uniform distribution). Comparing the in vivo functionality revealed the main complication to be thrombosis which was

encountered in the diabetic group. Despite the initial in vitro data (SMC differentiation and ability to promote SMC migration via secreted factors) showing functional deficiencies, all patent TEVGs in vivo regardless of group were able to remodel to a vascular-like construct similarly.

In the second part of this aim a mechanistic study was performed to identify the reason for the thrombosis encountered in the diabetic AD-MSC group. Using fibrinogen zymography, an enzymatic activity assay, and monitoring the degradation of fibrin-based constructs it was shown that diabetic AD-MSCs have a reduced fibrinolytic activity compared to healthy controls. Additionally, one molecular player – uPA – was identified to be decreased in diabetic AD-MSCs.

6.1.2 Specific Aim 2

The focus of Aim 2 was to evaluate the use of a culture-free adipose-derived cell population – SVF cells – for TEVG applications to reduce clinical barriers associated with fabrication time. It was shown that SVF cells were equipotent compared to paired cultured AD-MSCs at performing the two essential functions for TEVG maturation defined in Aim 1 (SMC differentiation, ability of secreted factors to promote SMC migration), seeding within TEVG scaffolds, and developing patent vascular-like TEVGs when implanting in vivo.

6.1.3 Specific Aim 3

The goal of Aim 3 was to perform a feasibility study for a novel TEVG construct incorporating microsphere encapsulating AD-MSC products as a replacement for cells themselves (termed as

"artificial AD-MSCs". This would allow for a functional TEVG regardless of deficiencies in autologous donor AD-MSCs (such as the lack of uPA production as determined in Aim 1-2). It was shown that microspheres can be seeded within TEVG scaffolds under redefined methodologies, microspheres remain embedded within TEVG scaffolds under flow conditions, their cargo and release can be customized, and they can release relevant biologic factors. This ultimately lays the ground work for future studies which can customize this technology to induce the in vivo processes seen when utilizing cells with a TEVG.

6.2 SUMMARY OF ACOMPLISHMENTS

The work of this dissertation, this work has led to the generation of the following scientific manuscripts:

1. **Krawiec JT**, Weinbaum JS, St. Croix CM, Phillippi JA, Watkins SC, Rubin JP, Vorp DA. "A Cautionary Tale for Autologous Vascular Tissue Engineering: Impact of Human Demographics on the Ability of Adipose-Derived Mesenchymal Stem Cells to Recruit and Differentiate Into Smooth Muscle Cells" *Tissue Engineering Part A*, 2014
2. **Krawiec JT**, et al. "In Vivo Functional Evaluation of Tissue Engineered Vascular Grafts Fabricated Using Human Adipose-Derived Stem Cells from High-Cardiovascular Risk Populations" [*in submission*]
3. **Krawiec JT**, et al. "Impaired Fibrinolytic Activity of Adipose-Derived Stem Cells from Diabetic Patients is Associated with Thrombotic Failure of Stem Cell-Based Tissue Engineered Vascular Grafts" [*in submission*]
4. **Krawiec JT**, et al. "Culture-Free Human Stromal Vascular Fraction Cells Produce a Functional Tissue Engineered Vascular Graft" [*in preparation*]

Additionally, a review and a book chapter were written pertaining to the background material utilized in this dissertation:

1. **Krawiec JT**, Vorp DA. "Adult stem cell-based tissue engineered blood vessels: A review," *Biomaterials*, 33(12):3388-3400, 2012.

2. Blose KJ, **Krawiec JT**, Weinbaum JS, Vorp DA. "Chapter 15: Bioreactors for Tissue Engineering Purposes," *Regenerative Medicine Applications in Organ Transplantation, 1st Edition*. Giuseppe Orlando, ed. Academic Press, 2013.

Finally, multiple individual fellowships were obtained by the author of this dissertation or by undergraduates who were mentored by the author:

1. **NIH T32 HL094295-02**, "Optimal Stem Cell Type and Effect of Donor Demographics on Engineered Autologous Human Blood Vessels", 9/2011-7/2012 [Training fellowship to Jeffrey Krawiec]

2. **AHA 12PRE12050163**, "Stem Cell Based-Tissue Engineered Vascular Grafts: Effect of Cell Type and Type-2 Diabetes", 7/2012-6/2014 [Predoctoral Fellowship to Jeffrey Krawiec]

3. **Undergraduate Summer Research Internship Scholarship**, Swanson School of Engineering (SSOE), University of Pittsburgh, 6/2013-8/2013 [Summer Fellowship to Alexander Josowitz (mentored undergraduate student)]

4. **Biomedical Engineering Summer Undergraduate Research Program (BME-SURP) Scholarship**, Carnegie Mellon University, 6/2013-8/2013 [Summer Fellowship to Katelyn Bruce (mentored undergraduate student)]

5. **Undergraduate Summer Research Internship Scholarship, Swanson School of Engineering (SSOE)**, University of Pittsburgh, 5/2014-7/2014 [Summer Fellowship to Dominic Pezzone (mentored undergraduate student)]

6. **Biomedical Engineering Summer Undergraduate Research Program (BME-SURP) Scholarship**, Carnegie Mellon University, 6/2014-8/2014 [Summer Fellowship to LaiYee (Lily) Kwan (mentored undergraduate student)]

7. **AHA Summer Undergraduate Research Program (AHA-SURP) in Cardiovascular Sciences Scholarship**, Vascular Medicine Institute, University of Pittsburgh, Summer 2015 [Summer Fellowship to Dominic Pezzone (mentored undergraduate student)]

6.3 FUTURE DIRECTIONS

The future directions of this dissertation are discussed within each Aim due to the independent nature of those projects. For the discussion of future directions in Aim 1-1 see **Section 2.6**, for Aim 1-2 see **Section 3.6**, for Aim 2 see **Section 4.6**, and for Aim 3 see **Section 5.5**.

APPENDIX A

APPENDIX A: DETERMINING APPROPRIATE CELL DENSITY FOR SMC SCRATCH MIGRATION ASSAY

Prior to performing the SMC scratch migration assay detailed in Aim 1 a pilot study was performed to determine the optimal number of SMCs to be plated to achieve a cell confluence enough to allow for unidirectional migration (i.e. towards to wound area) but to avoid a confluence that would allow cells to establish cellular adhesions which would prevent their migration. The results of this study can be seen in **Figure 80** which indicates that 18,750 cells per well in a 24 well plate allow for an optimal cell density for this assay.

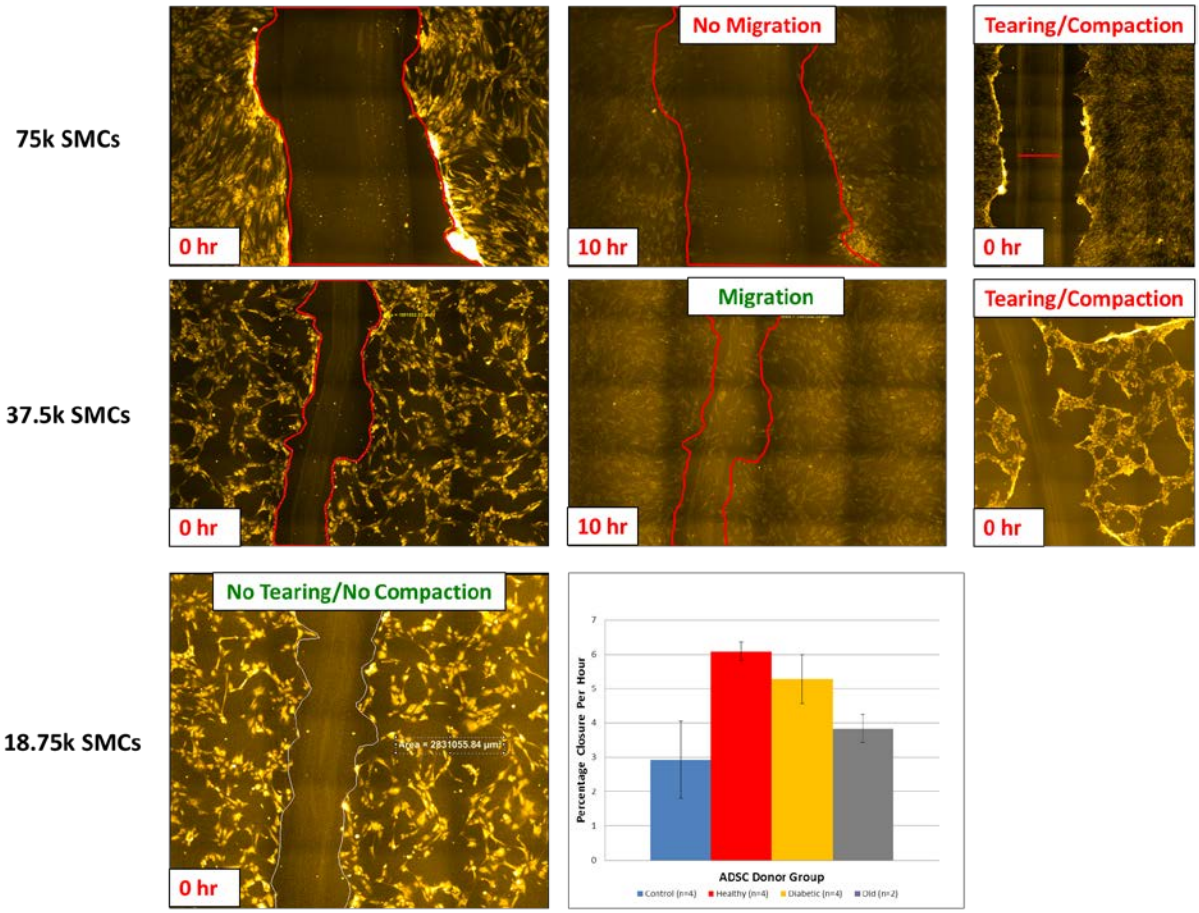

Figure 80. SMCs were plated at various densities to determine an ideal number to achieve confluence but not encounter tearing/compaction from too high an SMC density or lack of migration from cellular adhesion and/or extracellular matrix deposition. All cells were plated 1 day prior to experimentation to resist the aforementioned extracellular matrix deposition. At a plating density of 75,000 SMC per well of a 24 well plate both a lack of migration was denoted by the lack of cellular movement across the initial wound line (red line). Additionally, tearing was noted as cells retracted from the initial scratch wound (red line). At a cellular density of 37.5k SMCs, migratory effects were recovered but tearing and compaction was still denoted in some wells. Finally, at 18.75 SMCs neither tearing or compaction was shown and was utilized to generate data for all subsequent experiments (example for test assay shown). Although not shown, a density of less than 18.75k SMCs does not achieve enough cellular confluence.

APPENDIX B

APPENDIX B: IMAGEJ CELL COUNTING TOOL TUTORIAL AND SCRIPT

“Readme” written by Alex Josowitz

This is a guide for running the imageJ macro, analyze_Scaffolds.ijm, to count cells in fluorescent images of seeded scaffolds:

1. Before you do anything else, make sure the images you are using are in the "snapshot" format from the NIS Elements software. The original images do not open correctly on imageJ due to their imageJ type. RGB images are essential for this macro to work.

2. Open ImageJ or Fiji on your computer. This macro should work in both versions of the software.

3. Next, you may need to change one or two things in the macro itself. Depending on what color you used to mark the cells/particles you may have to change the number in the "selectImage()" command in Line 7 of the macro. To do this, click "File" and then "Open" in the ImageJ toolbar. You should select "analyze_Scaffolds.ijm" from wherever you have the file stored. In the lab computers, the file is in the Vorp Shared R-drive in the "Alex Josowitz" folder. The script for the macro should appear.

4. Find line 7 of the script which says "selectImage(#)". The # is either 1, 2, or 3, corresponding to red, green, and blue. If you used a TRITC dye (red), change the number to 1. If you used a FITC dye (green) change the number to 2. If you used a DAPI (blue) dye, change the number to 3. You must save the script (File-save) after making changes.

5. You must now install the script before it can be used. In the ImageJ toolbar, navigate to "Plugins" and click on it. A drop down menu should appear.

6. The first option in the dropdown menu is "Macros", which is another drop down menu. Hover over it and click the "Install" option.

7. Once you click "Install" a file browser window should appear. You should select "analyze_Scaffolds.ijm" from wherever you have the file stored. In the lab computers, the file is in the Vorp Shared R-drive in the "Alex Josowitz" folder. It is necessary to install the macro every time you open/reopen ImageJ.

8. Now you must open the image you wish to analyze. Simply click "File" and then "Open" and locate the image of your choice.

9. Once the image pops up, you are ready to use the analysis tool. Click on "Plugins" and then "Macros". At the bottom of the "Macros" menu should be a new option "analyze_Scaffolds". Click that.

10. The analysis tool should run its course. Multiple images should appear on the screen, representing the different modifications that the script performs on the original image. You can ignore those if you'd like. The only window that matters, if you are counting cells, is the small "Summary" window that pops up. It my be hiding behind the other images so you may have to move or delete the images to find it. The summary window should display the number of cells in the "Count" section.

11. There is also a small "Results" window that pops up. It details each individual particle, the particle's pixel area, and possibly coordinates for the particle's location. This "Results" window can be useful as the tool can be set to measure aspects of individual particles rather than simply counting them all. To do this, go to the ImageJ toolbar, click "Analyze" and then click "Set Measurements". A window should pop up with a variety of clickable options, including "Area", "Centroid", and "Perimeter" as well as other possibly useful measurements. You can click the box next to any of these measurements before running the macro and then the "Results" window should display values for the measurements you chose next to each particle.

12. In order to run a new image, you should close all of the residual images from your initial run. This can be done simply by clicking "File" and "Close All". This will not get rid of the "Summary" or "Results" sections, so you can still see them if need be.

13. Repeat steps 7-9 for each image you'd like to analyze.

ImageJ Cell Counting Script – “analyze_Scaffolds.ijm”

```
//Macro to count the number of cells in a multi-channel image of a seeded scaffold
//Created by Alex Josowitz
//splits channels between red, blue and green
//blue is on top
run("Split Channels");
//select red (1) green (2) blue (3)
selectImage(2)
//identifies image ID
```

```
idOrig = getImageID();
//converts to 32-bit to reduce rounding inaccuracies
run("32-bit");
//copies image
run("Duplicate...","title=[copy]");
//identifies copied image ID
idDup = getImageID();
selectImage(idOrig);
//applies Gaussian blur with small radius to original blue channel
run("Gaussian Blur...", "sigma=1");
selectImage(idDup);
//applies Gaussian blur with larger radius to duplicate
run("Gaussian Blur...", "sigma=3");
//subtracts duplicate blur from original blur to view distinct cells
imageCalculator("Subtract create", idOrig, idDup);
//applies Otsu threshold to image to remove unnecessary points
setAutoThreshold("Otsu dark");
//run("Threshold...");
setThreshold(26.5376, 170.7419);
//make binary
run("Make Binary");
//run Open command to clear small particles
run("Open");
//watershed separation
run("Watershed");
//counts cells and determines areas
run("Analyze Particles...", "size=10-Infinity circularity=0.00-1.00 show=Outlines display exclude clear summarize");
//Change “size=10-Inifinity” to “size=0-Infinity” for measuring microspheres instead of cells.
```

APPENDIX C

APPENDIX C: ANEURYSMAL TEVG HISTOLOGY FROM AIM 1

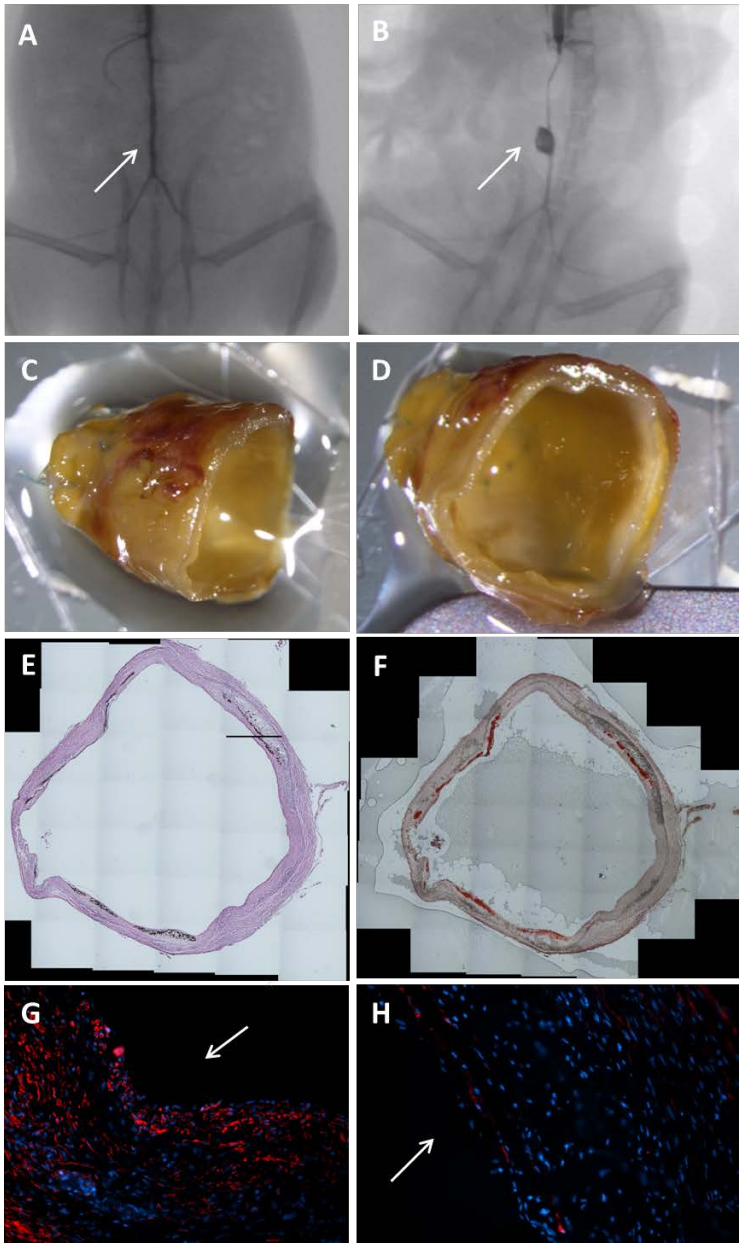

Figure 81. Aneurysmal TEVG explanted sample at 8 weeks. One TEVG sample from Aim 1-1 was implanted and incurred significant aneurysmal dilation (~4 mm diameter vs 1 mm diameter). (A,B) Angiography results show signifanct dilation of the aneurysmal TEVG (right, white arrow) compared to both the adjacent aorta and a non-dilated TEVG implant (right, white arrow). (C,D) Gross observation of transected the TEVG explant. (E, F) Von Kossa (E) and Alizarin Red (F) staining show general histological characteristics pointing to fragmentation of the TIPS scaffold layer and absence of the ES layer (i.e. a manufacturing defect) as a potential explanation for aneurysmal dilation and additionally show the presence of calcification (which occurred in other non-dilated TEVG explants). (G,H) Staining for SMC markers revealed prominent staining of SMA (G) but minimal staining for calponin (H).

APPENDIX D

APPENDIX D: GELATIN COATED SLIDES RECIPE

Ingredients:

Gelatin Type A (#Sigma G-2500) 0.75g
Chromium sulfate 0.125 g
Water 250 ml

Heat 250 mL water to 60#C. Remove from heat and dissolve 0.75g of Gelatin (Type A, #Sigma G-2500) with aid of a stir bar. After the gelatin has been completely dissolved, add chromium sulfate. Move solution to a Coplin staining jar and dip electrically charged slides (#Shandon Colorfrost Plus) for 5-10 seconds. Remove, pat dry, and repeat three times. Allow slides to dry for 24 hours prior to use.

BIBLIOGRAPHY

1. Standring, S., *Gray\'s Anatomy: The Anatomical Basis of Clinical Practice.* 2008.

2. Aird, W.C., *Phenotypic heterogeneity of the endothelium II. Representative vascular beds.* Circulation Research, 2007. **100**(2): p. 174-190.

3. Kelleher, C.M., S.E. McLean, and R.P. Mecham, *Vascular extracellular matrix and aortic development.* Current Topics in Developmental Biology, 2004. **62**: p. 153-188.

4. Alphonsus, C. and R. Rodseth, *The endothelial glycocalyx: a review of the vascular barrier.* Anaesthesia, 2014. **69**(7): p. 777-784.

5. Pacilli, A. and G. Pasquinelli, *Vascular wall resident progenitor cells: a review.* Experimental Cell Research, 2009. **315**(6): p. 901-914.

6. Torsney, E. and Q.B. Xu, *Resident vascular progenitor cells.* Journal of Molecular and Cellular Cardiology, 2011. **50**(2): p. 304-311.

7. Tang, Z., et al., *Differentiation of multipotent vascular stem cells contributes to vascular diseases.* Nature Communications, 2012. **3**: p. 875.

8. Nguyen, A.T., et al., *Smooth Muscle Cell Plasticity Fact or Fiction?* Circulation Research, 2013. **112**(1): p. 17-22.

9. Tang, Z., et al., *Smooth muscle cells: to be or not to be? Response to Nguyen et al.* Circulation Research, 2013. **112**(1): p. 23-26.

10. Herring, B.P., et al., *Previously differentiated medial vascular smooth muscle cells contribute to neointima formation following vascular injury.* Vascular cell, 2014. **6**(1): p. 1-14.

11. Cines, D.B., et al., *Endothelial cells in physiology and in the pathophysiology of vascular disorders.* Blood, 1998. **91**(10): p. 3527-3561.

12. Augustin, H.G., D.H. Kozian, and R.C. Johnson, *Differentiation of endothelial cells: analysis of the constitutive and activated endothelial cell phenotypes.* Bioessays, 1994. **16**(12): p. 901-906.

13. Kher, N. and J.D. Marsh. *Pathobiology of atherosclerosis--a brief review*. in *Seminars in Thrombosis and Hemostasis*. 2004.

14. Galley, H. and N. Webster, *Physiology of the endothelium.* British Journal of Anaesthesia, 2004. **93**(1): p. 105-113.

15. Aird, W.C., *Endothelial cell heterogeneity.* Cold Spring Harbor perspectives in medicine, 2012. **2**(1): p. a006429.

16. Franco, C.A., S. Liebner, and H. Gerhardt, *Vascular morphogenesis: a Wnt for every vessel?* Current Opinion in Genetics and Development, 2009. **19**(5): p. 476-483.

17. Aird, W.C., *Phenotypic heterogeneity of the endothelium I. Structure, function, and mechanisms.* Circulation Research, 2007. **100**(2): p. 158-173.

18. Aitsebaomo, J., et al., *Brothers and Sisters Molecular Insights Into Arterial–Venous Heterogeneity.* Circulation Research, 2008. **103**(9): p. 929-939.

19. Krawiec, J.T. and D.A. Vorp, *Adult stem cell-based tissue engineered blood vessels: A review*. Biomaterials, 2012. **33**(12): p. 3388-3400.

20. Zhang, P., et al., *Endothelial Differentiation of Adipose-Derived Stem Cells from Elderly Patients with Cardiovascular Disease.* Stem Cells and Development, 2011. **20**(6): p. 977-988.

21. Fischer, L.J., et al., *Endothelial differentiation of adipose-derived stem cells: effects of endothelial cell growth supplement and shear force.* Journal of Surgical Research, 2009. **152**(1): p. 157-166.

22. Cao, Y., et al., *Human adipose tissue-derived stem cells differentiate into endothelial cells in vitro and improve postnatal neovascularization in vivo.* Biochemical and biophysical research communications, 2005. **332**(2): p. 370-379.

23. Guan, L., et al., *In vitro differentiation of human adipose-derived mesenchymal stem cells into endothelial-like cells.* Chinese Science Bulletin, 2006. **51**(15): p. 1863-1868.

24. Planat-Benard, V., et al., *Plasticity of human adipose lineage cells toward endothelial cells - physiological and therapeutic perspectives.* Circulation, 2004. **109**(5): p. 656-663.

25. McIlhenny, S.E., et al., *Linear shear conditioning improves vascular graft retention of adipose-derived stem cells by upregulation of the alpha(5)beta(1) Integrin.* Tissue Engineering Part A, 2010. **16**(1): p. 245-255.

26. McIlhenny, S., et al., *eNOS transfection of adipose-derived stem cells yields bioactive nitric oxide production and improved results in vascular tissue engineering.* Journal of tissue engineering and regenerative medicine, 2013.

27. Bajpai, V.K. and S.T. Andreadis, *Stem cell sources for vascular tissue engineering and regeneration.* Tissue Engineering Part B: Reviews, 2012. **18**(5): p. 405-425.

28. Policha, A., et al., *Endothelial differentiation of diabetic adipose-derived stem cells.* Journal of Surgical Research, 2014. **192**(2): p. 656-663.

29. Owens, G.K., M.S. Kumar, and B.R. Wamhoff, *Molecular regulation of vascular smooth muscle cell differentiation in development and disease.* Physiological Reviews, 2004. **84**(3): p. 767-801.

30. Lacolley, P., et al., *The vascular smooth muscle cell in arterial pathology: a cell that can take on multiple roles.* Cardiovascular Research, 2012. **95**(2): p. 194-204.

31. Rzucidlo, E.M., K.A. Martin, and R.J. Powell, *Regulation of vascular smooth muscle cell differentiation.* Journal of Vascular Surgery, 2007. **45**(6): p. A25-A32.

32. Ailawadi, G., et al., *Smooth muscle phenotypic modulation is an early event in aortic aneurysms.* Journal of Thoracic and Cardiovascular Surgery, 2009. **138**(6): p. 1392-1399.

33. Starke, R.M., et al., *Vascular smooth muscle cells in cerebral aneurysm pathogenesis.* Translational stroke research, 2014. **5**(3): p. 338-346.

34. Liao, S., et al., *Accelerated replicative senescence of medial smooth muscle cells derived from abdominal aortic aneurysms compared to the adjacent inferior mesenteric artery.* Journal of Surgical Research, 2000. **92**(1): p. 85-95.

35. Bunton, T.E., et al., *Phenotypic alteration of vascular smooth muscle cells precedes elastolysis in a mouse model of Marfan syndrome.* Circulation Research, 2001. **88**(1): p. 37-43.

36. Sinha, A. and N.R. Vyavahare, *High-glucose levels and elastin degradation products accelerate osteogenesis in vascular smooth muscle cells.* Diabetes and Vascular Disease Research, 2013: p. 1479164113485101.

37. Sage, A.P., Y. Tintut, and L.L. Demer, *Regulatory mechanisms in vascular calcification.* Nature Reviews Cardiology, 2010. **7**(9): p. 528-536.

38. Johnson, R.C., J.A. Leopold, and J. Loscalzo, *Vascular calcification pathobiological mechanisms and clinical implications.* Circulation Research, 2006. **99**(10): p. 1044-1059.

39. Rudijanto, A., *The role of vascular smooth muscle cells on the pathogenesis of atherosclerosis.* Acta Med Indones, 2007. **39**(2): p. 86-93.

40. Gomez, D. and G.K. Owens, *Smooth muscle cell phenotypic switching in atherosclerosis.* Cardiovascular Research, 2012: p. cvs115.

41. Rensen, S., P. Doevendans, and G. Van Eys, *Regulation and characteristics of vascular smooth muscle cell phenotypic diversity.* Netherlands Heart Journal, 2007. **15**(3): p. 100-108.

42. Beamish, J.A., et al., *Molecular regulation of contractile smooth muscle cell phenotype: implications for vascular tissue engineering.* Tissue Engineering Part B: Reviews, 2010. **16**(5): p. 467-491.

43. McDaniel, D.P., et al., *The stiffness of collagen fibrils influences vascular smooth muscle cell phenotype.* Biophysical Journal, 2007. **92**(5): p. 1759-1769.

44. Vanhoutte, P.M., et al., *Modulation of vascular smooth muscle contraction by the endothelium.* Annual Review of Physiology, 1986. **48**(1): p. 307-320.

45. Triggle, C.R., et al., *The endothelium: influencing vascular smooth muscle in many ways.* Canadian Journal of Physiology and Pharmacology, 2012. **90**(6): p. 713-738.

46. Vorp, D.A., T. Maul, and A. Nieponice, *Molecular aspects of vascular tissue engineering.* Front Biosci, 2005. **10**: p. 768-89.

47. Neff, L.P., et al., *Vascular smooth muscle enhances functionality of tissue-engineered blood vessels in vivo.* Journal of Vascular Surgery, 2011. **53**(2): p. 426-434.

48. Matsumura, G., et al., *First evidence that bone marrow cells contribute to the construction of tissue-engineered vascular autografts in vivo.* Circulation, 2003. **108**(14): p. 1729-1734.

49. Matsumura, G., et al., *Evaluation of tissue-engineered vascular autografts.* Tissue Engineering, 2006. **12**(11): p. 3075-3083.

50. El-Kurdi, M.S., et al., *Transient elastic support for vein grafts using a constricting microfibrillar polymer wrap.* Biomaterials, 2008. **29**(22): p. 3213-20.

51. Krawiec, J.T., et al., *A Cautionary Tale for Autologous Vascular Tissue Engineering: Impact of Human Demographics on the Ability of Adipose-Derived Mesenchymal Stem Cells to Recruit and Differentiate into Smooth Muscle Cells.* Tissue Engineering Part A, 2014. **21**(3-4): p. 426-437.

52. Rodriguez, L.V., et al., *Clonogenic multipotent stem cells in human adipose tissue differentiate into functional smooth muscle cells.* Proceedings of the National Academy of Sciences of the United States of America, 2006. **103**(32): p. 12167-12172.

53. Wang, C., et al., *A small diameter elastic blood vessel wall prepared under pulsatile conditions from polyglycolic acid mesh and smooth muscle cells differentiated from adipose-derived stem cells.* Biomaterials, 2010. **31**(4): p. 621-630.

54. Wang, C., et al., *Differentiation of adipose-derived stem cells into contractile smooth muscle cells induced by transforming growth factor-beta 1 and bone morphogenetic protein-4.* Tissue Engineering Part A, 2010. **16**(4): p. 1201-1213.

55. Harris, L.J., et al., *Differentiation of adult stem cells into smooth muscle for vascular tissue engineering.* Journal of Surgical Research, 2011. **168**(2): p. 306-314.

56. Lee, W.C.C., J.P. Rubin, and K.G. Marra, *Regulation of alpha-smooth muscle actin protein expression in adipose-derived stem cells.* Cells Tissues Organs, 2006. **183**(2): p. 80-86.

57. Lee, W.C.C., et al., *Effects of uniaxial cyclic strain on adipose-derived stem cell morphology, proliferation, and differentiation.* Biomechanics and Modeling in Mechanobiology, 2007. **6**(4): p. 265-273.

58. Wagenseil, J.E. and R.P. Mecham, *Vascular extracellular matrix and arterial mechanics.* Physiological Reviews, 2009. **89**(3): p. 957-989.

59. Wells, R.G., *The role of matrix stiffness in regulating cell behavior.* Hepatology, 2008. **47**(4): p. 1394-1400.

60. Cavalcante, J.L., et al., *Aortic stiffness: current understanding and future directions.* Journal of the American College of Cardiology, 2011. **57**(14): p. 1511-1522.

61. Quint, C., et al., *Decellularized tissue-engineered blood vessel as an arterial conduit.* Proceedings of the National Academy of Sciences of the United States of America, 2011. **108**(22): p. 9214-9219.

62. Dahl, S.L., et al., *Readily available tissue-engineered vascular grafts.* Science Translational Medicine, 2011. **3**(68): p. 68-69.

63. Naito, Y., et al., *Beyond burst pressure: initial evaluation of the natural history of the biaxial mechanical properties of tissue-engineered vascular grafts in the venous circulation using a murine model.* Tissue Engineering Part A, 2013. **20**(1-2): p. 346-355.

64. Khosravi, R., et al., *Biomechanical Diversity Despite Mechanobiological Stability in Tissue Engineered Vascular Grafts Two Years Post-Implantation.* Tissue Engineering Part A, 2015. **21**(9-10): p. 1529-1538.

65. Kurobe, H., et al., *Development of Small Diameter Nanofiber Tissue Engineered Arterial Grafts.* PLoS ONE, 2015. **10**(4).

66. Tara, S., et al., *Evaluation of remodeling process in small-diameter cell-free tissue-engineered arterial graft.* Journal of Vascular Surgery, 2014.

67. Nivison-Smith, L. and A. Weiss, *Elastin based constructs*2011: INTECH Open Access Publisher.

68. Kielty, C.M., M.J. Sherratt, and C.A. Shuttleworth, *Elastic fibres.* Journal of Cell Science, 2002. **115**(14): p. 2817-2828.

69. Humphrey, J. and G.A. Holzapfel, *Mechanics, mechanobiology, and modeling of human abdominal aorta and aneurysms.* Journal of Biomechanics, 2012. **45**(5): p. 805-814.

70. Baldwin, A.K., et al., *Elastic fibres in health and disease.* Expert reviews in molecular medicine, 2013. **15**: p. e8.

71. Vrhovski, B. and A.S. Weiss, *Biochemistry of tropoelastin.* European Journal of Biochemistry, 1998. **258**(1): p. 1-18.

72. Weinbaum, J.S., et al., *Deficiency in microfibril-associated glycoprotein-1 leads to complex phenotypes in multiple organ systems.* J Biol Chem, 2008. **283**(37): p. 25533-43.

73. Deyl, Z., K. Macek, and M. Adam, *Studies on the chemical nature of elastin fluorescence.* Biochimica et Biophysica Acta (BBA)-Protein Structure, 1980. **625**(2): p. 248-254.

74. Boddy, A.M., et al., *Basic research studies to understand aneurysm disease.* Drug News and Perspectives, 2008. **21**(3): p. 142-8.

75. Davis, E.C., *Stability of elastin in the developing mouse aorta: a quantitative radioautographic study.* Histochemistry, 1993. **100**(1): p. 17-26.

76. Mithieux, S.M. and A.S. Weiss, *In Vivo Synthesis of Elastic Fiber*, 2012, Google Patents.

77. Kielty, C.M., *Elastic fibres in health and disease.* Expert reviews in molecular medicine, 2006. **8**(19): p. 1-23.

78. Hwang, J.-Y., et al., *Retrovirally mediated overexpression of glycosaminoglycan-deficient biglycan in arterial smooth muscle cells induces tropoelastin synthesis and elastic fiber formation in vitro and in neointimae after vascular injury.* The American Journal of Pathology, 2008. **173**(6): p. 1919-1928.

79. Huang, R., et al., *Inhibition of versican synthesis by antisense alters smooth muscle cell phenotype and induces elastic fiber formation in vitro and in neointima after vessel injury.* Circulation Research, 2006. **98**(3): p. 370-377.

80. Mitts, T.F., et al., *Aldosterone and mineralocorticoid receptor antagonists modulate elastin and collagen deposition in human skin.* Journal of Investigative Dermatology, 2010. **130**(10): p. 2396-2406.

81. Cenizo, V., et al., *LOXL as a target to increase the elastin content in adult skin: a dill extract induces the LOXL gene expression.* Experimental Dermatology, 2006. **15**(8): p. 574-581.

82. Davidson, J.M., O. Zoia, and J.-M. Liu, *Modulation of transforming growth factor-beta 1 stimulated elastin and collagen production and proliferation in porcine vascular smooth muscle cells and skin fibroblasts by basic fibroblast growth factor, transforming growth factor-α, and insulin-like growth factor-I.* Journal of Cellular Physiology, 1993. **155**(1): p. 149-156.

83. Lin, S., M. Sandig, and K. Mequanint, *Three-dimensional topography of synthetic scaffolds induces elastin synthesis by human coronary artery smooth muscle cells.* Tissue Engineering Part A, 2011. **17**(11-12): p. 1561-1571.

84. Liu, J.-m. and J.M. Davidson, *The elastogenic effect of recombinant transforming growth factor-beta on porcine aortic smooth muscle cells.* Biochemical and Biophysical Research Communications, 1988. **154**(3): p. 895-901.

85. Humphrey, J., *Vascular adaptation and mechanical homeostasis at tissue, cellular, and sub-cellular levels.* Cell Biochemistry and Biophysics, 2008. **50**(2): p. 53-78.

86. Webster, A.L., M.S.-C. Yan, and P.A. Marsden, *Epigenetics and cardiovascular disease.* Canadian Journal of Cardiology, 2013. **29**(1): p. 46-57.

87. Studies, I.C.f.B.P.G.-W.A., *Genetic variants in novel pathways influence blood pressure and cardiovascular disease risk.* Nature, 2011. **478**(7367): p. 103-109.

88. Berg, A.H. and P.E. Scherer, *Adipose tissue, inflammation, and cardiovascular disease.* Circulation Research, 2005. **96**(9): p. 939-949.

89. Bays, H.E., *Adiposopathy: is "sick fat" a cardiovascular disease?* Journal of the American College of Cardiology, 2011. **57**(25): p. 2461-2473.

90. Newby, A.C. and A.B. Zaltsman, *Molecular mechanisms in intimal hyperplasia.* The Journal of pathology, 2000. **190**(3): p. 300-309.

91. Vorp, D.A., *Biomechanics of abdominal aortic aneurysm.* Journal of Biomechanics, 2007. **40**(9): p. 1887-1902.

92. Vorp, D.A. and J.P.V. Geest, *Biomechanical determinants of abdominal aortic aneurysm rupture.* Arteriosclerosis, Thrombosis, and Vascular Biology, 2005. **25**(8): p. 1558-1566.

93. Vorp, D.A., et al., *Association of intraluminal thrombus in abdominal aortic aneurysm with local hypoxia and wall weakening.* Journal of Vascular Surgery, 2001. **34**(2): p. 291-299.

94. Geest, J.P.V., et al., *Towards a noninvasive method for determination of patient-specific wall strength distribution in abdominal aortic aneurysms.* Annals of Biomedical Engineering, 2006. **34**(7): p. 1098-1106.

95. Oparil, S., M.A. Zaman, and D.A. Calhoun, *Pathogenesis of hypertension.* Annals of Internal Medicine, 2003. **139**(9): p. 761-776.

96. Hathcock, J.J., *Flow effects on coagulation and thrombosis.* Arteriosclerosis, Thrombosis, and Vascular Biology, 2006. **26**(8): p. 1729-1737.

97. Gailani, D. and T. Renné, *Intrinsic pathway of coagulation and arterial thrombosis.* Arteriosclerosis, Thrombosis, and Vascular Biology, 2007. **27**(12): p. 2507-2513.

98. Mackman, N., R.E. Tilley, and N.S. Key, *Role of the extrinsic pathway of blood coagulation in hemostasis and thrombosis.* Arteriosclerosis, Thrombosis, and Vascular Biology, 2007. **27**(8): p. 1687-1693.

99. Collen, D. and H. Lijnen, *Basic and clinical aspects of fibrinolysis and thrombolysis.* Blood, 1991. **78**(12): p. 3114-3124.

100. Booth, G.L., et al., *Relation between age and cardiovascular disease in men and women with diabetes compared with non-diabetic people: a population-based retrospective cohort study.* The Lancet, 2006. **368**(9529): p. 29-36.

101. Federation, W.H. *Cardiovascular Disease Risk Factors*. 2015 [cited 2015; Available from: http://www.world-heart-federation.org/press/fact-sheets/cardiovascular-disease-risk-factors/.

102. Conroy, R., et al., *Estimation of ten-year risk of fatal cardiovascular disease in Europe: the SCORE project.* European heart journal, 2003. **24**(11): p. 987-1003.

103. Imazu, M., et al., *Influence of type 2 diabetes mellitus on cardiovascular disease mortality: findings from the Hawaii-Los Angeles-Hiroshima study.* Diabetes Research and Clinical Practice, 2002. **57**(1): p. 61-69.

104. Association, A.D. *Statistics About Diabetes*. 2015 [cited 2015; Available from: http://www.diabetes.org/diabetes-basics/statistics/.

105. Lakatta, E.G. and D. Levy, *Arterial and cardiac aging: major shareholders in cardiovascular disease enterprises part I: aging arteries: a "set up" for vascular disease.* Circulation, 2003. **107**(1): p. 139-146.

106. Fuster, J.J. and V. Andrés, *Telomere biology and cardiovascular disease.* Circulation research, 2006. **99**(11): p. 1167-1180.

107. Saliques, S., et al., *Telomere length and cardiovascular disease.* Archives of cardiovascular diseases, 2010. **103**(8): p. 454-459.

108. Brouilette, S., et al., *Telomere length is shorter in healthy offspring of subjects with coronary artery disease: support for the telomere hypothesis.* Heart, 2008. **94**(4): p. 422-425.

109. Tsamis, A., J.T. Krawiec, and D.A. Vorp, *Elastin and collagen fibre microstructure of the human aorta in ageing and disease: a review.* Journal of The Royal Society Interface, 2013. **10**(83): p. 20121004.

110. Noureddine, H., et al., *Pulmonary artery smooth muscle cell senescence is a pathogenic mechanism for pulmonary hypertension in chronic lung disease.* Circulation Research, 2011. **109**(5): p. 543-553.

111. Franklin, S.S., et al., *Does the relation of blood pressure to coronary heart disease risk change with aging? The Framingham Heart Study.* Circulation, 2001. **103**(9): p. 1245-1249.

112. Cheitlin, M.D., *Cardiovascular physiology—changes with aging.* The American journal of geriatric cardiology, 2003. **12**(1): p. 9-13.

113. Toda, N., *Age-related changes in endothelial function and blood flow regulation.* Pharmacology and Therapeutics, 2012. **133**(2): p. 159-176.

114. Yildiz, O., *Vascular smooth muscle and endothelial functions in aging.* Annals of the New York Academy of Sciences, 2007. **1100**(1): p. 353-360.

115. Zhou, R.-H., et al., *Mitochondrial oxidative stress in aortic stiffening with age the role of smooth muscle cell function.* Arteriosclerosis, Thrombosis, and Vascular Biology, 2012. **32**(3): p. 745-755.

116. Dokken, B.B., *The pathophysiology of cardiovascular disease and diabetes: beyond blood pressure and lipids.* Diabetes Spectrum, 2008. **21**(3): p. 160-165.

117. Mooradian, A.D., *Dyslipidemia in type 2 diabetes mellitus.* Nature clinical practice endocrinology & metabolism, 2009. **5**(3): p. 150-159.

118. Ciccone, M.M., et al., *Endothelial function in pre-diabetes, diabetes and diabetic cardiomyopathy: a review.* J Diabetes Metab, 2014. **5**(364): p. 2.

119. Giacco, F. and M. Brownlee, *Oxidative stress and diabetic complications.* Circulation Research, 2010. **107**(9): p. 1058-1070.

120. Artwohl, M., et al., *Insulin does not regulate glucose transport and metabolism in human endothelium.* European Journal of Clinical Investigation, 2007. **37**(8): p. 643-650.

121. Mann, G.E., D.L. Yudilevich, and L. Sobrevia, *Regulation of amino acid and glucose transporters in endothelial and smooth muscle cells.* Physiological Reviews, 2003. **83**(1): p. 183-252.

122. Bakker, W., et al., *Endothelial dysfunction and diabetes: roles of hyperglycemia, impaired insulin signaling and obesity.* Cell and Tissue Research, 2009. **335**(1): p. 165-189.

123. Brownlee, M., *Biochemistry and molecular cell biology of diabetic complications.* Nature, 2001. **414**(6865): p. 813-820.

124. Libby, P. and P. Theroux, *Pathophysiology of coronary artery disease.* Circulation, 2005. **111**(25): p. 3481-3488.

125. Yamagishi, S.-i., *Role of advanced glycation end products (AGEs) and receptor for AGEs (RAGE) in vascular damage in diabetes.* Experimental Gerontology, 2011. **46**(4): p. 217-224.

126. Mudau, M., et al., *Endothelial dysfunction: the early predictor of atherosclerosis: review article.* Cardiovascular journal of Africa, 2012. **23**(4): p. 222-231.

127. Lloyd-Jones, *Heart Disease and Stroke Statistics-2009 Update: A Report From the American Heart Association Statistics Committee and Stroke Statistics Subcommittee.* Circulation, 2009. **119**(3): p. E182-E182.

128. Organization, W.H., *Cardiovascular diseases: Fact sheet No. 317. September 2012.* Available on line at http://www. who. int/mediacentre/factsheets/fs317/en/index. html. Last retrieved September 4th, 2012.

129. Catto, V., et al., *Vascular tissue engineering: recent advances in small diameter blood vessel regeneration.* ISRN Vascular Medicine, 2014. **2014**.

130. Heidenreich, P.A., et al., *Forecasting the future of cardiovascular disease in the United States a policy statement from the American heart association.* Circulation, 2011. **123**(8): p. 933-944.

131. U.S. Renal Data System, U.A.D.R.A.o.E.S.R.D.i.t.U.S., National Institutes of Health, National Institute of Diabetes and Digestive and Kidney Diseases, Bethesda, MD, 2006.

132. Tatterton, M., et al., *The use of antithrombotic therapies in reducing synthetic small-diameter vascular graft thrombosis.* Vascular and Endovascular Surgery, 2012: p. 1538574411433299.

133. Klinkert, P., et al., *Saphenous vein versus PTFE for above-knee femoropopliteal bypass. A review of the literature.* European Journal of Vascular and Endovascular Surgery, 2004. **27**(4): p. 357-362.

134. Chiu, J.-J. and S. Chien, *Effects of disturbed flow on vascular endothelium: pathophysiological basis and clinical perspectives.* Physiological Reviews, 2011. **91**(1): p. 327-387.

135. Stewart, S.F. and D.J. Lyman, *Effects of a vascular graft/natural artery compliance mismatch on pulsatile flow.* J Biomech, 1992. **25**(3): p. 297-310.

136. Schmitto, J.D., T.K. Rajab, and L.H. Cohn, *Prevalence and variability of internal mammary graft use in contemporary multivessel coronary artery bypass graft.* Current Opinion in Cardiology, 2010. **25**(6): p. 609-612.

137. Calafiore, A.M., et al., *Internal mammary artery.* Multimedia Manual of Cardio-Thoracic Surgery, 2005. **2005**(1129).

138. Tranbaugh, R.F., et al., *Coronary Artery Bypass Grafting Using the Radial Artery Clinical Outcomes, Patency, and Need for Reintervention.* Circulation, 2012. **126**(11 suppl 1): p. S170-S175.

139. Otsuka, F., et al., *Why is the mammary artery so special and what protects it from atherosclerosis?* Annals of Cardiothoracic Surgery, 2013. **2**(4): p. 519.

140. Buxton, B.F., et al., *Radial artery patency and clinical outcomes: five-year interim results of a randomized trial.* The Journal of Thoracic and Cardiovascular Surgery, 2003. **125**(6): p. 1363-1370.

141. Conte, M.S., *Challenges of distal bypass surgery in patients with diabetes: patient selection, techniques, and outcomes.* Journal of the American Podiatric Medical Association, 2010. **100**(5): p. 429-438.

142. Lytle, B., et al., *Long-term (5 to 12 years) serial studies of internal mammary artery and saphenous vein coronary bypass grafts.* The Journal of Thoracic and Cardiovascular Surgery, 1985. **89**(2): p. 248-258.

143. Waller, B.F. and W.C. Roberts, *Remnant saphenous veins after aortocoronary bypass grafting: analysis of 3,394 centimeters of unused vein from 402 patients.* The American journal of cardiology, 1985. **55**(1): p. 65-71.

144. El-Kurdi, M.S., et al., *Ovine femoral artery bypass grafting using saphenous vein: a new model.* Journal of Surgical Research, 2015. **193**(1): p. 458-469.

145. Weintraub, W.S., et al., *Frequency of repeat coronary-bypass or coronary angioplasty after coronary-artery bypass-surgery using saphenous venous grafts.* American Journal of Cardiology, 1994. **73**(2): p. 103-112.

146. Deutsch, M., et al., *Long-term experience in autologous in vitro endothelialization of infrainguinal ePTFE grafts.* Journal of Vascular Surgery, 2009. **49**(2): p. 352-362.

147. Palmer, S.C., et al., *Antiplatelet therapy to prevent hemodialysis vascular access failure: systematic review and meta-analysis.* American Journal of Kidney Diseases, 2013. **61**(1): p. 112-122.

148. El-Kurdi, M.S., *In-situ Bioengineering of Arterial Vein Grafts*, 2008, University of Pittsburgh. p. 406.

149. El-Kurdi, M.S., et al. *Effecting in-situ remodeling of saphenous vein bypass grafts using a conformal electrospun external support*. in *International Society for Applied Biomechanics (ISACB) Biennial Meeting 2014*. 2014. Cleveland, OH.

150. Mehta, R.I., et al., *Pathology of explanted polytetrafluoroethylene vascular grafts.* Cardiovascular Pathology, 2011. **20**(4): p. 213-221.

151. Legout, L., et al., *Characteristics and prognosis in patients with prosthetic vascular graft infection: a prospective observational cohort study.* Clinical Microbiology and Infection, 2012. **18**(4): p. 352-358.

152. Weinberg, C.B. and E. Bell, *A blood vessel model constructed from collagen and cultured vascular cells.* Science, 1986. **231**(4736): p. 397-400.

153. Soletti, L., et al., *In vivo performance of a phospholipid-coated bioerodable elastomeric graft for small-diameter vascular applications.* J Biomed Mater Res A, 2011. **96**(2): p. 436-48.

154. Zeng, W., et al., *The promotion of endothelial progenitor cells recruitment by nerve growth factors in tissue-engineered blood vessels.* Biomaterials, 2010. **31**(7): p. 1636-1645.

155. Zeng, W., et al., *The use of BDNF to enhance the patency rate of small-diameter tissue-engineered blood vessels through stem cell homing mechanisms.* Biomaterials, 2012. **33**(2): p. 473-484.

156. Yu, J., et al., *The effect of stromal cell-derived factor-1α/heparin coating of biodegradable vascular grafts on the recruitment of both endothelial and smooth muscle progenitor cells for accelerated regeneration.* Biomaterials, 2012. **33**(32): p. 8062-8074.

157. Zilla, P., *Endothelialization of vascular grafts.* Current Opinion in Cardiology, 1991. **6**(6): p. 877-886.

158. Thomas, L.V., V. Lekshmi, and P.D. Nair, *Tissue engineered vascular grafts—preclinical aspects.* International Journal of Cardiology, 2013. **167**(4): p. 1091-1100.

159. Seifu, D.G., et al., *Small-diameter vascular tissue engineering.* Nature Reviews Cardiology, 2013. **10**(7): p. 410-421.

160. Udelsman, B.V., et al., *Characterization of evolving biomechanical properties of tissue engineered vascular grafts in the arterial circulation.* Journal of Biomechanics, 2014. **47**(9): p. 2070-2079.

161. Nieponice, A., et al., *In Vivo Assessment of a Tissue-Engineered Vascular Graft Combining a Biodegradable Elastomeric Scaffold and Muscle-Derived Stem Cells in a Rat Model.* Tissue Engineering Part A, 2010. **16**(4): p. 1215-1223.

162. Wu, W., R.A. Allen, and Y. Wang, *Fast-degrading elastomer enables rapid remodeling of a cell-free synthetic graft into a neoartery.* Nature medicine, 2012. **18**(7): p. 1148-1153.

163. Cho, S.W., et al., *Small-diameter blood vessels engineered with bone marrow-derived cells.* Annals of Surgery, 2005. **241**(3): p. 506-515.

164. Tara, S., et al., *Vessel bioengineering.* Circulation Journal, 2014. **78**(1): p. 12-19.

165. Soletti, L., et al., *A bilayered elastomeric scaffold for tissue engineering of small diameter vascular grafts.* Acta Biomaterialia, 2010. **6**(1): p. 110-122.

166. Rocco, K.A., et al., *In vivo applications of electrospun tissue-engineered vascular grafts: a review.* Tissue Engineering Part B: Reviews, 2014. **20**(6): p. 628-640.

167. Abruzzo, A., et al., *Using polymeric scaffolds for vascular tissue engineering.* International Journal of Polymer Science, 2014. **2014**.

168. Boland, E.D., et al., *Electrospinning collagen and elastin: preliminary vascular tissue engineering.* Frontiers in Bioscience, 2004. **9**(1422): p. C1432.

169. Lepidi, S., et al., *Hyaluronan biodegradable scaffold for small-caliber artery grafting: preliminary results in an animal model.* European journal of vascular and endovascular surgery, 2006. **32**(4): p. 411-417.

170. Ryan, E.A., et al., *Structural origins of fibrin clot rheology.* Biophysical Journal, 1999. **77**(5): p. 2813-2826.

171. Syedain, Z.H., et al., *Implantable arterial grafts from human fibroblasts and fibrin using a multi-graft pulsed flow-stretch bioreactor with noninvasive strength monitoring.* Biomaterials, 2011. **32**(3): p. 714-722.

172. Rana, D., et al., *Development of decellularized scaffolds for stem cell-driven tissue engineering.* Journal of Tissue Engineering and Regenerative Medicine, 2015.

173. Isenberg, B.C., C. Williams, and R.T. Tranquillo, *Small-diameter artificial arteries engineered in vitro.* Circulation Research, 2006. **98**(1): p. 25-35.

174. Kang, J., et al., *Granulocyte colony-stimulating factor minimizes negative remodeling of decellularized small diameter vascular graft conduits but not medial degeneration.* Annals of Vascular Surgery, 2013. **27**(4): p. 487-496.

175. Boneva, R.S., T.M. Folks, and L.E. Chapman, *Infectious disease issues in xenotransplantation.* Clinical Microbiology Reviews, 2001. **14**(1): p. 1-14.

176. Farndale, R., et al., *The role of collagen in thrombosis and hemostasis.* Journal of Thrombosis and Haemostasis, 2004. **2**(4): p. 561-573.

177. Sheridan, W.S., G.P. Duffy, and B.P. Murphy, *Injection techniques for bulk cell seeding decellularised vascular scaffolds.* International Journal of Nano and Biomaterials 17, 2012. **4**(2): p. 96-107.

178. L'Heureux, N., et al., *A completely biological tissue-engineered human blood vessel.* Faseb Journal, 1998. **12**(1): p. 47-56.

179. Gauvin, R., et al., *A Novel Single-Step Self-Assembly Approach for the Fabrication of Tissue-Engineered Vascular Constructs.* Tissue Engineering Part A, 2010. **16**(5): p. 1737-1747.

180. Gauvin, R., et al., *Mechanical Properties of Tissue-Engineered Vascular Constructs Produced Using Arterial or Venous Cells.* Tissue Eng Part A, 2011. **17**(15-16): p. 2049-2059.

181. Zhao, J., et al., *A Novel Strategy to Engineer Small-Diameter Vascular Grafts From Marrow-Derived Mesenchymal Stem Cells.* Artificial Organs, 2012. **36**(1): p. 93-101.

182. Yasuhide, N., I.-U. Hatsue, and T. Keiichi, *In Vivo Tissue-Engineered Small-Caliber Arterial Graft Prosthesis Consisting of Autologous Tissue (Biotube).* Cell Transplantation, 2004. **13**(4): p. 439-449.

183. Rehman, J., et al., *Secretion of angiogenic and antiapoptotic factors by human adipose stromal cells.* Circulation, 2004. **109**(10): p. 1292-1298.

184. Zimmerlin, L., et al., *Regenerative Therapy and Cancer: In Vitro and In Vivo Studies of the Interaction Between Adipose-Derived Stem Cells and Breast Cancer Cells from Clinical Isolates.* Tissue Engineering Part A, 2011. **17**(1-2): p. 93-106.

185. Moon, K.M., et al., *The effect of secretory factors of adipose-derived stem cells on human keratinocytes.* International journal of molecular sciences, 2012. **13**(1): p. 1239-1257.

186. Cherubino, M., et al., *Adipose-Derived Stem Cells for Wound Healing Applications.* Annals of Plastic Surgery, 2011. **66**(2): p. 210-215.

187. Kinnaird, T., et al., *Marrow-derived stromal cells express genes encoding a broad spectrum of arteriogenic cytokines and promote in vitro and in vivo arteriogenesis through paracrine mechanisms.* Circulation Research, 2004. **94**(5): p. 678-685.

188. Gnecchi, M., et al., *Paracrine mechanisms in adult stem cell signaling and therapy.* Circulation research, 2008. **103**(11): p. 1204-1219.

189. Schinköthe, T., W. Bloch, and A. Schmidt, *In vitro secreting profile of human mesenchymal stem cells.* Stem cells and development, 2008. **17**(1): p. 199-206.

190. Li, S., D. Sengupta, and S. Chien, *Vascular tissue engineering: from in vitro to in situ.* Wiley Interdisciplinary Reviews: Systems Biology and Medicine, 2014. **6**(1): p. 61-76.

191. Zimmerlin, L., et al., *Stromal vascular progenitors in adult human adipose tissue.* Cytometry A, 2010. **77**(1): p. 22-30.

192. Hibino, N., et al., *Evaluation of the use of an induced puripotent stem cell sheet for the construction of tissue-engineered vascular grafts.* The Journal of Thoracic and Cardiovascular Surgery, 2012. **143**(3): p. 696-703.

193. Soletti, L., *Development of a Stem Cell-Based Tissue Engineered Vascular Graft,* in *Bioengineering*2008, University of Pittsburgh: Pittsburgh.

194. Ju, Y.M., et al., *Bilayered scaffold for engineering cellularized blood vessels.* Biomaterials, 2010. **31**(15): p. 4313-4321.

195. Nieponice, A., et al., *Combination of muscle-derived stem cells and biodegradable scaffolds for arterial tissue-engineered vascular grafts in rat and pig models,* in *Tissue Engineering & Regenerative Medicine International Society (TERMIS North America)*2008: San Diego, CA.

196. Villalona, G.A., et al., *Cell-seeding techniques in vascular tissue engineering.* Tissue Engineering Part B: Reviews, 2010. **16**(3): p. 341-350.

197. Nieponice, A., et al., *Development of a tissue-engineered vascular graft combining a biodegradable scaffold, muscle-derived stem cells and a rotational vacuum seeding technique.* Biomaterials, 2008. **29**(7): p. 825-33.

198. Soletti, L., et al., *A seeding device for tissue engineered tubular structures.* Biomaterials, 2006. **27**(28): p. 4863-70.

199. Udelsman, B., et al., *Development of an operator-independent method for seeding tissue-engineered vascular grafts.* Tissue Engineering Part C: Methods, 2011. **17**(7): p. 731-736.

200. Kurobe, H., et al., *Comparison of a Closed System to a Standard Open Technique for Preparing Tissue-Engineered Vascular Grafts.* Tissue Engineering Part C: Methods, 2014. **21**(1): p. 88-93.

201. Breuer, C., T. Shinoka, and E. Snyder, *Seeding tissue-engineered vascular grafts in a closed, disposable filter–vacuum system.* BioProcess International, 2013. **11**: p. 52-56.

202. Orlando, G., *Regenerative medicine applications in organ transplantation*2013: Academic Press.

203. Maul, T., et al., *Mechanical stimuli differentially control stem cell behavior: morphology, proliferation, and differentiation.* Biomechanics and Modeling in Mechanobiology, 2011. **10**(6): p. 939-953.

204. Maul, T.M., *Mechanobiology of Stem Cells: Implications for Vascular Tissue Engineering*, 2008, University of Pittsburgh. p. 345.

205. Hong, Y., et al., *A small diameter, fibrous vascular conduit generated from a poly(ester urethane)urea and phospholipid polymer blend.* Biomaterials, 2009. **30**(13): p. 2457-2467.

206. Cho, S.W., et al., *Enhancement of in vivo endothelialization of tissue-engineered vascular grafts by granulocyte colony-stimulating factor.* Journal of Biomedical Materials Research Part A, 2006. **76A**(2): p. 252-263.

207. Shi, Q., et al., *Utilizing granulocyte colony-stimulating factor to enhance vascular graft endothelialization from circulating blood cells.* Annals of Vascular Surgery, 2002. **16**(3): p. 314-320.

208. Zhou, M., et al., *Beneficial effects of granulocyte-colony stimulating factor on small-diameter heparin immobilized decellularized vascular graft.* Journal of Biomedical Materials Research Part A, 2010. **95A**(2): p. 600-610.

209. Lee, K.-W., et al., *Human progenitor cell recruitment via SDF-1α coacervate-laden PGS vascular grafts.* Biomaterials, 2013. **34**(38): p. 9877-9885.

210. Janairo, R.R.R., et al., *Heparin-modified small-diameter nanofibrous vascular grafts.* NanoBioscience, IEEE Transactions on, 2012. **11**(1): p. 22-27.

211. Lee, Y.B., et al., *Polydopamine-mediated immobilization of multiple bioactive molecules for the development of functional vascular graft materials.* Biomaterials, 2012. **33**(33): p. 8343-8352.

212. Melchiorri, A.J., et al., *Development and assessment of a biodegradable solvent cast polyester fabric small-diameter vascular graft.* Journal of Biomedical Materials Research Part A, 2014. **102**(6): p. 1972-1981.

213. Shin, Y.M., et al., *Mussel-inspired immobilization of vascular endothelial growth factor (VEGF) for enhanced endothelialization of vascular grafts.* Biomacromolecules, 2012. **13**(7): p. 2020-2028.

214. Janairo, R.R.R., et al., *Mucin Covalently Bonded to Microfibers Improves the Patency of Vascular Grafts.* Tissue Engineering Part A, 2013. **20**(1-2): p. 285-293.

215. De Visscher, G., et al., *Improved endothelialization and reduced thrombosis by coating a synthetic vascular graft with fibronectin and stem cell homing factor SDF-1α.* Acta biomaterialia, 2012. **8**(3): p. 1330-1338.

216. Roh, J.D., et al., *Tissue-engineered vascular grafts transform into mature blood vessels via an inflammation-mediated process of vascular remodeling.* Proceedings of the National Academy of Sciences of the United States of America, 2010. **107**(10): p. 4669-4674.

217. Lovett, M., et al., *Tubular silk scaffolds for small diameter vascular grafts.* Organogenesis, 2010. **6**(4): p. 217-224.

218. Pavcnik, D., et al., *Angiographic evaluation of carotid artery grafting with prefabricated small-diameter, small-intestinal submucosa grafts in sheep.* Cardiovascular and interventional radiology, 2009. **32**(1): p. 106-113.

219. Torikai, K., et al., *A self-renewing, tissue-engineered vascular graft for arterial reconstruction.* The Journal of Thoracic and Cardiovascular Surgery, 2008. **136**(1): p. 37-45.e1.

220. Yokota, T., et al., *In situ tissue regeneration using a novel tissue-engineered, small-caliber vascular graft without cell seeding.* The Journal of Thoracic and Cardiovascular Surgery, 2008. **136**(4): p. 900-907.

221. Duncan, D.R., et al., *TGFβR1 Inhibition Blocks the Formation of Stenosis in Tissue-Engineered Vascular Grafts.* Journal of the American College of Cardiology, 2015. **65**(5): p. 512-514.

222. Hashi, C.K., et al., *Antithrombogenic modification of small-diameter microfibrous vascular grafts.* Arteriosclerosis, Thrombosis, and Vascular Biology, 2010. **30**(8): p. 1621-1627.

223. Bergmeister, H., et al., *Biodegradable, thermoplastic polyurethane grafts for small diameter vascular replacements.* Acta Biomaterialia, 2015. **11**: p. 104-113.

224. Otrock, Z.K., et al., *Understanding the biology of angiogenesis: review of the most important molecular mechanisms.* Blood Cells, Molecules, and Diseases, 2007. **39**(2): p. 212-220.

225. Grundmann, S., et al., *Arteriogenesis: basic mechanisms and therapeutic stimulation.* European Journal of Clinical Investigation, 2007. **37**(10): p. 755-766.

226. Allen, R.A., et al., *Nerve regeneration and elastin formation within poly (glycerol sebacate)-based synthetic arterial grafts one-year post-implantation in a rat model.* Biomaterials, 2014. **35**(1): p. 165-173.

227. Bowald, S., C. Busch, and I. Eriksson, *Absorbable material in vascular prostheses: a new device.* Acta Chirurgica Scandinavica, 1979. **146**(6): p. 391-395.

228. Hibino, N., et al., *Late-term results of tissue-engineered vascular grafts in humans.* Journal of Thoracic and Cardiovascular Surgery, 2010. **139**(2): p. 431-U233.

229. Shin'oka, T., et al., *Midterm clinical result of tissue-engineered vascular autografts seeded with autologous bone marrow cells.* Journal of Thoracic and Cardiovascular Surgery, 2005. **129**(6): p. 1330-1338.

230. Matsumura, G., et al., *Successful application of tissue engineered vascular autografts: clinical experience.* Biomaterials, 2003. **24**(13): p. 2303-2308.

231. Cleary, M.A., et al., *Vascular tissue engineering: the next generation.* Trends in Molecular Medicine, 2012. **18**(7): p. 394-404.

232. Kurobe, H., et al., *Concise review: tissue-engineered vascular grafts for cardiac surgery: past, present, and future.* Stem cells translational medicine, 2012. **1**(7): p. 566-571.

233. Udelsman, B.V., M.W. Maxfield, and C.K. Breuer, *Tissue engineering of blood vessels in cardiovascular disease: moving towards clinical translation.* Heart, 2013. **99**(7): p. 454-460.

234. Breuer, C.K., *The development and translation of the tissue-engineered vascular graft.* Journal of Pediatric Surgery, 2011. **46**(1): p. 8-17.

235. Hibino, N., et al., *A critical role for macrophages in neovessel formation and the development of stenosis in tissue-engineered vascular grafts.* Faseb Journal, 2011. **25**(12): p. 4253-4263.

236. Hibino, N., et al., *The innate immune system contributes to tissue-engineered vascular graft performance.* The FASEB Journal, 2015: p. fj. 14-268334.

237. Nelson, G.N., et al., *Functional small-diameter human tissue-engineered arterial grafts in an immunodeficient mouse model: preliminary findings.* Arch Surg, 2008. **143**(5): p. 488-94.

238. Tara, S., et al., *Well-organized neointima of large-pore poly (l-lactic acid) vascular graft coated with poly (l-lactic-co-ε-caprolactone) prevents calcific deposition compared to small-pore electrospun poly (l-lactic acid) graft in a mouse aortic implantation model.* Atherosclerosis, 2014. **237**(2): p. 684-691.

239. Hibino, N., et al., *Tissue-engineered vascular grafts form neovessels that arise from regeneration of the adjacent blood vessel.* Faseb Journal, 2011. **25**(8): p. 2731-2739.

240. Mirensky, T.L., et al., *Tissue-engineered vascular grafts: does cell seeding matter?* Journal of Pediatric Surgery, 2010. **45**(6): p. 1299-1305.

241. Naito, Y., et al., *Characterization of the natural history of extracellular matrix production in tissue-engineered vascular grafts during neovessel formation.* Cells, Tissues, Organs, 2012. **195**(1-2): p. 60-72.

242. Stacy, M.R., et al., *Targeted imaging of matrix metalloproteinase activity in the evaluation of remodeling tissue-engineered vascular grafts implanted in a growing lamb model.* The Journal of Thoracic and Cardiovascular Surgery, 2014. **148**(5): p. 2227-2233.

243. Hibino, N., et al., *Comparison of human bone marrow mononuclear cell isolation methods for creating tissue-engineered vascular grafts: novel filter system versus traditional density centrifugation method.* Tissue Engineering Part C: Methods, 2011. **17**(10): p. 993-998.

244. Hibino, N., et al., *The tissue-engineered vascular graft using bone marrow without culture.* Journal of Thoracic and Cardiovascular Surgery, 2005. **129**(5): p. 1064-1070.

245. Miller, K., et al., *Computational model of the in vivo development of a tissue engineered vein from an implanted polymeric construct.* Journal of Biomechanics, 2014. **47**(9): p. 2080-2087.

246. Harrington, J.K., et al., *Determining the fate of seeded cells in venous tissue-engineered vascular grafts using serial MRI.* The FASEB Journal, 2011. **25**(12): p. 4150-4161.

247. Vogel, G., *Mending the youngest hearts.* Science, 2011. **333**(6046): p. 1088-1089.

248. L'Heureux, N., T.N. McAllister, and L.M. de la Fuente, *Tissue-Engineered Blood Vessel for Adult Arterial Revascularization.* New England Journal of Medicine, 2007. **357**(14): p. 1451-1453.

249. McAllister, T.N., et al., *Effectiveness of haemodialysis access with an autologous tissue-engineered vascular graft: a multicentre cohort study.* Lancet, 2009. **373**(9673): p. 1440-6.

250. L'Heureux, N., et al., *Technology Insight: the evolution of tissue-engineered vascular grafts - from research to clinical practice.* Nature Clinical Practice Cardiovascular Medicine, 2007. **4**(7): p. 389-395.

251. Peck, M., et al., *Tissue engineering by self-assembly.* Materials Today, 2011. **14**(5): p. 218-224.

252. Konig, G., et al., *Mechanical properties of completely autologous human tissue engineered blood vessels compared to human saphenous vein and mammary artery.* Biomaterials, 2009. **30**(8): p. 1542-1550.

253. Wystrychowski, W., et al., *First human use of an allogeneic tissue-engineered vascular graft for hemodialysis access.* Journal of Vascular Surgery, 2014. **60**(5): p. 1353-1357.

254. Olausson, M., et al., *Transplantation of an allogeneic vein bioengineered with autologous stem cells: a proof-of-concept study.* The Lancet, 2012. **380**(9838): p. 230-237.

255. Zhu, C.H., et al., *Development of anti-atherosclerotic tissue-engineered blood vessel by A20-regulated endothelial progenitor cells seeding decellularized vascular matrix.* Biomaterials, 2008. **29**(17): p. 2628-2636.

256. Zhao, Y.L., et al., *The development of a tissue-engineered artery using decellularized scaffold and autologous ovine mesenchymal stem cells.* Biomaterials, 2010. **31**(2): p. 296-307.

257. Cho, S.W., et al., *Evidence for in vivo growth potential and vascular remodeling of tissue-engineered artery.* Tissue Engineering Part A, 2009. **15**(4): p. 901-912.

258. Lim, S.H., et al., *Tissue-engineered blood vessels with endothelial nitric oxide synthase activity.* Journal of Biomedical Materials Research Part B: Applied Biomaterials, 2008. **85B**(2): p. 537-546.

259. Lawson, J., et al., *VS5 human tissue-engineered grafts for hemodialysis: development, preclinical data, and early investigational human implant experience.* Journal of Vascular Surgery, 2014. **59**(6): p. 32S-33S.

260. He, W., et al., *Pericyte-based human tissue engineered vascular grafts.* Biomaterials, 2010. **31**(32): p. 8235-8244.

261. Hashi, C.K., et al., *Antithrombogenic property of bone marrow mesenchymal stem cells in nanofibrous vascular grafts.* Proceedings of the National Academy of Sciences of the United States of America, 2007. **104**(29): p. 11915-11920.

262. Hjortnaes, J., et al., *Intravital molecular imaging of small-diameter tissue-engineered vascular grafts in mice: a feasibility study.* Tissue Engineering Part C: Methods, 2010. **16**(4): p. 597-607.

263. L'Heureux, N., et al., *Human tissue-engineered blood vessels for adult arterial revascularization.* Nat Med, 2006. **12**(3): p. 361-5.

264. Quint, C., et al., *Allogeneic human tissue-engineered blood vessel.* Journal of Vascular Surgery, 2012. **55**(3): p. 790-798.

265. He, W., et al., *Rapid Engineered Small Diameter Vascular Grafts from Smooth Muscle Cells.* Cardiovascular Engineering and Technology, 2011: p. 1-11.

266. Krawiec, J.T., et al. *A Cautionary Tale for Autologous Vascular Tissue Engineering*. in *International Society of Applied Cardiovascular Biology (ISACB) 14th Biennial Meeting*. 2014. Cleveland, OH.

267. Kaushal, S., et al., *Functional small-diameter neovessels created using endothelial progenitor cells expanded ex vivo.* Nature Medicine, 2001. **7**(9): p. 1035-1040.

268. Liu, J.Y., et al., *Functional tissue-engineered blood vessels from bone marrow progenitor cells.* Cardiovascular Research, 2007. **75**(3): p. 618-628.

269. Brennan, M.P., et al., *Tissue-engineered vascular grafts demonstrate evidence of growth and development when implanted in a juvenile animal model.* Annals of Surgery, 2008. **248**(3): p. 370-376.

270. Zhang, L., et al., *A novel small-diameter vascular graft: in vivo behavior of biodegradable three-layered tubular scaffolds.* Biotechnol Bioeng, 2008. **99**(4): p. 1007-15.

271. He, H., et al., *Canine endothelial progenitor cell-lined hybrid vascular graft with nonthrombogenic potential.* The Journal of Thoracic and Cardiovascular Surgery, 2003. **126**(2): p. 455-464.

272. Koch, S., et al., *Fibrin-polylactide-based tissue-engineered vascular graft in the arterial circulation.* Biomaterials, 2010. **31**(17): p. 4731-9.

273. He, H. and T. Matsuda, *Newly designed compliant hierarchic hybrid vascular graft wrapped with microprocessed elastomeric film-II: Morphogenesis and compliance change upon implantation.* Cell Transplantation, 2002. **11**(1): p. 75-87.

274. Niklason, L., et al., *Functional arteries grown in vitro.* Science, 1999. **284**(5413): p. 489-493.

275. Hoerstrup, S.P., et al., *Functional Growth in Tissue-Engineered Living, Vascular Grafts.* Circulation, 2006. **114**(1 suppl): p. I-159-I-166.

276. Kelm, J.M., et al., *Functionality, growth and accelerated aging of tissue engineered living autologous vascular grafts.* Biomaterials, 2012. **33**(33): p. 8277-8285.

277. Watanabe, M., et al., *Tissue-engineered vascular autograft: inferior vena cava replacement in a dog model.* Tissue engineering, 2001. **7**(4): p. 429-439.

278. Cummings, I., et al., *Tissue-engineered vascular graft remodeling in a growing lamb model: expression of matrix metalloproteinases.* European Journal of Cardio-Thoracic Surgery, 2012. **41**(1): p. 167-172.

279. Soletti, L., *Development of a stem cell-based tissue engineered vascular graft* 2008, University of Pittsburgh: Pittsburgh. p. 404.

280. Roh, J.D., et al., *Construction of an autologous tissue-engineered venous conduit from bone marrow-derived vascular cells: optimization of cell harvest and seeding techniques.* Journal of Pediatric Surgery, 2007. **42**(1): p. 198-202.

281. Rexius, H., et al., *Mortality on the waiting list for coronary artery bypass grafting: incidence and risk factors.* The Annals of thoracic surgery, 2004. **77**(3): p. 769-774.

282. Rexius, H., et al., *Waiting time and mortality after elective coronary artery bypass grafting.* The Annals of thoracic surgery, 2005. **79**(2): p. 538-543.

283. Prestwich, G.D., et al., *What is the greatest regulatory challenge in the translation of biomaterials to the clinic.* Sci. Transl. Med, 2012. **4**: p. 160cm14.

284. Krawiec, J.T., et al., *Human Diabetic Adipose Stem Cells Display Reduced Fibrinolysis Due to Urokinase Activity Attributing to Their Pro-Thrombogenic Phenotype* Under Review, 2015.

285. Camilleri, J., et al., *Surface healing and histologic maturation of patent polytetrafluoroethylene grafts implanted in patients for up to 60 months.* Archives of Pathology and Laboratory Medicine, 1985. **109**(9): p. 833-837.

286. Formichi, M.J., et al., *Expanded PTFE prostheses as arterial substitutes in humans: late pathological findings in 73 excised grafts.* Annals of Vascular Surgery, 1988. **2**(1): p. 14-27.

287. Guidoin, R., et al., *Expanded polytetrafluoroethylene arterial prostheses in humans: histopathological study of 298 surgically excised grafts.* Biomaterials, 1993. **14**(9): p. 678-693.

288. Bergmeister, H., et al., *Healing characteristics of electrospun polyurethane grafts with various porosities.* Acta Biomaterialia, 2013. **9**(4): p. 6032-6040.

289. Ryu, Y.-J., et al., *Phenotypic characterization and in vivo localization of human adipose-derived mesenchymal stem cells.* Molecules and cells, 2013. **35**(6): p. 557-564.

290. Gimble, J.M., A.J. Katz, and B.A. Bunnell, *Adipose-derived stem cells for regenerative medicine.* Circulation research, 2007. **100**(9): p. 1249-1260.

291. Mizuno, H., *Adipose-derived stem cells for tissue repair and regeneration: ten years of research and a literature review.* Journal of Nippon Medical School, 2009. **76**(2): p. 56-66.

292. Wei, H.-J., et al., *Bioengineered cardiac patch constructed from multilayered mesenchymal stem cells for myocardial repair.* Biomaterials, 2008. **29**(26): p. 3547-3556.

293. Schoen, F.J., *Heart valve tissue engineering:< i> quo vadis?</i>*. Current Opinion in Biotechnology, 2011. **22**(5): p. 698-705.

294. Tedder, M.E., et al., *Assembly and testing of stem cell-seeded layered collagen constructs for heart valve tissue engineering.* Tissue Engineering Part A, 2010. **17**(1-2): p. 25-36.

295. Steinert, A.F., et al., *Concise review: the clinical application of mesenchymal stem cells for musculoskeletal regeneration: current status and perspectives.* Stem cells translational medicine, 2012. **1**(3): p. 237-247.

296. Richardson, S.M., et al., *Mesenchymal stem cells in regenerative medicine: opportunities and challenges for articular cartilage and intervertebral disc tissue engineering.* Journal of cellular physiology, 2010. **222**(1): p. 23-32.

297. da Silva Meirelles, L., P.C. Chagastelles, and N.B. Nardi, *Mesenchymal stem cells reside in virtually all post-natal organs and tissues.* Journal of Cell Science, 2006. **119**(11): p. 2204-2213.

298. Crisan, M., et al., *A perivascular origin for mesenchymal stem cells in multiple human organs.* Cell Stem Cell, 2008. **3**(3): p. 301-313.

299. Traktuev, D.O., et al., *A population of multipotent CD34-positive adipose stromal cells share pericyte and mesenchymal surface markers, reside in a periendothelial location, and stabilize endothelial networks.* Circulation Research, 2008. **102**(1): p. 77-85.

300. Bourin, P., et al., *Stromal cells from the adipose tissue-derived stromal vascular fraction and culture expanded adipose tissue-derived stromal/stem cells: a joint statement of the International Federation for Adipose Therapeutics and Science (IFATS) and the International Society for Cellular Therapy (ISCT).* Cytotherapy, 2013. **15**(6): p. 641-648.

301. Mitchell, J.B., et al., *Immunophenotype of human adipose-derived cells: temporal changes in stromal-associated and stem cell-associated markers.* Stem Cells, 2006. **24**(2): p. 376-385.

302. McIntosh, K., et al., *The Immunogenicity of Human Adipose-Derived Cells: Temporal Changes In Vitro.* Stem Cells, 2006. **24**(5): p. 1246-1253.

303. Kokai, L.E., K. Marra, and J.P. Rubin, *Adipose stem cells: biology and clinical applications for tissue repair and regeneration.* Translational Research, 2014. **163**(4): p. 399-408.

304. Schipper, B.M., et al., *Regional anatomic and age effects on cell function of human adipose-derived stem cells.* Ann Plast Surg, 2008. **60**(5): p. 538-44.

305. Aksu, A.E., et al., *Role of Gender and Anatomical Region on Induction of Osteogenic Differentiation of Human Adipose-Derived Stem Cells.* Annals of Plastic Surgery, 2008. **60**(3): p. 306-22.

306. Dudas, J.R., et al., *Leporine-Derived Adipose Precursor Cells Exhibit In Vitro Osteogenic Potential.* Journal of Craniofacial Surgery, 2008. **19**(2): p. 360-368.

307. Sorisky, A., *From preadipocyte to adipocyte: differentiation-directed signals of insulin from the cell surface to the nucleus.* Critical Reviews in Clinical Laboratory Sciences, 1999. **36**(1): p. 1-34.

308. Kirkland, J.L., C.H. Hollenberg, and W.S. Gillon, *Age, anatomic site, and the replication and differentiation of adipocyte precursors.* American Journal of Physiology-Cell Physiology, 1990. **258**(2): p. C206-C210.

309. Djian, P., A. Roncari, and C. Hollenberg, *Influence of anatomic site and age on the replication and differentiation of rat adipocyte precursors in culture.* Journal of Clinical Investigation, 1983. **72**(4): p. 1200.

310. Djian, P., D. Roncari, and C. Hollenberg, *Adipocyte precursor clones vary in capacity for differentiation.* Metabolism: Clinical and Experimental, 1985. **34**(9): p. 880-883.

311. Zuk, P.A., et al., *Multilineage cells from human adipose tissue: implications for cell-based therapies.* Tissue Engineering, 2001. **7**(2): p. 211-228.

312. Tsuji, W., J.P. Rubin, and K.G. Marra, *Adipose-derived stem cells: Implications in tissue regeneration.* World journal of stem cells, 2014. **6**(3): p. 312.

313. Bellas, E., et al., *Sustained volume retention in vivo with adipocyte and lipoaspirate seeded silk scaffolds.* Biomaterials, 2013. **34**(12): p. 2960-2968.

314. Zimmerlin, L., et al., *Human adipose stromal vascular cell delivery in a fibrin spray.* Cytotherapy, 2013. **15**(1): p. 102-108.

315. Kokai, L. and J.P. Rubin, *Whitening Effects of Adipose-Derived Stem Cells: An In Vivo Study.* Aesthetic Plastic Surgery, 2014. **38**(1): p. 234.

316. Zhang, P., et al., *A review of adipocyte lineage cells and dermal papilla cells in hair follicle regeneration.* Journal of Tissue Engineering, 2014. **5**: p. 2041731414556850.

317. Lin, Y.-C., et al., *Evaluation of a multi-layer adipose-derived stem cell sheet in a full-thickness wound healing model.* Acta Biomaterialia, 2013. **9**(2): p. 5243-5250.

318. Smith, D.M., et al., *Regenerative surgery in cranioplasty revisited: the role of adipose-derived stem cells and BMP-2.* Plastic and Reconstructive Surgery, 2011. **128**(5): p. 1053-1060.

319. Gerlach, J.C., et al., *Adipogenesis of human adipose-derived stem cells within three-dimensional hollow fiber-based bioreactors.* Tissue Engineering Part C: Methods, 2011. **18**(1): p. 54-61.

320. Du, Y., et al., *Adipose-derived stem cells differentiate to keratocytes in vitro.* Molecular Vision, 2010. **16**: p. 2680.

321. Santiago, L.Y.C.-A., Julio; Brayfield, Candace; Rubin, J. Peter; Marra, Kacey G, *Delivery of Adipose-Derived Precursor Cells for Peripheral Nerve Repair.* Cell Transplantation, 2009. **18**: p. 145-158.

322. Dudas, J.R., et al., *The Osteogenic Potential of Adipose-Derived Stem Cells for the Repair of Rabbit Calvarial Defects.* Annals of Plastic Surgery, 2006. **56**(5): p. 543-548.

323. Freese, K.E., et al., *Adipose-derived stems cells and their role in human cancer development, growth, progression, and metastasis: a systematic review*. Cancer Research, 2015. **75**(7): p. 1161-1168.

324. Linkov, F., et al., *The role of adipose-derived stem cells in endometrial cancer proliferation.* Scandinavian Journal of Clinical and Laboratory Investigation, 2014. **74**(sup244): p. 54-58.

325. Wang, H., J. Kirkland, and C. Hollenberg, *Varying capacities for replication of rat adipocyte precursor clones and adipose tissue growth.* Journal of Clinical Investigation, 1989. **83**(5): p. 1741.

326. Kirkland, J.L., C.H. Hollenberg, and W.S. Gillon, *Two preadipocyte subtypes cloned from human omental fat.* Obesity Research, 1993. **1**(2): p. 87-91.

327. Donnenberg, A.D., et al., *The cell-surface proteome of cultured adipose stromal cells.* Cytometry Part A, 2015.

328. Satish, L., et al., *Expression analysis of human adipose-derived stem cells during in vitro differentiation to an adipocyte lineage.* BMC Medical Genomics, 2015. **8**(1): p. 41.

329. Zimmerlin, L., et al., *Mesenchymal markers on human adipose stem/progenitor cells.* Cytometry A, 2013. **83**(1): p. 134-40.

330. Li, H., et al., *Adipogenic potential of adipose stem cell subpopulations.* Plast Reconstr Surg, 2011. **128**(3): p. 663-72.

331. Stolzing, A., et al., *Diabetes Induced Changes in Rat Mesenchymal Stem Cells.* Cells Tissues Organs, 2010. **191**(6): p. 453-465.

332. Cronk, S.M., et al., *Adipose-Derived Stem Cells From Diabetic Mice Show Impaired Vascular Stabilization in a Murine Model of Diabetic Retinopathy.* Stem cells translational medicine, 2015: p. sctm. 2014-0108.

333. Rennert, R.C., et al., *Diabetes impairs the angiogenic potential of adipose derived stem cells by selectively depleting cellular subpopulations.* Current stem cell research & therapy, 2014. **5**(79): p. 10.1186.

334. Cianfarani, F., et al., *Diabetes impairs adipose tissue–derived stem cell function and efficiency in promoting wound healing.* Wound Repair and Regeneration, 2013. **21.4**: p. 545-553.

335. Acosta, L., et al., *Adipose mesenchymal stromal cells isolated from type 2 diabetic patients display reduced fibrinolytic activity.* Diabetes, 2013. **62**(12): p. 4266-9.

336. Zhu, M., et al., *The effect of age on osteogenic, adipogenic and proliferative potential of female adipose-derived stem cells.* Journal of Tissue Engineering and Regenerative Medicine, 2009. **3**(4): p. 290-301.

337. Lavasani, M., et al., *Muscle-derived stem/progenitor cell dysfunction limits healthspan and lifespan in a murine progeria model.* Nature Communications, 2012. **3**(608): p. 1-12.

338. Cheleuitte, D., S. Mizuno, and J. Glowacki, *In Vitro Secretion of Cytokines by Human Bone Marrow: Effects of Age and Estrogen Status 1.* The Journal of Clinical Endocrinology & Metabolism, 1998. **83**(6): p. 2043-2051.

339. Madonna, R., et al., *Age-dependent impairment of number and angiogenic potential of adipose tissue-derived progenitor cells.* European Journal of Clinical Investigation, 2011. **41**(2): p. 126-133.

340. Tsuji, W., et al., *Effects of immunosuppressive drugs on viability and susceptibility of adipose-and bone marrow-derived mesenchymal stem cells.* Frontiers in immunology, 2015. **6**.

341. Sethe, S., A. Scutt, and A. Stolzing, *Aging of mesenchymal stem cells.* Ageing research reviews, 2006. **5**(1): p. 91-116.

342. Kim, Y.M., et al., *Angiotensin II-induced differentiation of adipose tissue-derived mesenchymal stem cells to smooth muscle-like cells.* The international journal of biochemistry & cell biology, 2008. **40**(11): p. 2482-2491.

343. van der Loop, F.T., et al., *Differentiation of smooth muscle cells in human blood vessels as defined by smoothelin, a novel marker for the contractile phenotype.* Arteriosclerosis, thrombosis, and vascular biology, 1997. **17**(4): p. 665-671.

344. Guan, J., et al., *Synthesis, characterization, and cytocompatibility of elastomeric, biodegradable poly(ester-urethane)ureas based on poly(caprolactone) and putrescine.* J Biomed Mater Res, 2002. **61**(3): p. 493-503.

345. Guan, J., et al., *Preparation and characterization of highly porous, biodegradable polyurethane scaffolds for soft tissue applications.* Biomaterials, 2005. **26**(18): p. 3961-71.

346. Koch, R.G., et al., *A custom image-based analysis tool for quantifying elastin and collagen micro-architecture in the wall of the human aorta from multi-photon microscopy.* Journal of biomechanics, 2014. **47**(5): p. 935-943.

347. Tsamis, A., et al., *Fiber micro-architecture in the longitudinal-radial and circumferential-radial planes of ascending thoracic aortic aneurysm media.* Journal of Biomechanics, 2013. **46**(16): p. 2787-2794.

348. Grosskreutz, C.L., et al., *Vascular Endothelial Growth Factor-Induced Migration of Vascular Smooth Muscle Cells< i> in Vitro</i>*. Microvascular research, 1999. **58**(2): p. 128-136.

349. Xu, X., et al., *Characteristic analysis of Otsu threshold and its applications.* Pattern recognition letters, 2011. **32**(7): p. 956-961.

350. WOLINSKY, H. and S. Glagov, *Nature of species differences in the medial distribution of aortic vasa vasorum in mammals.* Circulation Research, 1967. **20**(4): p. 409-421.

351. Lovett, M., et al., *Vascularization strategies for tissue engineering.* Tissue Engineering Part B: Reviews, 2009. **15**(3): p. 353-370.

352. Anderson, L.A., et al., *The effects of androgens and estrogens on preadipocyte proliferation in human adipose tissue: Influence of gender and site.* Journal of Clinical Endocrinology & Metabolism, 2001. **86**(10): p. 5045-5051.

353. van Harmelen, V., K. Rohrig, and H. Hauner, *Comparison of proliferation and differentiation capacity of human adipocyte precursor cells from the omental and subcutaneous adipose tissue depot of obese subjects.* Metabolism: Clinical and Experimental, 2004. **53**(5): p. 632-637.

354. Van Harmelen, V., et al., *Effect of BMI and age on adipose tissue cellularity and differentiation capacity in women.* International journal of obesity, 2003. **27**(8): p. 889-895.

355. Faries, P.L., et al., *Human vascular smooth muscle cells of diabetic origin exhibit increased proliferation, adhesion, and migration.* Journal of Vascular Surgery, 2001. **33**(3): p. 601-607.

356. Ruiz-Torres, A., et al., *Age-dependent decline of in vitro migration (basal and stimulated by IGF-1 or insulin) of human vascular smooth muscle cells.* The Journals of Gerontology Series A: Biological Sciences and Medical Sciences, 2003. **58**(12): p. B1074-B1077.

357. Gerthoffer, W.T., *Mechanisms of vascular smooth muscle cell migration.* Circulation research, 2007. **100**(5): p. 607-621.

358. Eringa, E.C., et al., *Endothelial dysfunction in (pre) diabetes: characteristics, causative mechanisms and pathogenic role in type 2 diabetes.* Reviews in Endocrine and Metabolic Disorders, 2013. **14**(1): p. 39-48.

359. Kovacic, J.C., et al., *Cellular Senescence, Vascular Disease, and Aging Part 1 of a 2-Part Review.* Circulation, 2011. **123**(15): p. 1650-1660.

360. Kovacic, J.C., et al., *Cellular senescence, vascular disease, and aging part 2 of a 2-part review: clinical vascular disease in the elderly.* Circulation, 2011. **123**(17): p. 1900-1910.

361. Caballero, S., et al., *Ischemic vascular damage can be repaired by healthy, but not diabetic, endothelial progenitor cells.* Diabetes, 2007. **56**(4): p. 960-967.

362. Fadini, G.P., et al., *Circulating endothelial progenitor cells are reduced in peripheral vascular complications of type 2 diabetes mellitus.* Journal of the American College of Cardiology, 2005. **45**(9): p. 1449-1457.

363. Tepper, O.M., et al., *Human endothelial progenitor exhibit impaired proliferation, cells from type II diabetics adhesion, and incorporation into vascular structures.* Circulation, 2002. **106**(22): p. 2781-2786.

364. Vasa, M., et al., *Number and migratory activity of circulating endothelial progenitor cells inversely correlate with risk factors for coronary artery disease.* Circulation Research, 2001. **89**(1): p. e1-e7.

365. Heiss, C., et al., *Impaired progenitor cell activity in age-related endothelial dysfunction.* Journal of the American College of Cardiology, 2005. **45**(9): p. 1441-1448.
366. Scheubel, R.J., et al., *Age-dependent depression in circulating endothelial progenitor cells inpatients undergoing coronary artery bypass grafting.* Journal of the American College of Cardiology, 2003. **42**(12): p. 2073-2080.

367. Chang, E.I., et al., *Age decreases endothelial progenitor cell recruitment through decreases in hypoxia-inducible factor 1α stabilization during ischemia.* Circulation, 2007. **116**(24): p. 2818-2829.

368. Porter, K.E. and K. Riches, *The vascular smooth muscle cell: a therapeutic target in Type 2 diabetes?* Clinical Science, 2013. **125**(4): p. 167-182.

369. Byrom, M.J., et al., *Animal models for the assessment of novel vascular conduits.* Journal of Vascular Surgery, 2010. **52**(1): p. 176-195.

370. Swartz, D.D. and S.T. Andreadis, *Animal models for vascular tissue-engineering.* Current opinion in biotechnology, 2013. **24**(5): p. 916-925.

371. Chow, J.P., et al., *Mitigation of diabetes-related complications in implanted collagen and elastin scaffolds using matrix-binding polyphenol.* Biomaterials, 2013. **34**(3): p. 685-695.

372. Minteer, D.M., et al., *Analysis of type II diabetes mellitus adipose-derived stem cells for tissue engineering applications.* Journal of Tissue Engineering, 2015. **6**: p. 2041731415579215.

373. Tchoukalova, Y.D., et al., *Sex-and Depot-Dependent Differences in Adipogenesis in Normal-Weight Humans.* Obesity, 2010. **18**(10): p. 1875-1880.

374. Rossmeislová, L., et al., *Weight loss improves the adipogenic capacity of human preadipocytes and modulates their secretory profile.* Diabetes, 2013. **62**(6): p. 1990-1995.

375. Goldstein, S., J.W. Littlefield, and J.S. Soeldner, *Diabetes mellitus and aging: diminished plating efficiency of cultured human fibroblasts.* Proceedings of the National Academy of Sciences, 1969. **64**(1): p. 155-160.

376. Rajagopalan, S., *Serious infections in elderly patients with diabetes mellitus.* Clinical Infectious Diseases, 2005. **40**(7): p. 990-996.

377. Brem, H., et al., *The synergism of age and db/db genotype impairs wound healing.* Experimental Gerontology, 2007. **42**(6): p. 523-531.

378. Lewis, J., et al., *Comparative hematology and coagulation: studies on rodentia (rats).* Comparative Biochemistry and Physiology Part A: Physiology, 1985. **82**(1): p. 211-215.

379. Bodary, P.F. and D.T. Eitzman, *Animal models of thrombosis.* Current Opinion in Hematology, 2009. **16**(5): p. 342-346.
380. Chen, L., et al., *Paracrine factors of mesenchymal stem cells recruit macrophages and endothelial lineage cells and enhance wound healing.* PLoS ONE, 2008. **3**(4): p. e1886.

381. Lee, K.-W., D.B. Stolz, and Y. Wang, *Substantial expression of mature elastin in arterial constructs.* Proceedings of the National Academy of Sciences, 2011. **108**(7): p. 2705-2710.

382. Potts, W.K., et al., *The role of infectious disease, inbreeding and mating preferences in maintaining MHC genetic diversity: an experimental test [and discussion]*. Philosophical Transactions of the Royal Society B: Biological Sciences, 1994. **346**(1317): p. 369-378.

383. Sommer, S., *The importance of immune gene variability (MHC) in evolutionary ecology and conservation.* Front Zool, 2005. **2**(1): p. 16.

384. Azizi, S.A., et al., *Engraftment and migration of human bone marrow stromal cells implanted in the brains of albino rats—similarities to astrocyte grafts.* Proceedings of the National Academy of Sciences, 1998. **95**(7): p. 3908-3913.

385. Berry, M.F., et al., *Mesenchymal stem cell injection after myocardial infarction improves myocardial compliance*. American Journal of Physiology-Heart and Circulatory Physiology, 2006. **290**(6): p. H2196-H2203.

386. Min, J.-J., et al., *In vivo bioluminescence imaging of cord blood derived mesenchymal stem cell transplantation into rat myocardium.* Annals of Nuclear Medicine, 2006. **20**(3): p. 165-170.

387. Inoue, S., et al., *Immunomodulatory effects of mesenchymal stem cells in a rat organ transplant model.* Transplantation, 2006. **81**(11): p. 1589-1595.

388. Chabannes, D., et al., *A role for heme oxygenase-1 in the immunosuppressive effect of adult rat and human mesenchymal stem cells.* Blood, 2007. **110**(10): p. 3691-3694.

389. Konieczynska, M., et al., *Prolonged duration of type 2 diabetes is associated with increased thrombin generation, prothrombotic fibrin clot phenotype and impaired fibrinolysis.* Thrombosis and Haemostasis, 2014. **111**(4): p. 685-693.

390. Grant, P.J., *Diabetes mellitus as a prothrombotic condition.* J Intern Med, 2007. **262**(2): p. 157-72.

391. Carr, M.E., *Diabetes mellitus: a hypercoagulable state.* Journal of Diabetes and Its Complications, 2001. **15**(1): p. 44-54.

392. Varma, V., et al., *Thrombospondin-1 is an adipokine associated with obesity, adipose inflammation, and insulin resistance.* Diabetes, 2008. **57**(2): p. 432-9.

393. Neuss, S., et al., *Secretion of fibrinolytic enzymes facilitates human mesenchymal stem cell invasion into fibrin clots.* Cells Tissues Organs, 2010. **191**(1): p. 36-46.

394. Kachgal, S. and A.J. Putnam, *Mesenchymal stem cells from adipose and bone marrow promote angiogenesis via distinct cytokine and protease expression mechanisms.* Angiogenesis, 2011. **14**(1): p. 47-59.

395. Ahmann, K.A., et al., *Fibrin degradation enhances vascular smooth muscle cell proliferation and matrix deposition in fibrin-based tissue constructs fabricated in vitro.* Tissue Eng Part A, 2010. **16**(10): p. 3261-70.

396. Weinbaum, J.S., J.B. Schmidt, and R.T. Tranquillo, *Combating Adaptation to Cyclic Stretching By Prolonging Activation of Extracellular Signal-Regulated Kinase.* Cell Mol Bioeng, 2013. **6**(3): p. 459-286.

397. Andreasen, P.A., et al., *The urokinase-type plasminogen activator system in cancer metastasis: a review.* International Journal of Cancer, 1997. **72**(1): p. 1-22.

398. Lijnen, H.R., et al., *Biochemical and thrombolytic properties of a low molecular weight form (comprising Leu144 through Leu411) of recombinant single-chain urokinase-type plasminogen activator.* Journal of Biological Chemistry, 1988. **263**(12): p. 5594-5598.

399. Duffy, M.J., *The urokinase plasminogen activator system: role in malignancy.* Current pharmaceutical design, 2004. **10**(1): p. 39-49.

400. Stump, D.C., H.R. Lijnen, and D. Collen, *Purification and characterization of a novel low molecular weight form of single-chain urokinase-type plasminogen activator.* Journal of Biological Chemistry, 1986. **261**(36): p. 17120-17126.

401. Blasi, F., J.-D. Vassalli, and K. Danø, *Urokinase-type plasminogen activator: proenzyme, receptor, and inhibitors.* The Journal of cell biology, 1987. **104**(4): p. 801-804.

402. Tang, L. and X. Han, *The urokinase plasminogen activator system in breast cancer invasion and metastasis.* Biomedicine & Pharmacotherapy, 2013. **67**(2): p. 179-182.

403. Sprengers, E. and C. Kluft, *Plasminogen activator inhibitors.* Blood, 1987. **69**(2): p. 381-387.

404. Cubellis, M.V., et al., *Accessibility of receptor-bound urokinase to type-1 plasminogen activator inhibitor.* Proceedings of the National Academy of Sciences, 1989. **86**(13): p. 4828-4832.

405. Kenichi, M., et al., *Renal synthesis of urokinase type-plasminogen activator, its receptor, and plasminogen activator inhibitor-1 in diabetic nephropathy in rats: Modulation by*

angiotensin-converting–enzyme inhibitor. Journal of Laboratory and Clinical Medicine, 2004. **144**(2): p. 69-77.

406. El-Remessy, A.B., et al., *Experimental diabetes causes breakdown of the blood-retina barrier by a mechanism involving tyrosine nitration and increases in expression of vascular endothelial growth factor and urokinase plasminogen activator receptor.* The American journal of pathology, 2003. **162**(6): p. 1995-2004.

407. Vasir, B., et al., *Effects of diabetes and hypoxia on gene markers of angiogenesis (HGF, cMET, uPA and uPAR, TGF-α, TGF-β, bFGF and Vimentin) in cultured and transplanted rat islets.* Diabetologia, 2000. **43**(6): p. 763-772.

408. Caldwell, R.B., et al., *Vascular endothelial growth factor and diabetic retinopathy: pathophysiological mechanisms and treatment perspectives.* Diabetes/metabolism research and reviews, 2003. **19**(6): p. 442-455.

409. Montuori, N. and P. Ragno, *Multiple activities of a multifaceted receptor: roles of cleaved and soluble uPAR.* Frontiers in bioscience, 2008. **14**: p. 2494-2503.

410. Ostrowski, S.R., et al., *Plasma concentrations of soluble urokinase-type plasminogen activator receptor are increased in patients with malaria and are associated with a poor clinical or a fatal outcome.* Journal of Infectious Diseases, 2005. **191**(8): p. 1331-1341.

411. Eugen-Olsen, J., et al., *Circulating soluble urokinase plasminogen activator receptor predicts cancer, cardiovascular disease, diabetes and mortality in the general population.* Journal of internal medicine, 2010. **268**(3): p. 296-308.

412. Heraclides, A., et al., *The pro-inflammatory biomarker soluble urokinase plasminogen activator receptor (suPAR) is associated with incident type 2 diabetes among overweight but not obese individuals with impaired glucose regulation: effect modification by smoking and body weight status.* Diabetologia, 2013. **56**(7): p. 1542-1546.

413. Backes, Y., et al., *Usefulness of suPAR as a biological marker in patients with systemic inflammation or infection: a systematic review.* Intensive care medicine, 2012. **38**(9): p. 1418-1428.

414. Persson, M., et al., *Soluble urokinase plasminogen activator receptor in plasma is associated with incidence of CVD. Results from the Malmö Diet and Cancer Study.* Atherosclerosis, 2012. **220**(2): p. 502-505.

415. Haugaard, S., et al., *The immune marker soluble urokinase plasminogen activator receptor is associated with new-onset diabetes in non-smoking women and men.* Diabetic Medicine, 2012. **29**(4): p. 479-487.

416. Cubellis, M.V., T.-C. Wun, and F. Blasi, *Receptor-mediated internalization and degradation of urokinase is caused by its specific inhibitor PAI-1.* The EMBO Journal, 1990. **9**(4): p. 1079.
417. Markus, G., J. DePasquale, and F.C. Wissler, *Quantitative determination of the binding of epsilon-aminocaproic acid to native plasminogen.* Journal of Biological Chemistry, 1978. **253**(3): p. 727-732.

418. Vassalli, J.-D., A. Sappino, and D. Belin, *The plasminogen activator/plasmin system.* Journal of Clinical Investigation, 1991. **88**(4): p. 1067.

419. Keohane, E., L. Smith, and J. Walenga, *Rodak's Hematology: Clinical Principles and Applications*2015: Elsevier Health Sciences.

420. Alkjaersig, N., A.P. Fletcher, and S. Sherry, *ε-aminocaproic acid: an inhibitor of plasminogen activation.* Journal of Biological Chemistry, 1959. **234**(4): p. 832-837.

421. Seetharam, R. and S.K. Sharma, *Purification and analysis of recombinant proteins*. Vol. 12. 1991: CRC Press.

422. Collen, D. and H.R. Lijnen, *The tissue-type plasminogen activator story.* Arteriosclerosis, Thrombosis, and Vascular Biology, 2009. **29**(8): p. 1151-1155.

423. Rijken, D.C., M. Hoylaerts, and D. Collen, *Fibrinolytic properties of one-chain and two-chain human extrinsic (tissue-type) plasminogen activator.* Journal of Biological Chemistry, 1982. **257**(6): p. 2920-2925.

424. Andreasen, P., R. Egelund, and H. Petersen, *The plasminogen activation system in tumor growth, invasion, and metastasis.* Cellular and Molecular Life Sciences CMLS, 2000. **57**(1): p. 25-40.

425. Carmassi, F., et al., *Coagulation and fibrinolytic system impairment in insulin dependent diabetes mellitus.* Thrombosis research, 1992. **67**(6): p. 643-654.

426. Aso, Y., et al., *Impaired fibrinolytic compensation for hypercoagulability in obese patients with type 2 diabetes: association with increased plasminogen activator inhibitor-1.* Metabolism, 2002. **51**(4): p. 471-476.

427. Vague, P., et al., *Correlation between blood fibrinolytic activity, plasminogen activator inhibitor level, plasma insulin level, and relative body weight in normal and obese subjects.* Metabolism, 1986. **35**(3): p. 250-253.

428. Jotic, A., et al., *Decreased Insulin Sensitivity and Impaired Fibrinolytic Activity in Type 2 Diabetes Patients and Nondiabetics with Ischemic Stroke.* International Journal of Endocrinology, 2015.

429. Ajjan, R.A., et al., *Diabetes is associated with posttranslational modifications in plasminogen resulting in reduced plasmin generation and enzyme-specific activity.* Blood, 2013. **122**(1): p. 134-142.

430. Lee, E.A., et al., *Reactive oxygen species mediate high glucose–induced plasminogen activator inhibitor-1 up-regulation in mesangial cells and in diabetic kidney.* Kidney international, 2005. **67**(5): p. 1762-1771.

431. Akinci, B., et al., *Hyperglycemia is associated with lower levels of urokinase-type plasminogen activator and urokinase-type plasminogen activator receptor in wound fluid.* Journal of Diabetes and its Complications, 2014. **28**(6): p. 844-849.

432. Belkacemi, L., et al., *Inhibition of human trophoblast invasiveness by high glucose concentrations.* The Journal of Clinical Endocrinology & Metabolism, 2005. **90**(8): p. 4846-4851.

433. Kim, H.K., et al., *Alterations in the proangiogenic functions of adipose tissue-derived stromal cells isolated from diabetic rats.* Stem Cells and Development, 2008. **17**(4): p. 669-680.

434. Schaffler, A. and C. Buchler, *Concise review: adipose tissue-derived stromal cells - basic and clinical implications for novel cell-based therapies.* Stem Cells, 2007. **25**(4): p. 818-827.

435. Divoux, A., et al., *Fibrosis in human adipose tissue: composition, distribution, and link with lipid metabolism and fat mass loss.* Diabetes, 2010. **59**(11): p. 2817-2825.

436. van der Poll, T. and E. de Jonge, *Cytokines as Regulators of Coagulation.* 2000.

437. Fuchs, T.A., et al., *Extracellular DNA traps promote thrombosis.* Proceedings of the National Academy of Sciences, 2010. **107**(36): p. 15880-15885.

438. Philips, B.J., et al., *Prevalence of endogenous CD34+ adipose stem cells predicts human fat graft retention in a xenograft model.* Plastic and Reconstructive Surgery, 2013. **132**(4): p. 845.

439. Suga, H., et al., *Functional implications of CD34 expression in human adipose-derived stem/progenitor cells.* Stem Cells and Development, 2009. **18**(8): p. 1201-1210.

440. Hong, Y., et al., *Synthesis, characterization, and paclitaxel release from a biodegradable, elastomeric, poly (ester urethane) urea bearing phosphorylcholine groups for reduced thrombogenicity.* Biomacromolecules, 2012. **13**(11): p. 3686-3694.

441. Fang, J., et al., *Biodegradable poly (ester urethane) urea elastomers with variable amino content for subsequent functionalization with phosphorylcholine.* Acta Biomaterialia, 2014. **10**(11): p. 4639-4649.

442. Karagiannides, I., et al., *Altered expression of C/EBP family members results in decreased adipogenesis with aging.* American Journal of Physiology-Regulatory, Integrative and Comparative Physiology, 2001. **280**(6): p. R1772-R1780.
443. Zhu, M., et al., *Manual isolation of adipose-derived stem cells from human lipoaspirates.* JoVE (Journal of Visualized Experiments), 2013(79): p. e50585-e50585.

444. Riordan, N.H., et al., *Non-expanded adipose stromal vascular fraction cell therapy for multiple sclerosis.* J Transl Med, 2009. **7**(29): p. 10.1186.

445. Keck, M., et al., *Power assisted liposuction to obtain adipose-derived stem cells: Impact on viability and differentiation to adipocytes in comparison to manual aspiration.* Journal of Plastic, Reconstructive and Aesthetic Surgery, 2014. **67**(1): p. e1-e8.

446. Tremp, M., et al., *Power-assisted liposuction (PAL) of multiple symmetric lipomatosis (MSL)—a longitudinal study.* Surgery for Obesity and Related Diseases, 2014.

447. Schafer, M.E., et al., *Acute adipocyte viability after third-generation ultrasound-assisted liposuction.* Aesthetic Surgery Journal, 2013. **33**(5): p. 698-704.

448. Aust, L., et al., *Yield of human adipose-derived adult stem cells from liposuction aspirates.* Cytotherapy, 2004. **6**(1): p. 7-14.

449. Soletti L, M.B., Hong Y, Wagner WR, Vorp DA. *A Novel Sliding Rotational Vacuum Seeding Device (S-RVSD) for Porous Tubular Scaffolds*. in *Tissue Engineering & Regenerative Medicine International Society (TERMIS North America)*. 2008. San Diego, CA.

450. Soletti L, N.A., Gharaibeh B, Gupta N, Guan J, Hong Y, Huard J, Wagner WR, Vorp DA. *Evaluation of a Stem Cell-Based Tissue-Engineered Vascular Graft in Small and Large Animal Models: Towards a Fully Autologous Approach*. in *Annual Hilton Head Tissue Engineering Workshop*. 2008.

451. Williams, S.K., et al., *Adipose Stromal Vascular Fraction Cells Isolated Using an Automated Point of Care System Improve the Patency of Expanded Polytetrafluoroethylene Vascular Grafts.* Tissue Engineering Part A, 2013. **19**(11-12): p. 1295-1302.

452. Strioga, M., et al., *Same or not the same? Comparison of adipose tissue-derived versus bone marrow-derived mesenchymal stem and stromal cells.* Stem cells and development, 2012. **21**(14): p. 2724-2752.

453. Casteilla, L., et al., *Adipose-derived stromal cells: Their identity and uses in clinical trials, an update.* World journal of stem cells, 2011. **3**(4): p. 25.

454. Yoshimura, K., et al., *Cell-assisted lipotransfer for cosmetic breast augmentation: supportive use of adipose-derived stem/stromal cells.* Aesthetic Plastic Surgery, 2008. **32**(1): p. 48-55.

455. Bai, X., et al., *Both cultured and freshly isolated adipose tissue-derived stem cells enhance cardiac function after acute myocardial infarction.* European Heart Journal, 2010. **31**(4): p. 489-501.

456. Garcia-Olmo, D., et al., *Treatment of enterocutaneous fistula in Crohn's disease with adipose-derived stem cells: a comparison of protocols with and without cell expansion.* International Journal of Colorectal Disease, 2009. **24**(1): p. 27-30.

457. Li, J., et al., *Factors affecting mesenchymal stromal cells yield from bone marrow aspiration.* Chinese Journal of Cancer Research, 2011. **23**(1): p. 43-48.

458. Benatti, F.B., F.S. Lira, and L.M. Oyama, *Strategies for reducing body fat mass: effects of liposuction and exercise on cardiovascular risk factors and adiposity.* Diabetes, metabolic syndrome and obesity: targets and therapy, 2011. **4**: p. 141.

459. Lee, M.H., et al., *Considerations for tissue-engineered and regenerative medicine product development prior to clinical trials in the United States.* Tissue Engineering Part B: Reviews, 2009. **16**(1): p. 41-54.

460. (FDA), U.F.a.D.A. *Cellular & Gene Therapy Guidances*. 2015 May 2015]; Available from: http://www.fda.gov/BiologicsBloodVaccines/GuidanceComplianceRegulatoryInformation/Guidances/CellularandGeneTherapy/.

461. Patterson, J.T., et al., *Tissue-engineered vascular grafts for use in the treatment of congenital heart disease: from the bench to the clinic and back again.* Regenerative medicine, 2012. **7**(3): p. 409-419.

462. (FDA), U.F.a.D.A. *Early Development Considerations for Innovative Combination Products*. 2015 May 2015]; Available from: http://www.fda.gov/RegulatoryInformation/Guidances/ucm126050.htm.

463. Tanaka, S., et al., *Stromal vascular fraction isolated from lipo-aspirates using an automated processing system: bench and bed analysis.* Journal of Tissue Engineering and Regenerative Medicine, 2013. **7**(11): p. 864-870.

464. Condé-Green, A., et al., *Comparison between Stromal Vascular Cells' Isolation with Enzymatic Digestion and Mechanical Processing of Aspirated Adipose Tissue.* Plastic and Reconstructive Surgery, 2014. **134**(4S-1): p. 54.

465. Gimble, J.M. and X. Wu, *Non-Enzymatic Method for Isolating Human Adipose-Derived Stromal Stem Cells*, 2012, Google Patents.

466. Millan, A., *Comparison Between Collagenase Adipose Digestion and StromaCell Mechanical Dissociation for Mesenchymal Stem Cell Separation.* McNair Scholars Journal - Sacramento State, 2014. **15**: p. 86.

467. Carvalho, P.P., et al., *Xenofree Enzymatic Products for the Isolation of Human Adipose-Derived Stromal/Stem Cells.* Tissue Engineering Part C: Methods, 2013.

468. Müller, A.M., et al., *Platelet lysate as a serum substitute for 2D static and 3D perfusion culture of stromal vascular fraction cells from human adipose tissue.* Tissue Engineering Part A, 2009. **15**(4): p. 869-875.

469. Taha, M.F. and V. Hedayati, *Isolation, identification and multipotential differentiation of mouse adipose tissue-derived stem cells.* Tissue & cell, 2010. **42**(4): p. 211-216.

470. Timmermans, F., et al., *Endothelial progenitor cells: identity defined?* Journal of cellular and molecular medicine, 2009. **13**(1): p. 87-102.

471. Dominici, M., et al., *Minimal criteria for defining multipotent mesenchymal stromal cells. The International Society for Cellular Therapy position statement.* Cytotherapy, 2006. **8**(4): p. 315-317.

472. Kim, S.E., et al., *Porous chitosan scaffold containing microspheres loaded with transforming growth factor-β1: implications for cartilage tissue engineering.* Journal of Controlled Release, 2003. **91**(3): p. 365-374.

473. Choi, Y.-H., et al., *Injectable PLGA microspheres encapsulating WKYMVm peptide for neovascularization.* Acta Biomaterialia, 2015.

474. Rui, J., et al., *Controlled release of vascular endothelial growth factor using poly-lactic-co-glycolic acid microspheres: in vitro characterization and application in polycaprolactone fumarate nerve conduits.* Acta Biomaterialia, 2012. **8**(2): p. 511-518.

475. Mooney, D.J., et al., *Localized delivery of epidermal growth factor improves the survival of transplanted hepatocytes.* Biotechnology and Bioengineering, 1996. **50**(4): p. 422-429.

476. Byeon, H.J., et al., *PEGylated apoptotic protein-loaded PLGA microspheres for cancer therapy.* International Journal of Nanomedicine, 2015. **10**: p. 739.

477. Ramazani, F., et al., *Formulation and characterization of microspheres loaded with imatinib for sustained delivery.* International Journal of Pharmaceutics, 2015. **482**(1): p. 123-130.

478. Kawai, K., et al., *Accelerated tissue regeneration through incorporation of basic fibroblast growth factor-impregnated gelatin microspheres into artificial dermis.* Biomaterials, 2000. **21**(5): p. 489-499.

479. Rothstein, S.N. and S.R. Little, *A "tool box" for rational design of degradable controlled release formulations.* Journal of Materials Chemistry, 2011. **21**(1): p. 29-39.

480. Blaber, S.P., et al., *Analysis of in vitro secretion profiles from adipose-derived cell populations.* Journal of translational medicine, 2012. **10**(1): p. 172.

481. Lopatina, T., et al., *Adipose-derived stem cells stimulate regeneration of peripheral nerves: BDNF secreted by these cells promotes nerve healing and axon growth de novo.* PloS one, 2011. **6**(3): p. e17899.

482. Barleon, B., et al., *Migration of human monocytes in response to vascular endothelial growth factor (VEGF) is mediated via the VEGF receptor flt-1.* Blood, 1996. **87**(8): p. 3336-3343.

483. Arshady, R., *Microspheres and microcapsules, a survey of manufacturing techniques: Part III: Solvent evaporation.* Polymer Engineering & Science, 1990. **30**(15): p. 915-924.

484. Huo, Y., X. Guo, and G.S. Kassab, *The flow field along the entire length of mouse aorta and primary branches.* Annals of Biomedical Engineering, 2008. **36**(5): p. 685-699.

485. Robb, H.J., *The role of micro-embolism in the production of irreversible shock.* Annals of Surgery, 1963. **158**(4): p. 685.

486. Jönsson, H., et al., *Circulating particles during cardiac surgery.* Interactive Cardiovascular and Thoracic Surgery, 2009. **8**(5): p. 538-542.

487. Leotot, J., et al., *Platelet lysate coating on scaffolds enhances directly and indirectly cell migration improving bone and blood vessel formation.* Acta biomaterialia, 2013.

488. Pevsner-Fischer, M., et al., *Toll-like receptors and their ligands control mesenchymal stem cell functions.* Blood, 2007. **109**(4): p. 1422-1432.

489. Tomchuck, S.L., et al., *Toll-Like Receptors on Human Mesenchymal Stem Cells Drive Their Migration and Immunomodulating Responses.* Stem Cells, 2008. **26**(1): p. 99-107.

490. Waterman, R.S., et al., *A New Mesenchymal Stem Cell (MSC) Paradigm: Polarization into a Pro-Inflammatory MSC1 or an Immunosuppressive MSC2 Phenotype.* Plos One, 2010. **5**(4).

491. Jay, S.M., et al., *Dual delivery of VEGF and MCP-1 to support endothelial cell transplantation for therapeutic vascularization.* Biomaterials, 2010. **31**(11): p. 3054-3062.

492. Chung, C.W., et al., *VEGF microsphere technology to enhance vascularization in fat grafting.* Annals of Plastic Surgery, 2012. **69**(2): p. 213-219.

493. Skop, N.B., et al., *Heparin crosslinked chitosan microspheres for the delivery of neural stem cells and growth factors for central nervous system repair*. Acta Biomaterialia, 2013. **9**(6): p. 6834-6843.

494. Marra, K.G., et al., *FGF-2 Enhances Vascularization for Adipose Tissue Engineering.* Plastic and Reconstructive Surgery, 2008. **121**(4): p. 1153-1164.

495. Royce, S.M., M. Askari, and K.G. Marra, *Incorporation of polymer microspheres within fibrin scaffolds for the controlled delivery of FGF-1*. Journal of Biomaterials Science, Polymer Edition, 2004. **15**(10): p. 1327-1336.

496. Richardson, T.P., et al., *Polymeric system for dual growth factor delivery*. Nature Biotechnology, 2001. **19**(11): p. 1029-1034.

497. Sun, Q., et al., *Sustained release of multiple growth factors from injectable polymeric system as a novel therapeutic approach towards angiogenesis.* Pharmaceutical Research, 2010. **27**(2): p. 264-271.

498. Elisseeff, J., et al., *Controlled-release of IGF-I and TGF-β1 in a photopolymerizing hydrogel for cartilage tissue engineering.* Journal of Orthopaedic Research, 2001. **19**(6): p. 1098-1104.

499. Chen, F.-M., et al., *In vitro cellular responses to scaffolds containing two microencapulated growth factors.* Biomaterials, 2009. **30**(28): p. 5215-5224.

500. Basmanav, F.B., G.T. Kose, and V. Hasirci, *Sequential growth factor delivery from complexed microspheres for bone tissue engineering.* Biomaterials, 2008. **29**(31): p. 4195-4204.

501. Wang, X., et al., *Growth factor gradients via microsphere delivery in biopolymer scaffolds for osteochondral tissue engineering.* Journal of Controlled Release, 2009. **134**(2): p. 81-90.

502. de Boer, R., et al., *Short-and long-term peripheral nerve regeneration using a poly-lactic-co-glycolic-acid scaffold containing nerve growth factor and glial cell line-derived neurotrophic factor releasing microspheres.* Journal of Biomedical Materials Research Part A, 2012. **100**(8): p. 2139-2146.

503. Kokai, L.E., A.M. Ghaznavi, and K.G. Marra, *Incorporation of double-walled microspheres into polymer nerve guides for the sustained delivery of glial cell line-derived neurotrophic factor.* Biomaterials, 2010. **31**(8): p. 2313-2322.

504. Liang, C.-z., et al., *Dual release of dexamethasone and TGF-β3 from polymeric microspheres for stem cell matrix accumulation in a rat disc degeneration model.* Acta Biomaterialia, 2013. **9**(12): p. 9423-9433.

505. Rubin, J.P., et al., *Encapsulation of adipogenic factors to promote differentiation of adipose-derived stem cells.* Journal of Drug Targeting, 2009. **17**(3): p. 207-215.

506. De Rosa, G. and G. Salzano, *PLGA Microspheres Encapsulating siRNA*, in *RNA Interference*2015, Springer. p. 43-51.

507. Tengood, J.E., et al., *Sequential delivery of vascular endothelial growth factor and sphingosine 1-phosphate for angiogenesis.* Biomaterials, 2010. **31**(30): p. 475-7812.

508. Tengood, J.E., et al., *Sequential delivery of basic fibroblast growth factor and platelet-derived growth factor for angiogenesis.* Tissue Engineering Part A, 2011. **17**(9-10): p. 1181-1189.

509. Balmert, S.C. and S.R. Little, *Biomimetic Delivery with Micro-and Nanoparticles.* Advanced Materials, 2012. **24**(28): p. 3757-3778.

510. Rothstein, S.N., W.J. Federspiel, and S.R. Little, *A simple model framework for the prediction of controlled release from bulk eroding polymer matrices.* Journal of Materials Chemistry, 2008. **18**(16): p. 1873-1880.

511. Rothstein, S.N., W.J. Federspiel, and S.R. Little, *A unified mathematical model for the prediction of controlled release from surface and bulk eroding polymer matrices.* Biomaterials, 2009. **30**(8): p. 1657-1664.

512. Rothstein, S.N., et al., *A retrospective mathematical analysis of controlled release design and experimentation.* Molecular pharmaceutics, 2012. **9**(11): p. 3003-3011.